



ESCUELA DE DOCTORADO  
INTERNACIONAL DE LA USC

Antonio  
Dopico López

Tesis doctoral

Preclinical studies on the  
protective effect of the  
recombinant human GOT  
enzyme in animal models of  
ischaemic stroke

Santiago de Compostela, 2021

**Programa de doctorado en Medicina Molecular**



TESIS DE DOCTORADO

**PRECLINICAL STUDIES ON THE  
PROTECTIVE EFFECT OF  
RECOMBINANT HUMAN GOT  
ENZYME IN ANIMAL MODELS OF  
ISCHAEMIC STROKE**

Antonio Dopico López

**ESCUELA DE DOCTORADO INTERNACIONAL DE LA UNIVERSIDAD DE  
SANTIAGO DE COMPOSTELA**

**PROGRAMA DE DOCTORADO EN MEDICINA MOLECULAR**

SANTIAGO DE COMPOSTELA

AÑO 2021



## **DECLARACIÓN DEL AUTOR DE LA TESIS**

### **Preclinical studies on the protective effect of the recombinant human GOT enzyme in animal models of ischaemic stroke**

D. Antonio Dopico López

Presento mi Tesis, siguiendo el procedimiento adecuado del Reglamento y declaro que:

- 1) La Tesis abarca los resultados de la elaboración de mi trabajo.
- 2) De ser el caso, en la Tesis se hace referencia a las colaboraciones que tuvo este trabajo.
- 3) Confirmando que la Tesis no incurre en ningún tipo de plagio de otros autores ni de trabajos presentados por mí para la obtención de otros títulos.
- 4) La Tesis es la versión definitiva presentada para su defensa y coincide la versión impresa con la presentada en formato electrónico.

En Santiago de Compostela, a 19 de diciembre de 2021.

Fdo.: Antonio Dopico López



## **AUTORIZACIÓN DEL DIRECTOR DE LA TESIS**

### **Preclinical studies on the protective effect of the recombinant human GOT enzyme in animal models of ischaemic stroke**

D. Francisco Campos Pérez

D. José Castillo Sánchez

INFORMAN:

Que la presente Tesis, se corresponde con el trabajo realizado por D. Antonio Dopico López, bajo mi dirección, y autorizo su presentación, considerando que reúne los requisitos exigidos en el Reglamento de Estudios de Doctorado de la USC, y que como director de esta no incurre en las causas de abstención establecidas en la Ley 40/2015.

De acuerdo con lo indicado en el Reglamento de Estudios de Doctorado, declara también que la presente Tesis doctoral es idónea para ser defendida en base a la modalidad de Monográfica con reproducción de publicaciones, en los que la participación del doctorando fue decisiva para su elaboración y las publicaciones se ajustan al Plan de Investigación.

En Santiago de Compostela, a 19 de diciembre de 2021.

Francisco Campos Pérez

José Castillo Sánchez



## **AUTORIZACIÓN DEL TUTOR DE LA TESIS**

### **Preclinical studies on the protective effect of the recombinant human GOT enzyme in animal models of ischaemic stroke**

D. Juan Bautista Zalvide Torrente

INFORMA:

Que la presente Tesis, se corresponde con el trabajo realizado por D. Antonio Dopico López, bajo mi tutorización, y autorizo su presentación, considerando que reúne los requisitos exigidos en el Reglamento de Estudios de Doctorado de la USC, y que como director de esta no incurre en las causas de abstención establecidas en la Ley 40/2015.

De acuerdo con lo indicado en el Reglamento de Estudios de Doctorado, declara también que la presente Tesis doctoral es idónea para ser defendida en base a la modalidad de Monográfica con reproducción de publicaciones, en los que la participación del doctorando fue decisiva para su elaboración y las publicaciones se ajustan al Plan de Investigación.

En Santiago de Compostela, a 19 de diciembre de 2021.

Juan Bautista Zalvide Torrente



## **Conflict of interest**

The author and the directors of the work agreed to present the results in this Thesis and declare no conflict of interest.



## **Research stay**

During the development of the Thesis, the PhD student performed a stay in an international laboratory, with the group of Prof. Dr. Devrim Gözüaçik in the Koç University Research Center for Translational Medicine (KUTTAM) in Istanbul, Turkey, during the period between June-September 2021.



## **Funding**

This study was partially supported by the Instituto de Salud Carlos III (PI17/00540, ICI19/00032 and AC19/00066, this list grant under the frame of EuroNanoMed III), the Miguel Servet program (CPII19/00020) and the European Union program FEDER and the European Regional Development Fund-ERDF.

During the development of this Thesis, the doctoral candidate benefited from a predoctoral scholarship granted by the Health Research Institute of Santiago de Compostela Foundation. During this period, Dr. Francisco Campos, Director of the Thesis, has been the beneficiary of the Miguel Servet contract, of the Instituto de Salud Carlos III (CP14/00154).



## Agradecimientos

Como reza el dicho, es de buen nacido el ser agradecido, y como siempre nos recuerda Pepe (con mucho tino), ninguna Tesis doctoral es el trabajo de una única persona, aunque sea un único nombre el que aparece en la portada. Por lo tanto, no podría dar por terminada esta Tesis sin antes agradecer a la gente que ha participado en ella.

En primer lugar, debo agradecer al Prof. José Castillo y al Dr. Francisco Campos, directores de esta Tesis. Sin su supervisión y sus consejos no habría sido posible llevar esta empresa a buen puerto. Gracias también al Dr. Tomás Sobrino por su ayuda.

Gracias a los profesores David Mirelman y Marc Gauthier, que participaron en este proyecto como si fuese el suyo propio. Y por supuesto, gracias a la Dra. Ahlem Zaghmi, con la que compartí poyata y risas. Mi experiencia contigo no pudo haber sido más agradable.

Gracias al Prof. Devrim Gözüaçik y al resto de miembros de su laboratorio, especialmente a la Dra. Öyküm Kaplam, por su amabilidad y su paciencia a la hora de enseñarme el poco turco que sé. Me acogisteis como uno más y me permitisteis disfrutar todo lo posible de Estambul y de Turquía. Tesekkürler.

Por supuesto, gracias a todos los miembros del LINC, tanto los que siguen como los que ya no, con los que he compartido alegrías y penas (aunque ahora sean los LINCS, yo lo sigo sintiendo como uno solo). Todos habéis contribuido a esta Tesis, ya sea con vuestras manos o con vuestras cabezas. Jamás he necesitado ayuda y me he sentido olvidado o abandonado por ninguno de vosotros. Sin embargo, sería injusto no nombrar a aquellos que han contribuido especialmente a esta Tesis. Ramón, que aguantó con

infinita paciencia mis preguntas sobre átomos, spines y demás mientras me brindaba perlas de sabiduría sobre otros temas menos... científicos. Andrés, al que acosé a preguntas sobre el glutamato, la GOT y a saber cuántas cosas más, quien siempre tuvo una palabra amable (y un chiste, aunque no diré sobre que) mientras me ayudaba. Clara, a quien esta Tesis le robó horas de sueño (y es posible que también algún que otro año de vida) pero que siempre estuvo ahí para remangarse y arrimar el hombro. Hervella, quien fue, y sigue siendo, la prueba viviente de que el ser un buen científico no está reñido con el consumo de vermut. Por último, pero no por ello menos importante, a María. Si el título de doctor se pudiese compartir, María se merecería, al menos, la mitad del mío. Me ha aconsejado, me ha enseñado y me ha ayudado; ha tenido que lidiar con mis errores y se ha sido responsable de muchos de mis aciertos; todo ello sin una sola palabra desagradable ni un mal gesto. Nadie podría desear una mejor compañera que ella.

Por supuesto, no sólo la gente que ha participado en esta Tesis merece mi agradecimiento. Otros han contribuido de forma igualmente importante a esta Tesis, puede que no con ciencia, pero sin ellos este trabajo tampoco habría sido posible. Que mejor sitio para empezar que por la más joven. Antía, que se negó a aceptar al señor mayor que llevo dentro y que no ha dejado de intentar contagiarme algo de su espíritu juvenil, aunque a veces haya sido una tarea infructuosa. A la Dra. Garrote, compañera de tropelías y consejera espiritual. Al contrario que su tocaya, sus consejos suelen venir acompañados de una mirada hosca y/o un comentario sarcástico, pero no por ello son menos bienvenida o menos útiles. Y cómo no, gracias a Manuel y Nacho, los otros dos miembros del triunvirato. No podrían ser más diferentes y a la vez más iguales. Ni Nacho es tan bueno como parece ni Manuel tan malo. Las tardes infinitas en el laboratorio con ellos y las más

aún infinitas cañas me salvaron en más de una ocasión de caer en la desesperación.

Gracias a mis padres, a mi hermano y a toda mi familia, que me ha apoyado en todo lo que he hecho, desde que un jovencito imberbe (aunque ahora no es que tenga mucha más barba) vino a Santiago con 18 años. Sé que se han sentido orgullosos de mí (a pesar de que mi madre quizás no me perdona los eventos familiares que me he perdido) y eso me ha animado a seguir más de lo que se imaginan.

Finalmente, a Vanessa. Nada de lo que diga aquí podría hacer justicia a lo que has sido, y eres, para mí. Me has aguantado en los días buenos y los malos, en los felices y en los tristes, y el saber que me esperabas a la salida, ha hecho cada uno de los largos días de trabajo un poco más corto. También me has ayudado a entrenar la paciencia, que dicen que es la madre de la ciencia. No pierdas jamás tu inocencia ni tu sonrisa, a pesar de este gruñón con el que te ha tocado vivir.



# INDEX



<b>Resumo</b>	1
ABBREVIATIONS	11
INTRODUCTION	19
1.- SECTION I: STROKE	21
1.1.- Definition	21
1.2.- Epidemiology	21
1.3.- Classification	23
1.3.1.- HAEMORRHAGIC STROKE	23
1.3.2.- ISCHAEMIC STROKE	23
1.4.- Risk factors	26
1.4.1.- NON-MODIFIABLE RISK FACTORS	26
1.4.2.- MODIFIABLE RISK FACTORS	26
1.5.- Pathophysiology of Ischaemic Stroke	27
1.6.- Therapeutic Approaches for Ischaemic Stroke	32
1.6.1.- REPERFUSION THERAPIES	32
1.6.2.- NEUROPROTECTION	35
1.6.2.1.- Calcium Blockers	38
1.6.2.2.- Glutamate antagonists	38
1.6.2.3.- Antioxidants	39
1.6.2.4.- Phospholipid Precursors	39
1.6.2.5.- Inhibitors of Glutamate Release	40
1.6.2.6.- GABA Agonists	40
1.6.2.7.- Anti-inflammatories	41
1.6.2.8.- Other compounds	41
1.6.3.- NEUROREPAIR	41
1.6.3.1.- Neurogenesis	42
1.6.3.2.- Angiogenesis	42
1.6.3.3.- Neurogenesis and Angiogenesis	43

1.6.3.4.- The Role of Oligodendrocytes, Astrocytes and Axons in Neurorepair	44
2.- SECTION II: GLUTAMATE AND EXCITOTOXICITY	45
2.1.- Glutamate	45
2.2.- Compartmentalization	45
2.3.- Glutamate Transporters	46
2.3.1.- EXCITATORY AMINO ACID TRANSPORTERS	46
2.3.1.1.- Brain Location	47
2.3.1.2.- Function	48
2.3.2.- VESICULAR GLUTAMATE TRANSPORTERS	49
2.3.2.1.- Function	49
2.3.2.2.- Brain Location	50
2.4.- Metabolism and Cycling	50
2.5.- Excitotoxicity	53
2.6.- Therapeutic Strategies for Glutamate Excitotoxicity	54
2.7.- Blood Glutamate Grabbing	55
3.- SECTION III: GOT	59
3.1.- Chemical Structure	59
3.2.- Mechanism of Action	61
3.3.- Tissue Distribution	62
3.4.- Function	65
3.4.1.- MALATE-ASPARTATE SHUTTLE	65
3.4.2.- GLUCOSE METABOLISM	67
3.4.3.- GLYCERONEOGENESIS	70
3.4.4.- HYDROGEN SULPHIDE SYNTHESIS	71
3.4.5.- KYNURENIC ACID SYNTHESIS	72
3.4.6.- FATTY ACID BINDING PROTEIN	73

3.5.- Therapeutic Applications of GOT	74
3.5.1.- ISCHAEMIC STROKE	74
3.5.2.- TRAUMATIC BRAIN INJURY	76
3.5.3.- SUBARACHNOID HAEMORRHAGE	78
3.5.4.- MIGRAINE HEADACHE	79
3.5.5.- ORGANOPHOSPHATE INTOXICATION	80
3.5.6.- FOETAL ASPHYXIA AND HYPOXIC-ISCHAEMIC ENCEPHALOPATHY	81
3.5.7.- AMYOTROPHIC LATERAL SCLEROSIS	82
3.5.8.- GLIOMA	83
3.5.9.- ALZHEIMER’S DISEASE	83
3.5.10.- OTHER PATHOLOGIES	84
HYPOTHESIS	85
OBJECTIVES	89
MATERIALS AND METHODS	93
4.- SECTION I: ENDOGENOUS GOT1 INHIBITION STUDIES	95
4.1.- Synthesis and Production of Anti-rGOT1 Antibody	95
4.2.- <i>In vitro</i> Dose-response Analysis of AbGOT1	96
4.3.- Animal Procedures	96
4.3.1.- ANIMAL CARE	97
4.3.2.- INHIBITION OF BLOOD GOT1 IN HEALTHY ANIMALS	98
4.3.3.- ABGOT1 EFFECT IN AN ISCHAEMIC RAT MODEL	98
4.3.3.1.- Surgical Procedures	99
4.3.3.2.- <i>In vivo</i> Magnetic Resonance Imaging	101
4.3.3.3.- <i>In vivo</i> Magnetic Resonance Spectroscopy	103
4.3.3.4.- Sensorimotor Tests	103
4.3.3.5.- Image Analysis	105

4.4.- Biochemical Analysis	105
4.4.1.- BLOOD GOT AND GPT ACTIVITY ANALYSIS	105
4.4.2.- BLOOD GLUTAMATE ANALYSIS	105
4.4.3.- ANALYSIS OF GOT1 LEVELS IN CEREBROSPINAL FLUID AND BRAIN TISSUE	106
4.5.- Statistical Analysis	107
5.- SECTION II: RGOT1 THERAPEUTIC EFFECT	107
5.1.- Protein Synthesis	107
5.1.1.- BIOSYNTHESIS	108
5.1.2.- PURIFICATION	110
5.1.3.- CHARACTERIZATION	111
5.1.3.1.- Sequencing	112
5.1.3.2.- Secondary Structure Analysis	112
5.1.3.3.- Specific Activity	112
5.2.- Animal Procedures	113
5.2.1.- ANIMAL CARE	113
5.2.2.- PHARMACOKINETICS AND DOSE RESPONSE STUDY	114
5.2.3.- SURGICAL PROCEDURES	115
5.2.4.- THERAPEUTIC TIME WINDOW	115
5.2.5.- THERAPEUTIC EFFECT ON SEVERE AND MILD ISCHAEMIA	116
5.2.6.- INJECTION PROTOCOL	117
5.2.7.- ANALYSIS OF GOT1 LEVELS IN CEREBROSPINAL FLUID	118
5.3.- Statistical Analysis	118
6.- SECTION III: RGOT1 BIOCONJUGATION	119
6.1.- Synthesis of mPEG-rGOT1 and Angiopep-PEG- rGOT1	119
6.2.- Animal Procedures	121

6.2.1.- ANIMAL CARE	122
6.2.2.- SURGICAL PROCEDURES	122
6.2.3.- PHARMACOKINETICS AND PHARMACODYNAMICS IN HEALTHY RATS	122
6.2.4.- PHARMACOKINETICS IN ISCHAEMIC RATS AND PROTECTIVE STUDY	123
6.3.- Biochemical Analysis	123
6.3.1.- ANALYSIS OF GOT ACTIVITY IN SERUM AND CSF	124
6.3.2.- MONITORING OF GLUTAMATE CONCENTRATION IN SERUM AND CSF BY HPLC	124
6.4.- Statistical Analysis	125
7.- SECTION IV: RGOT1 AND RTPA INTERACTIONS	125
7.1.- <i>In vitro</i> Analysis	125
7.2.- Animal Procedures	126
7.2.1.- ANIMAL CARE	127
7.2.2.- THROMBIN-INDUCED STROKE MODEL	127
7.2.2.1.- Surgical Procedures	128
7.2.3.- EMBOLIC STROKE MODEL	129
7.2.3.1.- Surgical Procedures	129
7.3.- Statistical Analysis	131
RESULTS	133
8.- SECTION I: ENDOGENOUS GOT1 INHIBITION STUDIES	135
8.1.- <i>In Vitro</i> and <i>In Vivo</i> Analysis of AbGOT1 on GOT1	135
8.2.- Effect of AbGOT1 in an ischaemic animal model	137
8.3.- Analysis of Sensorimotor Deterioration in Control and AbGOT1 Treated Animals	141
8.4.- Effect of AbGOT1 on Brain Glutamate and Lactate Levels in the Ischaemic Animal Model	143

8.5.- GOT1 Activity in CSF and Brain Tissue	144
9.- SECTION II: RGOT1 THERAPEUTIC EFFECT	147
9.1.- Protein Synthesis	147
9.1.1.- SIZE AND SEQUENCE ANALYSIS	147
9.1.2.- SECONDARY STRUCTURE	149
9.1.3.- SPECIFIC ACTIVITY	150
9.2.- Pharmacokinetics and Dose Response Study	151
9.3.- Therapeutic Time Window	154
9.4.- Therapeutic Effect on Mild and Severe Ischaemia	156
9.4.1.- SEVERE ISCHAEMIA	156
9.4.2.- MILD ISCHAEMIA	163
9.5.- Injection Protocol	166
9.6.- Therapeutic Effect on Mild and Severe Ischaemia: 4 Injections Protocol	168
9.6.1.- SEVERE ISCHAEMIA	168
9.6.2.- MILD ISCHAEMIA	172
9.7.- GOT1 Activity in CSF	178
10.- SECTION III: RGOT1 BIOCONJUGATION	180
10.1.- Synthesis of mPEG-rGOT1 and Angiopep-PEG- rGOT1	181
10.2.- Pharmacokinetics	182
10.3.- Protective Study	185
10.4.- GOT1 Activity in CSF	190
11.- SECTION IV: RGOT1 AND RTPA INTERACTION	191
11.1.- <i>In Vitro</i> Analysis	192
11.2.- Thrombin-Induced Stroke Model	194
11.3.- Embolic Stroke Model	197

DISCUSSION	202
12.- SECTION I: ENDOGENOUS GOT1 INHIBITION STUDIES	203
13.- SECTION II: RGOT1 THERAPEUTIC EFFECT	209
14.- SECTION III: RGOT1 BIOCONJUGATION	217
15.- SECTION IV: RGOT1 AND RTPA INTERACTION	221
CONCLUSIONS	225
SECTION I: ENDOGENOUS GOT1 INHIBITION STUDIES	227
SECTION II: RGOT1 THERAPEUTIC EFFECT	227
SECTION III: RGOT1 BIOCONJUGATION	228
SECTION IV: RGOT1 AND RTPA INTERACTION	228
BIBLIOGRAPHY	233
ANNEXES	267



## Resumo

O ictus isquémico é unha enfermidade neurolóxica de orixe vascular causada pola obstrución dunha arteria cerebral e que supón a segunda causa de morte nos países desenvolvidos, afectando a 15 millóns de persoas en todo o mundo. Esta situación é aínda máis grave en Galicia, onde o envellecemento da poboación fai que as enfermidades de orixe vascular se convertan na primeira causa de morte. Ademais do custo en vidas e anos de vida útiles, o ictus supón unha gran carga económica, cun custo aproximado de dous mil millóns de euros ó ano.

Pese a que a aparición das unidades de ictus, os avances nas técnicas de neuroimaxe, a maior concienciación e educación da poboación á hora de detectar os síntomas e o uso das terapias de reperfusión, como o activador tisular do plasminóxeno recombinante e, máis recentemente, a trombectomía mecánica, conseguiron reducir considerablemente tanto a mortalidade como as secuelas neurolóxicas derivadas do ictus isquémico. Así e todo, segue a existir a necesidade dun tratamento que axude a reducir o dano provocado polo ictus isquémico, sobre todo naqueles doentes que non son elixibles para as terapias reperfusoras.

Tras o bloqueo da arteria, a falta de fluxo sanguíneo provoca unha caída drástica dos niveis de oxíxeno e glucosa, o que deriva finalmente nunha falta de enerxía nas células da zona afectada. Este fallo enerxético da lugar a unha serie de eventos moleculares que finalmente provocan a morte celular e o dano no parénquima cerebral. Un dos procesos máis importantes neste dano é a liberación descontrolada de glutamato ó espazo extracelular. A falta de enerxía derivada da redución do fluxo sanguíneo provoca un fallo na bomba de sodio/potasio, o que provoca unha despolarización da membrana das neuronas, o que da lugar á liberación de glutamato. Esta liberación masiva

de glutamato ó espazo sináptico activa os receptores glutamatérxicos NMDA e AMPA, o que provoca unha entrada de calcio na célula e a morte celular.

Debido a esta excitotoxicidade provocada polo glutamato, durante anos, decenas de estudos estiveron enfocados ó bloqueo, en diversos puntos da ruta, da liberación ou a toxicidade deste neurotransmisor. A pesar dos resultados prometedores de moitos deles nos ensaios con animais, ningún foi capaz de mostrar un verdadeiro beneficio nos doentes de ictus, en gran medida por mor dos efectos secundarios indesexables provocados por moitos deles, debido a que alteraban o normal funcionamento fisiolóxico do glutamato (cabe recordar que o glutamato é o neurotransmisor máis abundante do sistema nervioso). Polo tanto, plantexaronse novas estratexias enfocadas a abordar a excitotoxicidade do glutamato sen afectar ó seu normal funcionamento. Unha destas estratexias, nomeada como os atrapadores de glutamato, consiste na redución dos niveis extracelulares de glutamato mediante a redución dos niveis deste aminoácido na sangue, facilitando o seu fluxo dende o parénquima cerebral cara o torrente sanguíneo. Entre estes atrapadores de glutamato atópase a glutamato-oxalacetato transaminase (GOT).

As transaminases son un conxunto de encimas que transfiren grupos amino dun metabolito a outro, xeralmente aminoácidos. No caso da GOT, esta encima cataliza a reacción de transferencia dun grupo amino entre o glutamato e o aspartato de forma reversible. A reacción completa desta encima utiliza unha molécula de glutamato e unha de oxalacetato para producir unha molécula de aspartato e outra de  $\alpha$ -cetoglutarato. Existen dúas isoformas da GOT, a GOT1 (citosólica) e a GOT2 (mitocondrial), que catalizan a mesma reacción, aínda que existen algunhas diferencias nos procesos nos que están implicadas. A GOT é unha encima crucial no metabolismo cerebral do glutamato, aínda que tamén participa noutros

procesos fisiolóxicos, sendo o máis destacable a lanzadeira malato-aspartato.

Tendo en conta todo o anteriormente exposto, a hipótese desta Tese é que o uso dunha versión recombinante da encima GOT1 humana (rGOT1) podería levar a unha redución dos niveis de glutamato en sangue, reducindo o volume do infarto e a mellora do déficit neurolóxico dos animais, todo isto sen desencadear ningún efecto secundario adverso.

Polo tanto, propuxéronse unha serie de obxectivos para dar resposta a esta hipótese:

- 1.- Análise do efecto do bloqueo da GOT1 endóxena mediante a utilización dun anticorpo policlonal específico nun modelo animal de isquemia.
- 2.- Estudo da farmacocinética e o efecto terapéutico da versión recombinante da GOT1 humana en modelos animais de isquemia.
- 3.- Análise da farmacocinética e o efecto terapéutico de dous bioconxugados da rGOT1 en modelos animais de isquemia.
- 4.- Estudo da interacción entre o rtPA e a rGOT1.

En primeiro lugar, levouse a cabo un estudo do efecto do bloqueo da GOT1 endóxena en modelos animais de isquemia, co fin de dilucidar o verdadeiro impacto desta encima na patoloxía cerebral isquémica. A síntese dun anticorpo policlonal contra a GOT1 endóxena, levouse a cabo en colaboración co Prof. David Mirelman, do Instituto Weizmann en Israel. En canto a análise *in vitro*, esta mostrou un potente efecto inhibitor do anticorpo, que se repetiu nos ensaios *in vivo* con animais sans, conseguindo unha inhibición significativa da actividade da GOT1 en sangue (inclusive por debaixo dos niveis mínimos

detectables) durante oito días. Para comprobar a especificidade do anticorpo, a actividade en sangue de outra transaminase, a GPT, foi tamén analizada. Sen embargo, a actividade encimática en sangue desta transaminase, moi próxima tanto en función como en estrutura á GOT, non se veu afectada polo anticorpo, o que demostrou que este actúa de forma específica contra a GOT1. Seguidamente, e utilizando o modelo animal de isquemia do filamento intraluminal (este modelo consiste na introdución dun pequeno filamento a través da carótide común dos animais, que é despois avanzado polo lumen da arteria ata chegar a taponar o comeza da arteria cerebral media) os animais foron sometidos a isquemia. Aqueles animais que foron tratados co anticorpo mostraron un maior volume de infarto en comparación con aqueles que foron tratados con soro salino, incluídos no grupo control. En canto ós resultados obtidos nos test motores, os animais que foran previamente tratados co anticorpo mostraron unha peor evolución funcional fronte aqueles animais pertencentes ó grupo control. Aínda que os datos dos volumes de infarto e os test funcionais indicaron unha peor evolución dos animais tratados co anticorpo, a análise dos niveis de glutamato en sangue non mostraron ningún cambio significativo entre os animais tratados e o grupo control. En base a isto, e co fin de determinar se o anticorpo podería ter un efecto local no lugar dun efecto sistémico, decidiuse levar a cabo un estudo de espectroscopia por resonancia magnética, co fin de analizar os niveis intracerebrais de glutamato. Neste caso si se observou un incremento significativo dos niveis deste aminoácido no hemisferio ipsilateral dos animais isquémicos. Ademais do glutamato, analizouse tamén, utilizando a mesma técnica, os niveis de lactato intracerebral. Igual que no caso do glutamato, observouse un aumento significativo da concentración de lactato no hemisferio ipsilateral dos animais sometidos a isquemia. Este aumento dos niveis de glutamato e lactato explican o aumento do dano isquémico asociado ó uso do anticorpo, xa que provocan un estado de susceptibilidade do tecido. Finalmente, o uso deste anticorpo demostrou un efecto

inhibitorio sobre a GOT1 tanto no líquido cefalorraquídeo como no tecido cerebral. Os datos obtidos neste estudo demostran a importancia da GOT1 durante a isquemia cerebral e apoian o seu uso como terapia fronte o ictus.

A continuación estudouse o efecto terapéutico dunha versión recombinante da GOT1 humana. Para iso, sintetizouse unha nova versión da encima, diferente da utilizada en estudos anteriores, utilizando a tecnoloxía SUMO. Esta tecnoloxía permite a obtención dunha proteína recombinante que segue os criterios de calidade CGMP (Current Good Manufacturing Practices), unha serie de guías elaboradas pola Food and Drug Administration (FDA) que regulan a produción de alimentos, cosméticos e fármacos destinados para ser utilizados en humanos. Os resultados obtidos da caracterización desta nova versión da encima demostraron que a rGOT1 conserva a mesma secuencia e estrutura que a GOT1 humana, así como a súa actividade encimática.

En canto á farmacocinética da rGOT1, o seu análise en animais sans mostrou un aumento significativo na actividade da GOT1 en sangue tras a administración da rGOT1, cunha vida media aproximada de 2 horas. Do mesmo xeito que no caso dos estudos co anticorpo, non se observou un efecto sobre os niveis de glutamato en sangue, aínda que si se veu unha eliminación do glutamato máis rápida en animais que foron inxectados previamente cunha dose 1M do aminoácido. Tendo en conta estes experimentos e estudos publicados anteriormente polo noso grupo, seleccionouse a dose de 0.24 mg/kg.

Seguidamente realizouse un novo estudo para determinar a fiestra terapéutica da rGOT1. A encima foi inxectada a diferentes tempos tras a reperusión, máis ningún dos grupos experimentais mostrou efecto algún sobre os volumes de infarto ou os test funcionais. A falta de efectos positivos debeuse a unha dose insuficiente da rGOT1. A pesar de que a dose utilizada mostrou uns niveis de actividade en sangue similares

ós obtidos nos nosos estudos anteriores, a utilización dun protocolo diferente para a síntese da rGOT1 poido ter repercusións sobre o funcionamento da encima. Debido a isto, probáronse de novo diferentes doses da proteína recombinante nun modelo animal de isquemia, co fin de dilucidar cal é a nova dose adecuada para obter un efecto terapéutico visible nos animais.

En base a estes experimentos, que se realizaron en animais sometidos tanto a unha isquemia severa coma moderada (a distinción entre isquemia severa e moderada realizouse en función da desviación da liña media como resultado do infarto cerebral, avaliada ás 24 horas tras a cirurxía) escolleuse a dose de 1 mg/kg como a máis axeitada para os futuros estudos. Esta dose demostrou unha redución significativa do volume de infarto e unha mellora nos test funcionais. Non obstante, tampouco neste caso se observaron cambios significativos nos niveis de glutamato en sangue.

Unha vez rematados estes ensaios e seleccionada a dose efectiva para a rGOT1, decidimos comparar o efecto da administración de catro doses da encima fronte a unha soa inxección. Para isto, en primeiro lugar, probáronse tres protocolos de inxección diferentes, co obxectivo de establecer cal de eles representaba unha opción máis axeitada. Unha vez seleccionado o protocolo, repetíronse os experimentos levados a cabo anteriormente, con animais sometidos a isquemias severas e moderadas e tratados con catro administracións da rGOT1. Non só a dose de 1 mg/kg volveu a demostrar a súa eficacia reducindo os volumes de infarto e mellorando a evolución neurolóxica dos animais, se non que o uso de múltiples administracións da rGOT1 potenciou o efecto terapéutico da encima, reducindo aínda máis o tamaño da lesión, tanto en animais cunha isquemia severa coma moderada. Con todo, e a pesar do claro efecto da proteína sobre a lesión isquémica, novamente non se observou ningún cambio nos niveis de glutamato en sangue, igual que ocurría no caso dos animais tratados cunha única dose da encima.

Sen embargo, cabe destacar que os efectos beneficiosos da rGOT1 sobre o infarto e o déficit neurolóxico desapareceron unha vez que a administración da proteína foi retrasada, sendo administrada dúas horas despois da reperfusión, no canto de ser inxectada tras a reperfusión. Isto pon de manifesto a importancia dunha pronta administración da rGOT1, máis tendo en conta o papel crucial que o tempo xoga na enfermidade cerebral vascular.

Por último, analizouse a actividade da GOT1 no líquido cefalorraquídeo en animais tratados con rGOT1, tanto sans coma isquémicos. Observouse que aqueles animais tratados ca encima recombinante sufriron un incremento significativo da actividade da GOT1 no líquido cefalorraquídeo, o que abre a posibilidade a unha acción directa da rGOT1 neste fluído, no canto de na sangue.

En base ós resultados obtidos dos estudos con catro administracións de rGOT1, e co gallo de mellorar a vida media en sangue da rGOT1, sintetizáronse dous bioconxugados da rGOT1. En colaboración co Prof. Marc Gauthier, do Institut National de la Recherche Scientifique, en Québec, Montreal, a rGOT1 foi modificada de dúas formas diferentes, engadíndolle polietilenglicol (PEG) ou PEG asociado a Angiopep, un péptido utilizado para aumentar a acumulación e o traspaso da proteína na barreira hematoencefálica. Ningunha destas modificacións afectou de forma notable á actividade encimática da rGOT1. En canto á farmacocinética dos bioconxugados, a utilización de PEG conseguiu alongar a vida media da rGOT1 de forma considerable, mantendo un aumento significativo da actividade da GOT1 na sangue de animais sans ata 4 días despois da súa administración, tempo que aumentou ata os 8 días no caso dos animais isquémicos. Non obstante, a adición do Angiopep non tivo ningún efecto adicional fronte usar soamente o PEG.

Con respecto ó efecto terapéutico, o uso dos bioconxugados mostrou unha maior redución nos volumes de infarto e unha

melloría máis pronunciada nos test funcionais, comparado cos animais que foron tratados ca versión nativa da rGOT1. Non só os bioconxugados tiveron un maior efecto terapéutico cando se compararon cos animais tratados cunha única dose de rGOT1, se non que tamén conseguiron unha maior redución da lesión isquémica que aqueles animais que foron tratados con catro administracións da rGOT1. Isto demostra que a acción terapéutica da rGOT1 débese máis a un efecto tempo dependente que a un efecto dose dependente. Pola contra, igual que no caso da vida media, o uso do péptido Angiopep non tivo ningún efecto a maiores sobre esta melloría. Tamén se levou a cabo un estudo dos niveis de actividade da GOT1 no líquido cefalorraquídeo de animais sans. Neste caso, aqueles animais tratados ca rGOT1 conxugada con PEG mostraron unha maior actividade encimática no líquido cefalorraquídeo, posiblemente debido a un maior tempo de residencia na sangue do bioconxugado.

A pesar de existir outras alternativas (como é o caso da tenecteplase ou a trombectomía mecánica) o rtPA segue a ser o tratamento máis empregado naqueles doentes que sofren un ictus isquémico. Polo tanto, todos aqueles tratamentos en fase de desenvolvemento, como é o caso da rGOT1, e que estean destinados a ser utilizados na mesma fiestra terapéutica que o rtPA deben de ser coidadosamente analizados co fin de detectar posibles interaccións indesexables entre ambos compostos. En primeiro lugar, realizáronse dous tipos de ensaios *in vitro*, unha dose resposta e unha cinética. Ningún dos experimentos mostrou ningún tipo de inhibición do rtPA por parte da rGOT1, do mesmo xeito que o rtPA non tivo ningún efecto sobre a actividade da rGOT1. No caso dos estudos *in vivo*, utilizáronse dous modelos diferentes de isquemia, un modelo de trombo inducido por trombina (realizado en ratos) e un modelo no que se formou un trombo utilizando sangue autóloga (realizado en ratas). En ámbolos dous casos, o uso da rGOT1 non mostrou ningún tipo de efecto prexudicial sobre a capacidade reperfusora do rtPA, demostrando a falta de interacción entre o

axente fibrinolítico e a nosa proteína recombinante. O uso das dúas terapias combinadas tampouco tivo un efecto negativo sobre a mortalidade dos animais. Inclusive, unha administración temperán (antes da reperusión) da rGOT1 mostrou unha melloría na redución dos volumes de infarto. Os datos deste estudo, xunto cos publicados anteriormente polo noso grupo, nos que se demostra que o uso da rGOT1 non aumenta o volume do hematoma no caso dos ictus hemorráxicos, abren a porta a unha posible administración prehospitalaria desta encima no caso dunha sospeita de ictus, acurtando o tempo entre o inicio do evento isquémico e a administración do tratamento, e evitando unha demora que, en moitos casos, pode ser crucial, especialmente nunha enfermidade coma o ictus, no que o tempo xoga un papel crítico.

Aínda que os análises levados a cabo durante a realización desta Tese non mostraron cambios significativos nos niveis de glutamato en sangue, a rGOT1 si mostrou un claro efecto terapéutico, tanto en relación co tamaño da lesión isquémica coma na melloría do déficit neurolóxico dos animais. Na bibliografía existen diferentes estudos que poden dar explicación a este efecto beneficioso da encima, sen a necesidade de implicar unha redución dos niveis periféricos de glutamato. Tal e como se mencionou anteriormente, ademais de na síntese e metabolismo do glutamato, a GOT, tanto na súa forma citosólica (GOT1) como mitocondrial (GOT2), ten un papel crucial na lanzadeira malato-aspartato, esencial no equilibrio redox entre a mitocondria e o citosol. A función desta lanzadeira é a de transportar os equivalentes reductores, producidos en diferentes vías metabólicas, dende o citosol cara a mitocondria, xa que a membrana mitocondrial é impermeable ás moléculas de NADH. A implicación desta lanzadeira no metabolismo enerxético e a capacidade da GOT para sintetizar intermediarios do ciclo dos ácidos tricarboxílicos (principalmente o  $\alpha$ -cetoglutarato) explicaría a capacidade da GOT de preservar o tecido fronte a isquemia. Segundo esta

hipótese, a GOT actuaría como intermediaria en situacións de estrés metabólico (como é o caso do ictus isquémico), producindo estes intermediarios do ciclo dos ácidos tricarbóxicos sen a necesidade de utilizar glucosa para a produción de enerxía, usando no seu lugar o glutamato como fonte de enerxía. Neste sentido, diversos traballos publicados, tanto na patoloxía isquémica como en cancro, demostran o importante papel que a GOT desenrola na regulación da morte celular. Ademais de este mecanismo no que a GOT serviría para reencher de intermediarios ó ciclo de Krebs (nun proceso denominado anaplerose), tamén se observou, en estudos en cancro, que o bloqueo da GOT producía un arresto das células canceríxenas na fase G1. Do mesmo xeito, este mesmo bloqueo aumentaba de forma significativa as células que sufrían ferroptose (un tipo de morte celular non apoptótica dependente do ferro). Estes mecanismos poderían explicar o efecto terapéutico da GOT observado na presente Tese, sen que estivera implicado unha redución dos niveis de glutamato en sangue.

En base ós resultados obtidos nesta Tese, pódese concluír que: a GOT1 xoga un papel crucial no ictus isquémico axudando a reducir o dano provocado pola isquemia a rGOT1 ten un efecto terapéutico sobre os volumes de infarto e o déficit neurolóxico en modelos animais de isquemia cerebral; que a bioconxugación da rGOT1 con PEG estende a vida media da proteína no sangue e potencia o efecto terapéutico da rGOT1; que o uso da rGOT1 non causa ningún tipo de interacción co rtPA nin provoca unha perda da súa capacidade fibrinolítica, polo que pode ser administrado conxuntamente con este fármaco de forma segura.

## ABBREVIATIONS



- AbGOT1:** Anti-GOT1 antibody
- ADC:** Apparent Diffusion Coefficient
- AGC:** Aspartate-Glutamate Carrier
- ALS:** Amyotrophic Lateral Sclerosis
- AMPA:**  $\alpha$ -amino-3-hydroxy-5-methyl-4-isoxazol propionic acid
- AMPAr:**  $\alpha$ -amino-3-hydroxy-5-methyl-4-isoxazol propionic acid receptors
- AST:** Aspartate Transaminase
- ATP:** Adenosine Tri-Phosphate
- AU:** Arbitrary Units
- BBB:** Blood Brain Barrier
- BTPH:** BiotechPharma UAB
- CAT:** Cysteine Aminotransferase
- CBF:** Cerebral Blood Flow
- CBS:** Cystathionine  $\beta$ -synthase
- CD:** Circular Dichroism
- CGMP:** Current Good Manufacturing Practice
- CM:** Cisterna Magna
- COX-2:** Cyclooxygenase-2
- CSD:** Cortical Spreading Depression
- CSE:** Cystathionine  $\gamma$ -lyase
- DTT:** Dithiothreitol
- EAATs:** Excitatory Amino Acid Transporters

Antonio Dopico López

**ET:** Echo Time

**FA:** Flip Angle

**FOV:** Field of View

**FPLC:** Fast Protein Liquid Chromatographer

**GABA:** Gamma-aminobutyric Acid

**GAPDH:** Glyceraldehyde 3-phosphate Dehydrogenase

**GBD:** Global Burden Disease, Injuries and Risk Factors Study

**GNG:** Glyceroneogenesis

**GOT:** Glutamate-Oxaloacetate Transaminase

**GOT1:** Glutamate-Oxaloacetate Transaminase 1

**H<sub>2</sub>S:** Hydrogen Sulphide

**HPLC:** High Performance Liquid Chromatography

**I.M.:** Intramuscular

**I.P.:** Intraperitoneal

**I.V.:** Intravenous

**ICH:** Intracerebral Haemorrhage

**iGluR:** Ionotropic Glutamate Receptor

**iNOS:** Inducible Nitric Oxide synthase

**IPTG:** Isopropyl-β-D-1-thiogalactopyranoside

**KATs:** Kynurenine Aminotransferases

**KYNA:** Kynurenic Acid

**LRP1:** Low-density Lipoprotein Receptor-related Protein 1

**Mal-PEG:**  $\alpha$ -maleimide,  $\omega$ -succinimidyl carboxymethyl ester  
PEG

**MAS:** Malate-Aspartate Shuttle

**MCT<sub>1</sub>:** Monocarboxylic Acid Transporter

**MDH1:** Malate Dehydrogenase 1

**MDH2:** Malate Dehydrogenase 2

**mGluR:** Metabotropic Glutamate Receptor

**MMPs:** Matrix Metalloproteinases

**mPEG:**  $\alpha$ -Methoxy,  $\omega$ -succinimidyl carboxymethyl ester  
poly(ethyleneglycol)

**MR:** Magnetic Resonance

**MRA:** Magnetic Resonance Angiography

**MRI:** Magnetic Resonance Imaging

**MRS:** Magnetic Resonance Spectroscopy

**MWCO:** Molecular Weight Cut Off

**NA:** Number of Averages

**NMDA:** N-methyl-D-aspartate glutamatergic

**NMDAr:** N-methyl-D-aspartate glutamatergic receptors

**nNOS:** Nitric Oxide synthase

**NO:** Nitric Oxide

**OGC:** Oxoglutarate/Malate Carrier

**PBRs:** Peripheral Benzodiazepine Receptors

**PEP:** Phosphoenolpyruvate

**PEPCK-C:** Phosphoenolpyruvate Carboxykinase

Antonio Dopico López

**PI3-Akt:** Phosphatidylinositol-3-kinase

**PLP:** Pyridoxal Phosphate

**PLP:** Pyridoxal-5'-phosphate

**PMP:** Pyridoxamine 5'-phosphate

**PSD-95:** Postsynaptic Density Protein of 95 kDa

**RBC:** Red Blood Cells

**RF:** Radio Frequency

**rGOT1:** Human Recombinant Glutamate-Oxaloacetate  
Transaminase 1

**ROS:** Reactive Oxygen Species

**RT:** Repetition Time

**SAH:** Subarachnoid Haemorrhage

**SAT<sub>1</sub>:** Glutamine System A Transporter 1

**SDF-1:** Stromal Cell-Derived Factor 1

**SE:** Status Epilepticus

**SEC:** Size-Exclusion Chromatography

**SN<sub>1</sub>:** Glutamine System N Transporter 1

**SNAREs:** Soluble N-ethylmaleimide-sensitive factor Attachment  
Protein Receptors

**STAIR:** Stroke Therapy Academic Industry Roundtable

**SUMO:** Small Ubiquitin-like Molecule

**SVZ:** Subventricular Zone

**SW:** Spectral Bandwidth

**TBI:** Traumatic Brain Injury

**TCA:** Tricarboxylic Acids

**tMCAO:** Transient Middle Cerebral Artery Occlusion

**TOF-MRA:** Time-of-Flight Magnetic Resonance Angiography

**Ulp1:** Ubiquitin-like-specific protease 1

**VEGF:** Vascular Endothelial Growth Factor

**VEGFr2:** Vascular Endothelial Growth Factor Receptor

**X<sub>c</sub>:** Cysteine/glutamate Antiporter



# INTRODUCTION



## 1.- SECTION I: STROKE

### 1.1.- Definition

The most common definition of stroke, as provided by the American Stroke Association/American Heart Association) is “a neurological deficit attributed to an acute focal injury of the central nervous system (CNS) by a vascular cause, including cerebral infarction, intracerebral haemorrhage (ICH) and subarachnoid haemorrhage (SAH), and is a major cause of disability and death worldwide”.<sup>1</sup>

Although there are different types of stroke and multiple causes, they share a few common symptoms<sup>2</sup>:

- Weakness or numbness on one side of the body.
- Vision difficulties in one or both eyes.
- Difficulty to speak or comprehend language.
- Dizziness or instability, as well as headache more intense than usual, as long as they are associated with one or more of the symptoms mentioned above.

Nevertheless, a number of strokes occurred without noticeable symptoms and imaging techniques are necessary in order to diagnosed them.

### 1.2.- Epidemiology

According to the data obtained by the Global Burden Disease, Injuries and Risk Factors Study (GBD) from 2015, over 6 million people died from cerebrovascular diseases that year, a 5.1% increase compared to the 2005 GBD. Furthermore, the data indicates there is a shift from communicable diseases, maternal

and nutritional causes towards non-communicable diseases like stroke. This shift, especially in stroke and ischaemic heart disease, is most likely due to the decrease in communicable diseases mortality and the progressive aging of the population.<sup>3</sup>

In Spain, stroke mortality represented a 6.1% (25,712) of total deaths in 2019, being stroke the main cause of death in women. Once divided by sex, the mortality rate is higher in women, being a 7.1% (14,626) and a 5.2% (11,086) on men.<sup>4</sup> Despite the fact that mortality due to stroke has decreased over the years, different studies had shown a mortality rate of 39-60% within the first five years, being specially high early after stroke, when 8-22% of the deaths occur.<sup>5</sup>

Regarding hospitalization, the average length of hospital stay for stroke patients is 13.6 days. After hospitalization, up to 53% of stroke patients present some kind of disability after 6 months<sup>6</sup> and this percentage is only reduced to a 41.5% after a year.<sup>7</sup> Due to this, stroke has become the most common cause of complex disability in adults and one of the leading causes of disability-adjusted life-years.<sup>8</sup>

Besides the personal cost, stroke entails a huge economic burden. Yebenes *et al.*, in an observational, prospective multicentre study, estimated that the cost for each stroke patient in 2017 was 27,711 € during the first year.<sup>9</sup> According to the Sociedad Española de Neurología, in 2019 the incidence of stroke in Spain was 187.4 cases per 100,000 people, making a total of 71,780 new cases of stroke,<sup>10</sup> implying a total cost of about 1,989 million euros. Different studies show the distribution of this expenditure: 46% of the cost on the first year is because patients' follow-up<sup>11</sup> and 86.5% is due to outpatient treatment.<sup>12</sup> Nevertheless, most of the cost is not direct health related but informal care and social cost programs, among others, which become more important during the following years after stroke, representing a 58.3% of the total cost during

the first years and increasing up to a 72.4% after the second year.<sup>13</sup>

### 1.3.- Classification

There are two main types of stroke, depending on the nature of the lesion: haemorrhagic and ischaemic stroke. Nevertheless, this two large groups can be further divided (**Figure 1**) based on different parameters as progression profile, neuroimaging characteristics, stroke subtype, lesion size, location of the lesion, mechanisms and aetiology.<sup>2</sup>

#### 1.3.1.- HAEMORRHAGIC STROKE

Haemorrhagic stroke represents only 15% of total strokes and it is associated with a high mortality rate. This type of stroke is caused by a non-traumatic rupture of a blood vessel, leading to a bleeding into the ventricular space or the brain parenchyma. The accumulation of blood inside the cranium provokes an increase of the intracranial pressure and cell toxicity due to some of the blood components, which leads to necrosis of the affected area and a global stress for the brain. There are different causes of haemorrhagic stroke, being the most common arterial hypertension, anticoagulant treatments or amyloid angiopathy. Other possible causes are vascular malformations, toxics, drugs, brain vasculopathies, tumours and haematological diseases, among others.<sup>14</sup>

#### 1.3.2.- ISCHAEMIC STROKE

Is the most common type of stroke, representing 85% of all stroke cases. In this case, the cerebrovascular event occurs due to an impairment of the fibrinolysis-coagulation equilibrium and other metabolic cycles, which leads to a blockade of a vessel, most commonly because of the presence of a clot. This prevent

the blood for reaching the vascular territory irrigated by this vessel.

There are different subtypes of ischaemic strokes depending on aetiology, size and the vascular territory affected, among others<sup>15,16</sup>. The most common classification for ischaemic strokes is as follows: large-artery atherosclerotic, cardioembolic, lacunar, other aetiology and unknown or undetermined aetiology.

- **Atherosclerotic stroke:** also called large-artery stroke, it represents around 20% of ischaemic strokes. Patients show a significant stenosis (>50%) or an occlusion of a major brain artery due to atherosclerosis. It appears with cortical, brain stem or cerebellar symptomatology and it can be seen in neuroimaging studies when large lesions are present.<sup>15,16</sup>
- **Cardioembolic stroke:** its cause is an embolus originated and released from the heart and it accounts for 20% of the ischaemic strokes. Symptomatology and neuroimaging are similar to atherosclerotic strokes but the diagnosis is based on the presence of cardiac risk factors related with embolism (atrial fibrillation, atrial thrombus, recent myocardial infarction, mechanical prosthetic valve, etc.).<sup>15,16</sup>
- **Lacunar stroke:** or small-artery strokes, are the 25% of total strokes. They are provoked mostly by micro-atheromatosis and lipohyalinosis, although cardiac embolism, arterial embolism, infectious arthritis or prothrombotic states can also cause lacunar strokes. The most defining characteristic is their small size (between 3 and 20 mm in diameter) and localization in the penetrating arterioles territory.<sup>15,16</sup>

- **Stroke of other aetiology:** these are strokes of uncommon aetiologies, like arterial dissection, non-atherosclerotic vasculopathies or hematologic disorders. They represent only 5% of ischaemic strokes.<sup>15,16</sup>
- **Stroke of undetermined aetiology:** 30% of ischaemic strokes belong to this category. They present medium or large size lesions with two or more potential aetiologies or an unknown origin.<sup>15,16</sup>

This classification is not made based only on aetiological parameters, rather than being constituted as a useful tool for daily clinical practice, allowing physicians to treat patients more efficiently based on stroke subtypes.

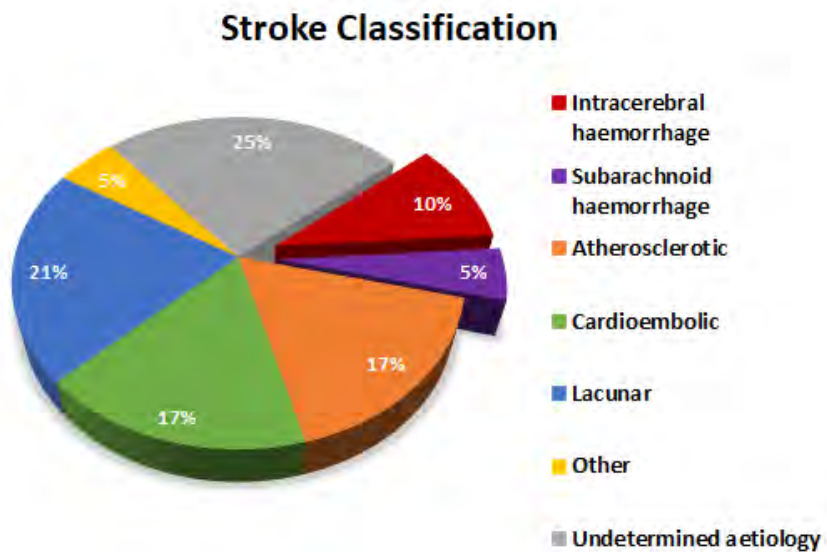


**Figure 1.** Classification and percentage of the different stroke subtypes.<sup>15,16</sup>  
Self-created image.

## 1.4.- Risk factors

There are several risk factors related to stroke, which can be divided in two major groups, modifiable and non-modifiable.

### 1.4.1.- NON-MODIFIABLE RISK FACTORS

The non-modifiable risk factors associated with stroke are three:

- **Age:** one of the most important risk factors in stroke. Age is exponentially correlated with incidence of stroke, reaching its maximum values after 65 years old.<sup>17</sup>
- **Sex:** there is a correlation between sex and stroke incidence, being higher in men.<sup>18</sup>
- **Race:** there are differences in stroke subtypes depending on the race. Large-vessels strokes affect more to Caucasian while small-vessels strokes are more common in Africans and Asians.<sup>17</sup>

### 1.4.2.- MODIFIABLE RISK FACTORS

Several modifiable risk factors are associated with stroke incidence:

- **Systemic hypertension:** the major risk factor both in ischaemic and haemorrhagic stroke. Both systolic and diastolic hypertension increase the risk of stroke, even with moderate values. For values of 140-160 mm Hg in systolic and 90-94 mm Hg in diastolic, for example, the risk of having a stroke increases 1.5 fold.<sup>19,20</sup>
- **Cardiopathy:** most heart diseases are associated with the incidence of stroke, especially atrial fibrillation,

valvulopathies, left ventricular hypertrophy, myocardial infarction and cardiomegaly.<sup>19,20</sup>

- **Hyperlipidaemia:** it is related to the development of ischaemia and atheromatosis, both coronary and carotid.<sup>19,20</sup>
- **Diabetes mellitus:** its influence is higher in women, increasing the risk of suffering a stroke by 2.2-fold, contrary to the 1.8-fold in men. The link between stroke and diabetes resides in the influence of the latter in atherosclerosis development.<sup>19,20</sup>
- **Smoking:** Tobacco consumption increases the chance of having a stroke by predisposition to develop atherosclerosis, both in men and women. Smoking facilitates endothelial damage and arterial spasms. This increased risk due to smoking disappears only after five years of abstinence.<sup>19,20</sup>
- **Other factors:** besides the risk factors mentioned above, there are several others which can increase the incidence of stroke to a greater or lesser extent, as sedentarism, night snoring, obesity, alcoholism or oral contraceptives for example.<sup>19,20</sup>

### 1.5.- Pathophysiology of Ischaemic Stroke

As described above, an ischaemic stroke occurs after the blockade of a brain vessel due to a variety of causes. This leads to a focal ischaemia, a sudden reduction of blood flow in the irrigated area. However, this reduction is not homogeneous and varies depending on different factors, like the occluded vessel, collateral irrigation or the type of occlusion.<sup>21</sup>

A gradient of blood flow reduction can be distinguished in the ischaemic region, being greater the closer the tissue is to the affected vessel. The most affected area, called **ischaemic core**, is the closest to the occluded vessel, while in the surrounding tissue, called **ischaemic penumbra**, the ischaemia is less severe due to the compensation of blood flow provided by collateral arteries.<sup>22</sup> Two major factors determine the severity of the ischaemia, the level of the artery occlusion and the time of the occlusion. Due to the latter, the duration of the blood flow reduction is of utmost importance.

During the ischaemic event, a series of molecular changes and processes occur in the short and long term. These events (**Figure 2**) start with an energetic failure because of a shortage in oxygen and glucose in the affected area of the brain and the following interruption of oxidative phosphorylation and consequently, the insufficient production of adenosine triphosphate (ATP).

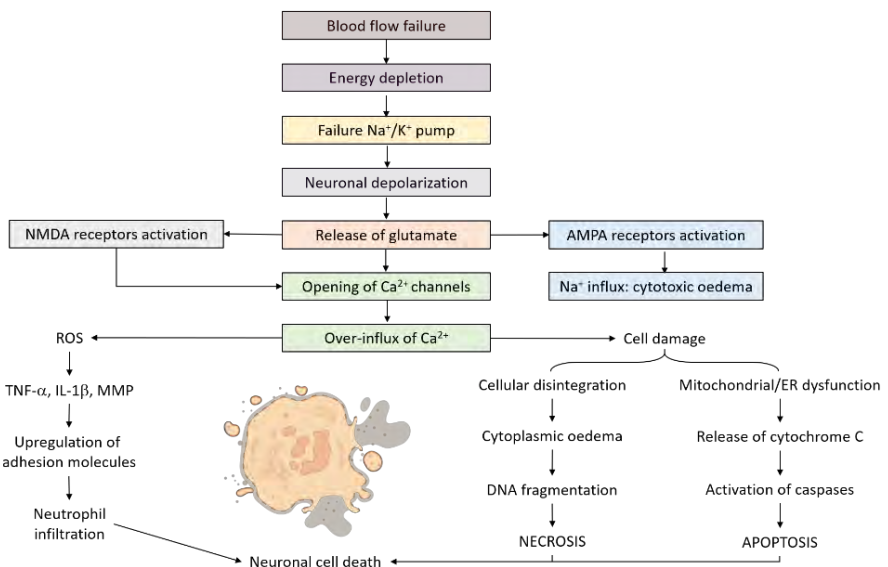


**Figure 2.** Physiopathological events following cerebral ischaemia. Self-created image.

The key event in the physiology of ischaemia is the depolarization of the cellular membrane. This occurs due to failure of ATP-dependant pumps, especially sodium-potassium-ATPase pump and it is particularly important in cell death inside the ischaemic core.<sup>23</sup> After the pumps failure, neurons and glial cells undergo a massive entrance of sodium, chloride and water into the cytoplasm<sup>24</sup> and an exit of potassium, inducing an increment of its extracellular levels and the depolarization of these cells.<sup>25</sup> Due to the energetic failure and the consequent ionic changes, there is an huge increase of extracellular glutamate, which leads to a hyperexcitability of N-methyl-D-aspartate glutamatergic receptors and  $\alpha$ -amino-3-hydroxy-5-methyl-4-isoxazol propionic acid receptors, followed by an increase of the intracellular calcium (**Figure 3**).<sup>26-28</sup> **Due to the central role glutamate plays in this Thesis, its implications in ischaemic stroke will be further discussed in a later section.**

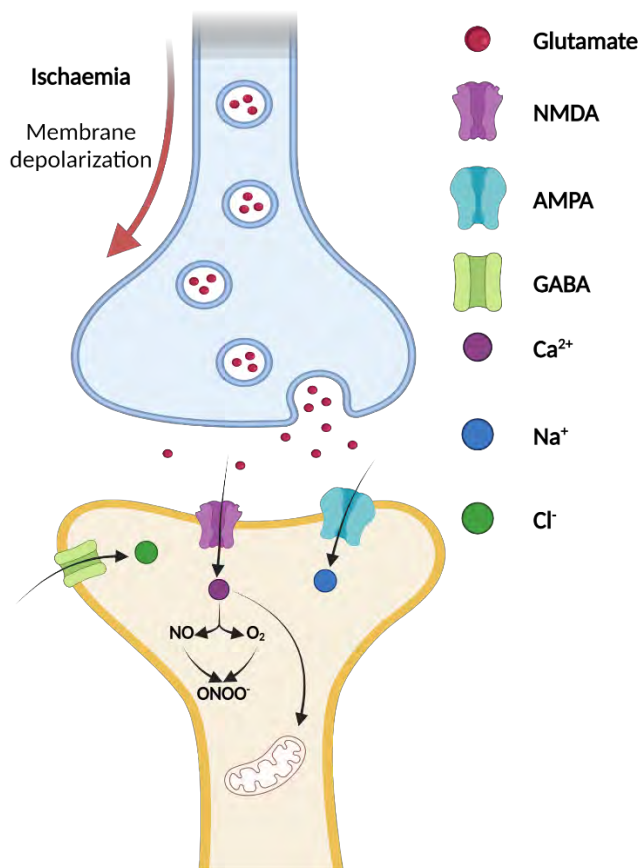


**Figure 3.** Stimulation of AMPA and NMDA receptors by glutamate during ischaemia. Self-created image using BioRender software.

However, this calcium increase is not only dependant on the activation of these receptors but also on the stimulation of the calcium voltage-dependant channels. These two events lead to a depolarization of the cell membrane and an increase of the energetic cost since the cell tries to repolarize itself.<sup>22,29,30</sup> Besides the increase of calcium, peri-infarct depolarization and acidosis are the starters of tissue damage. After the initial damage, inflammation and apoptotic processes continue to extent the lesion size.<sup>28,31</sup>

Along with these processes, another molecular event that play a major role in ischaemic damage is the generation of free radicals, especially during the artery reperfusion phase. Free radicals are highly reactive species produced both during early and late phases of ischaemia through several mechanisms. The most important radicals in brain ischaemia are reactive oxygen species (ROS), produced either through metabolic pathways of arachidonic acid or activity of neuronal Nitric Oxide (NO) synthase (nNOS) during the first stages of ischaemic stroke. After this first stage, ROS are produced mostly via to neutrophils infiltration into the affected area. Finally, at the later stages of ischaemia, ROS are produced due to the synthesis and activation of inducible NO synthase (iNOS) enzymes and cyclooxygenase-2(COX-2).<sup>32,33</sup>

All the events described above lead to the final cell death and the consequent neuronal damage. Cell death can occur through two different mechanisms, **necrosis** and **apoptosis (Figure 4)**, being the first the most common one.<sup>34</sup> Acute energetic failure is responsible for necrosis, which take place mainly in the lesion core. This kind of cell death is characterized by quick morphological changes and cell lysis. The cellular components released because of cell lysis lead to inflammatory processes that further expand tissue damage.<sup>35</sup> Apoptosis, on the other hand, takes place in the ischaemic penumbra and it is a cell response to energy-dependant mechanisms that lead to cell degradation and death.<sup>31,36</sup>

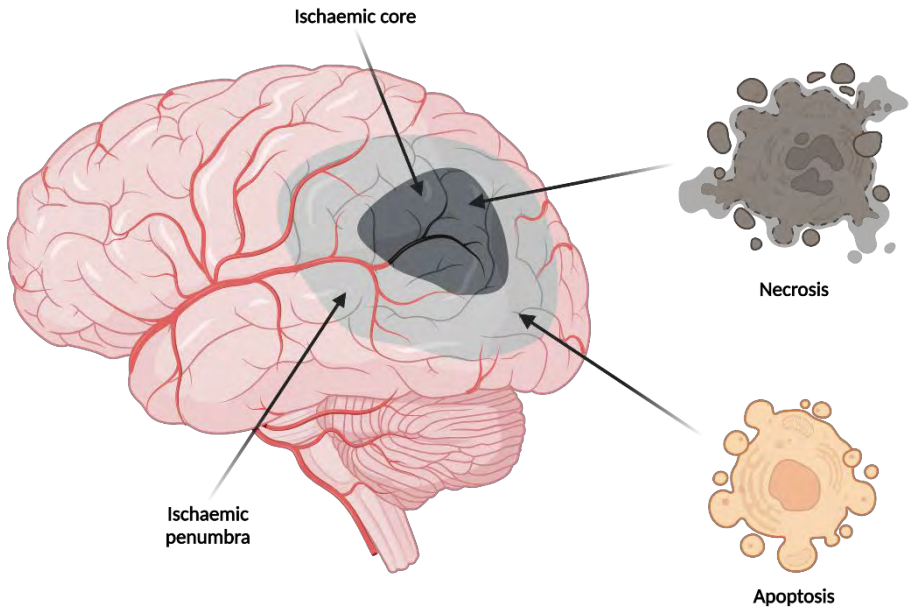


**Figure 4.** Representation of ischaemic core and penumbra and the cell death types associated with each of the ischaemic regions. Self-created image using BioRender software.

## 1.6.- Therapeutic Approaches for Ischaemic Stroke

Since ischaemia is a common cause of mortality and disability, different therapeutic approaches have been developed throughout the years in order to assess this pathology. These strategies can be divided in three major groups: recanalization therapies, neuroprotection and neurorepair.

### 1.6.1.- REPERFUSION THERAPIES

There are two different approaches regarding reperfusion therapies, **pharmacological thrombolysis** or **mechanical thrombectomy** (Figure 5), both focused in removing the

occlusion of the affected artery during the early stages of stroke. In regard to pharmacological thrombolysis, the most common thrombolytic agent is the recombinant tissue plasminogen activator (rtPA), a recombinant version of tPA (enzyme involved in the conversion of plasminogen to plasmin), which is used in order to degrade the clot occluding the affected vessel. Despite rtPA being the most common pharmacological fibrinolytic in clinical use (also called *alteplase* in its commercial name), different modifications of this molecule have been developed in order to overpass some of its disadvantages. This is the case of *demoteplase*, *tenecteplase* and *reteplase*, developed by modifying or removing some of rtPA domains.<sup>37</sup>

On the other hand, mechanical thrombectomy is a minimally-invasive procedure designed to physically remove the thrombus using a mechanical device. In brief, an interventional radiologist inserts a catheter into an artery distal to the site of the thrombus. Aided by radiological techniques, the catheter is then guided through the patient's arteries until reaching the clot's localization. Then, the thrombus is removed using a stent retriever using the catheter as a guide. Nowadays, advanced endovascular recanalization technology based on the use of mechanical catheters has significantly improved the recanalization rates, showing a better overall outcome in treated patients. However, this mechanical therapy is effective when stroke events are caused by a large vessel occlusion, which represents less than 30% of the patients. Moreover, in occlusions located in small vessels, where the rtPA has a successful recanalization rate, the efficacy of mechanical thrombectomy is also limited. In addition, some clinical trials have shown that pre-treatment with intravenous rtPA provides additional benefits to patients undergoing mechanical thrombectomy. These evidences reflect that rtPA thrombolysis remains the gold standard treatment for acute stroke.<sup>38</sup>

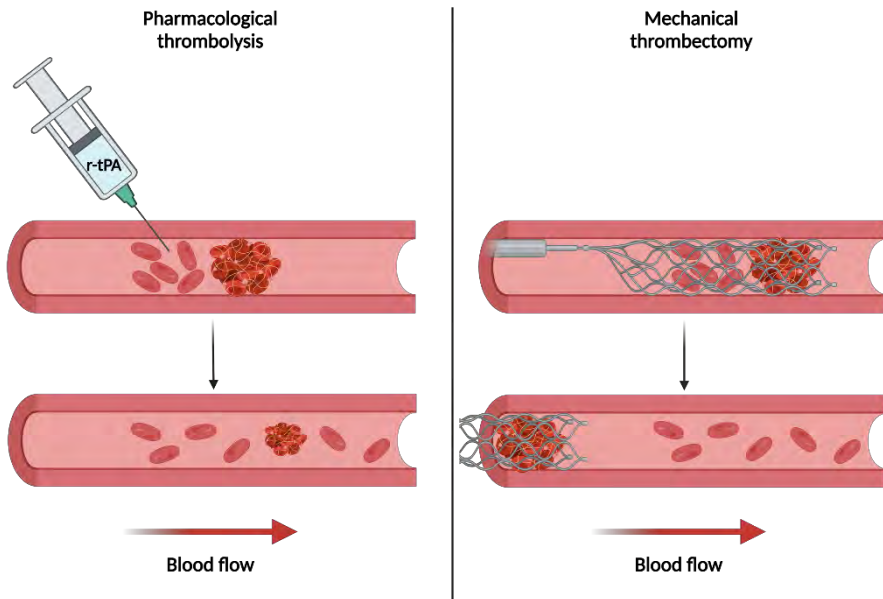


**Figure 5.** Recanalization therapies in ischaemic stroke. Self-created image using BioRender software.

Although these therapies have reduced mortality rates and disability in stroke patients, studies show that the number of patients who benefit for these treatments is very low. For pharmacological thrombolysis, only a small number of patients arrive within the therapeutic window of rtPA and only a 45-50% are eligible for the treatment.<sup>39</sup> The situation is even more daring looking at recanalization rates. According to a meta-analysis, after intravenous administration of rtPA, only a 46.2% of treated patients underwent successful recanalization.<sup>40</sup> In the case of mechanical thrombectomy, although the recanalization rates are higher than those in pharmacological thrombolysis, the small number of patients eligible for this treatment (10%) makes that the total amount of patients who benefit from this therapy even less.<sup>41,42</sup> The reason behind these reduced numbers is the existence of different factors, including the narrow therapeutic

window and high risk of haemorrhage transformation. The development of neuroprotective approaches requires to work addressing both problems, trying to widen the therapeutic window and reducing the risk factors. One way of extend the therapeutic window is by developing new parameters to select patients eligible for recanalization with rtPA, for example, including candidate patients with a large ischaemic penumbra.<sup>43</sup>

### 1.6.2.- NEUROPROTECTION

Neuroprotection is a wide term, encompassing a set of different strategies focused in reducing cell death with or without addressing reperfusion. A variety of molecules have been developed in order to stop the ischaemic damage by focusing different steps of the ischaemic cascade. Despite of its success in experimental studies and promising results, none of them showed positive results in clinical trials so far.<sup>44</sup> An overview of recently finished (**Table 1**) and ongoing (**Table 2**) clinical trials for neuroprotective agents is depicted below.

Despite of the huge number of studies and the variety of compounds used, neuroprotective drugs can be classified into different groups regarding their mechanism.

Agent	Trial Name	Trial No./Phase/ Location	Time of intervention (post-stroke)	Proposed mechanisms of neuroprotection
Human urinary kallidinogenase (HUK)	-	NCT03431909 Phase IV China	Within 72 hours	Anti-oxidative and anti-inflammatory agent
Statins	ASSORT	NCT02549846 Phase IV Japan	Within 24h of admission; Atorvastatin (20 mg), or Pitavastatin (4 mg) or Rosuvastatin (5 mg)	Pleiotropic effect with anti-inflammatory and anti-oxidant activity; reduces BBB dysfunction and enhances cerebral blood flow
	NeuSTART2	NCT01976936 Phase II USA	Withing 0 to 24h of symptom onset; Lovastatin-640 mg/day for 3 days	
Edavarone	-	NCT02430350 Phase III China/Japan	Every 2 hours for 2 weeks (37.5 mg/dose)	Potent anti-oxidant with other neuroprotective properties
NA-1 (nerinetide)	ESCAPE	NCT02930018 Phase III Canada & USA	As soon as they meet the enrollment criteria, withing 2h (2.6 mg/kg)	Targets NMDA receptor mediated excitotoxicity
3K3A-APC	RHAPSODY	NCT02222714 Phase II USA	Within 30 min to 120 min of r-tPA infusion or mechanical thrombectomy; q12h, 5 doses in 3 days; (120 ug, 240 ug, 360 ug or 540 ug/kg)	Anti-inflammatory agent that also supresses intracerebral haemorrhage
GM602	GMAIS	NCT01221246 Phase II USA	Within 18h; three consecutive daily doses (320 mg or 480 mg)	Multi-target drug with anti-inflammatory, anti-oxidative and anti-apoptotic properties
Natazulimab	ACTION2	NCT02730455 Phase II Europe & USA	Within 9h or 9-24h Dose - 300 or 600 mg, IV	Anti-inflammatory agent
Vinpocetine	-	NCT02878772 Phase II China	Between 4.5h to 48h after symptom onset and 1h (30 mg)	Cerebra vasodilator with anti-oxidative and anti-inflammatory properties

**Table 1.** Recently finished clinical trials for neuroprotective agents. Self-created image using data from Candelario-Jalil *et al.*<sup>45</sup>

Agent	Trial Name	Trial No./Phase/Location	Time of intervention (post-stroke)	Proposed mechanisms of neuroprotection
Ginkgolide	GIANT	NCT03772847 Phase IV China	To be administered along with r-tPA	Reduces BBB permeability, ER stress, inflammation and oxidative stress
Butylphthalide (NBP)	-	NCT03394950 Phase IV China	Within 4.5h; infusion for 14 days; 25 mg/day	Reduces oxidative damage, inflammation, apoptosis and mitochondrial dysfunction
	EBCAS	NCT03539445 Phase III China	Within 6h: 100 mL twice/day for 14 days; 60 mg/day from day 15 to day 90	
	-	NCT02905565 Phase II USA	Within 12h for 30 days, 800 mg/day	
BIIB093 (IV Glibenclamide)	CHARM	NCT02864953 Phase III USA	Bolus within 10h followed by continuous intravenous infusion for 72h	Reduces oedema and inflammation
HLCM051 (Multi Stem)	MASTERS-2	NCT03545607 Phase III USA	Within 18-36h; 1.2 billion HLCM051 cells	Reduces peripheral inflammatory response
	TREASURE	NCT02961504 Phase II/III Japan	Within 18-36h; 1.2 billion HLCM051 cells	
Imatinib	-	NCT03639922 Phase III Sweden	Within 8h; for 6 days; 800 mg/day	Ameliorates neuroinflammation by preserving BBB integrity
Exenatide (GLP-1R antagonist)	TEXAIS	NCT03287076 Phase II Australia	Within 9h; 5 ug, twice daily for 5 days	Reduces oxidative stress, inflammation and oedema
JPI-289 (Amelparib)	-	NCT03062397 Phase II Korea	Within 24h (low or high dose)	Attenuates NAD and ATP depletion, mitochondrial dysfunction and immune response
Neu2000	SONIC	NCT02831088 Phase II Korea	Within 8h (750 mg); nine follow-up infusion at 12h intervals (500 mg)	NR2B-selective NMDA receptor antagonist and antioxidant
Remot ischemic conditioning (RIC)	RIC-ACS	NCT03868007 China	Within 4h, twice daily for 14 days	Triggers anti-oxidative, anti-inflammatory, and mitochondria modulatory protective effects
	RICAMIS	NCT03740971 China	Within 48h, twice daily	
	RESIST	NCT03481777 Denmark	After 6h, twice daily for 7 days	
	REMOTE-CAT	NCT03375762 Spain	Within 8h, prehospital setting – single treatment	

**Table 2.** Currently ongoing clinical trials for neuroprotective agents. Self-created image using data from Candelario-Jalil *et al.*<sup>45</sup>

### 1.6.2.1.- Calcium Blockers

As explained in the previous section, calcium plays a major role in cell death during ischaemia. Therefore, blocking calcium channels stops the intake of calcium by neurons and reduces cell death. One example of this strategy is nimodipine. There are hundreds of studies using ***nimodipine*** as an ischaemic stroke treatment but only a few have shown positive results.<sup>44</sup> Similar to ***nimodipine***, none of the drugs aimed to block calcium intake have demonstrated a clear neuroprotective effect on clinical trials. One of the most important reasons for this is the fact that, in most of the studies with positive results, animals were treated in a very short time window (normally within the first 15 minutes after ischaemia) which is almost impossible to translate to clinical practice.

### 1.6.2.2.- Glutamate antagonists

Another molecule that plays a very important role during the ischaemic event is glutamate. Besides its role as the major excitatory CNS neurotransmitter, its capability of inducing an excitotoxic effect during ischaemia has made it an important target in neuroprotection studies. Most of the strategies focus on glutamate are aimed at its interactions with neuronal receptors, specially NMDA and AMPA receptors.<sup>46</sup>

Contrary to calcium blockers, NMDA antagonists have shown beneficial effects regarding infarct volume and neurological deficit. Nevertheless, the side effects linked to their use have made them non-viable once on clinical trials. For example, a competitive antagonist of NMDA receptors, ***selfotel***, showed outcome improvement and no significant increase of mortality in a phase III clinical trial but the high incidence of adverse psychiatric effects forced its withdrawal from clinical phases. Another example, ***dextromethorphan*** and its metabolites,

*dextrorphan* and *aptiganel*, were discontinued because of an unfavourable balance between risk and benefit and their adverse side effects. On the other hand, *eliprodil* and *gavestinel*, showed no side effects and great tolerance, but no efficacy.<sup>47</sup>

Several AMPA antagonists had positive results in preclinical phase, both for focal and global ischaemia, but they were not successful in clinical trials.<sup>46</sup>

### 1.6.2.3.- Antioxidants

As mentioned before, the production of ROS and oxidative stress are two mechanisms deeply involved in ischaemic damage. Due to this, different antioxidants drugs have been developed and tested for ischaemic stroke treatment. The best example of this kind of compounds is *NXY-059*, which reduced the lesion size by 66% in preclinical studies and had a wide therapeutic window, up to 5 hours. It showed positive results in a first clinical trial by improving functional outcome in patients, but failed to show the same results in a second trial.<sup>48</sup>

Similar to *NXY-059*, *uric acid* showed promising results in preclinical studies. Nevertheless, a clinical trial aimed to assess its neuroprotective capacity by measuring functional outcome at 90 days showed no side effects but no improvement compared to placebo.<sup>49</sup>

### 1.6.2.4.- Phospholipid Precursors

*Citicoline*, also called *CDP-choline*, is a precursor during the synthesis of phosphate-choline, a component of neuron cell membrane. *Citicoline* also inhibits dopamine and norepinephrine levels at CNS level and is able to restore ATPase activity in mitochondrias.<sup>50</sup> In preclinical studies, citicoline reduced oxidative stress after brain ischaemia by lowering phospholipase 2 activation, therefore reducing arachidonic acid

levels and the production of free radicals. It also seems to be involved in excitotoxicity reduction and promoting brain plasticity.<sup>51</sup> *Citicoline* improved functional outcomes at 28 days in preclinical studies when administered after reperfusion.<sup>52</sup> A pool-data analysis showed a significant increment in complete recovery after mild or severe stroke when the treatment was started within the first 24 hours and maintained for 6 weeks,<sup>53</sup> but a later clinical trial did not show protective effect in stroke patients.<sup>54</sup>

#### 1.6.2.5.- Inhibitors of Glutamate Release

These neuroprotective drugs work by blocking presynaptic channels, preventing membrane depolarization and glutamate release. **Lubezol**, a drug capable of deregulate glutamate induced nitric oxide synthase pathway, has shown hippocampal neuroprotection from nitric oxide toxicity. In preclinical studies, it showed a 50% infarct reduction with a therapeutic window of 3 hours after ischaemia onset. However, clinical trials showed no improvement and one of them had to be cancelled due to an increment in mortality.<sup>55</sup>

#### 1.6.2.6.- GABA Agonists

These drugs are aimed to upregulate the activity of GABA, the major inhibitory neurotransmitter in the brain and prevent cellular depolarization. **Clomethiazole** showed no result in two different studies involving patients suffering total anterior circulation infarcts.<sup>56</sup> **Maxipost**, another GABA agonist which produces hyperpolarisation by opening potassium channels, also failed to show beneficial results in clinical trials.<sup>46</sup>

### 1.6.2.7.- Anti-inflammatories

Anti-inflammatory molecules work by inhibiting different steps of the inflammatory response during ischaemia. **Enlimomab**, a monoclonal antibody against ICAM-1, was able to reduce infarct size in preclinical studies by inhibiting leukocyte adhesion and migration through vascular endothelium. Nonetheless, a phase III study not only did not show no beneficial results but also had a high number of complications. On the other hand, UK-279276, an inhibitor of CD11b/CD18 receptor showed a very low efficacy.<sup>44</sup>

### 1.6.2.8.- Other compounds

Besides the aforementioned studies, there is a plethora of compounds focused on different neuroprotective strategies, like membrane fluidity modifiers (**Piracetam**), opioid antagonists (**Namefene**), neuronal potassium channel activators (**BMS-204352**), growth factors acting as intracellular calcium regulators and several others. Same as before, none of them showed enough efficacy as neuroprotective agents in order to be used in clinical practice.<sup>46</sup>

### 1.6.3.- NEUROREPAIR

Contrary to recanalization therapies and neuroprotective agents, neurorepair strategies work in the late stages (days or weeks after) of ischaemic stroke. They are aimed either to regenerate damaged tissue (neuroregeneration) or to establish new synapses and neuronal pathways capable of substituting the ones lost. Neurorepair therapies aim to recover the neurovascular unit by enhancing synaptogenesis and angiogenesis processes. Same as neuroprotection, despite of the huge number of different strategies, they can be divided in a few major groups according to their mechanism of action.<sup>57</sup>

### 1.6.3.1.- Neurogenesis

Despite the low replacement rate compared with other cell lines, the production of neural stem cells continues in adult brain, localized in the dentate gyrus of the hippocampus and, mostly, in the subventricular zone of the lateral ventricles (SVZ).<sup>58</sup> In normal conditions, neuroblasts produced in the SVZ migrate to the olfactory bulb before differentiating into new neurons. After focal brain ischaemia onset in rat, the formation of neuroblasts increases and they migrate towards the surrounding regions of the lesion instead to the olfactory bulb.<sup>57</sup> This mechanism was also demonstrated in humans.<sup>59</sup>

Although the increase of neuroregeneration after an ischaemic insult is well known, most of the new neural stem cells are not able to integrate into neuronal circuits after their differentiation. The idea behind most neuroregenerative strategies is to enhance this endogenous neurogenesis and thus increase the probability of survival and integration in neural networks, improving functional recovery. In order to do this, both pharmacological and cellular therapies have been developed, for example, the activation of the phosphatidylinositol-3-kinase (PI3-Akt) pathway. PI3-Akt is involved in cell proliferation, differentiation, migration and survival.<sup>60</sup>

### 1.6.3.2.- Angiogenesis

Another neurorepair strategy is focused on the vascular component of the neurovascular unit. In adults, the proliferation of endothelial cells stops under normal physiological conditions. Nevertheless, after an ischaemic insult, proliferation of brain capillaries around the damaged tissue begins and new vessels are formed after 2-28 days since ischaemia.<sup>61-64</sup>

Angiogenesis occurs in different steps from endothelial cell proliferation and migration, tubule formation, branching and

finally, anastomosis. The process is started by Vascular Endothelial Growth Factor (VEGF) and its receptor VEGFr2. Later, angiopoietin 1 and 2 and their receptor TIE-2 are responsible for maturation, stabilization and vascular remodelling.<sup>65</sup> VEGF and VEGF2 promote vascular ramification, forming highly permeable vessels. Fully developed blood vessels are formed through vessel maturation promoted by angiopoietins and their receptor, TIE-2. Strategies focused on angiogenesis are developed in order to improve blood vessel formation around infarct region, either by using VEGF or by increasing the expression of VEGF, VEGF2, angiopoietins or TIE-2.<sup>65</sup>

This angiogenic process is of utmost importance for brain recovery after an ischaemic insult. Both cellular and pharmacological approaches have been used in preclinical studies in order to increase angiogenesis after brain ischaemia, achieving functional recovery.<sup>66</sup>

### 1.6.3.3.- Neurogenesis and Angiogenesis

In spite of the existence of therapeutic agents addressing neurogenesis or angiogenesis alone, they are not isolated processes during brain ischaemia recovery, that is why some strategies have been developed aiming both pathways. Angiogenesis is indispensable for neurogenesis in peri-infarct area, since its responsible for restoring energy and oxygen supply. Also, endothelial cells release growth factors which increase neurons survival and regulate metabolic activity of neural precursors. Among these growth factors are Stromal Cell-Derived Factor 1 (SDF-1), VEGF and Matrix Metalloproteinases (MMPs). These factors induce and facilitate neural stem cells to migrate to the injured site. Furthermore, neural progenitor cells increase angiogenesis by overexpressing angiopoietin 2 and VEGFr2.<sup>67</sup>

Both *in vitro* and *in vivo* studies have shown the relation between both processes.<sup>67,68</sup> For example, TIE-2 inhibitors reduce

angiogenesis, as expected, but they also interfere with neuroblasts migration to peri-infarct area. On the other side, grafting neural progenitor cells into the affected area induces angiogenesis. These studies show the interconnection between angiogenesis and neurogenesis and the importance of controlling both during ischaemia recovery.<sup>69,70</sup>

#### 1.6.3.4.- The Role of Oligodendrocytes, Astrocytes and Axons in Neurorepair

Despite neurons being the main focus of both neuroprotective and neurorepair strategies, other cell lines and cellular components have been addressed, as they are involved in neurorepair as well. Astrocyte proliferation, for example, occurs after an ischaemic insult. Astrocytes proliferate and surround the lesion area, forming a glial scar and releasing proteoglycans that inhibit axonal growth. Consequently, some strategies are aimed to reduce glial scar formation and stimulate axonal growth.<sup>71</sup> On the other hand, oligodendrocytes are a cell line especially vulnerable to brain ischaemia and are responsible for myelination in CNS, an essential process for the correct functioning of neurons. Due to this, several strategies have been developed in order to increase oligodendrocytes survival, using AMPA (*topiramate*, *SPD502*) or NMDA (*MK801*, *memantine*) antagonists, antioxidants (*edaravone*, *ebiselen*) or antiapoptotic agents (*IGF-1*, *estradiol*), among others.<sup>72</sup>

## 2.- SECTION II: GLUTAMATE AND EXCITOTOXICITY

### 2.1.- Glutamate

Glutamate is an  $\alpha$ -amino acid and the most abundant excitatory neurotransmitter in vertebrates. It is also considered to be involved in almost all aspects of normal brain function, including cognition, memory and learning. Furthermore, it plays a major role in CNS development, including synapse induction. Glutamate is also involved in signalling in peripheral organs and tissue as well as endocrine cells.<sup>73</sup>

Despite the huge amount of glutamate present in the brain (around 5-15 mM/kg of wet weight, depending on the region)<sup>74</sup>, only a very small fraction is present in extracellular space. Under normal conditions, glutamate is stored mainly intracellularly.<sup>75</sup> In extracellular fluid and plasma, normal concentration for glutamate is about 1-10  $\mu$ M and 40-60  $\mu$ M, respectively.<sup>76,77</sup> Nevertheless, glutamate concentration and distribution is highly sensitive to energy supply changes and its dynamic equilibrium can change quickly.

### 2.2.- Compartmentalization

In the brain, glutamate appears in three different locations: extracellularly (in a very low concentration) and as a free amino acid divided both in astrocytes and neurons.<sup>78</sup> In astrocytes, it appears as an only separated pool that is quickly converted into glutamine. On the other hand, in neurons there are two or more pools, located either in the neuronal dendrites and soma or in vesicles in the neuron terminals. When a nerve impulse reaches a neuron, it triggers glutamate release from the presynaptic neuron into the synaptic cleft, where it binds to glutamate

receptors on the postsynaptic neuron, transmitting the nerve impulse. Neurotransmission is ended by neurons and astrocytes when they uptake glutamate from the synaptic cleft. Only a tiny fraction of glutamate is believed to be able to escape this uptake and diffuse from the synapse.<sup>79-81</sup>

## 2.3.- Glutamate Transporters

### 2.3.1.- EXCITATORY AMINO ACID TRANSPORTERS

Excitatory amino acid transporters (EAATs) are polypeptides between 500-600 amino acids and exhibit 50-60% homology between the 5 described subtypes to date. Their topology consists of six to eight transmembrane domains, one to two re-entrant loops and both C and N terminal are cytoplasmic.<sup>82</sup>

The complete glutamate transport and the reset of the transporter (**Figure 6**) consists on different stages, each linked to a conformational change. The first stage begins with the recruitment of one molecule of glutamate, three sodium ions and one proton from the extracellular space. The binding of these substrates triggers a conformational change of the receptor from its outward-facing conformation to the inward-facing one. After the EAATs conformational change, cargo is released and the second stage begins. In this step, a potassium ion from the cytoplasm binds to the receptor, which returns to its outward-facing conformation, releasing the potassium into the extracellular space and starting the cycle again.<sup>83</sup>

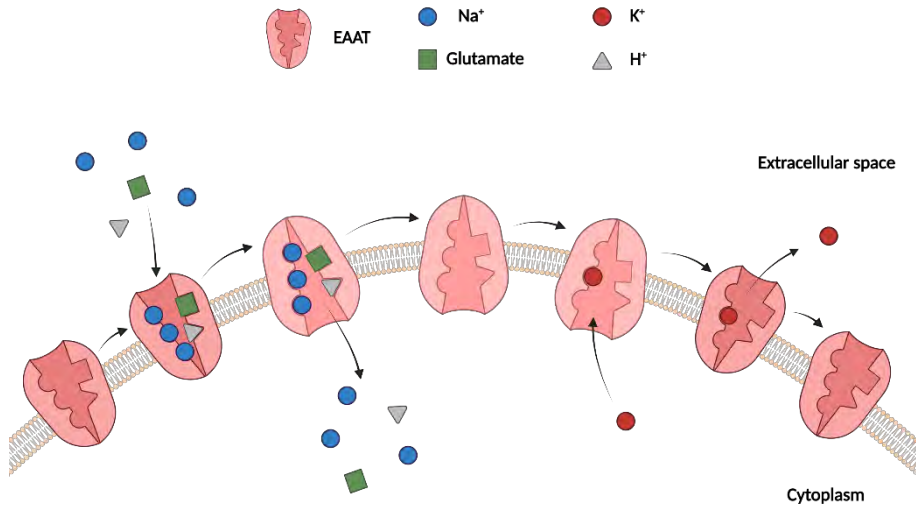


**Figure 6.** Glutamate transport from extracellular space to cytoplasm by the actions of EAATs. Self-created image using BioRender software.

### 2.3.1.1.- Brain Location

EAATs subtypes 1, 2 and 3 are widely distributed in CNS, while EAATs subtypes 4 and 5 are mostly expressed in cerebellum and retina, respectively. EAAT<sub>1</sub> and EAAT<sub>2</sub> are located in astrocytes membrane, with a higher density in the membrane that faces neuropil. EAAT<sub>1</sub> is exclusively expressed in astrocytes, while EAAT<sub>2</sub> is mostly expressed in astrocytes but can also be found (10%) in hippocampal nerve terminals. EAAT<sub>3</sub> is neuron selective but its expression is two orders of magnitude lower than EAAT<sub>2</sub> and it is limited to dendrites and cell bodies.<sup>84</sup> According to different studies, EAATs can also be found in brain capillary endothelial cells, where they are involved in brain glutamate efflux.<sup>85</sup>

### 2.3.1.2.- Function

The main role of EAATs (**Figure 7**) is the regulation of glutamate extracellular concentration and the maintenance of said concentration at low physiological levels, in order to avoid toxic effects. During synapse, after it is released into the synaptic cleft, glutamate is quickly absorbed into glial cells and neurons through EAATs. EAAT<sub>2</sub> is responsible for more than 90% of glutamate removal.<sup>86</sup> EAAT<sub>4</sub>, on the other hand, is responsible for neuronal excitability regulation by counteracting neuron depolarization. EAATs 4 and 5 possess a thermodynamically uncouple chlorine flux, translating into a high chloride conductance and a relatively low glutamate uptake.<sup>83</sup>

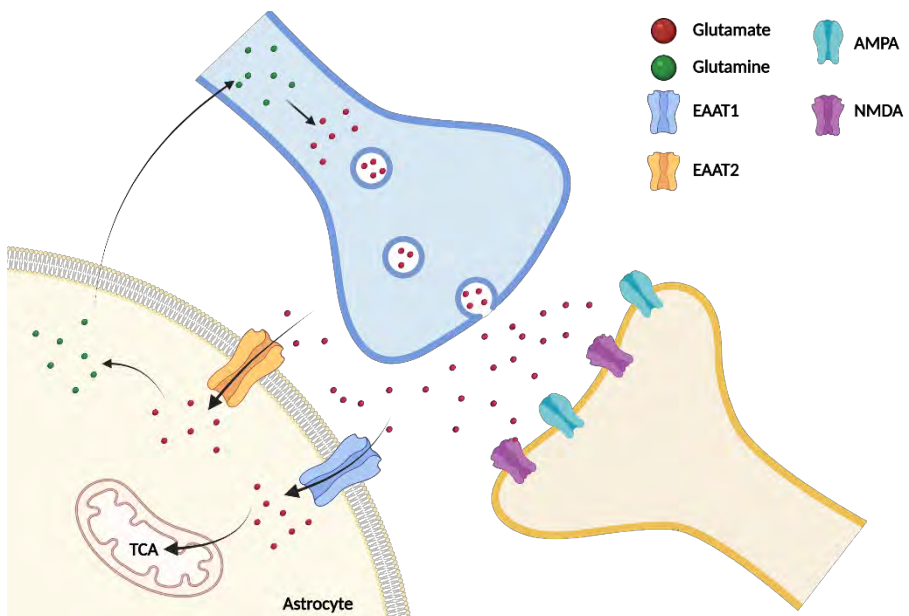


**Figure 7.** EAATs regulate the extracellular glutamate concentration in order to maintain it at low physiological levels, avoiding toxic effects. Self-created image using BioRender software.

### 2.3.2.- VESICULAR GLUTAMATE TRANSPORTERS

There are 3 subtypes of Vesicular Glutamate Transporters (VGLUTs), consisting in 560-589 amino acid residues. They have between 6 and 12 transmembrane domains and a C- and N-terminal both intracellular. The transmembrane domains of the three subtypes share more than a 90% homology while the C- and N-terminal regions have little homology and contribute to functional differences. A highly conserved glycosylation site is presented between transmembrane domains 1 and 2. Genes for the three subtypes are highly conserved throughout evolution, as multiple VGLUTs isoforms have been identified in many organisms, like *Drosophila*, zebrafish or frog.<sup>82,87</sup>

The glutamate transport by VGLUTs depends on a proton gradient inside the synaptic vesicles. A vacuolar ATPase, located in the vesicle membrane, hydrolyses the ATP, enabling the flow of H<sup>+</sup> into the synaptic vesicle, making it more acidic and generating a pH gradient across the membrane. The final consequence of this pH gradient is the creation of a membrane potential by making the inside of the vesicle more positive and thus allowing the entrance of the glutamate (an anion) through VGLUTs.<sup>83,87</sup>

#### 2.3.2.1.- Function

VGLUTs are responsible for the transport and accumulation of glutamate into synaptic vesicles. The accumulation of this neurotransmitter inside storage vesicles makes possible the quantal character of neurotransmission. Furthermore, it controls the neurotransmitter concentration gradient along the plasma membrane and protects neurons from toxicity derived from glutamate accumulation.<sup>83,87</sup>

### 2.3.2.2.- Brain Location

VGLUT<sub>1</sub> and VGLUT<sub>2</sub> are located mostly in glutamatergic neurons and have a complementary expression pattern, with only a limited overlap. VGLUT<sub>1</sub> is expressed in neocortex, hippocampus and amygdale while VGLUT<sub>2</sub> can be found in olfactory bulb, cerebral cortex, dentate gyrus, thalamus and hypothalamus. On the other hand, VGLUT<sub>3</sub> is localized in multiple brain regions (neocortex, olfactory bulb, substantia nigra, hippocampus, hypothalamus), although it is only present in a limited number of glutamatergic neurons. Additionally, it can also be observed in some hippocampal and cortical GABAergic neurons, cholinergic neurons in striatum and serotonergic neurons in raphe nuclei.<sup>83,87</sup>

### 2.4.- Metabolism and Cycling

There are three important metabolic pathways responsible for producing glutamate: 1) Glutamate-Glutamine cycle, 2) synthesis in astrocytes from glucose and 3) synthesis inside neurons from lactate delivered from astrocytes.

Not all the brain glutamate can be regenerated through glutamate-glutamine cycle in neurons and astrocytes, since part of it can be oxidized. Furthermore, glutamate does not cross the blood brain barrier (BBB), so it cannot be replenished into the CNS by diet. Therefore, it is necessary to *de novo* synthesize new glutamate.

*De novo* synthesis of glutamate from glucose can only occur in astrocytes, since neurons do not express pyruvate carboxylase, which is the major substrate for glutamate synthesis<sup>88</sup>. The sodium influx produced during nerve impulse transmission stimulates glucose uptake in astrocytes by GLUT<sub>1</sub> (glucose transporter). This glucose is then metabolized via glycolysis into pyruvate, which can be either reduce to lactate or enter the

tricarboxylic acids (TCA) cycle, producing  $\alpha$ -ketoglutarate as a carbon backbone for glutamate. Then, it can be converted into glutamate either by glutamate-oxaloacetate transaminase (GOT) or by glutamate dehydrogenase.<sup>89</sup> In neurons, glutamate can also be synthesized from lactate provided from astrocytes. In some neurons, glutamate can be then converted to gamma-aminobutyric acid (GABA) through glutamate decarboxylase.

Once synthesized, vesicles containing glutamate interact with soluble N-ethylmaleimide-sensitive factor attachment protein receptors (SNAREs) and glutamate is released into the synaptic cleft from presynaptic neurons, where it binds to either ionotropic (iGluR) or metabotropic (mGluR) receptors, located both on presynaptic and postsynaptic neurons. After it has been released, EAATs start transporting glutamate into astrocytes (EAATs 1 and 2) and neurons (EAAT<sub>3</sub>),<sup>90</sup> in order to re-establish adequate extracellular glutamate levels.

Both the glutamate transported into astrocytes and that synthesized from glucose can then be converted into glutamine, in an ATP-dependent process, through glutamine synthetase (an enzyme specific of astrocytes and oligodendrocytes). Nevertheless, not all glutamate molecules are converted into glutamine, as a tiny fraction is transformed into  $\alpha$ -ketoglutarate and enters the TCA cycle. This glutamine is released into the extracellular space through glutamine system N transporter 1 (SN<sub>1</sub>) and is uptaken by neurons through glutamine system A transporter 1 (SAT<sub>1</sub>). Then, glutamine is transformed into glutamate by phosphate-activated glutaminase<sup>91</sup> and loaded into synaptic vesicles through VGLUTs and the cycle starts again (**Figure 8**).

Besides EAATs and VGLUTs, another transport mechanism for glutamate has been described. The cysteine/glutamate antiporter (X<sub>c</sub><sup>-</sup>) exchange intracellular glutamate and extracellular cysteine. Cysteine transported from the synaptic

cleft into astrocytes is then used for glutathione synthesis, either in the astrocyte itself or by prior transportation to neurons.<sup>92,93</sup>

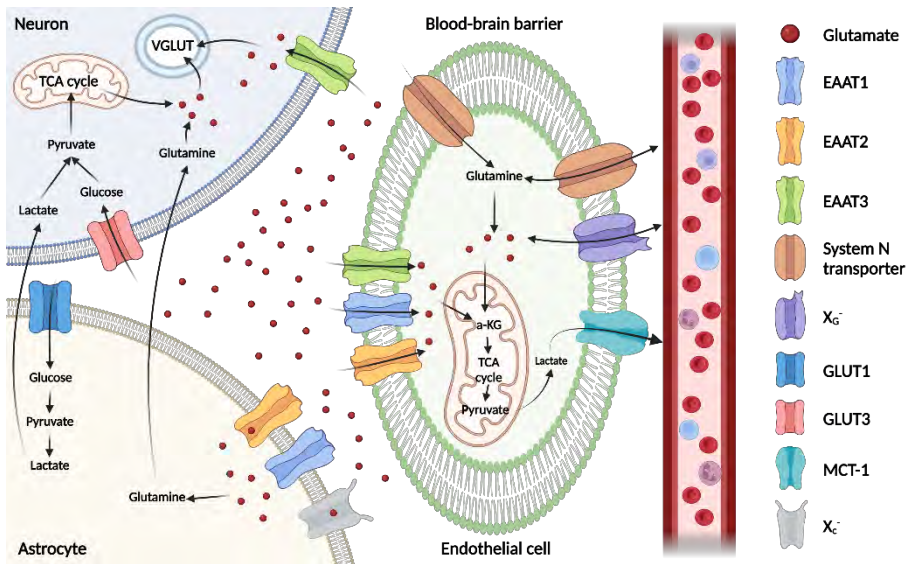


**Figure 8.** Metabolism and cycling of glutamate. Self-created image using BioRender software.

Furthermore, EAATs can also transport glutamate into endothelial cells, which is an important step in glutamate metabolism. The presence of EAATs in the abluminal membrane of brain endothelial cells shows their ability to accumulate glutamate. The fate of this glutamate may involve its transport, metabolism of glutamate and the transport of its metabolites or a combination of both processes.<sup>94</sup> The first case, glutamate transport, is supported by *in vivo* studies. These studies show a facilitative transport of glutamate in the luminal membrane, by means of a sodium independent transport through the X<sub>C</sub><sup>-</sup> transporter.<sup>95</sup> Several studies show a high mitochondrial density in brain endothelial cells and it has been proposed that these cells might be using glutamate as energy substrate in order to fuel the ABC-transporters.<sup>96</sup> Endothelial cells also express branched chain aminotransferases, involved in the conversion of

glutamate into  $\alpha$ -ketoglutarate, which is then included into the TAC cycle. This  $\alpha$ -ketoglutarate can be converted into pyruvate and, finally, into lactate in the cell cytosol and then transported into the blood by the monocarboxylic acid transporter (MCT<sub>1</sub>), located in the luminal membrane of endothelial cells.<sup>85</sup> Furthermore, there are transporters in the abluminal capable of uptake glutamine from the extracellular fluid into endothelial cells and hydrolyse it through glutaminase, transforming it into glutamate.<sup>78</sup>

## 2.5.- Excitotoxicity

Although not all the genes and proteins involved in glutamate excitotoxicity have been described, most of the major pathways of this process are well known.<sup>97,98</sup> The disruption of glutamate homeostasis has been linked to acute CNS injuries, such as stroke,<sup>99-102</sup> trauma, chronic neurodegenerative disorders (Parkinson's disease, multiple sclerosis, amyotrophic lateral sclerosis, etc.)<sup>100,103-105</sup> and surgical procedures involving blood flow interruption.<sup>106</sup>

During a stroke, the depolarization of the cell membrane due to an energy failure increases glutamate release. This same energetic failure blocks also the reuptake of glutamate.<sup>107</sup> This sudden release of glutamate overwhelms the regulating mechanisms and leads to the accumulation of glutamate in the extracellular space. Glutamate excess starts a series of downstream events that end in neuroexcitotoxicity. Neuroexcitotoxicity causes cell death, increasing even more the amount of glutamate released to the extracellular space, provoking a positive feedback that expands the damage.<sup>108</sup>

NMDAr are the major glutamate receptors involved in glutamate excitotoxicity, normally involved in neuronal plasticity (learning and memory formation).<sup>109</sup> Nevertheless, during the ischaemic event, the dysregulated activation of NMDAr leads to

neuroexcitotoxicity by receptor-mediated influx of calcium into the cells.<sup>110</sup> Calcium influx triggers other mechanisms, like activation of NOS and mitochondrial toxicity.<sup>75,111,112</sup>

NO production has an important role in glutamate excitotoxicity. Neuronal damage has been linked to nNOS translocation from the cytosol to cell membrane where it interacts with NMDAR.<sup>112</sup> NMDAR is also related to NOS through postsynaptic density protein of 95 kDa (PSD-95).<sup>113-115</sup> When glutamate binds to NMDAR, calcium influx induces the activation of nearby NOS and production of NO.<sup>75,98</sup> This can trigger the production of free radicals and harmful oxidants, causing lipid peroxidation, direct DNA damage, protein nitration, protein oxidation and Glyceraldehyde 3-phosphate dehydrogenase (GAPDH) depletion.<sup>115</sup> Free radicals can also be generated due to mitochondrial damage after a vast excitotoxic event.<sup>98,116</sup> NMDAR activation and the consequent calcium influx also trigger mitochondrial sequestration through high capacity sodium/calcium exchangers.<sup>117</sup> Besides mitochondria sequestration, these exchangers can induce metabolic acidosis and activation of superoxide and other ROS production. Furthermore, mitochondrial damage leads to calpain-mediated cleavage of regulatory proteins and activation of apoptotic pathways.<sup>108</sup>

## 2.6.- Therapeutic Strategies for Glutamate Excitotoxicity

The major role of glutamate excitotoxicity in ischaemic stroke and other pathologies has yielded a large number of studies addressing this mechanism. The first approach to glutamate toxicity was targeting NMDAR with antagonists. Being the primary effector of other downstream effects, NMDAR antagonists represented a promising strategy. Furthermore, the important role of these receptors in normal brain physiology

lead to an exhaustive understanding of their structure and function.<sup>118</sup>

Divers types of NMDAr antagonists were developed: competitive NMDAr antagonists acting on glutamate or glycine binding sites, non-competitive allosteric inhibitors and NMDAr channel blockers.<sup>119</sup> Despite their success in preclinical studies, all of them failed once translated to clinical trials (i.e. *Selfotel*, *Gavestinel* or *Traxoprodil*). Some of the reasons behind their failure could be their low brain penetrance and the dose-limiting side effects, like hallucinations, agitations, peripheral sensory loss, nausea, catatonia and increased blood pressure.<sup>46,119,120</sup> Another reason for NMDAr antagonists failure can be the therapeutic time window. In acute CNS insults, like traumatic brain injury (TBI) and stroke, it has been proposed that glutamate only produce its harmful effect within a narrow time frame and it returns to its normal function soon after. Thus, these therapeutic agents may have not only missed the therapeutic window but also have undesired side effects due to continue NMDAr blocking after glutamate normal function restoration.<sup>121</sup>

Despite initial setbacks, research focused on NMDAr antagonists continued. *Amantadine* and *Memantine*, for example, proved to be valuable in Parkinson's and Alzheimer's diseases, respectively.<sup>115</sup> Nevertheless, along the years, strategies focused on new targets, both upstream and downstream from NMDAr, have been developed.

## 2.7.- Blood Glutamate Grabbing

As mentioned above, glutamate homeostasis between blood and brain is controlled by different glutamate transporters. It has been shown that glutamate excitotoxicity during synapse is prevented by rapid glutamate uptake from synaptic cleft by glutamate transporters located both in the postsynaptic neuron

and the surrounding astrocytes.<sup>122</sup> Nevertheless, in endothelial cells, exists an unfavourable gradient between brain and blood glutamate concentrations (1-10  $\mu\text{M}$  to 40-60  $\mu\text{M}$ ).<sup>107</sup> When the glutamate concentration is higher inside endothelial cells compared to the blood, this glutamate is transported into the blood by a mechanism that allows the brain to get rid of the glutamate excess. Due to the presence of EAATs in the BBB and their ability to accumulate glutamate inside endothelial cells, a new hypothesis was proposed, called the **blood glutamate grabbing hypothesis**, regarding the possibility of reducing blood glutamate levels,<sup>123</sup> further increasing the gradient between brain and blood and facilitating the glutamate efflux towards the blood (**Figure 9**).

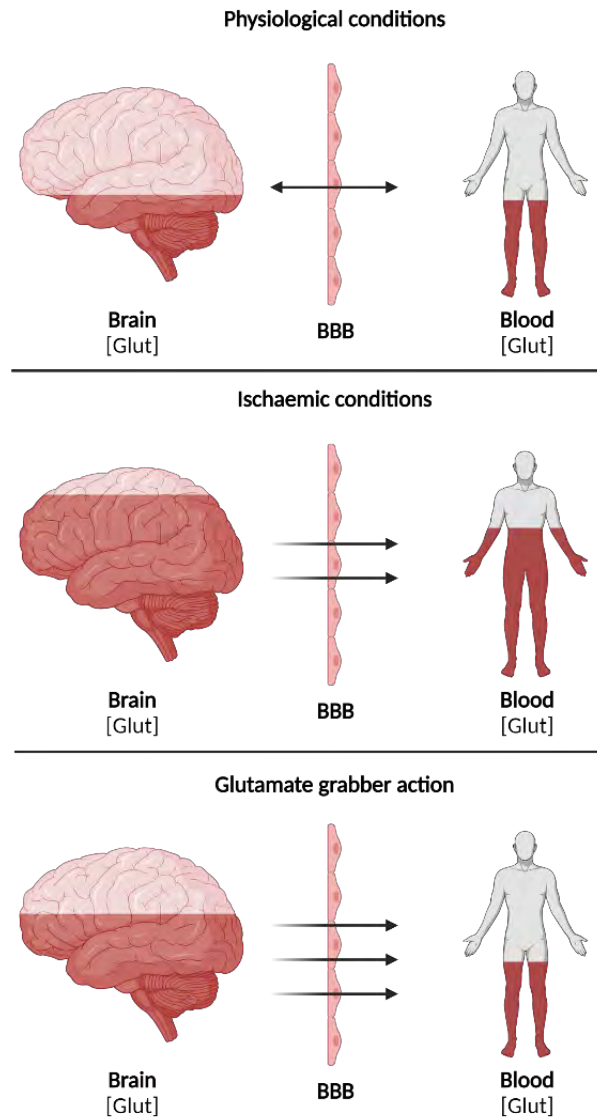


**Figure 9.** Under physiological conditions the BBB acts as a semi permeable membrane preventing the diffusion of glutamate from blood to brain. During ischaemia, glutamate concentrations in brain rise to levels 10 times above normal, leading to an increase in blood levels. With a glutamate grabber treatment, the washing effect of glutamate from brain to blood is increased, preventing secondary brain damage. Self-created image using BioRender software.

In order to prove this hypothesis, the glutamate-oxaloacetate transaminase (GOT), a transaminase which converts glutamate (using oxaloacetate as a cosubstrate) into  $\alpha$ -ketoglutarate and aspartate, was used. The idea behind this hypothesis was using artificially increased levels of oxaloacetate in order to shift the enzyme equilibrium and decreasing glutamate levels in blood. A study, conducted by Gottlieb et al.<sup>124</sup>, proved this hypothesis by injecting radioactive glutamate into animals and using oxaloacetate as a treatment. The use of oxaloacetate effectively decreased glutamate levels in blood, increasing the diffusion of radioactive glutamate (located in the brain) towards the blood. Other studies showed similar results by using two microdialysis probes, one infusing and the other collecting glutamate. Oxaloacetate treatment resulted in a reduction of glutamate collection by the second probe. Additionally, using malate (a GOT blocker) as a pre-treatment, showed an inhibition of the oxaloacetate-dependent blood glutamate clearing, proving the role of this enzyme. In addition to improving the GOT activity, the direct use of the enzyme as a treatment has also been proposed. Similar to previous studies, the use of a recombinant version of the enzyme as a treatment showed a significant reduction on blood glutamate levels, as well as a therapeutic effect in animal models of stroke.<sup>125</sup> Nevertheless, the role of GOT in glutamate metabolism and its potential use as a therapeutic agent will be discussed in detail in future sections.

On account of these results, different studies were done addressing blood glutamate grabbing in pathologies related with glutamate excitotoxicity (i.e. ischaemia, closed head injury, TBI, SAH or paraoxon intoxication). Even though these studies used different strategies to reduce blood glutamate levels, all of them reached the same general conclusion: lowering blood glutamate levels improved morbidity through better neuron survival, better recovery or smaller stroke volumes.<sup>85</sup> Contrary to NMDAr antagonists, which were either ineffective or potentially harmful, blood glutamate grabbers do not interfere with

physiological cellular signalling processes. They act only in the blood and they improve normal physiological mechanisms only in areas where glutamate levels are elevated.<sup>75</sup> These characteristics made them a suitable option for the development of novel, effective and safe therapeutic agents. The use of the GOT as a glutamate grabber in different pathologies will be further discussed in following sections.

### 3.- SECTION III: GOT

Glutamate-oxaloacetate transaminase (GOT), also known as aspartate transaminase (AST), AspAT, ASAT and AAT, is a pyridoxal-phosphate (PLP) dependent enzyme. First described in 1955<sup>126</sup>, it belongs to the transaminases protein family, which catalyses the reversible transfer of the alpha amino nitrogen of an amino acid to an alpha-keto acid with the synthesis of a second amino acid and a second alpha-keto acid. Particularly, GOT is responsible for the reversible conversion of one glutamate and one oxaloacetate into one aspartate and one  $\alpha$ -ketoglutarate.

Initially, it was believed that the transamination reaction was catalyzed by two independent enzymes: glutamate aminoferase and aspartate aminoferase. In 1942, Cohen demonstrated, that it is AST that catalyzes the transamination reaction. In 1950 the presence of GOT isoforms, cytosolic GOT1 and mitochondrial GOT2, was described.<sup>127</sup>

#### 3.1.- Chemical Structure

The human GOT isoforms are homodimers encoded by two separate genes: GOT1 and GOT2. The GOT1 gene, located on chromosome 10 at positions q24.1 - 25, consists of 9 exons and its product is a protein of 413 amino acids and a molecular weight of 46.248 kDa. The GOT2 gene is located on

chromosome 16 at position q21 and encodes a protein of 430 amino acids in length and a molecular weight of 47.476 kDa.<sup>128</sup>

GOT1 and human GOT2 are identical in a 48%, and differences in the sequence of amino acids relate to regions 1-31, 120-137, 275-295, 335-349AA. Analysis of the amino acid sequence of GOT1 in various organisms (human, pig, horse, rat, mouse, chicken) revealed the presence of many conserved regions, but the amino acids His-46, Lys-54, Val-186, Ile-198, Phe-250, Glu-278, Gln-282, Val-389, Ser-390 are characteristic only for human GOT1.<sup>127</sup>

The three-dimensional structure of both isozymes has been described, being almost identical.<sup>128-130</sup> The dimensions of a subunit of the protein are approximately 70x50x40 Å. The two subunits have an overlapping region, with the dimensions of the whole protein being 105x60x50 Å. The top and the sides of the protein are mainly formed by  $\alpha$ -helices while the bottom presents mostly  $\beta$ -sheets and extended loops. Four different domains have been proposed for every subunit, although the division responds principally to arbitrary criteria. First of all, a PLP binding domain; a small domain separated into two different parts (one located right after the N-terminal and the other on the C-terminal); the N-terminal arm; and two bridges binding the two parts of the small domain with the PLP binding domain. A visual representation of GOT1 is reproduced in **Figure 10**.

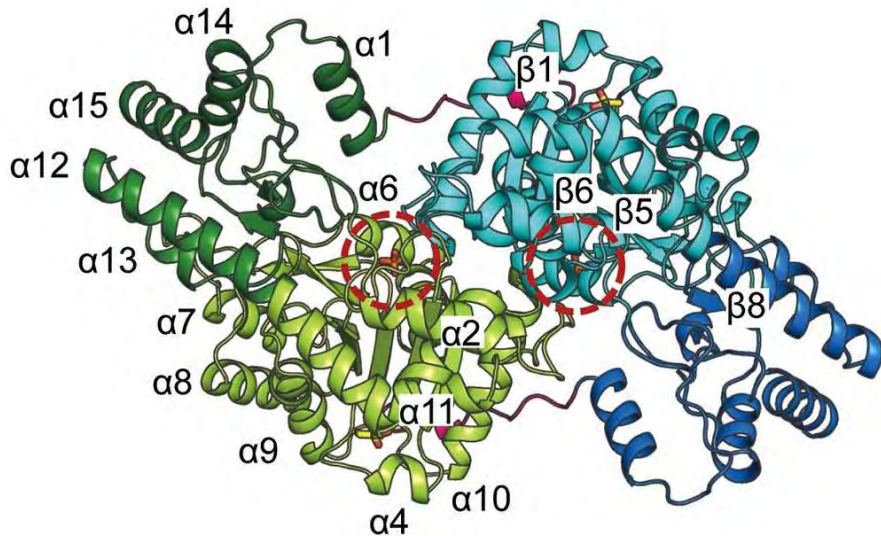


**Figure 10.** Three-dimensional structure of GOT1 from *Schizosaccharomyces pombe*. Shades of green and blue represent the two homodimers and the dashed red circles the active sites of the protein. Image modified from Chang *et al.*<sup>131</sup>

### 3.2.- Mechanism of Action

As described before, GOT is responsible for the reversible conversion of aspartate and  $\alpha$ -ketoglutarate into oxaloacetate and glutamate. The overall reaction is divided in two half-reactions through a ping-pong kinetic mechanism. Ping-pong mechanism occurs in enzymes which use two or more substrates to produce two or more products. This non-sequential mechanism is characterized by two traits. First, the change of the enzyme into a temporal intermediate form during the reaction of the first product and, second, the release of the first product before the binding of the second substrate.<sup>132</sup>

In the case of GOT, the first step consists on the addition of the cofactor PLP, forming the PLP-GOT, and the first substrate, L-Aspartate. Next, the PLP-GOT enzyme reacts with the L-

Aspartate, forming oxaloacetate and the pyridoxamine 5'-phosphate (PMP) form of the enzyme. In the second step, the reverse process occurs. The PMP-GOT reacts with  $\alpha$ -ketoglutarate, producing L-Glutamate and restoring the PLP-GOT.<sup>133,134</sup> An schematic view of the two-step reaction is shown in **Figure 11**.

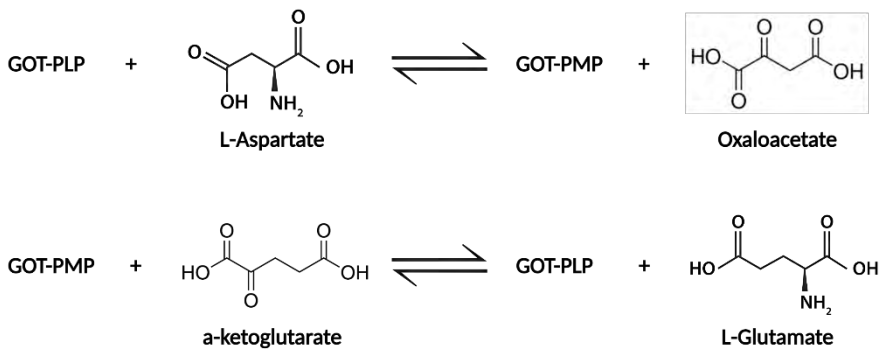


**Figure 11.** Schematic representation of the two-step ping pong reaction of GOT. Self-created image using BioRender software.

### 3.3.- Tissue Distribution

Since its central role in glutamate metabolism and the importance of this amino acid in the whole body, GOT is present in all tissues except for bone. Despite its global expression, the relative importance of GOT is not equal in all tissues, hence there are significant differences in GOT levels expression and distribution. Myocardium, liver and skeletal muscle are the tissues with a higher GOT activity,<sup>135,136</sup> followed by kidney, brain and pancreas. GOT activity in serum, on the other hand, is relatively low compared with the other tissues and most of the GOT activity in blood is present inside erythrocytes.<sup>137</sup> The relative distribution of GOT1 and GOT2 is very similar in most tissues, but it is not always the same. For example, in human liver, there is a 20% of cytosolic GOT (GOT1) against an 80% of

GOT2,<sup>135,138</sup> while in cardiac muscle, the mitochondrial isoform (GOT2) represents about 65% of total GOT.<sup>139</sup> In blood, GOT1 represents around 97% of total GOT, with an estimated concentration of 100 µg/L, while GOT2 concentration is only 2.8 µg/L.<sup>140,141</sup> Although in most organs the amount of protein detected and the enzyme activity are almost identical, in serum exists a significant amount of immunologically active GOT with no catalytic activity,<sup>142</sup> suggesting a rapid loss of catalytic activity once released into peripheral circulation. Meanwhile, inactive protein or protein fragments remain in the blood for some time, demonstrating the shift between catalytic inactivation and clearance.<sup>143,144</sup> **Figure 12** represents the relative expression of GOT1 and GOT2 in several tissues, showing a wide expression among most of the systems.

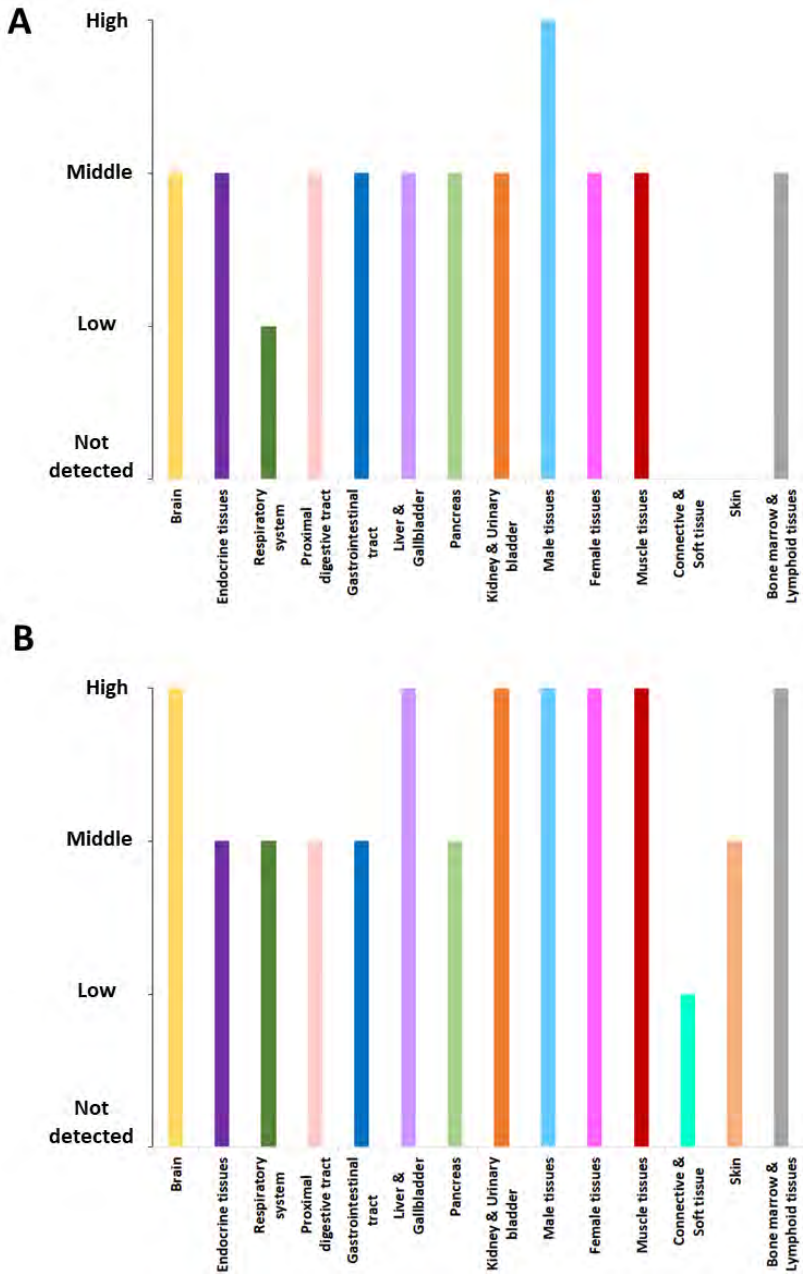


**Figure 12.** Relative expression of cytosolic GOT1 (A) and mitochondrial GOT2 (B) in different body tissues. Self-created image using The Human Protein Atlas data.<sup>140,141</sup>

### 3.4.- Function

As explained before, the main role of GOT is *de novo* synthesis of glutamate in astrocytes by using the  $\alpha$ -ketoglutarate provided by the TCA cycle and its implication in CNS synapses. Nevertheless, over the years, other functions of the enzyme have been described (**Figure 13**), along with the implication of its main role in several metabolic pathways and physiological processes.

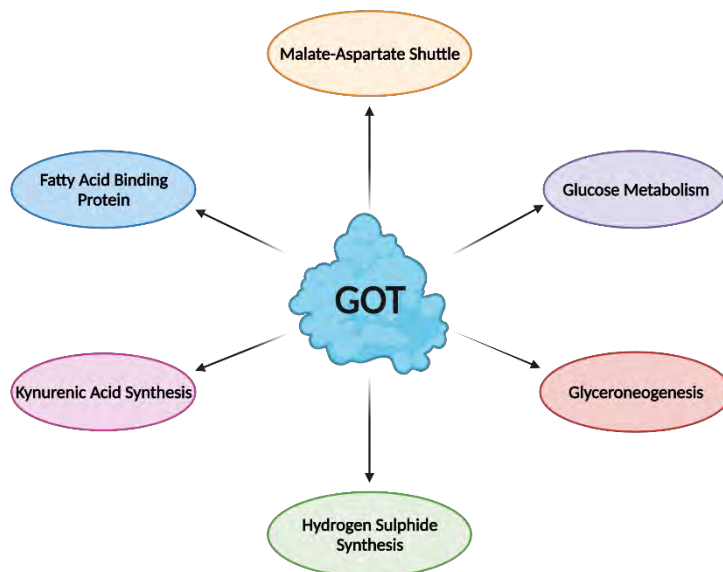


**Figure 13.** Described functions of GOT in different metabolic pathways and physiological processes. Self-created image using BioRender software.

#### 3.4.1.- MALATE-ASPARTATE SHUTTLE

The malate-aspartate shuttle (MAS) is a redox shuttle, essential for the redox balance in the mitochondria and the cytosol. The role of the MAS is to transport the cytosolic reducing equivalents

produced in different metabolic pathways, since the inner mitochondrial membrane is impermeable to NADH molecules.<sup>145,146</sup> This transport has two different goals: to allow the supply of electrons to the electron-transport chain for ATP production and the regeneration of cytosolic NAD<sup>+</sup>, permitting it to function as a reducing equivalent once again. Besides its main role, the MAS is involved in the synthesis of aspartate in glutamate in the brain, where it plays a very important role.<sup>147,148</sup>

The MAS is composed by six different elements, four enzymes and two mitochondrial carriers. The four enzymes involved in the shuttle are the mitochondrial and cytosolic versions of both malate dehydrogenase (MDH1 and MDH2) and glutamate-oxaloacetate transferase (GOT1 and GOT2). The two carriers are the oxoglutarate/malate carrier (OGC) and the two isoforms of the aspartate-glutamate carrier (AGC1 and AGC2). Due to the MAS role in metabolism, these components are highly expressed in energy demanding tissues, such as CNS, heart and skeletal muscle.<sup>140</sup>

Taking oxaloacetate as the starting point of the MAS, this metabolite is reduced to malate by MDH1, with the consequent oxidation of NADH to NAD<sup>+</sup>. Malate can then enter the mitochondria by an antiporter mechanism, exchanging cytosolic malate for mitochondrial  $\alpha$ -ketoglutarate through the OGC. Afterwards, malate is oxidized once again into oxaloacetate by MDH2 in the mitochondrial matrix, NAD<sup>+</sup> is then reduced to NADH and it is ready to participate in the electron-transport chain. The oxaloacetate in the mitochondrial matrix is then transformed into aspartate by the GOT2, using glutamate as an amino group donor. Aspartate is transported back to the cytosol by AGC carriers using glutamate and a proton in an antiporter mechanism. The last step of the MAS is the conversion of aspartate into oxaloacetate by GOT1, regenerating both oxaloacetate and glutamate and allowing the cycle to start again (**Figure 14**).<sup>149,150</sup>

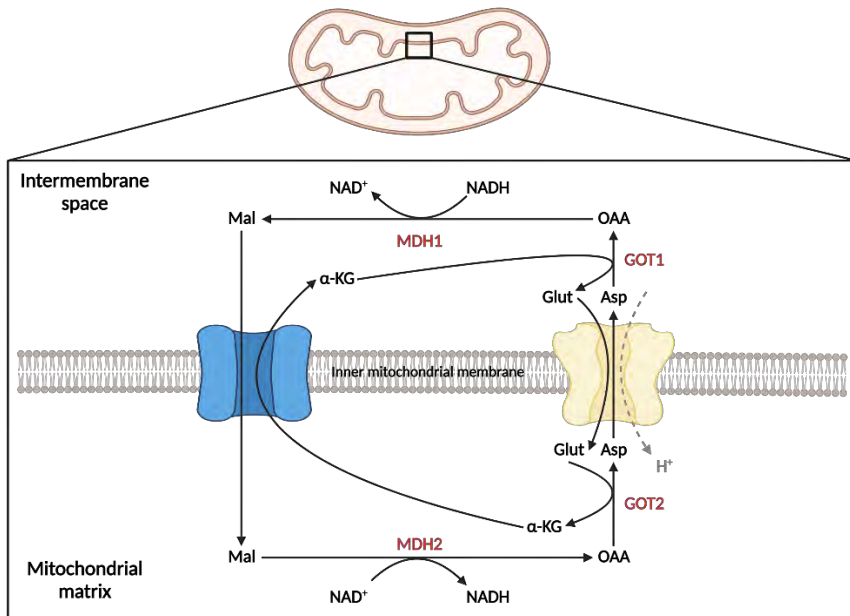


**Figure 14.** The Malate-Aspartate shuttle is responsible for transporting the cytosolic reducing equivalents produced in metabolic pathways.  $\alpha$ -KG:  $\alpha$ -ketoglutarate; Asp: aspartate; Glut: glutamate; Mal: malate; MDH: malate dehydrogenase; OAA: oxaloacetate. Self-created image using BioRender software.

### 3.4.2.- GLUCOSE METABOLISM

Different studies have shown the role of GOT at different levels of glucose metabolism. Ferré *et al.*<sup>151</sup> demonstrated the role of GOT in hepatic glucose synthesis by using an inhibitor of the GOT, which caused a significant hypoglycaemia and an accumulation of lactate in suckling new-born rats. Similar results were obtained *in vitro* using GOT inhibitors in isolated liver cells from adult rats<sup>152,153</sup>. In line with this, glucagon and cAMP, both gluconeogenesis-inducing molecules, increased the activity of GOT in a primary culture of liver cells from rat.<sup>154</sup> All these results prove the role of GOT in gluconeogenesis during both developmental states and adulthood.

Additionally, GOT has been related with the secretion of insulin, the most important hormone in glucose levels regulation. A simpler version of the metabolic pathway linking GOT and insulin secretion is represented in **Figure 15**. Briefly,  $\alpha$ -ketoglutarate produced by GOT in pancreatic islets can then be converted to succinyl-CoA by the  $\alpha$ -ketoglutarate dehydrogenase complex. The role of GOT, along with glutamate dehydrogenase, in the synthesis of  $\alpha$ -ketoglutarate in this metabolic pathway is especially important since they are capable of forming a complex with the  $\alpha$ -ketoglutarate dehydrogenase complex, improving substrate channelling.<sup>155</sup> Afterwards, succinyl-CoA can be metabolized by succinyl-CoA-acetoacetate transferase, producing succinate and acetoacetyl-CoA which then reacts with acetyl-CoA to form HMG-CoA by the action of HMG-CoA synthase. In the last step, HMG-CoA is reduced to mevalonate by the HMG-CoA reductase.<sup>156</sup> Different studies have shown the relation between levels of mevalonate and insulin secretion, finally linking GOT with the production of this hormone.<sup>156,157</sup>

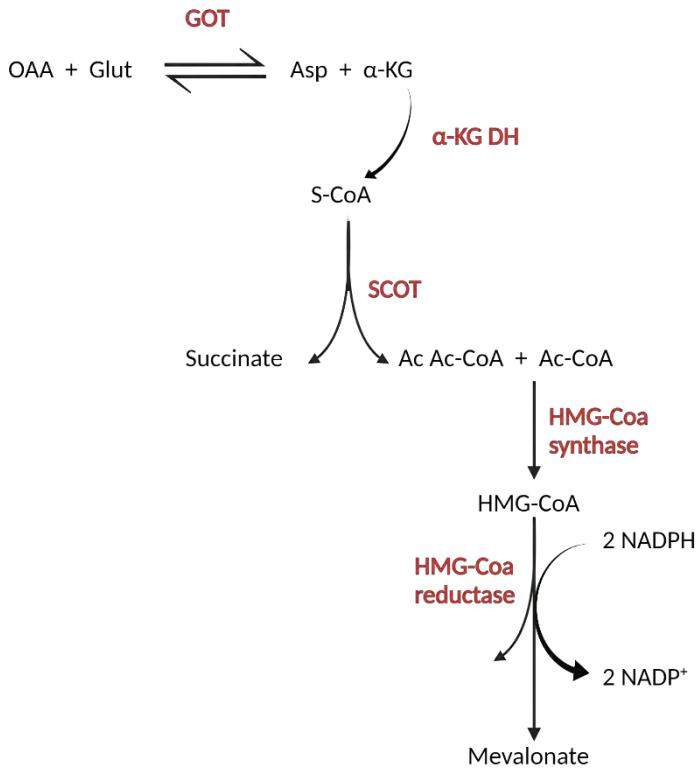


**Figure 15.** Simplified version of GOT-induced insulin secretion. Ac Ac-CoA: acetoacetyl-CoA; Ac-CoA: acetyl-CoA; a-KG: a-ketoglutarate; a-KG DH: a-ketoglutarate dehydrogenase; Asp: Aspartate; Glut: Glutamate; OAA: Oxaloacetate; S-CoA: Succinyl-CoA; SCOT: succinyl-CoA-acetoacetate transferase. Self-created image using BioRender software.

Another explanation for the influence of GOT activity in the insulin secretion has been proposed.<sup>158</sup> In this case, GOT is involved in incretin-induced insulin secretion through the action of cAMP. Incretins GLP-1 and GIP are secreted by enteroendocrine cells in response to meal ingestion, triggering cAMP signalling in  $\beta$ -cells and promoting insulin secretion. This cAMP signalling is responsible for the transport of glutamate into insulin secretory granules by VGLUTs, which triggers the granule exocytosis.<sup>159</sup> Although the exact mechanism behind glutamate-induced exocytosis has not been completely elucidated, it seems to be related to vacuolar proton pump

ATPase and chloride transport protein CIC3, which regulate granule electric potential, facilitating its fusion to the plasma membrane.<sup>160</sup> The glutamate necessary for this process is produced in a glucose-dependant manner by the GOT1 linked to the MAS in pancreatic  $\beta$ -cells.<sup>158,161</sup>

### 3.4.3.- GLYCERONEOGENESIS

Glyceroneogenesis (GNG) is a shorter version of gluconeogenesis responsible for the production of glycerol-3-phosphate using precursors other than glycerol or glucose when glucose utilization is reduced, mainly during fasting. GNG allows re-esterification of fatty acids for triacylglycerol synthesis while they are being metabolized through lipolysis. This mechanism prevents an excessive release of fatty acids into the blood by recycling some of them in anabolic reactions.<sup>162</sup> Different studies have estimated that 50% of fatty acids are re-esterified through this process; of them, one fifth occurs in adipocytes and the other 80% in other tissues (mostly in liver).<sup>163</sup> The most important enzyme in GNG, the phosphoenolpyruvate carboxykinase (PEPCK-C), uses oxaloacetate as a substrate, producing phosphoenolpyruvate (PEP). Finally, PEP is converted to glycerol-3-phosphate through glycerol-3-phosphate dehydrogenase (GPDH).<sup>163,164</sup>

Several studies have correlated a low glucose, fasting or diabetes scenario with an increase in GOT activity and mRNA, especially the cytosolic isomer, GOT1.<sup>165-167</sup> Furthermore, the region of the promoter that mediates the negative glucose regulation of GOT1 gene expression has been identified.<sup>167</sup> Also, GOT1 gene transcription is induced by thiazolidinediones, a family of antidiabetic drugs, resulting in an increased production of glycerol-3-phosphate and triacylglycerol synthesis.<sup>162</sup> All this data support the importance of GOT1 in GNG since it is a source of oxaloacetate, the first precursor of this metabolic pathway.

### 3.4.4.- HYDROGEN SULPHIDE SYNTHESIS

In 1978<sup>168</sup> and 1982,<sup>169</sup> two studies focused on the purification and characterization of cysteine aminotransferase (CAT) in mitochondria and cytosol respectively, discovered that this two isomers of the enzyme, based on substrate specificity, enzyme inhibition and physicochemical properties, were identical to cytosolic and mitochondrial GOT. CAT (GOT1 will be called CAT in this section in order to match most of the bibliography), is an enzyme deeply involved in the metabolism of hydrogen sulphide (H<sub>2</sub>S).

H<sub>2</sub>S, was first described a few centuries ago as a toxic gas due to its capacity to reversibly inhibiting cytochrome c oxidase, preventing oxidative phosphorylation and lowering ATP production. Nevertheless, in the last decade, different studies showed the role of H<sub>2</sub>S in several physiological and pathological processes, including induction of angiogenesis, regulation of neuronal activity, vascular relaxation, glucose homeostatic regulation or production of glutathione.<sup>170</sup> Regarding ischaemic stroke, H<sub>2</sub>S is also related with some major events involved in ischaemic injury. Several studies have observed the protective effect of H<sub>2</sub>S in ischaemia-reperfusion injury in different pathologies, including stroke<sup>171</sup> and endogenous H<sub>2</sub>S has been observed to play a significant role in BBB disruption after transient focal ischaemia.<sup>172</sup>

There are three main pathways for H<sub>2</sub>S synthesis, involving three different enzymes. First, it can be produced from combination of L-homocysteine and L-cysteine due to the action of cystathionine β-synthase (CBS) or cystathionine γ-lyase (CSE), producing H<sub>2</sub>S and cystathionine. The second pathway involve also CBS, which can produce H<sub>2</sub>S and serine directly from L-cysteine. Finally, the third pathway (**Figure 16**) is composed by two different reactions. First, a transamination through CAT, using L-cysteine and α-ketoglutarate and producing glutamate

and 3-mercaptopyruvate (3MP). The second reaction of this pathway is catalysed by 3-mercaptopyruvate sulfurtransferase (3MST), using 3MP and producing pyruvate and H<sub>2</sub>S.<sup>170</sup> Another pathway has been proposed in recent years, but its relevance in H<sub>2</sub>S synthesis has not yet been elucidated.<sup>173</sup> Although the relevance of CAT pathway in the synthesis of H<sub>2</sub>S was considered minor or even negligible, some studies have shown its major role in H<sub>2</sub>S in different tissues, including peripheral neurons and vascular endothelium.<sup>174,175</sup>

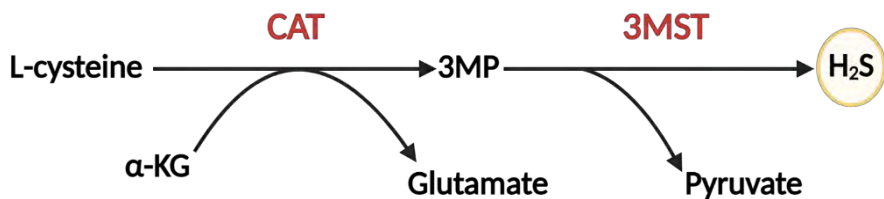


**Figure 16.** Synthesis of H<sub>2</sub>S in the CAT pathway. 3MP: 3-mercaptopyruvate; CAT: cysteine aminotransferase. 3MST: 3-mercaptopyruvate sulfurtransferase; α-KG: α-ketoglutarate. Self-created image using BioRender software.

### 3.4.5.- KYNURENIC ACID SYNTHESIS

Besides the canonical reaction catalysed by GOT and the cysteine transamination described in the previous section, another reaction has been described involving GOT. There are four kynurenine aminotransferases (KATs) enzymes, responsible for the synthesis of kynurenic acid (KYNA). The mitochondrial isomer of the GOT (GOT2) was first proposed and characterized by Guidetti *et al.*<sup>176</sup> as the fourth KAT. Further studies confirmed the identity of GOT2 as KAT-IV and its biochemistry and structure were determined.<sup>177</sup> Nevertheless, the relative relevance of KAT-IV in this metabolic pathway has yet to be elucidated.

KYNA is a product of tryptophan degradation metabolised through the kynurenine pathway, responsible for the

degradation of 95% of the tryptophan not used in protein synthesis. KYNA acts as a NMDAR and  $\alpha 7$ -nicotinic acetylcholine receptors endogenous antagonist as well as a ligand for the G-protein-coupled receptor 35 and the aryl hydrocarbon receptor, involved in immunomodulation processes.<sup>178,179</sup> KYNA also acts as a ROS scavenger.<sup>180</sup> Furthermore, abnormal levels of KYNA have been linked to different pathologies, including Alzheimer's disease, Huntington's disease, schizophrenia<sup>181</sup> and cognitive deficits.<sup>182</sup>

The first step in the kynurenine pathway is the degradation of tryptophan into N-formylkynurenine by the action of tryptophan 2,3-dioxygenase or indoleamine dioxygenase, which is then converted into L-kynurenine through formamidase. Finally, L-kynurenine is transformed into KYNA by kynurenine aminotransferases KATs. KATs also participate in another branch of the kynurenine pathway. L-kynurenine can be transformed into 3-hydroxykynurenine by kynurenine mono-oxygenase, and then transformed into xanthurenic acid through KATs. Different studies have partially elucidated the functions of xanthurenic acid, including acting as an aryl hydrocarbon receptor ligand,<sup>183</sup> a putative neurotransmitter, its implications in mGluR 1 and 2 signalling and inhibition of VGLUTs. Xanthurenic acid was also related to schizophrenia, although most of these processes are not well known and the extent of the role of xanthurenic acid is not clear.<sup>184</sup>

#### 3.4.6.- FATTY ACID BINDING PROTEIN

Fatty acid-binding proteins (FABPs) are a family of small and highly conserved lipid chaperone molecules involved in varied functions.<sup>185</sup> Initially it was thought that FABPs bound long-chain fatty acids almost exclusively, but they are able to bind to other hydrophobic molecules, such as endocannabinoids and lipophilic drugs. FABPs have specific tissue functions as well as regulatory effects outside their tissues. There are nine FABPs

described to the date, but this section will be focused on the first one, FABP1.<sup>186</sup>

FABP1, also called liver FABP, was the first FABP described and is expressed mostly in liver and intestine. Several studies by Berk *et al.* showed, first, that FABP1 was actually the mitochondrial GOT2<sup>187,188</sup> and, second, the relationship of this protein with fatty acids uptake.<sup>189,190</sup> Interestingly, FABP1 was found in the plasma membrane of hepatocytes and enterocytes as well as in the mitochondria.<sup>191</sup> Crystallographic studies have also identified a specific domain for long chain fatty acids binding.<sup>192</sup>

Different studies have identified several functions for FABP1. For instance, it plays a central role in  $\beta$ -oxidation of unesterified fatty acids, both through fatty acid trafficking and the regulation of gene expression through interactions with PPAR $\alpha$ , a transcription factor deeply involved in lipid metabolism in the liver. FABP1 is also related with the maintenance of intracellular lipid droplets in hepatic stellate cells, a process related with fibrogenesis in the liver. It is also involved in hepatic steatosis and regulates endogenous endocannabinoid levels by decreasing their uptake and enhancing their hydrolysis. In enterocytes, FABP1 has been related to cell proliferation and formation of prechylomicron transport vesicles. Finally, it has been suggested its potential regulatory role in other tissues where it is not expressed, such as skeletal muscle.<sup>186,193</sup>

### 3.5.- Therapeutic Applications of GOT

#### 3.5.1.- ISCHAEMIC STROKE

As described in previous sections, glutamate plays a major role in neuronal damage<sup>194</sup> during brain ischaemia and higher glutamate concentrations in blood and cerebrospinal fluid (CSF) are associated with poor neurological outcome in stroke patients.<sup>100,101</sup> Several studies have linked glutamate levels with

neuronal damage after an ischaemic insult.<sup>99-102,195</sup> Moreover, plasma levels of glutamate at admission above 200  $\mu\text{M}$  have been proved to be a good predictor of stroke outcome at 48 hours.<sup>101</sup>

Furthermore, elevated levels of glutamate during at least 24 hours were associated with early neurological deterioration. On the other hand, plasma glutamate levels of patients with a stable stroke returned to normal levels before 6 hours.<sup>101</sup> These data proved the pivotal role of glutamate in stroke and its relation with ischaemic damage and opened new possibilities for stroke treatment, focused on the inhibition of glutamate toxicity by means of blood glutamate grabbers.

The first studies addressing the therapeutic effect of blood glutamate grabbers were performed using oxaloacetate in ischaemic rats subjected to photothrombotic lesions.<sup>196,197</sup> Oxaloacetate attenuated the reduction of somatosensory evoked potentials provoked by the photothrombotic lesion, reduced infarct size, assessed histologically, and prevented long term potentiation impairment in rat CA1 hippocampal region in a 2-vessel occlusion model.<sup>198</sup> Similar to these results, Campos *et al.*<sup>199</sup>, demonstrated the reduction of blood glutamate levels, oedema and motor deficit by using an intravenous (I.V.) injection of oxaloacetate. In order to prove the protective effect of oxaloacetate through reduction of brain glutamate levels, magnetic resonance spectroscopy (MRS) was performed in the ischaemic region. MRS showed a reduction of brain glutamate levels in treated animals compared to the control group after ischaemia.<sup>199</sup> Additionally, injection of peripheral pyruvate, either with or without glutamic-pyruvic transaminase (GPT), also now as ALT, after ischaemia showed smaller blood glutamate levels, lesion volume, oedema, neurological deficit and mortality.<sup>200</sup>

In stroke patients, it has also been reported the association between higher levels of GOT and GPT (even greater for GOT

compared to GPT) and good outcome.<sup>201</sup> Furthermore, patients with higher glutamate levels and lower levels of GOT had a worse outcome and a greater lesion volume after 3 months, highlighting the important role of GOT in glutamate homeostasis.<sup>197,202</sup> Other studies also showed the critical role of GOT in the metabolic processing of glutamate, converting the glutamate excess after stroke in a potential source of metabolic energy.<sup>203,204</sup> All this findings led to the use of GOT as a therapeutic agent in stroke. Two major approaches have been used: the direct use of the enzyme as a therapeutic agent and the induction of endogenous GOT expression. In the first case, Campos *et al.* showed the potential therapeutic effect of GOT by the use of a recombinant version of the enzyme.<sup>125,205</sup> On the other side, Khanna *et al.* demonstrated the beneficial effect of an increased GOT expression, either oxygen-induced<sup>203</sup> or by using a phytoestrogen as a chemical inducer of GOT expression.<sup>206</sup>

### 3.5.2.- TRAUMATIC BRAIN INJURY

TBI is the disruption of the normal function of the brain due to a blow or jolt to the head or a penetrating head injury. It is one of the leading causes of death and disability in Europe and USA and a major health and socioeconomic problem worldwide.<sup>207,208</sup> According to the Centers for Disease Control and Prevention, between 2002 and 2006, 1.7 million TBIs occurred every year in the USA, being most of them mild TBIs. From this 1.7 million, 275,000 cases needed hospitalization and 52,000 ended in death. Most common causes of TBI are motor-vehicle traffic crashes, falls, struck by/against events and assaults. Besides these common causes, TBI has a high incidence among military personal, being blast injuries the major cause of TBI among soldiers in modern wars.<sup>209</sup> According to the *Joint Theater Trauma Registry*, made by US Army Institute of Surgical Research, soldiers suffering head or neck injuries, including severe TBI, represented 25% of all personnel evacuated from Iraq

and Afghanistan.<sup>209,210</sup> Mild TBI in soldiers serving in Iraq is related with post-traumatic stress disorder and depression and derived physical health problems after returning home.<sup>211</sup> Besides directly health related problems, TBI has major economic and social burden, especially with the increasing use of motor-vehicle in developed and developing countries.<sup>212</sup>

Clinical manifestations of TBI include concussion, coma or even death, depending on the severity of the lesion. The major pathophysiology processes behind TBI are two: primary injury, due to the direct action of the mechanical impact, and secondary injury, started right after trauma and involving cell and tissue damage due to the effects of the primary injury. Secondary injury continues to develop for several hours or even days after the initial trauma.<sup>213</sup> Due to the rapid development of primary injury, this kind of lesion is normally irreversible. On the other hand, the slower progression of secondary injury makes it possible to be reversed by addressing different steps of cell death processes. Different strategies have been proposed focused on the treatment of TBI by targeting neurotransmitter release, free radical mediated-damage, proapoptotic gene activation, calcium overload, mitochondrial dysfunction and inflammatory response, all involved in secondary injury pathogenesis.<sup>214,215</sup> All of these processes are induced by synaptic transmission and the consequent activation of postsynaptic receptors. Several postsynaptic membrane proteins form a special structure known as the postsynaptic density. This structure functions as a multi-protein complex that mediates a molecular network in neurons after injury.

In relation with glutamate, different studies showed an increase of glutamate levels in CSF after TBI, both in patients and animals.<sup>216-218</sup> Shortly after TBI, extracellular concentration of glutamate greatly increases due to massive depolarization of neurons derived from the traumatism and the associated energetic failure. Following the same processes described in stroke, glutamate excess leads to sodium and calcium influx

into the cytosol. Calcium overload then induces cell damage mechanisms and apoptosis through caspase activation.<sup>219</sup> Same as for stroke, regulating glutamate concentration has been used as a potential therapy for TBI and different studies showed a better neurological outcome by using oxaloacetate as a glutamate grabber.<sup>103,220,221</sup>

Moreover, the effect of oxaloacetate in blood glutamate reduction seems to be dose dependant, since smaller doses of oxaloacetate (5 mM) did not yield any reduction in blood glutamate.<sup>220</sup> On the contrary, this effect can be rescued when low doses of oxaloacetate are combined with a recombinant version of GOT. Other studies showed that treatment with oxaloacetate resulted in an improvement of neuron survival in five different hippocampal regions after 30 days. However, when administered with maleate, a GOT blocker, the glutamate reduction was reverted.<sup>103,197</sup> In another study, Jia *et al.* observed an improvement of synaptic plasticity in rats submitted to TBI after a combined treatment of GOT and oxaloacetate, in accordance with the previous data and demonstrating, once again, the beneficial role of GOT.<sup>222</sup>

### 3.5.3.- SUBARACHNOID HAEMORRHAGE

SAH is a common condition associated with high mortality and morbidity. Mortality rates are about 45% within the first 30 days and 10-15% cases are fatal even before hospitalization.<sup>223-226</sup> In almost 30% of the cases, a reactive vasospasm can occur at the time of the initial bleed, causing a critical reduction in cerebral blood flow as the regional intracranial pressure increases and approaches the systemic arterial pressure. This blood flow reduction triggers a cerebral vasospasm and consequent swelling of perivascular astrocytes, neurons and endothelial cells.<sup>75</sup> Even though the delayed effects of SAH are well known, early brain injury pathophysiology is not, and early treatment is still a challenge.<sup>227</sup> Different studies have shown the role of high

glutamate levels both in interstitial fluid (IF) and CSF in injury mechanisms of divers acute brain insults.<sup>97,100,101,228</sup> Similarly, some studies have shown a massive release of glutamate after SAH and a following overstimulation of NMDAr.<sup>229,230</sup>

These increased levels of glutamate are correlated with neurological status of SAH patients.<sup>231</sup> After SAH, the loss of BBB integrity leads to cerebral swelling and disturbance of intracranial hemodynamic.<sup>232</sup> These events further increase BBB disruption, creating a harmful positive feedback. Furthermore, NO pathway is also dysregulated in SAH, worsening early ischaemic injury.<sup>233</sup> NO is produced from L-arginine by the three isozymes of NOS (nNOS, iNOS and endothelial NOS) and it plays a major role in maintaining cerebrovascular tone and cerebral blood flow. A calcium sensitive nNOS enzyme is physically associated with NMDAr and is activated after SAH glutamate neuroexcitotoxicity.<sup>233,234</sup>

Following the same principles used in stroke and TBI, some studies have utilized glutamate grabbers as a therapeutic agent for SAH. These studies observed a reduction in blood and CSF glutamate and an improvement of neurological outcome at 24 hours, measured by BBB disruption, neurological severity score and oedema.<sup>75,200</sup> This opens the possibility of using GOT as a therapeutic agent for this pathology.

### 3.5.4.- MIGRAINE HEADACHE

Migraine affects around 14.7% of people in Europe from childhood to old age, being less common in women during the postmenopausal years.<sup>235</sup> The relation between glutamate homeostasis and migraine has been described in several studies.<sup>195,236-238</sup> Elevated glutamate levels and the consequent over-activation of NMDAr are implicated in the triggering, propagation and duration of cortical spreading depression (CSD).<sup>238,239</sup> Moreover, NMDA-mediated glutamatergic transmission is implicated in the activation of the trigeminus-

vascular system<sup>239,240</sup> and might be involved in the clinical symptoms of migraine and central sensitization.<sup>241</sup> As in other pathologies, NMDAR antagonists have been used for CSD suppression in preclinical studies,<sup>242</sup> but their harmful side effects in clinical trials caused their withdrawal.<sup>243</sup>

The role of glutamate in this pathology has open new possibilities for glutamate grabbers to be used as prophylactic treatment for migraine.<sup>236</sup> To further explore this hypothesis, the relation between GOT activity in blood with blood glutamate levels and clinical parameters in migraine patients was studied.<sup>111</sup> In this study, migraine patients had higher blood glutamate levels and lower GOT activity compare with the control group. Additionally, GOT activity was inversely associated with glutamate levels during interictal period, whereas elevated glutamate levels were associated with duration of pain during ictal period, though no relation was observed between GOT activity and clinical parameters.<sup>111</sup> These results support the idea of using blood glutamate grabbers as therapeutic agents for migraine, although more studies are necessary.

### 3.5.5.- ORGANOPHOSPHATE INTOXICATION

Organophosphates are highly toxic compounds used as pesticides (malathion and paraoxon) and nerve agents in chemical warfare (somain, sarin). Poisoning due to pesticides is one of the most common causes of poisoning, responsible for one million cases every year and several hundred thousand deaths.<sup>244</sup> These compounds affect to the acetylcholine esterase, a serine protease responsible for the hydrolysis of acetylcholine. Poisoning with organophosphates leads to acetylcholine accumulation which triggers overstimulation of cholinergic receptors and a quick and vast excitotoxicity and malfunction of cholinergic neurons.<sup>245</sup>

Exposure to organophosphates affects diverse regions of the brain, such as the entorhinal and piriform cortex, amygdala and hippocampus CA1 and CA3.<sup>246</sup> Contrary to other pathologies, brain damage due to organophosphates is not usually an acute event and it is the secondary neuronal damage the one responsible for most of the neuronal loss. The extent of the damage depends directly on the severity of convulsions, which it is related to an increase in the density of peripheral benzodiazepine receptors (PBRs).<sup>247</sup> PBRs density increase after glia activation following tissue damage.<sup>248</sup>

Glutamate plays an important role in the propagation and maintenance of seizures induced by organophosphates, contributing to secondary brain damage.<sup>249,250</sup> For this reason, NMDA antagonists have been proposed as antidotes against organophosphates poisoning.<sup>250</sup> Standard treatment for poisoning with organophosphates is a pre-treatment with pyridostigmine (a reversible inhibitor of Acetyl-cholinesterase) and the use of anticholinergic agents, like atropine sulfate.<sup>251</sup> Also it was reported the potential beneficial effect of benactyzine or benzodiazepines when administered soon enough.<sup>252</sup>

Due to the important role of glutamate in this pathology, a recent study observed reduced neuronal damage and prevention of the increase in PBRs density in rats treated with oxaloacetate and GOT, after exposure to paraoxon.<sup>253</sup> These promising results showed the potential use of glutamate grabbers as a treatment in organophosphate intoxication.

### 3.5.6.- FOETAL ASPHYXIA AND HYPOXIC-ISCHAEMIC ENCEPHALOPATHY

Foetal asphyxia and hypoxic-ischaemic encephalopathy are two significant causes of perinatal death and developmental disability. In foetal asphyxia, among other causes, the increase

of glutamate extracellular levels plays an important role in neuronal damage. Due to this, the use of glutamate antagonists has been proposed as a therapeutic agent in patients.<sup>254</sup> Nevertheless, the central role of glutamate during brain development has discourage the use of these agents in new-borns. Previous studies have shown a higher concentration of GOT in foetal blood compared with maternal blood.<sup>255</sup> These higher levels of GOT were also related to the blood glutamate, and this is why GOT activity has been proposed to be involved in maintaining non-toxic concentrations of glutamate during brain development, suggesting the potential use of GOT to lower the elevated glutamate levels present in foetal asphyxia.

The relationship between GOT activity and glutamate levels was studied in arterial blood collected from the umbilical cord of new-borns presenting symptoms of hypoxia-ischaemia and control infants. Glutamate concentration and GOT levels were higher in the infants with symptoms compared with the control group. An analysis of perinatal distress markers (Apgar scores and blood pH) showed that severe stress distress conditions were correlated with higher GOT and glutamate levels. The researchers proposed the possibility of GOT acting as an endogenous protective mechanism during foetal development.<sup>256</sup>

### 3.5.7.- AMYOTROPHIC LATERAL SCLEROSIS

The role of glutamate excitotoxicity in amyotrophic lateral sclerosis (ALS) has been extensively documented and remains one of the prominent hypotheses of ALS pathogenesis. Therefore, the development of a therapeutic agent capable of eliminating glutamate excess from brain and spinal cord extracellular fluid without the need of crossing the BBB and with minimal or no adverse effects, could provide a major breakthrough in the ALS treatment. A study conducted by Ruban *et al*, where they combined treatment with oxaloacetic acid and

a recombinant version of the GOT in animal models of sporadic ALS, showed significant protection of spinal cord motor neurons.<sup>257</sup>

### 3.5.8.- GLIOMA

In the last years, the role of glutamate in the growth and development of malignant gliomas, as well as the development of seizures that often accompany them, has been studied.<sup>258-262</sup> Glioma cells in culture have been seen to release huge amounts of glutamate, causing a 1,000-fold increase (100  $\mu$ M) in extracellular glutamate compared with normal conditions.<sup>262</sup> Extracellular glutamate increase has also been observed in peritumoral space in rats<sup>263</sup> and in malignant gliomas and oligodendrogliomas in patients.<sup>264,265</sup> According with these findings, rats and mice treated with a combination of oxaloacetate and GOT had smaller tumour volume, reduced tumour invasiveness and prolonged survival times.<sup>266</sup> All this data suggest the possibility of using glutamate grabbers as a therapeutic agent and add glioma to the list of pathologies involving glutamate excitotoxicity.

### 3.5.9.- ALZHEIMER'S DISEASE

Tohda *et al.* demonstrated that the treatment of cultured cortical neurons with a recombinant version of GOT1 extended axonal growth. Furthermore, continuous intracerebroventricular administration in normal mice for 14 days resulted in enhanced axonal densities and c-Fos expression. Additionally, the treated mice showed a better object recognition ability, assessed by the novel object test.<sup>267</sup> These results suggest the possibility of using GOT as a therapeutic agent in dementia or other memory loss pathologies. In the same way, Rowan *et al.* analysed the effect of GOT in an animal model of Alzheimer`s disease, produced by injecting exogenous amyloid- $\beta$  oligomers or by using a

transgenic rat model. Their results showed that a repeated administration of GOT1 reversed the deleterious effect of the exogenous amyloid- $\beta$  on synaptic plasticity as well as its inhibitory effect on long term potentiation.<sup>268</sup> Similar results were obtained by the same group when GOT was activated through the use of oxaloacetate.<sup>269</sup>

### 3.5.10.- OTHER PATHOLOGIES

Besides diseases mentioned above, there is existing data, to a greater or lesser extent, of the potential use of GOT in other pathologies. In the first place, as we mentioned above, there is an abnormal increase of glutamate levels in serum during and after stroke. Additionally to the implications in ischaemic stroke, discussed before, these glutamate levels during ischaemic injury have also been related with the development of post-stroke depression.<sup>270</sup> In correlation with this, some authors have proposed glutamate blood scavenging strategy, where the use of GOT is included, as a potential therapeutic approach for this pathology.<sup>271</sup>

Finally, it has been observed that there is an excess of glutamate concentration in multiple sclerosis, as well as multiple abnormalities in glutamate degrading enzymes, glutamate transporters, glutamate receptors and glutamate signalling. Furthermore, T cells, one of the main agents involved in this pathology, express several types of functional GluRs and glutamate can activate resting normal human T cells and induce T cell functions, like T cell adhesion, chemotactic migration, cytokine secretion or gene expression. Moreover, T cells are capable of producing and releasing glutamate, affecting both other cells and themselves. Due to this, it has been proposed that the glutamate scavenging strategy, in particular the use of GOT, could be a suitable therapy for this disease, although no experimental studies have been conducted yet.<sup>272</sup>

# HYPOTHESIS



Stroke continues to be one of the main causes of mortality and disability in the world and its prevalence is expected to increase in the incoming years. Despite the amount of effort, no neuroprotective drug has shown successful results for this pathology so far.

Glutamate, the most common excitatory neurotransmitter, plays a central role in neuroexcitotoxicity related with ischaemic injury, being responsible for the neuronal damage produced during the acute phase of ischaemic stroke. GOT, a transaminase enzyme, plays a major role in glutamate metabolism and homeostasis. High levels of this protein have been correlated with a better clinical outcome in stroke patients. In preclinical studies, the use of GOT demonstrated a significant effect in lowering glutamate blood levels and its therapeutic use has shown promising results in animal models of ischaemia, both regarding infarct volume and sensorimotor outcome. However, for a future clinical application of this therapy, the protective efficacy of the recombinant form of the human GOT1 has never been validated.

**Based on the above-mentioned observations, we hypothesize that the use of a recombinant version of the human enzyme GOT1 could lead to a reduction of blood glutamate levels, resulting in a reduction of infarct volume and the amelioration of neurological deficit, without triggering undesirable adverse side effects.**



## OBJECTIVES



The main goal of this Thesis was to study the effect on ischaemic stroke and the therapeutic potential of a recombinant version of the human GOT1 (rGOT1). In order to do that, the following secondary objectives were established.

- 1.- Analysis on an ischaemic animal model of the blockade of endogenous GOT1 by means of a specific monoclonal antibody.
- 2.- Study of pharmacokinetics and therapeutic effect of rGOT1 on ischaemic animals.
- 3.- Analysis of pharmacokinetics and therapeutic effect on ischaemic animals of rGOT1 bioconjugates.
- 4.- Study of the interaction between rtPA and the rGOT1.



# MATERIALS AND METHODS



## 4.- SECTION I: ENDOGENOUS GOT1 INHIBITION STUDIES

The aim of this additional study was to evaluate how the inhibition of GOT1 affects brain metabolism and ischaemic damage. In order to do so, we administered a monoclonal antibody targeting the endogenous GOT1 to block its activity and measured different parameters regarding brain infarct and behaviour.

### 4.1.- Synthesis and Production of Anti-rGOT1 Antibody

The synthesis and production of an anti-GOT1 antibody was performed in collaboration with Dr. Aharon Rabinkov and Prof. Dr. David Mirelman, from the Weizmann Institute of Science (Rehovot, Israel).

The synthesis of the anti-GOT1 antibody (AbGOT1) was done using the following protocol.<sup>273</sup> A human GOT1 cDNA was cloned from a human hepatoma cell line (hepG2). Then, the recombinant version of the enzyme, identical to the native version, was expressed in *Escherichia coli* cells, purified by Ni-agarose chromatography as previously described<sup>125,274</sup> and used as the immunization antigen. Then, two albino rabbits were injected intramuscularly (I.M.) with 50 µg of the rGOT1 in complete Freund's adjuvant and boosted three times with a three-week interval. Three weeks after each administration, test bleedings were performed as well as the titer of antibodies against rGOT1 in blood. For this, ELISA tests were performed using plastic plates coated with 5 µg/mL of rGOT1 and determined with a secondary goat anti-Rabbit antibody (Jackson ImmunoResearch Labs, West Grove, PA, USA) conjugated to horse radish peroxidase and diluted 1:50,000. Tetra Methyl Benzidine

substrate (Medicago, Quebec, Canada) was used for colour development and measured in an ELISA reader. Immune serums with the highest titer for AbGOT1 were purified on a Hi-trap Protein A HP 5 mL column (17-0403-0, GE Healthcare, Chicago, Illinois, USA) using the binding buffer and diluent, following the recommendations from the manufacturer. Yields for purified AbGOT1 antibodies were around 10 mg/mL. The purified antibody was capable of neutralizing >95% of human rGOT1 (1.3 ng/mL) at a 1:1,000 dilution (17 µg/mL). The purified AbGOT1 was also capable of reacting on Western Blots at high dilutions (1:5,000).

#### 4.2.- *In vitro* Dose-response Analysis of AbGOT1

To test blocking activity of AbGOT1 on GOT1, blood samples (500 µL) were taken from the tail vein of healthy rats and collected in test tubes (365968, BD, Franklin Lakes, NJ, USA). Samples were allowed to clot for 45 minutes, centrifuged at 1700 g for 7 minutes and serum was collected. Different amounts of AbGOT1 were diluted in 30 µL of PBS and mixed with 20 µL of serum (for a final volume of 50 µL). The different concentrations of AbGOT1 were incubated for 30 minutes at 37°C and then GOT1 enzymatic activity was measured using the Reflotron GOT specific activity tests. For validation of the specific blocking of AbGOT1 on GOT1 activity, an isotype form of the antibody (105009, Thermo Fisher Scientific, Waltham, MA, USA) was used as a negative control.

#### 4.3.- Animal Procedures

For the purpose of this study, 75 animals were used. The summary of all animals, included and excluded, is shown in **Figure 17**.

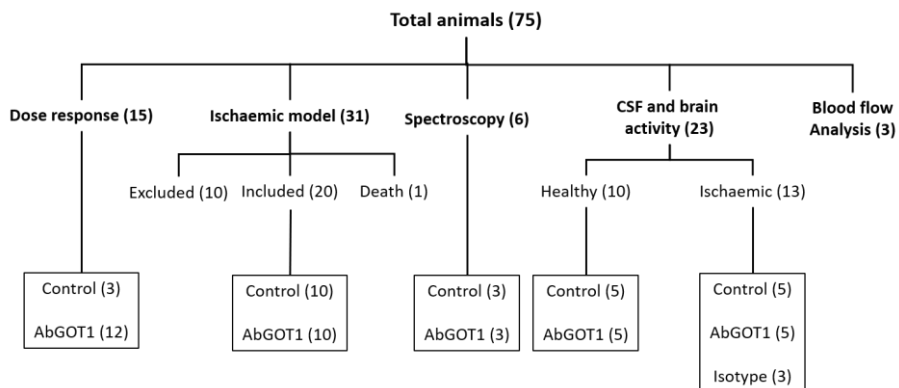


**Figure 17.** Overview of all the animals used in the AbGOT1 studies.

#### 4.3.1.- ANIMAL CARE

Experimental protocols were approved by the University Clinical Hospital of Santiago de Compostela Animal Care Committee under the procedure number: 15010/2019/004, according to the European Union (EU) rules (86/609/CEE, 2003/65/CE and 2010/63/EU) and within the ARRIVE guidelines. Male Sprague-Dawley rats (7-8 weeks) with a weight of 250-300 g were used. Animals were housed at an environmental temperature of 23 °C with 40% relative humidity and had a 12 h light-dark cycle. Rats were watered and fed *ad libitum*. Surgical procedures and magnetic resonance analysis were performed under anaesthetic conditions induced by inhalation of 5% sevoflurane in a nitrous oxide/oxygen mixture (70/30). Rectal temperature was maintained at 37°C + 0.5°C by using a feedback-controlled heating pad (Neos Biotec, Pamplona, Spain). Glucose levels were analysed before surgery (ranging from 180 to 220 mg/dl).

#### 4.3.2.- INHIBITION OF BLOOD GOT1 IN HEALTHY ANIMALS

Similar to *in vitro* analysis, different concentrations were tested in healthy animals in order to determine the right dose for the correct blockade of GOT1 activity. All animals were injected intraperitoneal (I.P.) either with 1 mL of PBS (drug vehicle) or 1 mL of different doses of AbGOT1 (1, 2.5, 4 or 5 mg/rat, n=3/group). Whole blood samples were collected from tail vein (200  $\mu$ L) into test tubes (365975, BD, Franklin Lakes, NJ, USA) under basal conditions (before administration) and after 1, 2, 3, 4, 6, 8 and 10 hours and 1, 2, 3, 4, 6, 8, 10 and 14 days after injection. Blood GOT1 activity was measured using Reflotron.

#### 4.3.3.- ABGOT1 EFFECT IN AN ISCHAEMIC RAT MODEL

To analyse the effect of GOT1 blocking on ischaemia, the dose selected from the previous study was tested in ischaemic rats. The study was divided in two experimental groups, on group treated I.P. with 1 mL of PBS (drug vehicle) and the other treated with 1 mL of AbGOT1 (5  $\mu$ L/rat, n=10/group). Both groups were injected one hour before surgery. Blood samples (500  $\mu$ L) for GOT, GPT and glutamate analysis were collected under basal conditions (before administration) and 1 hour after the injections (right before surgery). Additional blood samples were also collected right after MCA reperfusion (75 minutes after occlusion) and 2, 4 and 6 hours and 1, 2, 4, 7 and 14 days after ischaemia onset.

Cerebral infarct lesion was assessed by means of *in vivo* Magnetic Resonance Imaging (MRI) during arterial occlusion (defined as  $T_0$ ) and 1, 7 and 14 days after ischaemia. Sensorimotor tests were performed in healthy conditions (1 day before surgery) and 7 and 14 days after surgery.

Another two groups of animals, conforming a different set of experimental animals, were also administrated PBS or AbGOT1 as described below (n=3/group). Cerebral glutamate and lactate levels were determined before ischaemia, during MCA occlusion (75 minutes) and 120 minutes after reperfusion, both in ipsilateral and contralateral hemispheres, using the non-invasive Magnetic Resonance Spectroscopy (MRS) technique.

### 4.3.3.1.- Surgical Procedures

Transient focal ischaemia was induced using the transient middle cerebral artery occlusion (tMCAO) model as previously described.<sup>125,199,273</sup> Briefly, under an operating microscope, a midline neck incision was performed and connective tissue was dissected from both common carotids. The right external carotid and the pterygopalatine artery were isolated and ligated by a 6-0 silk suture. A silicon rubber-coated monofilament (403512PK5Re, Docol Corporation, Sharon, MA, USA) was inserted through the external carotid into the left common carotid artery and advanced into the internal carotid artery to 20 mm from the bifurcation to occlude the origin of the MCA. The left common carotid was ligated by a 6-0 silk suture right before the occlusion of the MCA. A laser-Doppler flow probe (MT B500-0L240, Perimed, Järfälla, Sweden) attached to a flowmeter (PeriFlux 5000, Perimed AB, Järfälla, Sweden) was located over the thinned skull in the MCA territory (4 mm lateral to bregma) to obtain a continuous measure of relative cerebral blood flow during the occlusion. Once the artery occlusion was reached, as indicated by Doppler signal reduction, animals were carefully moved from the surgical bench to the MRI system to assess the ischaemic lesion using apparent diffusion coefficient (ADC) maps (defined as  $T_0$ ). Magnetic resonance angiography (MRA) was also performed to ensure that the artery remained occluded throughout the magnetic resonance (MR) procedure. After MR analysis, animals were returned to the surgical bench and the Doppler probe was repositioned. The monofilament was

removed after 75 minutes of occlusion. After its removal, the left pterygopalatine and the right common carotid artery were reperfused while left external carotid (used to introduce the monofilament) remained tied to avoid bleeding. As it has been described elsewhere,<sup>275</sup> this surgical ischaemic protocol, based on the combination of laser Doppler monitoring and ADC and MRA represents a reliable inclusion protocol during ischaemic surgery to reduce intergroup variability and to guarantee the infarct volumes to be reproducible. A schematic view of the surgery can be seen in **Figure 18**.

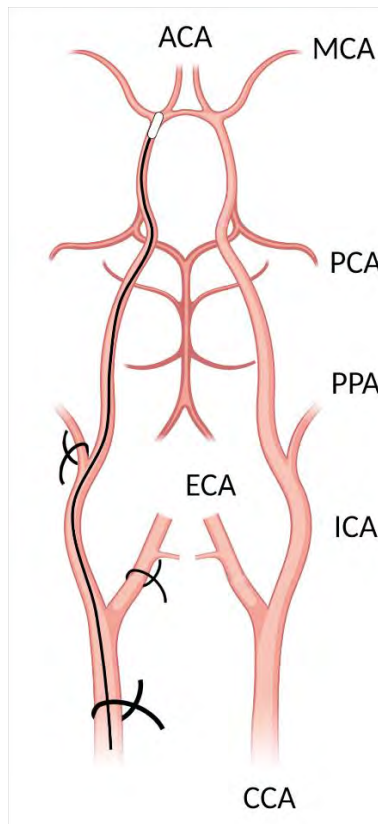


**Figure 18.** Schematic view of tMCAO surgery using the monofilament model. ACA: anterior cerebral artery; CCA: common carotid artery; ECA: external carotid artery; ICA: internal carotid artery; MCA: middle cerebral artery; PCA: posterior cerebral artery; PPA: pterygopalatine artery. Self-created image using BioRender software.

The following exclusion criteria were used: (1) less than 70% reduction in relative cerebral blood flow; (2) vascular abnormalities, as determined by MRA; (3) baseline lesion volume of less than 35% or greater than 45% of the ipsilateral hemisphere, measured using ADC maps; (4) absence of reperfusion or prolonged reperfusion (more than 10 minutes until achievement of at least 50% of the basal cerebral blood flow) after monofilament removal. All excluded or deceased animals were replaced until the total number of animals indicated for each group was attained.

Experimental procedures were performed following 5 criteria derived from the Stroke Therapy Academic Industry Roundtable (STAIR) group guidelines for preclinical evaluation of stroke therapeutics<sup>276,277</sup>: (1) cerebral blood flow was measured to confirm the vascular occlusion as an index of the reliability of the ischaemic model; (2) animals were randomly assigned to treatment groups of the study; (3) researchers were blinded to treatment administration; (4) researchers were blinded to treatments during outcome assessment; (5) temperature was controlled during the ischaemic period.

### 4.3.3.2.- *In vivo* Magnetic Resonance Imaging

Infarct size was assessed by means of MRI. MRI studies were conducted on a 9.4-T horizontal bore magnet (Bruker BioSpin, Ettlingen, Germany) with 12-cm wide actively shielded gradient coils (440 mT/m). Radiofrequency (RF) transmission was achieved with a birdcage volume resonator; signal was detected using a 4-element arrayed surface coil, positioned over the head of the animal. The head of the animal was then fixed with a teeth bar, earplugs, and adhesive tape. Transmission and reception coils were actively decoupled from each other. Gradient-echo pilot scans were performed at the beginning of each imaging session for accurate positioning of the animal inside the magnet bore.

ADC maps were acquired during MCA occlusion (40 minutes after the onset of ischaemia) using a spin-echo echo-planar imaging sequence with the following acquisition parameters: echo time (ET)= 26.91 ms, repetition time (RT)= 4 s, spectral bandwidth (SW) 200 KHz, 7 b-values of 0, 300, 600, 900, 1200, 1600, and 2000 s/mm<sup>2</sup>, flip angle (FA)= 90°, number of averages (NA)= 4, 14 consecutive slices of 1 mm, 24x16 mm<sup>2</sup> field of view (FOV) (with saturation bands to suppress signal outside this FOV), a matrix size of 96x64 (isotropic in-plane resolution of 250 µm/pixel x 250 µm/pixel) and implemented with fat suppression option. Based on previous studies, the values of ADC in the healthy rat brain normally do not fall below 0.55x10<sup>3</sup> mm<sup>2</sup>/s; Therefore, this threshold provides a convenient means of segmenting abnormal tissue.<sup>278</sup>

tMCAO status was evaluated in a non-invasive manner with the time-of-flight magnetic resonance angiography (TOF-MRA). TOF-MRA scan was performed with a 3D-Flash sequence with the following parameters: ET= 2.5 ms, RT=15 ms, FA= 20°, NA= 2, SW= 98 KHz, 1 slice of 14 mm, 30.72x30.72x14 mm<sup>3</sup> FOV (with saturation bands to suppress signal outside this FOV), a matrix size of 256x256x58 (resolution of 120 µm/pixel x 120 µm/pixel x 241 µm/pixel) and implemented without fat suppression option.

Ischaemic lesions were determined from T2-maps calculated from T2-weighted images acquired 1, 7 and 14 days after the onset of ischaemia using a Multi Slice Multi Echo (MSME) sequence with: ET= 9 ms, RT= 3 seconds, 16 echoes with 9 ms echo spacing, FA= 180°, NA= 2, SW= 75 KHz, 14 slices of 1 mm, 19.2x19.2 mm<sup>2</sup> FOV (with saturation bands to suppress signal outside this FOV), a matrix size of 192x192 (isotropic in-plane resolution of 100 µm/ pixel x 100 µm/pixel) and implemented without fat suppression option.

#### 4.3.3.3.- *In vivo* Magnetic Resonance Spectroscopy

MRS was acquired as previously described.<sup>279,280</sup> Local shimming was performed by manual adjustment of first and second-order shim coil currents using a proton-stimulated-echo acquisition mode (STEAM)-waterline sequence. The field homogeneity in a 3x3x3 mm<sup>3</sup> voxel typically resulted in signal line widths of 10-20 Hz for the water signal. *In vivo* 1H magnetic resonance spectra of both hemispheres of the rat brain were acquired by using a STEAM-1H sequence with: ET= 3 ms, mixing time (TM)=10 ms, RT=1500 ms, FA= 90°, NA=128, cubic voxel =3x3x3 mm<sup>3</sup> and acquisition time= 3:15 minutes. Water signal was suppressed by variable power RF pulses with optimized relaxation delays.

Spectra were processed using MestReNova software (Mestrelab Research, Santiago de Compostela, Spain). For the quantitative analysis, glutamate and lactate signals were normalized to the creatine peak/phosphocreatine areas for each single spectrum. MRS was acquired under basal conditions (before the occlusion), during the occlusion (75 minutes) and after reperfusion (40, 80, and 120 minutes after reperfusion).

#### 4.3.3.4.- Sensorimotor Tests

In order to assess the sensorimotor deficits after ischaemic insult a series of different test were performed, using a modified version of already described protocols.<sup>281-283</sup>

- a) **Cylinder test:** this test evaluates asymmetry of forelimbs during the exploratory activity. Animals were put in a cylinder of transparent base of 20 cm diameter. A video camera is located under the cylinder in order to record the vertical exploratory movement of the animal with forelimbs during 5 minutes. For recording analysis, the Virtual Dub (free software) was used. Analysed

behaviours were as follows: number of times that the animal touches the cylinder wall and independent use of each limb in contact with the cylinder wall in each upward movement. Laterality index was calculated as the number of times that the animal touches the cylinder with the impaired forelimb during the ascendant movement divided by the number of total touches (impaired and nonimpaired forelimb contacts). This index is close to 0.5 for healthy animals, and tends to be 0 or 1 for animals that have a preferential use of the right or left paw, respectively.

- b) **Neuroscore:** the animal was suspended by the tail, with its front paws touching a table or another stable surface. The rodent's walking pattern was observed during 1 minute. A sensorimotor score on a scale of 0 to 3 was assigned to rats on the basis of their gait behaviour, being: 0: walking to both sides equally; 1: partial circling; 2: fully circling; 3: death of the animal.
- c) **Rotarod test:** the test was performed using a rotarod apparatus (47650, UgoBasile, Comerio, Italy). The animals were trained for 3 days before ischaemia, 3 times per day. The speed was constant and set at 20 rpm. The time that the animal could stay on the rotarod was measured, establishing 120 seconds as the cut-off limit.

All the sensorimotor tests were performed during the darkness cycle of animal housing, with environmental conditions consistently maintained across examinations and by a researcher blinded to the animal grouping. These tests were performed 1 day before surgery and 7 and 14 days after ischaemia. Baseline functional evaluation is required to test for preoperative bias.

### 4.3.3.5.- Image Analysis

Images were processed using ImageJ (National Institutes of Health, Bethesda, MD, USA) on an independent computer workstation. Ischaemic damage was determined from ADC maps and T2-maps by manually selecting areas of reduced ADC values or hyper intense T2 signal by a researcher blinded to the animal protocols. Infarct size was indicated as the percentage of ischaemic damage with respect to the ipsilateral hemisphere volume, corrected for brain oedema.

### 4.4.- Biochemical Analysis

In addition to the previous studies, focused on the effect of GOT1 blockade on the infarct lesion, we also analysed a series of different biochemical parameters in order to determine what repercussions has the blocking of GOT1 on glutamate and GOT1 levels.

#### 4.4.1.- BLOOD GOT AND GPT ACTIVITY ANALYSIS

35 mL of blood were collected into test tubes and GOT/GPT activity were determined by means of Reflotron GOT/GPT specific activity tests strips following the manufacturer's technical specifications.

#### 4.4.2.- BLOOD GLUTAMATE ANALYSIS

Blood samples were collected in test tubes and centrifuged at 3000 rpm (5804, Eppendorf, Hamburg, Germany) for 7 minutes. Serum was removed and immediately frozen and stored at -80°C. Serum glutamate concentration was determined by high performance liquid chromatography (HPLC) (1260 Infinity II, Agilent Technologies, Santa Clara, CA, USA) using the AccQ-Tag

Precolumn derivatization method for amino acid analysis (Waters, Milford, MA68DX), following a previously described method.<sup>284</sup> In brief, serum samples were centrifuged at 21130 g for 30 minutes using 3 kDa filters (Merck Millipore, Burlington, MA, USA) in order to obtain deproteinized samples. 70  $\mu$ L of borate buffer and 20  $\mu$ L of AccQ-Tag reagent were used for every 10  $\mu$ L of deproteinized sample and incubated in a thermoblock at 55 °C for 10 minutes. Then, samples were analysed using an increasing concentration of acetonitrile as a mobile phase. Chromatograms were analysed using the software provided by the manufacturer and values were expressed as concentration ( $\mu$ M).

#### 4.4.3.- ANALYSIS OF GOT1 LEVELS IN CEREBROSPINAL FLUID AND BRAIN TISSUE

The CSF was obtained from the cisterna magna (CM) and was carried out using the protocol described previously.<sup>285</sup> Briefly, by using the occipital crest as a reference point, a midline incision was made between the ears. The fascia was retracted and muscles dissected until the CM was exposed, which appears as a tiny inverted triangle, outlined by the cerebellum above and medulla below, behind the translucent dural membrane. Once identified the CM, a glass capillary was inserted and a volume of 5  $\mu$ L of CSF was collected at every puncture. Clear CSF was collected in healthy and ischaemic animals (n= 5/group) under basal conditions (before treatment administration) and 2, 4 and 24 hours after administration (in case of healthy animals) or arterial reperfusion (in ischaemic animals). CSF was transferred to a tube and kept frozen at -80°C. GOT activity in CSF was determined by Aspartate Aminotransferase Activity Assay Kit (ab105135, Abcam, Cambridge, UK) which requires a minimum volume of 5  $\mu$ L to perform the analysis.

GOT activity was analysed in the brain tissue of ischaemic animals 2 hours after ischaemic reperfusion. Animals were

sacrificed with overdose of anaesthesia and immediately perfused with cold PBS. The brain was then removed and homogenized on ice to preserve protein levels. Samples were stored at -80°C until further analysis, which was carried out by means of Reflotron GOT specific activity tests following the manufacturer's technical specifications. Total protein content in samples was determined by the BCA protein assay (Thermo Scientific, Waltham, MA, USA). The results were expressed in U/L per mg of protein.

### 4.5.- Statistical Analysis

All data are expressed as mean  $\pm$  SEM. The data were analysed using GraphPad Prism v.8.3.0 for Windows. The criterion for statistical significance was  $P < 0.05$ . Two-way ANOVA test was used to identify significant differences in multiple comparisons followed by a Bonferroni post hoc test. The Student-test was used to identify significant differences between two groups. Data were first examined to assess distribution using the D'Agostino and Pearson omnibus normality test.

## 5.- SECTION II: rGOT1 THERAPEUTIC EFFECT

In this section, we aimed to study the therapeutic effect of the human rGOT1 enzyme on stroke volume and neurological outcome. In order to do that, several experiments were performed either in healthy or ischaemic animals.

### 5.1.- Protein Synthesis

The manufacture of the rGOT1 used in these studies was externalised and performed by **BiotechPharma UAB** (Vilnius, Lithuania), from now on called BTPH. Due to the differences and novelties with respect to the recombinant protein used in our previous studies,<sup>125</sup> the procedure for the synthesis of the

Human Recombinant Glutamate-Oxaloacetate Transaminase 1 (rGOT1) will be presented, including the purification and characterization steps.

### 5.1.1.- BIOSYNTHESIS

rGOT1 is a homodimer polypeptide, consisting of two identical subunits, each one of 412 amino acids with the exact same sequence as the native Glutamate-Oxaloacetate Transaminase 1 (GOT1). Each monomer is bound to a pyridoxal-5'-phosphate (PLP) coenzyme.

A recombinant expression system for the expression of a polyamino acid, peptide, or protein is provided. The polyamino acid of interest is expressed as a fusion protein that includes an amino acid sequence recognized and cleaved by the Ubiquitin-like-specific protease 1 (Ulp1). The amino acid sequence joined to the polyamino acid of interest is preferably from a small ubiquitin-like molecule (SUMO) protein. This sequence imparts favourable solubility and refolding properties to the fusion protein. The Ulp1 protease rapidly and specifically cleaves the fusion proteins at the Ulp1 cleavage site. Research cell bank SUMOGOT1/ $\Delta$ His/pET28/E.coli BL21(DE3) (without His6x-link) was prepared by BTPH.

The recombinant organism *Escherichia coli* SUMO-GOT1/ $\Delta$ His/pET28/E.coli BL21(DE3) from the research cell bank was grown for 17-19 hours in a 1 L Erlenmeyer flask containing 0.5 L of growth medium. The flask is incubated in a shaker incubator at  $30\pm 2^\circ\text{C}$  and  $300\pm 50$  rpm shaking speed. Then, the optical density of the inoculum is measured at a 600 nm wavelength and seeding volume is calculated in order to obtain approximately 0.5 arbitrary units (AU) cell density in a 12 L working volume (15L total volume) fermenter (Applikon, Delft, Netherlands). A sample for culture purity is taken and tested by plating on nutrient media.

Fermentation media is prepared (7.7 L) and autoclaved together with 15 L fermenter. 0.7 seven litres of glucose and phosphate solutions are prepared and autoclaved separately and are transferred to the fermenter aseptically before fermentation. Base solution for pH maintenance and antifoam solution for foam control are also prepared separately and connected to the fermenter system before biosynthesis. The phosphate feeding solution and glucose feeding solution are prepared and autoclaved prior to biosynthesis. Isopropyl- $\beta$ -D-1-thiogalactopyranoside (IPTG) solution for induction of SUMO-GOT1 cells during biosynthesis is prepared and sterilized using a sterile 0.2  $\mu$ m filter shortly prior to usage. Before seeding the calculated volume of inoculum, pH, temperature, agitation and dissolved oxygen control are established.

Set points of fermentation parameters are 37°C (up to the induction point) and 25°C (after induction point). Temperature is ensured by controlled water flow in jacketed fermenter. pH is adjusted to 6.8 with ammonia solution. O<sub>2</sub> is maintained at 20% with air and oxygen gasses. The culture is grown at 37°C until cell optical density reaches 65-85 AU at which point sterile IPTG solution is added. After induction the culture is grown for 3.5 hours at 25°C. Concentration of glucose (maintained at 17.0 g/L at feeding point) is measured and adjusted every 30 min after cell density reaches 20 AU, and every 15 min after cell density reaches 60-70 AU. Carbon feed is adjusted according to measured glucose concentration in the growth media. Four portions of phosphate solution are added during fermentation. The first portion is added when cell density reaches 60-70 AU and the rest are added: 1 hour, 1.5 hours and 2 hours after induction. At the end of the fermentation the biomass is harvested and centrifugation is performed. After the end of the fermentation, testing of the purity and the plasmid stability are performed by plating samples on nutrient media. The biomass from the fermenter is transferred to centrifugation bottles and centrifuged at 12,227 $\times$ g for 20 minutes at 4°C. The biomass is

then removed from the centrifuge bowls and transferred to plastic bags for further storage. The bags are placed in refrigerator at -33°C. For total concentration of proteins, a sample is taken not earlier than 12 hours since freeze storage and tested by SDS-PAGE analysis and gel scanning for SUMO-GOT1 quantity.

### 5.1.2.- PURIFICATION

Frozen pieces of the biomass (1570-1830 g) were removed from bags. The cells are reconstituted in a vessel with buffer solution W-A02 at 3 mL/g of cell paste at temperature 4-8°C. The cells are disrupted using a high-pressure homogenizer at a pressure of 900 bar for 3 cycles. The suspension is centrifuged, precipitate is discarded, and protein solution is used for the next steps.

Suspension is heated with stirring in the water bath and when 50°C is reached  $\alpha$ -ketoglutarate (COW-B01) and PLP hydrate (COW-B02) are added to final concentration of 10 mM ( $\alpha$ -ketoglutarate) and 20  $\mu$ M (PLP). Temperature is increased to 65-70°C and incubated at this temperature for  $10 \pm 1$  min. After cooling to 2-10°C, the denatured material is removed by centrifugation. The supernatant is collected and the pH is adjusted to 7.90-8.10.

Add 1 mM of dithiothreitol (DTT) to the protein solution after the heating treatment. One millilitre of SUMO protease is added and the temperature for cleavage is kept at 4-10°C for 10-24 hours.

After deSUMOylation solid ammonium sulfate is added to the protein solution, to a concentration of 300 g/L. This solution is stirred at room temperature for 20 minutes and centrifuged. The pellets are discarded and additional amount of ammonium sulfate (130 g/L) are added to the supernatant fluid under continuous stirring. After 20-min storage at 4-10°C the final

pellets are collected by centrifugation and dissolved in PBS buffer at 20 mL/g of pellets.

Three chromatographic steps are utilized to purify the rGOT1 intermediate material: Mixedmode interaction using medium PPA Hyper Cel Resin (bed high 15.3-15.8 cm), Ion-Exchange chromatography using CM-Sepharose FF (bed high 9.4-9.9 cm), and Q Sepharose FF (bed high 9.2-10.2 cm).

After pellets are dissolved, PPA Hyper Cel Resin chromatography is performed. Protein solution pH is adjusted to 4.75-4.85, loaded and then eluted with a low pH buffer solution (W-D02) into a vessel. Fractions with optical density between 80 mAU (up) and 45 mAU (down) are collected.

The eluted protein after Mixedmode chromatography is loaded and then eluted with an increasing pH (W-E02) into a clean vessel. The protein fraction is collected from 80 mAU (up) till 35 mAU (down), the pH is adjusted to 5.90-6.10, and conductivity to 2.0-2.2 mS/cm.

The protein fraction is diluted until conductivity is less than 2 mS/cm; pH is adjusted to pH 6.00 and loaded on the column. The protein fraction in flow-through is collected from 35 mAU (up) to 30 mAU (down).

The protein fraction after Q Sepharose FF is concentrated, using a 30 kDa membrane, to 15-20 mg/mL. One hundred diafiltration volumes are used for buffer exchange to 20 mM sodium acetate, pH 5.0. Final protein concentration is  $10 \pm 2$  mg/mL. Transmembrane pressure is from 0.3 to 0.6 bar.

### 5.1.3.- CHARACTERIZATION

In order to characterize the sequence, size, secondary structure and specific activity of the rGOT1, different analyses were performed.

### 5.1.3.1.- Sequencing

First, a preliminary SDS-PAGE analysis was done in order to compare the rGOT1 with the native enzyme isolated from red blood cells (RBC). Then, the sequence analysis and comparison between the two proteins were performed twice.

The first attempt was carried out by Smoler Proteomics Center (Haifa, Israel). Human RBC GOT1 and rGOT1 protein samples were reduced, carbamidomethylated, and digested with trypsin. The second attempt was carried out by the National Proteomics Center (Israel). Samples were prepared in two ways: digestion with trypsin followed by desalting and microwave-assisted acid hydrolysis followed by desalting. In both comparisons, the resulting peptides were analysed by liquid chromatography-tandem mass spectrometry and compared to peptide sequence databases.

### 5.1.3.2.- Secondary Structure Analysis

The secondary structures of human RBC GOT1 and rGOT1 were determined using circular dichroism (CD) spectroscopy. Samples of both proteins were diluted to achieve matching absorbance so the protein solutions had the same concentration.

### 5.1.3.3.- Specific Activity

GOT1 specific activity was measured using Reflotron (Roche, Basel, Switzerland). Specific activity tests for GOT1 were conducted according to the manufacturer's technical specifications.

## 5.2.- Animal Procedures

For the evaluation of the therapeutic effect of the rGOT1, 586 animals were used (between included and excluded animals) divided in several groups for the different analyses, as shown in **Figure 19**.

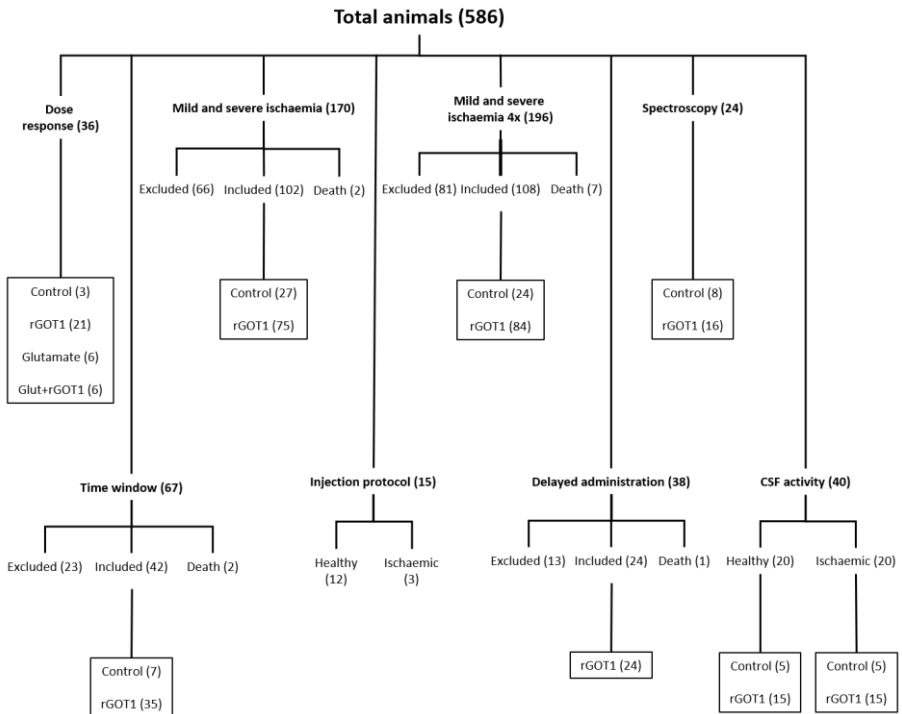


**Figure 19.** Overview of all the animals used in the rGOT1 therapeutic effect studies.

### 5.2.1.- ANIMAL CARE

Experimental protocols were approved by the University Clinical Hospital of Santiago de Compostela Animal Care Committee under the procedure number: 15010/2019/004, according to the European Union (EU) rules (86/609/CEE, 2003/65/CE and

2010/63/EU) and within the ARRIVE guidelines. Male Sprague-Dawley rats (7-8 weeks) with a weight of 250-300 g were used. Animals were housed at an environmental temperature of 23 °C with 40% relative humidity and had a 12 h light-dark cycle. Rats were watered and fed *ad libitum*. Surgical procedures and magnetic resonance analysis were performed under anaesthetic conditions induced by inhalation of 5% sevoflurane in a nitrous oxide/oxygen mixture (70/30). Rectal temperature was maintained at 37°C + 0.5°C by using a feedback-controlled heating pad (Neos Biotec, Pamplona, Spain). Glucose levels were analysed before surgery (ranging from 180 to 220 mg/dl).

#### 5.2.2.- PHARMACOKINETICS AND DOSE RESPONSE STUDY

In order to analyse the pharmacokinetics of rGOT1 and its effect on blood glutamate concentration, a set of animals (n=3/group) were injected either with PBS (control group) or with different amounts of rGOT1 (0.06, 0.12, 0.24, 0.50, 1, 2 and 4 mg/kg). Animals were injected I.V. and blood was collected in test tubes under basal conditions (previous to injection) and at 1, 2, 3, 4, 5 and 6 hours and 1, 2, 4, 6, 8 and 10 days. GOT levels were measured using Reflotron and blood glutamate concentration was analysed using HPLC as previously described (see **Sections 4.4.1 and 4.4.2**).

To further analyse the effect of rGOT1 on blood glutamate, another set of animals (n=6) were injected I.V. with 1 mL of glutamate 1 M 30 minutes after being injected I.V. either with 1 mL of PBS or 1 mL of rGOT1(0.24 mg/kg). Blood was collected into test tubes under basal conditions (prior to PBS or rGOT1 administration) and at 30 minutes, 1, 2, 4 and 6 hours and 1 and 2 days. GOT and glutamate measures were performed as in previous sections.

### 5.2.3.- SURGICAL PROCEDURES

The ischaemic model selected for these studies was the tMCAO. All the experiments were performed following the STAIR criteria and the same inclusion and exclusion criteria as before. To see the detailed version of inclusion criteria, STAIR criteria and tMCAO protocol, refer to previous section (**Section 4.3.3.1**).

### 5.2.4.- THERAPEUTIC TIME WINDOW

After analysing the behaviour of rGOT1 in healthy animals, a study to analyse the therapeutic time window of the enzyme was done. Several groups of ischaemic animals (n=7 animals/group) were injected either with PBS (right after reperfusion) or with 0.24 mg/kg of rGOT1 at different times (0, 1, 2, 4 and 6 hours after reperfusion).

Blood samples were collected under basal conditions (previous to surgery), right after reperfusion and every 2 hours until 6 hours after reperfusion or 4 hours after treatment administration, whichever came later. GOT measures were done using the Reflotron. MRI analysis were performed as described above (**Section 4.3.3.2**) during the occlusion of the MCA (MRA and ADC maps) and 1, 7 and 14 days after ischaemia (T2 maps). Sensorimotor tests were performed one day before surgery and 7 and 14 days after ischaemia as previously described (**Section 4.3.3.4**). In addition to the test previously described, another test was added to the battery, the grip strength test. This test, performed as described elsewhere<sup>286</sup>, consisted of a small leaky rack attached to a digital measure system to analyse the grip strength of the animals. In brief, animals were handled by the tail and carefully approached to the grip rack, allowing them to grab on it just with the forelimbs, to finally pull back the animal to measure the strength they grabbed the rack with.

### 5.2.5.- THERAPEUTIC EFFECT ON SEVERE AND MILD ISCHAEMIA

After the time window analysis, a study to evaluate the different therapeutic effect of rGOT1 in long and short occlusion times was done. Mild ischaemia was defined as an infarct volume of 20-30% at 24 hours without a midline shift. On the other hand, severe ischaemia was defined as animals presenting an infarct volume of 30-40% at 24 hours with a pronounced midline shift (**Figure 20**). For this study, two different occlusion times were selected: 75 (severe ischaemia) and 45 (mild ischaemia) minutes. For the 45 minutes occlusion, animals (n=15 per group) were treated either with PBS or rGOT1 (1 mg/kg). In the 75 minutes occlusion, various sets of animals (n=12 animals/group) were injected either with PBS or with different doses of rGOT1 (0.24, 0.5, 1, 2 and 4 mg/kg). Treatments were administered right after reperfusion.



**Figure 20.** T2-weighted images at 24 hours of three representative animals: healthy and submitted to mild and severe ischaemi. The dotted line represents the midline.

Then, four doses of the treatment were injected in two new groups of mild and severe ischaemia. Animals submitted to severe ischaemia (n=12 per group) were injected with the same treatments as before, while the mild ischaemia group (n=12 per group) was treated either with PBS or with 0.5 or 1 mg/kg of

rGOT1. Treatments were administered 0, 2, 5 and 8 hours after reperfusion.

Blood and serum samples were collected under basal conditions (right before surgery) and after 0, 2, 5 and 8 hours and 1, 7 and 14 days after reperfusion. GOT measures were done using a Reflotron device and a fraction of the animals from the 75 minutes occlusion (n=6 animals/group) were randomly selected to perform glutamate measurements using HPLC analysis. MRI imaging was performed during occlusion (MRA and ADC maps) and 1, 7 and 14 days after ischaemia (T2 maps). Sensorimotor tests were performed under basal conditions (1 day before surgery) and 7 and 14 days after occlusion, using the same protocols as described in **Section 5.2.4**.

### 5.2.6.- INJECTION PROTOCOL

In order to mimic a perfusion administration of the drug, different injection protocols were performed to analyse the pharmacokinetics of the drug and obtain the most suitable time points of administration.

Three different protocols were tested in healthy rats (n=3 animals/group) using the dose of 0.24 mg/kg, injected at different times. The third protocol, selected as the most suitable, was repeated with a dose of 0.50 mg/kg. Blood extractions were done under basal conditions (before the first injection), every hour up to 11 hours and at 24 and 48 hours.

A group of ischaemic animals (n=3) was treated using the third protocol. Blood extractions were done under basal conditions (prior to surgery) and at 0, 2, 5, 8, 11, 24 and 48 hours after reperfusion. All GOT measures were performed using a Reflotron device. A schematic view of the protocols is presented, along with the results obtained, in **Section 9.5**.

### 5.2.7.- ANALYSIS OF GOT1 LEVELS IN CEREBROSPINAL FLUID

The CSF was obtained using the protocol described in previous sections (see **Section 4.4.3**). A volume of 5  $\mu$ L of CSF was collected at every puncture.

For GOT1 measures, animals (n=5 animals/group) were treated either with saline or with different doses of rGOT1: 1 and 4 mg/kg (one injection) and 1 mg/kg (four injections following the injection protocol selected in **Section 5.2.6**). Clear CSF was collected in healthy and ischaemic animals under basal conditions (before treatment administration) and 2, 4 and 24 hours after administration (in case of healthy animals) or arterial reperfusion (in ischaemic animals).

CSF was transferred to a tube and kept frozen at  $-80^{\circ}\text{C}$ . GOT activity in CSF was determined by Aspartate Aminotransferase Activity Assay Kit (ab105135, Abcam, Cambridge, UK) which requires a minimum volume of 5  $\mu$ L to perform the analysis. Glutamate was measured using the Glutamate Assay Kit (ab252893, Abcam, Cambridge, UK). Both measures were performed following the manufacturer guidelines.

### 5.3.- Statistical Analysis

All data are expressed as mean  $\pm$  SEM. The data were analysed using GraphPad Prism v.8.3.0 for Windows. The criterion for statistical significance was  $P < 0.05$ . Two-way ANOVA test was used to identify significant differences in multiple comparisons followed by a Bonferroni post hoc test. The Student-test was used to identify significant differences between two groups. Data were first examined to assess distribution using the D'Agostino and Pearson omnibus normality test.

## 6.- SECTION III: rGOT1 BIOCONJUGATION

In order to extend the half-life of rGOT1, a bioconjugation of the enzyme was proposed.<sup>287</sup> The synthesis and purification of the bioconjugates, as well as the protective studies, were performed in collaboration with Dr. Ahlem Zaghmi and Prof. Dr. Marc Gauthier, from the Institut National de la Recherche Scientifique (Québec, Canada).

### 6.1.- Synthesis of mPEG-rGOT1 and Angiopep-PEG-rGOT1

To prepare mPEG-rGOT1, a 3 mL solution of rGOT1 (7 mg/mL) was prepared in potassium phosphate buffer (100 mM, pH 7.2). To this solution, 50 equivalents of  $\alpha$ -Methoxy,  $\omega$ -succinimidyl carboxymethyl ester poly(ethyleneglycol) (mPEG) were added and the reaction mixture was mildly stirred for 30 minutes at room temperature in a sealed glass vial. After this period, mPEG-rGOT1 was purified by size-exclusion chromatography (SEC) using a fast protein liquid chromatographer (FPLC) (ÅKTA Start, Thermo Fisher Scientific, Waltham, MA, USA) equipped with a HiPrep 16/60 Sephacryl™ S200 HR column (Thermo Fisher Scientific, Waltham, MA, USA).

Filtered (0.2  $\mu$ m) potassium phosphate buffer (100 mM, pH 7.2) was used to elute samples at a flow rate of 0.8 mL/min. The column was equilibrated for 0.2 column volumes before sample injection and elution occurred over 120 mL (1 column volume) while continuously collecting 4mL fractions. To prepare Angiopep-PEG-rGOT1, rGOT1 was modified with  $\alpha$ -maleimide,  $\omega$ -succinimidyl carboxymethyl ester poly(ethyleneglycol) (Mal-PEG) and purified according to the procedure above. Following purification by SEC, the collected fractions containing Mal-PEG-rGOT1 were concentrated by centrifugal dialysis at 30 kDa molecular weight cut off (MWCO) and added directly to a vial

containing Angiopep (2 equivalent relatives to the expected amount of Mal on the conjugate). The solution was left for 30 min at room temperature, then incubated for 24 h at 4 °C in the dark.

Angiopep-PEG-rGOT1 was isolated from residual Angiopep by centrifugal dialysis (MWCO 30 kDa) at 5000xg for 60 min at 4 °C. The conjugates were stored frozen at -20 °C until used.

To determine the degree of PEGylation of the bioconjugates, SDS-PAGE was performed. rGOT1 (5 µg in 3 µL water) and rGOT1 bioconjugates (5 µg protein in 3 µL water) were mixed with 5 µL of loading buffer (65mM Tris-HCl, pH 6.8, 2% SDS, 10% glycerol, and 0.1% bromophenol blue). Gels were run in Tris/glycine/SDS (3.0/14.4/1.0 g/L) buffer pH 8.3, under constant voltage (100 V) for ~90 min.

The gels were imaged using an UVP Biodoc-it (Thermo Fisher Scientific, Waltham, MA, USA) imaging system running UVP VisionWorksLS™ software.

The degree of PEGylation was determined by <sup>1</sup>H NMR spectroscopy using an Av300 spectrometer (Bruker, Billerica, MA, USA) operating at 300 MHz for protons, as described elsewhere<sup>288</sup>. This parameter was also determined by UV-Vis spectroscopy. For this, a known mass of bioconjugate was dissolved in a known volume of distilled water. The number of moles of the rGOT1 component of the bioconjugate in the solution was determined via the absorbance at 280 nm and the extinction coefficient of rGOT1 (140,000/M.cm). Dividing the mass of the bioconjugate by the number of moles of the rGOT1 component yields the molecular weight of the bioconjugate, from which the degree of PEGylation can be determined ( $[MW_{\text{Bioconjugate}} (\text{kDa}) - MW_{\text{rGOT1}} (\text{kDa})] \div MW_{\text{PEG}} (5 \text{ kDa})$ ). mPEG does not absorb significantly at this wavelength and thus does not interfere with quantification of molecular weight.

The molecular weight distribution of the bioconjugates was analysed by aqueous SEC using a 1260 HPLC (Agilent Technologies, Santa Clara, CA, USA) equipped with two Bio-SEC5 columns (Agilent Technologies, Santa Clara, CA, USA) mounted in series (5  $\mu\text{m}$ , 7.8  $\times$  300 mm), with 1000 Å and 2000 Å nominal pore sizes, a 1200 Infinity photodiode array detector VL, and a 1290 Infinity II evaporative light scattering detector. 100  $\mu\text{L}$  of a 0.5 mg/mL sample solution prepared in ammonium formate buffer (100 mM, pH 3.5) was injected and eluted with ammonium formate buffer (100 mM, pH 3.5) at 1 mL/min at 25  $^{\circ}\text{C}$ .

## 6.2.- Animal Procedures

For the purpose of this study, 67 animals were used. The summary of all animals, included and excluded, is shown in **Figure 21**.

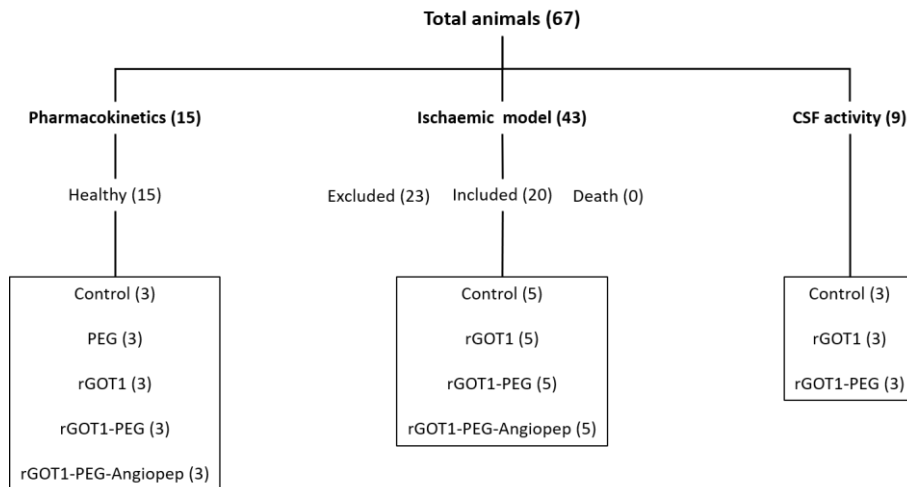


**Figure 21.** Overview of all the animals used in the rGOT1 modifications studies.

### 6.2.1.- ANIMAL CARE

Experimental protocols were approved by the University Clinical Hospital of Santiago de Compostela Animal Care Committee, according to the European Union (EU) rules (86/609/CEE, 2003/65/CE and 2010/63/EU) and within the ARRIVE guidelines. Male Sprague-Dawley rats (Harlan Laboratories, Barcelona Spain) weighing 250-300 g (8-10 weeks) were used. Animals were housed at an environmental temperature of 23 °C with 40% relative humidity and had a 12 h light-dark cycle. Rats were watered and fed *ad libitum*. Surgical procedures and magnetic resonance analysis were performed under anaesthetic conditions induced by inhalation of 5% sevoflurane in a nitrous oxide/oxygen mixture (70/30). Rectal temperature was maintained at 37°C + 0.5°C by using a feedback-controlled heating pad (Neos Biotec, Pamplona, Spain). Glucose levels were analysed before surgery (ranging from 180 to 220 mg/dl).

### 6.2.2.- SURGICAL PROCEDURES

The ischaemic model selected for these studies was the tMCAO. All the experiments were performed following the STAIR criteria and the same inclusion and exclusion criteria as before. To see the detailed version of inclusion criteria, STAIR criteria and tMCAO protocol, refer to previous section (**Section 4.3.3.1**).

### 6.2.3.- PHARMACOKINETICS AND PHARMACODYNAMICS IN HEALTHY RATS

Several groups of healthy animals (n=3 animals/group) were administered 1mg/kg (protein equivalent) of rGOT1, mPEG-rGOT1, or Angiopep-PEG-rGOT1 in 1mL sterile saline by I.V. injection via the tail vein. Control groups (n=3 animals/group) received either 1mL of saline or 1.3mg/kg mPEG (equivalent to

the amount administered for the bioconjugates). Serum samples were collected at 1, 2, 4, and 6 h and 1, 2, 4, 6, 8, 14, 21, and 30 days.

Furthermore, CSF was collected from rats treated with 1 mg/kg (protein equivalent) of rGOT1, mPEG-rGOT1 or saline (control). CSF was obtained from the CM following the protocol described before (see **Section 4.4.3**). A volume of 3–5  $\mu\text{L}$  of CSF was collected under basal conditions (prior to administration) and at 2, 4 and 24 hours. CSF was transferred to a tube and kept frozen at  $-80\text{ }^{\circ}\text{C}$  until used.

### 6.2.4.- PHARMACOKINETICS IN ISCHAEMIC RATS AND PROTECTIVE STUDY

Different sets of animals ( $n=5$  animals/group) were injected either with 1 mL of saline (control group) or with 1 mg/kg (protein equivalent) of rGOT1, mPEG-rGOT1 or Angiopep-PEG-rGOT1. Treatments were administered via tail vein injection immediately after reperfusion. The serum GOT activity was determined under basal conditions (before surgery) and at 1 and 6 hours and 1, 2, 3, 4, 6, 8, 14, 21 and 30 days after arterial reperfusion. MRI imaging was performed as previously described (**Section 4.3.3.2**) during occlusion (MRA and ADC maps) and 1, 3, 7, 14, 21 and 30 days after ischaemia (T2 maps). Cylinder and Rotarod test (as described in **Section 4.3.3.4**) were performed under basal conditions (1 day before surgery) and 3, 7, 14, 21 and 30 days after occlusion.

### 6.3.- Biochemical Analysis

In addition to the previous studies, focused on the effect of GOT1 blockade on the infarct lesion, we also analysed a series of different biochemical parameters in order to determine the

repercussions the blocking of GOT1 has on glutamate and GOT1 levels.

### 6.3.1.- ANALYSIS OF GOT ACTIVITY IN SERUM AND CSF

Blood samples were collected in test tubes and immediately centrifuged at 3170 g for 7 min for collection of serum that was stored frozen ( $-80\text{ }^{\circ}\text{C}$ ) until analysed. GOT activity, in serum and CSF, was determined by means of an Aspartate Aminotransferase activity assay kit (Abcam, Cambridge, UK) following the manufacturer's recommended protocol.

### 6.3.2.- MONITORING OF GLUTAMATE CONCENTRATION IN SERUM AND CSF BY HPLC

The concentration of glutamate was determined using a pre-column derivatization HPLC method. For serum, samples ( $7.5\text{ }\mu\text{L}$ ) were deproteinized with  $30\text{ }\mu\text{L}$  ice-cold methanol. The solution was vortexed and then centrifuged at  $20,000 \times g$  for 5min at  $4\text{ }^{\circ}\text{C}$ . The pellet was discarded and  $25\text{ }\mu\text{L}$  of the supernatant was collected and mixed with  $5\text{ }\mu\text{L}$  20% SDS in water and  $25\text{ }\mu\text{L}$  0.1M sodium tetraborate (pH 9.5). Thereafter,  $50\text{ }\mu\text{L}$  of o-phthaldialdehyde/2-mercaptoethanol derivatization solution (freshly prepared by dissolving 50mg of o-phthaldialdehyde in 1.25mL of absolute methanol, followed by the addition of  $50\text{ }\mu\text{L}$  of 2-mercaptoethanol and 11.2mL of 0.1M sodium tetraborate, pH 9.5) was added and mixed thoroughly.

Subsequently,  $50\text{ }\mu\text{L}$  of 1M sodium acetate (pH 7.2) was added and the mixture was injected into the equilibrated HPLC column. For the CSF, the same volume ratios were followed using a sample volume of  $3.5\text{ }\mu\text{L}$ . Samples were analysed using an increasing concentration of acetonitrile as a mobile phase. Analytes were separated at  $30 \pm 2\text{ }^{\circ}\text{C}$  on a ZORBAX Eclipse AAA C18 reverse-phase column (Agilent Technologies, Santa Clara,

CA, USA) and detected by fluorescence ( $\lambda_{\text{ex}}=340$  nm and  $\lambda_{\text{em}}=450$  nm). Chromatograms were analysed using the software provided by the manufacturer and values were expressed as concentration ( $\mu\text{M}$ ).

### 6.4.- Statistical Analysis

All data are expressed as mean  $\pm$  SEM. The data were analysed using GraphPad Prism v.8.3.0 for Windows. The criterion for statistical significance was  $P < 0.05$ . Results from pharmacokinetic data were compared by one-way ANOVA followed by a Tukey post hoc test. Infarct volumes and motor tests data were compared by a two-way ANOVA followed by a Bonferroni post hoc test. Data were first examined to assess distribution using the D'Agostino and Pearson omnibus normality test.

## 7.- SECTION IV: rGOT1 AND rtPA INTERACTIONS

The purpose of this study is to analyse the possible interactions between the rtPA and rGOT1, in case rtPA eligible subjects could be treated in combination with rGOT1.

### 7.1.- *In vitro* Analysis

For the tPA activity measures, the SensoLyte AMC tPA Activity Assay Kit (AS-72160, AnaSpec, Fremont, CA, USA) was used following the protocol provided by the manufacturer. In brief, the kit contains a fluorogenic substrate used as an indicator of the tPA activity.

Two different experiments were performed regarding the *in vitro* analysis. For the first one, a single time point was used (30 minutes) and rtPA ( $0.1 \mu\text{M}$ ) was incubated with different

concentrations of the inhibitor (Leupeptine) or rGOT1, ranging from 0.01 ( $\mu\text{M}$  for the inhibitor and mg/mL for rGOT1) to 10000 in ten-fold increases.

For the second experiment, a kinetic of the rtPA activity was done, using measures between 0 and 60 minutes, every five minutes. In this case, the rtPA (0.1  $\mu\text{M}$ ) was incubated with a fixed concentration either of the inhibitor (10 mM) or rGOT1 (10 mg/mL).

## 7.2.- Animal Procedures

For the purpose of this study, 136 animals were used. The summary of all animals, included and excluded, is shown in **Figure 22**.

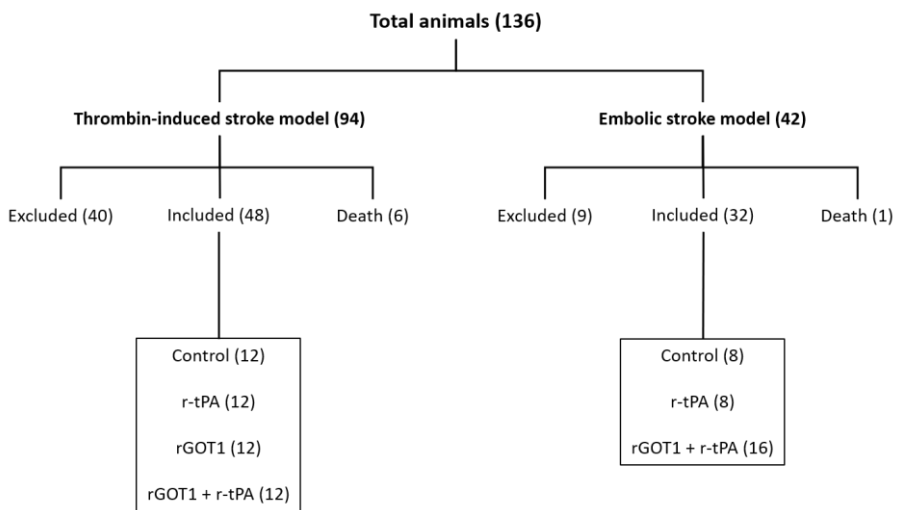


**Figure 22.** Overview of all the animals used in the rGOT1 and rtPA interactions studies.

### 7.2.1.- ANIMAL CARE

Experimental protocols were approved by the University Clinical Hospital of Santiago de Compostela Animal Care Committee, according to the European Union (EU) rules (86/609/CEE, 2003/65/CE and 2010/63/EU) and within the ARRIVE guidelines. Male Sprague-Dawley rats (7-8 weeks) with a weight of 250-300 g and male Swiss mice with a weight of 25-30 g (4-5 weeks) were used. Animals were housed at an environmental temperature of 23 °C with 40% relative humidity and had a 12 h light-dark cycle. Rats were watered and fed *ad libitum*. Surgical procedures and magnetic resonance analysis were performed under anaesthetic conditions induced by inhalation of 5% sevoflurane in a nitrous oxide/oxygen mixture (70/30). Rectal temperature was maintained at 37°C ± 0.5°C by using a feedback-controlled heating pad. Glucose levels were analysed before surgery (ranging from 180 to 220 mg/dl).

### 7.2.2.- THROMBIN-INDUCED STROKE MODEL

Four sets of ischaemic animals (n=12 animals/group) were treated with saline (control group), rtPA (10 mg/kg), rGOT1 (0.24 mg/kg) or a combination of rtPA and rGOT1. The treatments were administered I.V. through the tail vein as a 10% bolus and 90% perfusion (rtPA) or as a bolus (saline and rGOT1). In the combined treatment group, the rtPA was administered right after the rGOT1 bolus. Blood samples (50 µL) were collected under basal conditions (prior to surgery), 60 minutes after occlusion (30 minutes after treatment administration) and 24 h after surgery. Both MRI analysis and sensorimotor tests were performed 1, 3, 7 and 14 days after surgery. Sensorimotor tests were done as previously described (see **Sections 4.3.3.4** and **5.2.4**). Blood GOT1 activity was measured using a Reflotron device.

### 7.2.2.1.- Surgical Procedures

For this study, the thromboembolic stroke model was selected and performed as described elsewhere<sup>289</sup>. In brief, mice were placed in a stereotaxic frame, the skin between the right ear and the eye was cut and the temporal muscle retracted in order to expose the temporal and parietal bones. The artery bifurcation was located and a small craniotomy was done. The meninges were then removed using a 25 G needle (300600, BD Microlance, Franklin Lakes, NJ, USA).

A micropipette (tip size: 20-40 mm) made with hematologic glass capillaries (World Precision Instruments, Sarasota, Florida, USA) using a puller (Sutter Instruments, Novato, California, USA) was pneumatically filled with 1.5  $\mu$ L of 1 U/ $\mu$ L thrombin (Stago, Parsippany, NJ, USA). The micropipette was placed on a micromanipulator and 1  $\mu$ L of thrombin solution was injected into the lumen of the artery bifurcation to induce the formation of a clot. The micropipette was removed 15 minutes later once the clot had stabilized. The treatment administrations were done 15 minutes after the removal of the micropipette.

CBF was monitored before injection of the thrombin and throughout all the surgery with a Periflux 5000 laser Doppler perfusion monitor by placing the Doppler probe in the parietal territory of the MCA.

The following exclusion criteria were used: less than 60% reduction in relative CBF; spontaneous reperfusion (defined as reperfusion in the first 30 minutes, before treatment administration); parenchymal or arterial damage during surgery. All excluded or deceased animals were replaced until the total number of animals indicated for each group was attained.

Experimental procedures were performed following 5 criteria derived from the STAIR group guidelines for preclinical evaluation of stroke therapeutics<sup>276,277</sup>.

### 7.2.3.- EMBOLIC STROKE MODEL

Four sets of ischaemic animals (n=8 animals/group) were treated with saline (control group), rtPA (10 mg/kg), rGOT1 (1 mg/kg) plus rtPA or rGOT1 administered 30 minutes before rtPA. The treatments were administered I.V. through the jugular vein as a 10% bolus and 90% perfusion (rtPA) or as a bolus (saline and rGOT1). Blood samples (200  $\mu$ L) were collected under basal conditions (prior to surgery), and 0, 2, 5, 8 and 24 h after treatment administration. MRI analysis were performed as previously described (**Section 4.3.3.2**). ADC and MRA images were done 30 minutes (before treatment administration) and 90 minutes (right after treatment administration) after occlusion. T2 maps were done 24 hours after surgery. Blood GOT1 activity was measured using a Reflotron device.

#### 7.2.3.1.- Surgical Procedures

The model used for this experiment was a modification of a previously established protocol.<sup>290,291</sup> In brief, 500  $\mu$ L of blood collected from the tail vein were injected into a 0.58 mm (internal diameter) polythene tube (800/100/200, Smiths Medical, Minneapolis, MN, USA) and incubated for 2 hours at 37 °C for clot formation. Then, the clot was flushed with saline into a Petri dish and rinse with saline. A 5 cm portion was cut and collected, alongside with saline, into a 0.28 mm (internal diameter) polythene tube (800/100/100, Smiths Medical, Minneapolis, MN, USA).

During the clot formation, and under an operating microscope, a midline neck incision was performed and connective tissue was dissected from both common carotids. The right external carotid and the pterygopalatine artery were isolated and ligated by a 6-0 silk suture. The left common carotid was ligated by a 6-0 silk suture right before the occlusion of the MCA. The

polythene tube containing the clot was then inserted into the common carotid and moved through the internal carotid until pterygopalatine bifurcation. The clot was then injected using a syringe with a needle connected to the other side of the tube, using saline as a vehicle, until a drop in CBF was registered. A laser-Doppler flow probe attached to a flowmeter was located over the thinned skull in the MCA territory (4 mm lateral to bregma) to obtain a continuous measure of relative CBF during the occlusion.

After reaching the artery occlusion, as indicated by Doppler signal reduction, animals were maintained for 30 minutes on the surgical bench to assure clot stability (in the rGOT1 30 minutes before rtPA group, rGOT1 was administrated at this point). Then, they were carefully moved from the surgical bench to the MRI system to assess the ischaemic lesion using ADC maps (defined as  $T_0$ ). MRA was also performed to ensure that the artery remained occluded throughout the magnetic resonance procedure. After MR analysis, animals were returned to the surgical bench and the Doppler probe was repositioned. 60 minutes after occlusion, either rGOT1 (as a bolus through tail vein), rtPA (10% bolus, 90% in 30 minutes perfusion through jugular vein) or a combination of both were administered. 90 minutes after occlusion, left common carotid artery was reperfused, while right common carotid (used to introduce the tube) remained tied to avoid bleeding and animals were moved to the MRI system to reassess the ischaemic lesion using ADC maps. MRA was also performed again to analyse the recanalization of the MCA.

The following exclusion criteria were used: less than 50% reduction in relative cerebral blood flow; vascular abnormalities, as determined by MRA; presence of spontaneous reperfusion (described as reperfusion during the first 60 minutes after occlusion, before rtPA administration). All excluded or deceased animals were replaced until the total number of animals indicated for each group was attained.

Experimental procedures were performed following 5 criteria derived from the STAIR group guidelines for preclinical evaluation of stroke therapeutics.<sup>276,277</sup>

### 7.3.- Statistical Analysis

All data are expressed as mean  $\pm$  SEM. The data were analysed using GraphPad Prism v.8.3.0 for Windows. The criterion for statistical significance was  $P < 0.05$ . Infarct volumes and motor tests data were compared by a two-way ANOVA followed by a Bonferroni post hoc test. Fisher's exact test was used for analysis of binary data. Data were first examined to assess distribution using the D'Agostino and Pearson omnibus normality test.



## RESULTS



## 8.- SECTION I: ENDOGENOUS GOT1 INHIBITION STUDIES

### 8.1.- *In Vitro* and *In Vivo* Analysis of AbGOT1 on GOT1

In order to validate the blocking efficacy of the AbGOT1 on the enzyme activity, AbGOT1 was tested first *in vitro* in blood samples and later *in vivo* in healthy animals. *In vitro* analysis showed that even a tiny amount of antibody (0.5  $\mu\text{g}$ ) was sufficient to induce a reduction  $>80\%$  of the GOT1 activity (**Figure 23, A**). Doses greater than 2  $\mu\text{g}$  of AbGOT1 showed an inhibition  $>95\%$  respect to the basal levels. On the other hand, the IgG isotype control did not show any GOT1 inhibition. *In vivo* dose-response analysis in healthy animals confirmed the same inhibitory effect observed in the previous study as summarized in **Table 3**. I.P. administration of 1 mL of AbGOT1 (1 mg/rat) induced a reduction of 55% (respect to the control group) of GOT1 activity one day after injection. A higher dose (2.5 mg/rat) induced an inhibition of 80%, which lasted at least four days after administration. However, with a dose of 4 and 5 mg/rat, endogenous blood GOT activity was below detectable values ( $<5$  U/L) during at least 8 days. Temporal analysis at 1, 2, 3, 4, 5, 6 and 8 hours and 1, 2, 3, 4, 6, 8, 10 and 14 days after AbGOT1 injection confirmed that a single I.P. administration of 5 mg/rat was enough to induced a significant reduction of blood GOT1 activity which lasted for 8 days. Endogenous GOT1 activity recovered 14 days after antibody administration (**Figure 23, B**). Based on this inhibition, the dose of 5 mg/rat was used for further studies in ischaemic animals.

AbGOT1 mg/rat	GOT, day 1	GOT, day 2	GOT, day 4	GOT, day 8	GOT, day 14
Control	78	82	86	80	89
1	45	105	95	92	91
2.5	18	19	17	22	97
4	<5	<5	<5	15	92
5	<5	<5	<5	10	112

**Table 3.** Dose-response analysis of AbGOT1 on blood GOT activity in healthy animals.

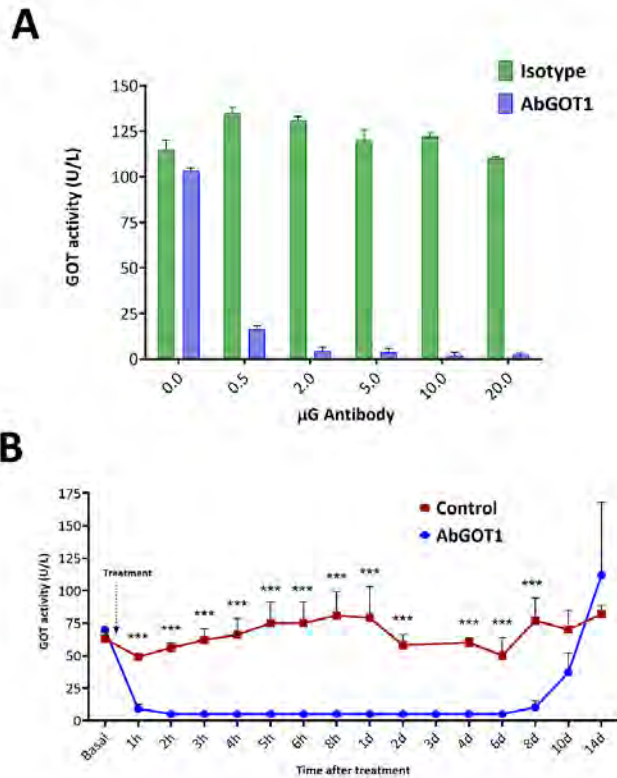


**Figure 23. A.** *In vitro* analysis of AbGOT1 and IgG isotype on blood GOT1 activity. The blocking efficacy of the AbGOT1 on GOT1 enzyme activity was tested on blood samples obtained from the tail vein of healthy rats (500 µL). **B.** *In vivo* analysis of AbGOT1 on blood GOT activity in healthy animals. Control animals were treated (i.p.) with 1 mL of PBS (drug vehicle), and AbGOT1 animals were treated with 1 mL (i.p.) 5 mg/mL of antibody. Basal samples were obtained before treatment. Data are shown as mean ± SEM. \*\*\**P* < 0.001 compared with the control group (n = 3).

## 8.2.- Effect of AbGOT1 in an ischaemic animal model

Cerebral ischaemic injury in control animals induced a significant increase of blood GOT1 levels during at least 2 days after ischaemia with respect to basal levels (before ischaemia). Maximum increase was observed one day after ischaemic damage ( $446 \pm 122$  U/L) compared with basal levels ( $77 \pm 11$  U/L). Blood GOT1 levels returned to basal levels 4 days after ischaemia ( $89 \pm 7$ ; **Figure 24, A**). In line with the findings observed in healthy animals, AbGOT1 treatment in ischaemic animals led to a complete inhibition of blood GOT1 below detectable levels ( $< 5$  U/L) one hour after administration and also abolished the natural increase of endogenous GOT1 enzyme activity caused by the ischaemic damage observed in the control group. GPT activity, the other blood-resident transaminase enzyme involved on the blood glutamate homeostasis,<sup>292</sup> was also increased after brain injury during at least one day after ischaemia, and returned to basal levels one day later. The maximum increase was observed at 6 hours after ischaemic damage ( $59 \pm 10$  U/L), as compared to the basal levels ( $26 \pm 2$  U/L). In contrast to what was seen with GOT1, this increase in blood GPT activity was not affected by the AbGOT1 treatment (**Figure 24, B**). No changes in blood glutamate levels were observed during the follow-up period in both control and AbGOT1 treated groups (**Figure 25**).

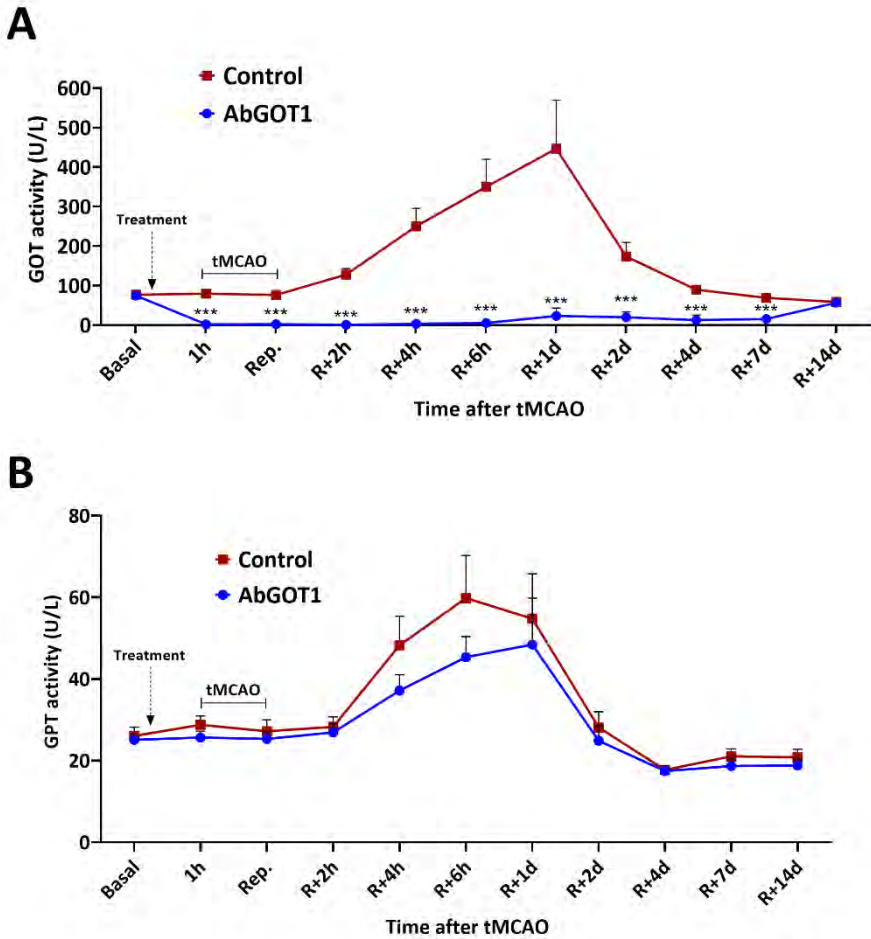


**Figure 24. A.** Temporal analysis of the effect of the AbGOT1 on blood GOT activity in ischaemic animals. **B.** Temporal analysis of the effect of the AbGOT1 on blood GPT activity in ischaemic animals. Control animals were treated (I.P.) with 1 mL of PBS (drug vehicle), and AbGOT1 animals were treated with 1 mL (I.P.) 5 mg/mL. Treatments were injected 1 hour before ischaemic surgery. tMCAO was induced during 75 minutes. Basal samples were obtained before treatment and surgery. Data are shown as mean  $\pm$  SEM. \*\*\* $P < 0.001$  compared with the control group (n=10).

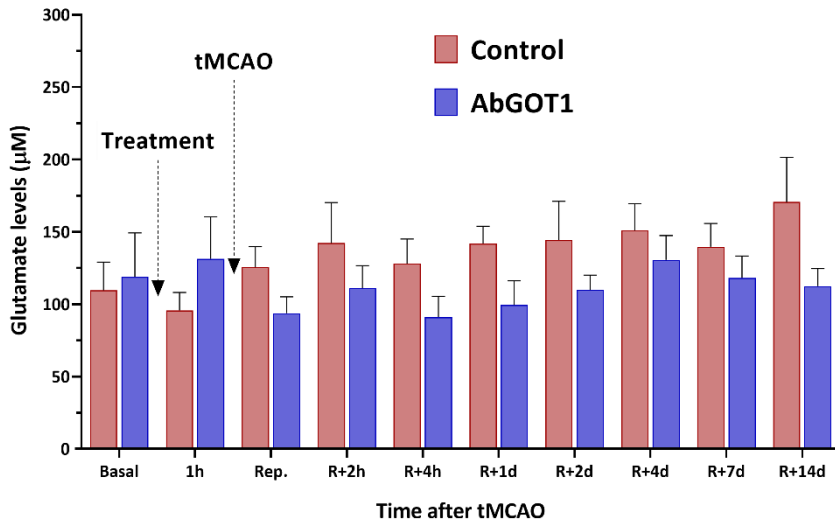


**Figure 25.** Temporal analysis of the effect of the AbGOT1 on blood glutamate levels in ischaemic animals. Control animals were treated (I.P.) with 1 mL of PBS (drug vehicle), and AbGOT1 animals were treated with 1 mL (I.P.) 5 mg/mL. Treatments were injected 1 hour before ischaemic surgery. tMCAO was induced during 75 minutes. Basal samples were obtained before treatment and surgery. Data are shown as mean  $\pm$  SEM (% respect the basal levels (n=10)).

Meanwhile, comparative analysis of ischaemic lesions between controls and treated animals showed that blockade of endogenous GOT1 blood activity by AbGOT1 caused larger lesions following ischaemia induction and 7 and 14 days after, compared with the control group (**Figure 26**). Doppler analysis of the cerebral blood flow determined before and after AbGOT1 administration in healthy animals, showed that the blocking of the GOT1 activity had no impact on this physiological parameter (**Figure 27**).

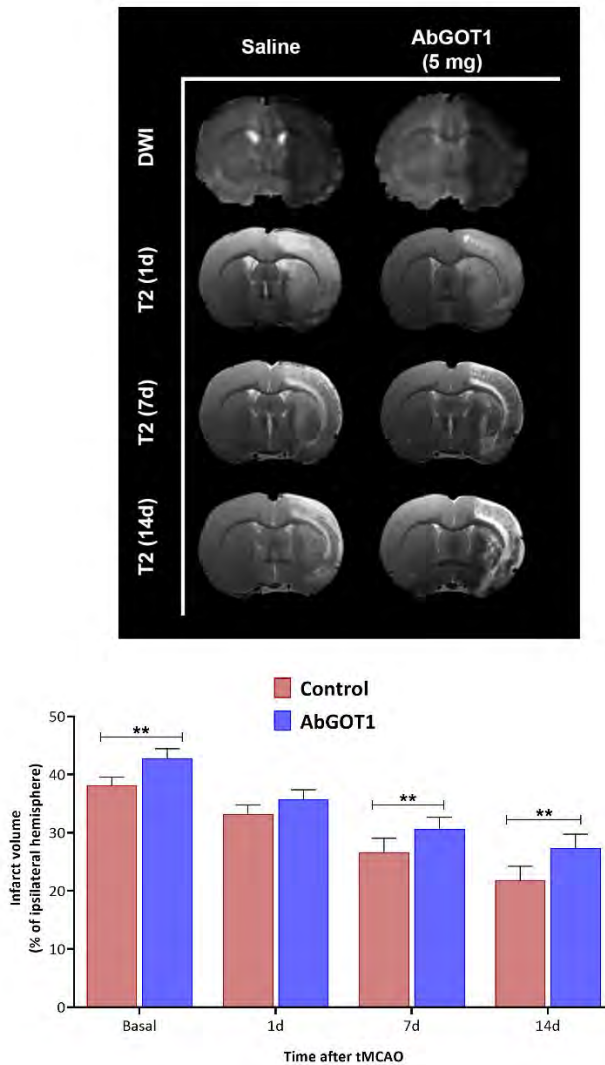


**Figure 26.** MRI assessments of ischaemic injury evolution. ADC maps were recorded during cerebral artery occlusion (defined as basal). Lesion volume evolution was assessed using T2-weighted images recorded 24 hours and 7 and 14 days after ischaemia induction. Control animals were treated (I.P.) with 1 mL of PBS (drug vehicle), and AbGOT1 animals were treated with 1 mL (I.P.) 5 mg/mL. Treatments were injected 1 hour before ischaemic surgery. tMCAO was induced during 75 minutes. T2 lesions are represented as % adjusted to the ipsilateral hemisphere and corrected by oedema. Data are shown as mean  $\pm$  SEM. \*\*P < 0.01 compared with the control group (n=10).

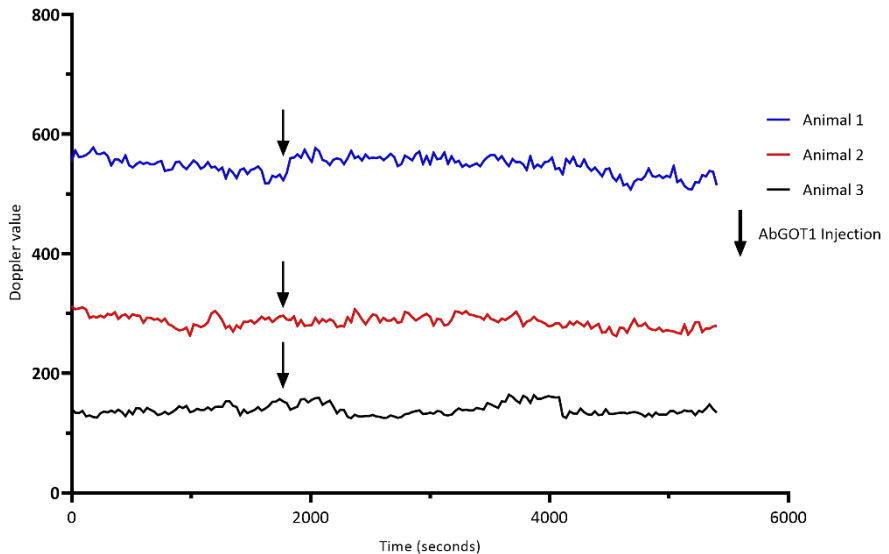


**Figure 27.** Cerebral blood flow of three different healthy animals measure with a laser-Doppler flow probe. Measures were taken during 90 minutes (30 minutes before injection and 60 minutes after AbGOT1 treatment).

### 8.3.- Analysis of Sensorimotor Deterioration in Control and AbGOT1 Treated Animals

Ischaemic injury was associated with sensorimotor deficit, evaluated by cylinder, rotarod and neuroscore tests. AbGOT1 treated animals had higher deficits compared to the control group, as detected with the rotarod test at 7 days (**Figure 28**). In the cylinder test and the neuroscore, despite not being statistically significant, animals treated with AbGOT1 showed a trend toward worse recovery (**Figure 28, B and C**). Functional evaluation performed 1 day before AbGOT1 treatment and surgery confirmed that none of the animals included had previous disability.

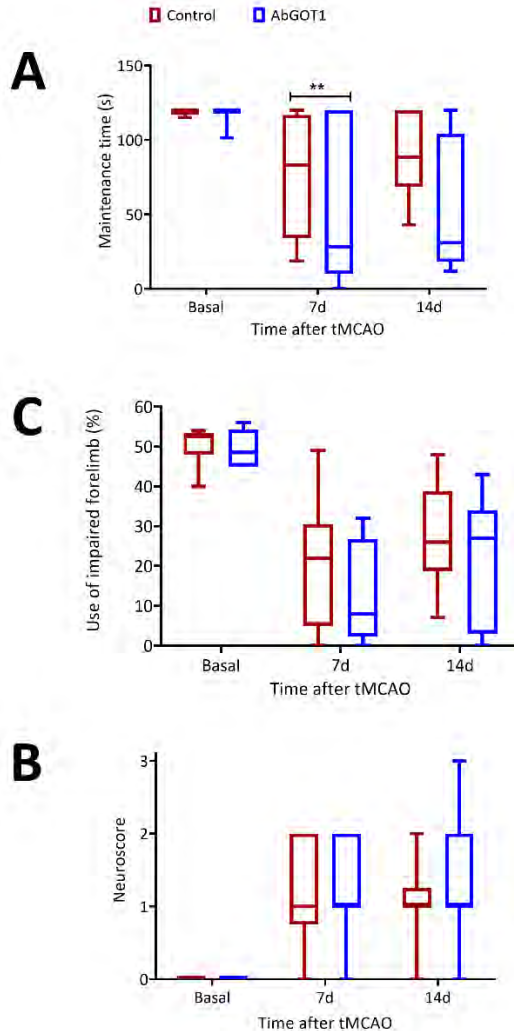


**Figure 28.** Box plots showing the assessment of sensorimotor function using rotarod test (A) cylinder test (B) and neuroscore (C). Functional tests were performed before ischaemic injury (baseline) 7 and 14 days after injury in control (vehicle) and treated animals. Control animals were treated (I.P.) with 1 mL of PBS (drug vehicle), and AbGOT1 treated animals with 1 mL (I.P.) 5 mg/mL. Treatments were injected 1 hour before ischaemic surgery. tMCAO was induced during 75 minutes. Boxes represent interquartile ranges. The line across each box indicates the median, and the whiskers (T) are the highest and lowest values. Baseline reflects pre-treatment and preoperative functional evaluation. Data are shown as mean  $\pm$  SEM. \*\* $P < 0.01$  compared with the control group ( $n = 10$ ).

#### 8.4.- Effect of AbGOT1 on Brain Glutamate and Lactate Levels in the Ischaemic Animal Model

Analysis of brain glutamate and lactate levels by means of MRS showed a persistent increase in brain glutamate after tMCAO in the AbGOT1 treated group compared with basal levels and the contralateral (healthy) brain region as shown in **Figure 29 (A and B)**. In line with the brain glutamate response, analysis of lactate levels, used as a marker of ischaemic brain lesion<sup>293,294</sup>, showed a significant increase in the ischaemic region in animals submitted to GOT1 blocking (**Figure 29, A and C**).

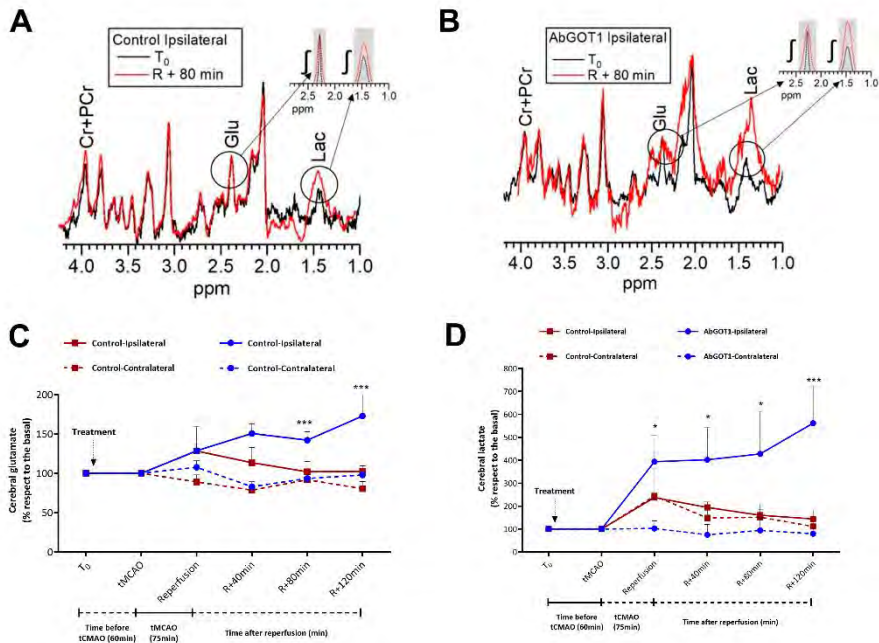


**Figure 29.** Brain glutamate (C) and lactate (D) levels were determined in control and AbGOT1 treated animals before ischaemia (T<sub>0</sub>), during occlusion (75 minutes) and 40, 80, and 120 minutes after reperfusion (R) using MRS technique. Glutamate (Glu), and lactate (Lac) peaks in the MR spectrum were normalized to the creatine (Cr) peak/phosphocreatine (PCr) areas for each single spectrum and then represented as % adjusted to basal levels. On the right and up panels are represented the automatic software integration of the area of glutamate and lactate spectral peaks. Figures (A) and (B) represent the differences in the glutamate and lactate peaks at T<sub>0</sub> and at 80 minutes after reperfusion in a control and treated animal respectively. Control animals were treated (I.P.) with 1 mL of PBS (drug vehicle), and AbGOT1 treated animals with 1 mL (I.P.) 5 mg/mL. Treatments were injected 1 hour before ischaemic surgery. tMCAO was induced during 75 minutes. Data are shown as mean ± SEM. \*  $P < 0.05$ , \*\*\*  $P < 0.001$  compared with the control group (n = 3).

## 8.5.- GOT1 Activity in CSF and Brain Tissue

To analyse whether administration of AbGOT1 had any impact on the activity of GOT1 in the brain, GOT1 activity was determined in healthy and ischaemic animals both in CSF and brain tissue. AbGOT1 caused an inhibition of blood GOT1

activity (**Figure 30**, A and C) and GOT1 activity in CSF for at least 24 hours in healthy and ischaemic animals (**Figure 30**, B and D), although this reduction was significantly lower (50% respect to CSF basal levels) compared with the effect observed in blood. In order to confirm AbGOT1 specificity, an isotype form of the antibody was tested on brain GOT1 in a new group of animals. The results confirmed again the inhibition of brain and blood GOT1 activity by AbGOT1 as shown in **Figure 31**, but no effect was observed with the isotype form.

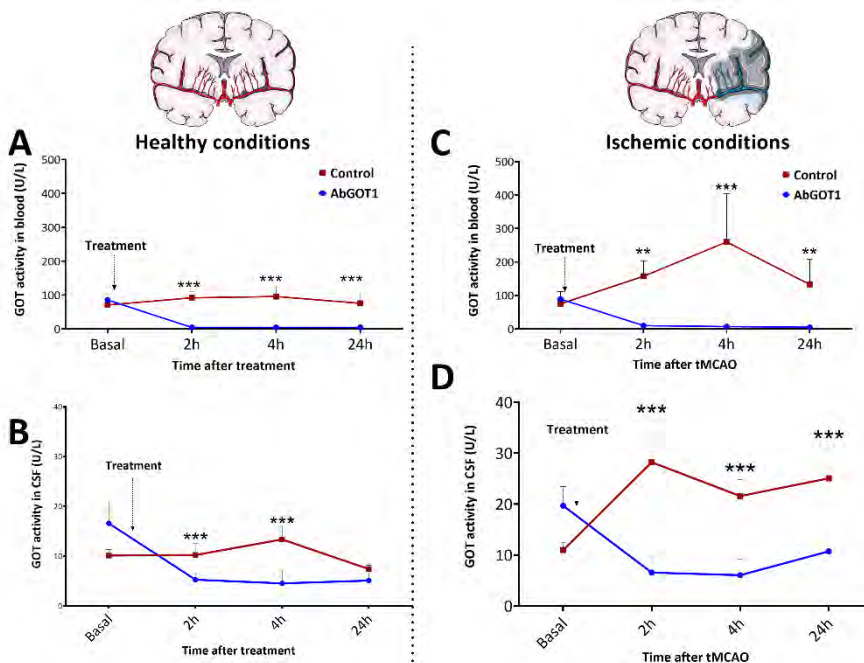


**Figure 30.** GOT1 activity was determined in blood and CSF from healthy (**A**, **B**) and ischaemic (**C**, **D**) animals. Control animals were treated (I.V.) with 1 mL of PBS (drug vehicle), and AbGOT1 treated animals with 1 mL (I.V.) 5 mg/mL. Treatments were injected right after reperfusion. tMCAO was induced during 75 minutes. Data are shown as mean  $\pm$  SEM. \*\* $P < 0.01$ , \*\*\* $P < 0.001$  compared with the control group ( $n=5$ ).

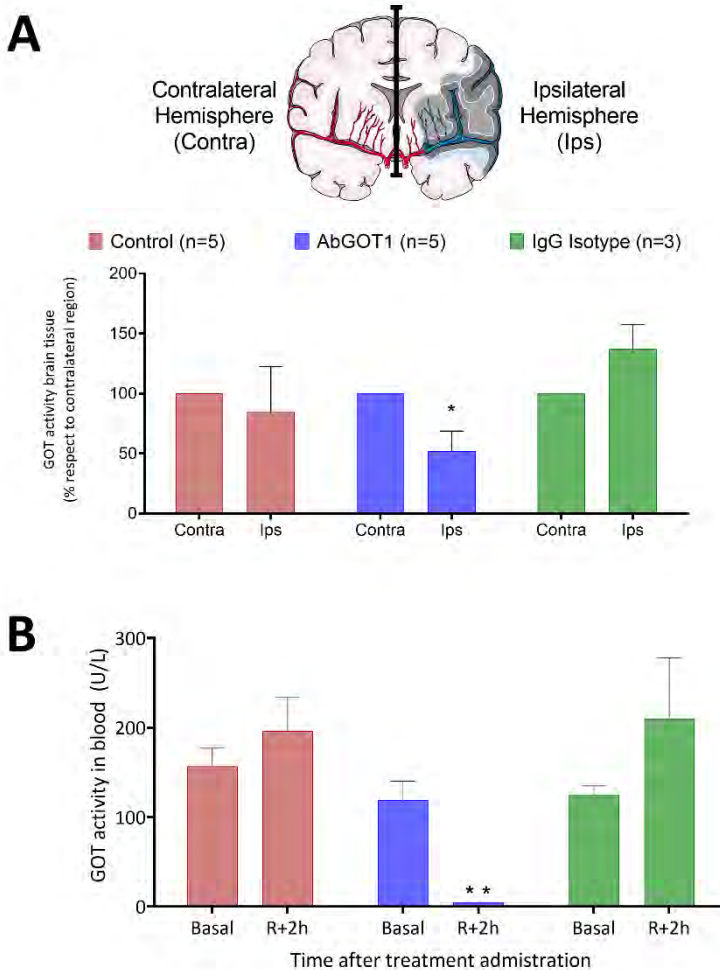


**Figure 31.** The specificity of AbGOT1 on GOT1 activity was determined in the brain tissue and blood of ischaemic animals using an isotype form. In **A**, a 50% reduction of the GOT1 activity in the brain tissue of the animals treated with AbGOT1 was observed, while the isotype form had no effect on the GOT activity. Also, in the same group of ischaemic animals GOT1 activity was measured in the blood (**B**), and the same results were observed as previously described: AbGOT1 significantly reduced GOT1 activity and the isotype form did not induce changes in GOT1 activity. Data are shown as mean  $\pm$  SEM. \* $P < 0.05$ , \*\* $P < 0.01$  compared with the control group (n = 5).

## 9.- SECTION II: rGOT1 THERAPEUTIC EFFECT

### 9.1.- Protein Synthesis

In order to evaluate the successful synthesis of the recombinant protein, three different characterization studies were performed: sequence and size analysis, secondary structure analysis and specific activity analysis.

#### 9.1.1.- SIZE AND SEQUENCE ANALYSIS

Size analysis by SDS-PAGE showed equal sizes for rGOT1 and GOT1 isolated from RBC (**Figure 32**). The weight of the bands (between the 37 and 50 kDa) corresponds to a single monomer of the protein (46 kDa) instead of the total protein (92 kDa). This is due to denaturation of the protein during the heating process necessary for SDS-PAGE.

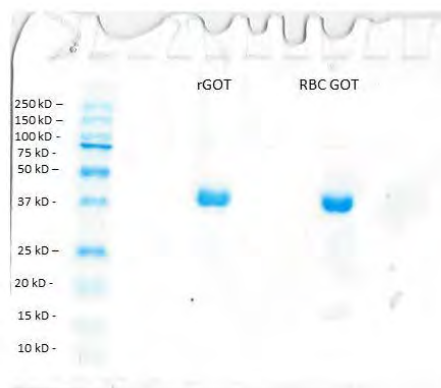


**Figure 32.** SDS-PAGE comparison of human RBC GOT1 and rGOT1 proteins.

Furthermore, sequence analysis of both RBC GOT1 and rGOT1 was performed twice. In the first study, the digested human RBC GOT1 showed 78.69% coverage compared to the database sequence for human cytoplasmic GOT (E.C. 2.6.1.1), while rGOT1 showed a 79.18% coverage, with similar segments of the peptide sequence matching, as shown in **Figure 33**.



**Figure 33.** Protein sequencing with trypsin digest of human RBC GOT1 (A) and rGOT1 (B) compared to human cytoplasmic GOT.

In the second sequencing study (**Figure 34**) the digested recombinant rGOT1 showed 96% coverage compared to the database sequence for human GOT1. The assembled sequence is provided, showing areas of “weak supporting evidence” highlighted in yellow and “no supporting evidence” highlighted in red. The remainder of the sequence is supported by high confidence data from either the microwave assisted acid hydrolysis or trypsin digested samples.

APPSVFAEVPQAQPVLVFKLTADFRED **PDPR**KVNLGVGAYRTDDCHPWVLPVVKKVEQK  
 IANDNSLNHEYLPILGLAEFRSCASRLALGDDSPALKEKRVGGVQSLGGTGALRIGADFL  
 ARWYNGTNNKNTPVYVSSPTWENHNAVFSAAAGFKDIRSYRWDAEKRGLDLQGFLNDLEN  
 APEFSIVVLHACAHNPTGIDPTPEQWKQIASVMKHRFLFPFFDSAYQGFASGNLERDAWA  
 IRYFVSEGF~~EFFCAQSF~~**SK**NFGLYNERVGNLTVVGKEPESILQVLSQMEKIVRITWSNPP  
 AQGARIVASTLSNPELFEEWGTVNVTMADRILTMRSELRA**LE**ALKTPGTWNHITDQIGM  
 FSFTGLNPKQVEYLVNEKHIIYLLPSGRINVSGLTTKNLDYVATSIHEAVTKIQ

**Figure 34.** Protein Sequencing with trypsin digest and microwave assisted acid hydrolysis of rGOT1 compared with human GOT1. Yellow: weak supporting evidence; Red: no supporting evidence.

While neither study captured the entire human GOT1 sequence, the protein sequence areas with weak or no supporting evidence in the National Proteomics Center study were captured in the sequencing performed at the Smoler Proteomics Center. Therefore, taken together, these studies demonstrate 100% protein sequence coverage of rGOT1 to the published human GOT1 sequence.

### 9.1.2.- SECONDARY STRUCTURE

In order to determine the secondary structures of human RBC GOT1 and rGOT1 circular dichroism (CD) spectroscopy was used. The CD spectra (**Figure 35**) comparing the two proteins indicates similar secondary protein structures. The most common configuration for this protein is the helix, representing up to one third of the total structure. These results match the existing data for human cytoplasmic GOT (E.C. 2.6.1.1), showing that the recombinant version of the enzyme preserves the correct folding pattern. The small differences detected may be due to slight folding differences because the synthesis was

carried out in a prokaryotic microenvironment instead of in a eukaryotic one.

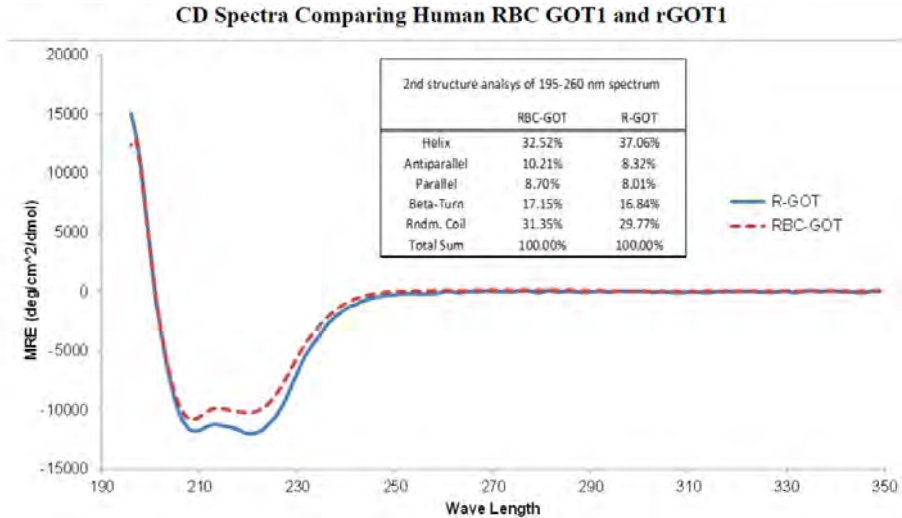


**Figure 35.** CD spectra comparing human RBC GOT1 and rGOT1.

### 9.1.3.- SPECIFIC ACTIVITY

As commented in previous sections, GOT activity measures were done using a Reflotron device, according to the manufacturer`s specifications. The specific activity of RBC GOT1 was 437 U/mg, compared to 530 U/mg for the recombinant version of the enzyme. The activity data suggest that the small differences found in the secondary structure between these two proteins has no detrimental effect on the catalytic activity of rGOT1.

## 9.2.- Pharmacokinetics and Dose Response Study

To analyse the pharmacokinetics of the rGOT1, first, different doses of rGOT1 were tested in healthy animals. Animals showed an exponential increase of blood GOT activity with the doses of 0.50, 1, 2, and 4 mg/kg (**Figure 36**). Maximum increase was achieved 1 hour after treatment administration and the half-time for all doses was roughly 2 hours.

No effect on glutamate blood levels was observed (data not shown) with any of the doses, probably due to the rapid clearance of glutamate from the blood. To be able to detect a significant effect of rGOT1 on blood glutamate lowering, we increased the basal levels of glutamate by injecting the animals with 1 mL of a 1 M glutamate solution. The dose of 0.24 mg/kg was selected based on previous results from our group.<sup>125</sup> In this case, as shown in **Figure 37 (A)**, we observed a significant reduction of glutamate levels 2 hours after rGOT1 treatment (this time point corresponds to 90 minutes after glutamate administration). We also analysed GOT activity in blood. On this occasion, the dose of 0.24 mg/kg did show a significant effect on the GOT activity. The administration of glutamate did not induce an increment of GOT activity (**Figure 37, B**).

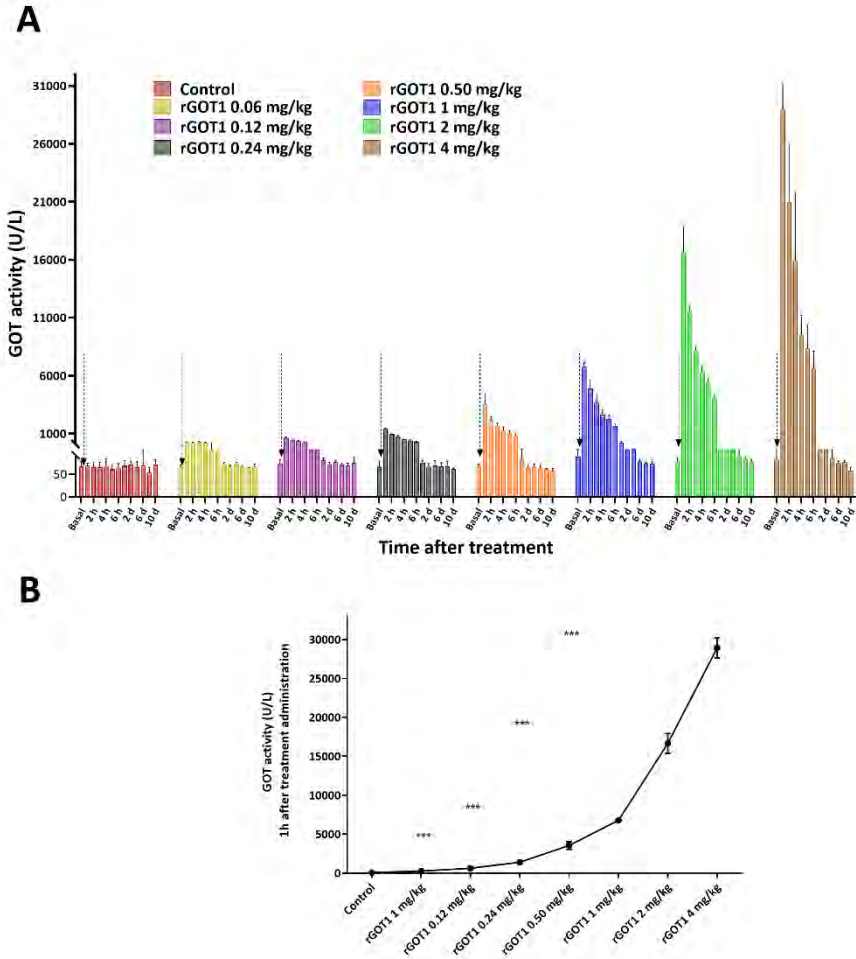


**Figure 36. A.** Temporal analysis of blood GOT activity in healthy animals. Control animals were injected (I.V.) with 1 mL of PBS (drug vehicle) and treated animals with 1 mL of rGOT1 (I.V.) at different concentrations. **B.** GOT activity 1 hour after treatment. Basal samples were obtained before treatment. Arrows indicate treatment administration. Data are shown as mean  $\pm$  SEM. \*\*\* $P$ <0.001 compared to the control group (n=3).

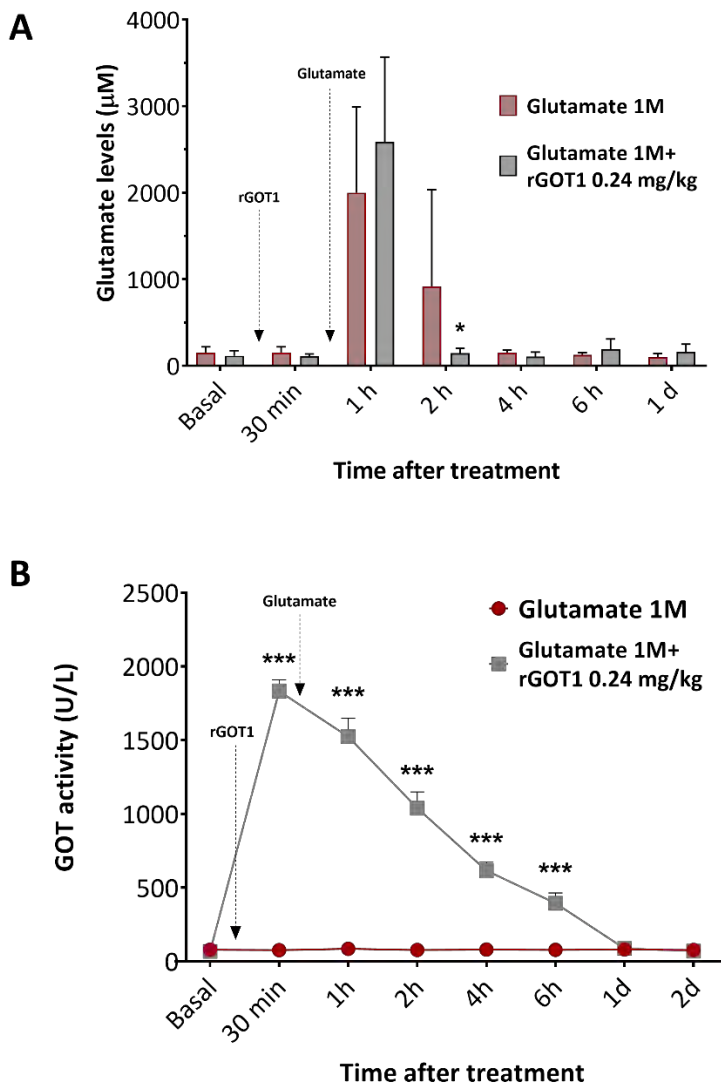


**Figure 37. A.** Temporal analysis of the effect of rGOT1 on blood glutamate levels in healthy animals. Control animals were treated (I.V.) with 1 mL of PBS (drug vehicle) and treated animals with 1 mL of rGOT1 (I.V.) 0.24 mg/kg. 1 mL of glutamate 1 M was injected 30 minutes after rGOT1 injection in both groups. Basal samples were obtained before treatment. **B.** Temporal analysis of blood GOT activity in healthy animals. Data are shown as mean  $\pm$  SEM. \* $P < 0.05$ , \*\*\* $P < 0.001$  compared to the control group ( $n = 6$ ).

### 9.3.- Therapeutic Time Window

Once the dose was established, we decided to analyse the potential therapeutic window of the enzyme. In order to do that, different sets of ischaemic animals were treated with the same amount of rGOT1 (0.24 mg/kg) administered at different times after reperfusion. In previous studies<sup>125</sup>, we observed that a dose of 0.12 mg/kg induced an increase of GOT levels in blood to ~1.500 U/L with significant protective effect. With this new human recombinant form similar increase of blood GOT levels was obtained with a dose of 0.24 mg/kg, therefore, this last dose was selected to perform this Therapeutic Time Window study. Time points of administration and GOT1 activity in blood are represented in **Figure 38**. Regarding the infarct volume, no significant differences were observed in any of the groups once compared to control animals (**Figure 39**). The same result was obtained for sensorimotor tests, where none of them showed significant differences between the control and the treated groups (data not shown).

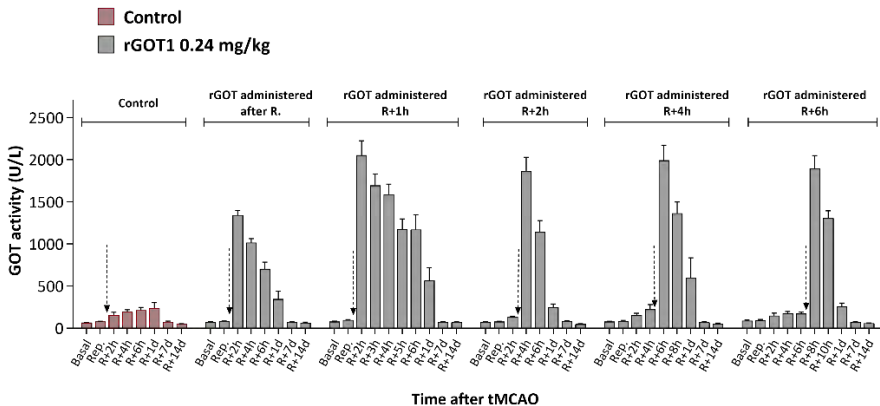


**Figure 38.** Temporal analysis of blood GOT activity in ischaemic animals. Control animals were injected (i.v.) with 1 mL of PBS (drug vehicle) and treated animals with 1 mL of rGOT1 (i.v.) 0.24 mg/kg. Treatments were injected at different times after reperfusion. tMCAO was induced during 75 minutes. Basal samples were obtained before treatment. Arrows indicate treatment administration. Data are shown as mean  $\pm$  SEM (n=7).

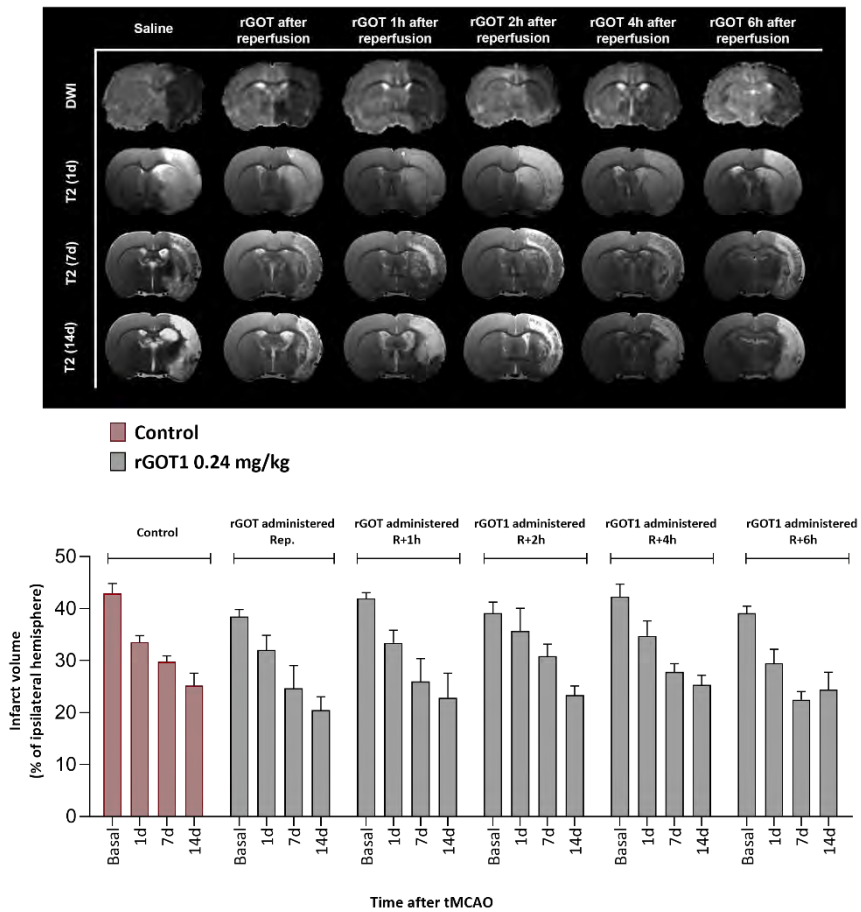


**Figure 39.** MRI assessments of ischaemic injury evolution. ADC maps were recorded during cerebral artery occlusion (defined as basal). Lesion volume evolution was assessed using T2-weighted images recorded 1, 7 and 14 days after ischaemia induction. Control animals were treated (I.V.) with 1 mL of PBS (drug vehicle), and rGOT1 animals were treated with 1 mL (I.V.) 0.24 mg/kg. Treatments were injected at different times after reperfusion. tMCAO was induced during 75 minutes. T2 lesions are represented as % adjusted to the ipsilateral hemisphere and corrected by oedema. Data are shown as mean  $\pm$  SEM (n=7).

## 9.4.- Therapeutic Effect on Mild and Severe Ischaemia

### 9.4.1.- SEVERE ISCHAEMIA

Since we did not find any effect with the dose of 0.24 mg/kg, we decided to test different doses from **Section 9.2** to evaluate which dose had a greater efficacy. First, we tested them in ischaemic animals suffering severe ischaemia, that is, a prolonged tMCAO (75 minutes). All doses caused a significant increase of GOT activity in blood, as seen in **Figure 40**. However, only the 1 mg/kg dose had some effect on infarct volume at 7 days (**Figure 41**), but this beneficial outcome was not present at the end point of our study (14 days). Furthermore, higher doses of rGOT1 (2 and 4 mg/kg) did not show any effect regarding the size of the lesion. Once again, none of the treatments utilized induced a significant reduction of glutamate concentration in blood (**Figure 42**). Finally, we analysed sensorimotor deficits with different test. Only the dose of 1 mg/kg showed a significant improvement in the cylinder at 7 days (**Figure 43, B**), which correlates with a significant reduction on infarct volume at the same time. Because of this, we selected 1 mg/kg as the effective dose for the next studies.

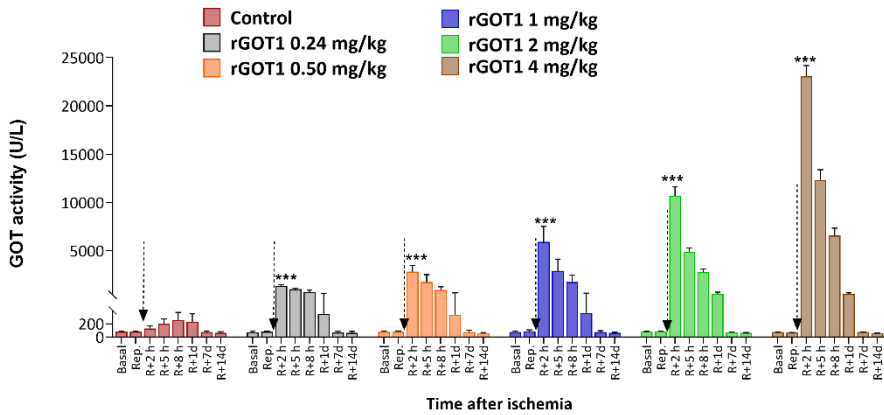


**Figure 40.** Temporal analysis of blood GOT activity in ischaemic animals. Control animals were injected (i.v.) with 1 mL of PBS (drug vehicle) and treated animals with 1 mL of rGOT1 (i.v.) at different concentrations. Treatments were injected right after reperfusion. tMCAO was induced during 75 minutes. Basal samples were obtained before treatment. Arrows indicate treatment administration. Data are shown as mean  $\pm$  SEM. \*\*\* $P$ <0.001 compared to the control group ( $n=12$ ).

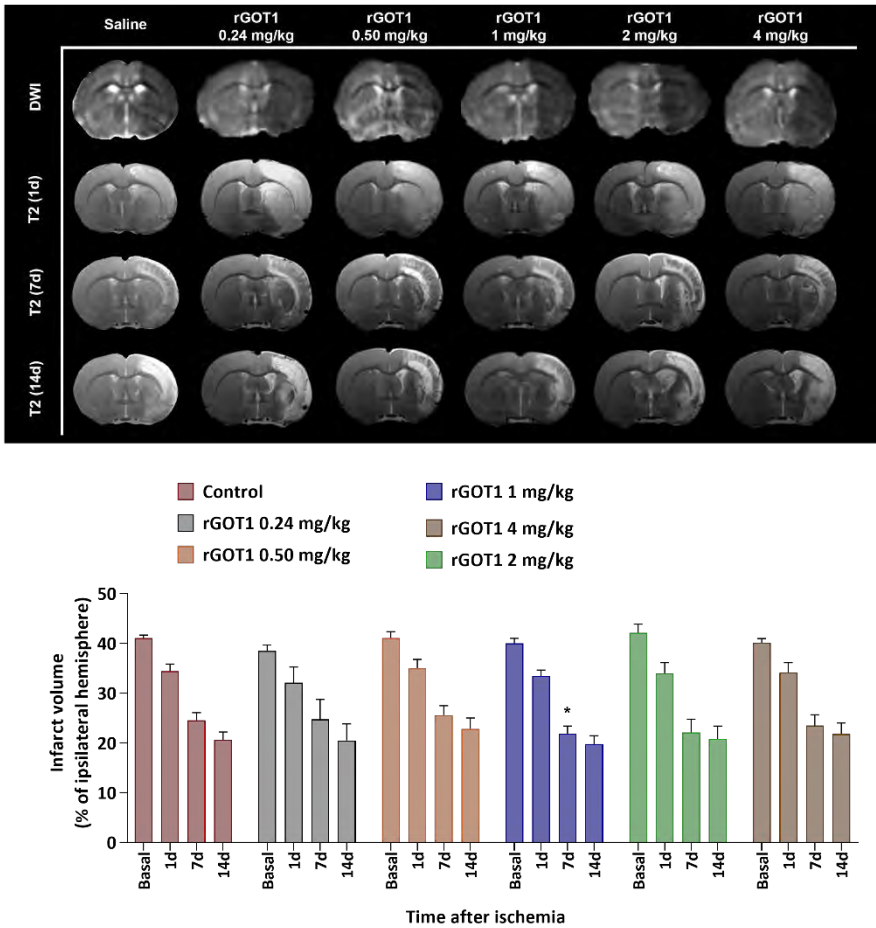


**Figure 41.** MRI assessments of ischaemic injury evolution. ADC maps were recorded during cerebral artery occlusion (defined as basal). Lesion volume evolution was assessed using T2-weighted images recorded 1, 7 and 14 days after ischaemia induction. Control animals were treated (I.V.) with 1 mL of PBS (drug vehicle), and rGOT1 animals were treated with 1 mL (I.V.) at different concentrations. Treatments were injected right after reperfusion. tMCAO was induced during 75 minutes. T2 lesions are represented as % adjusted to the ipsilateral hemisphere and corrected by oedema. Data are shown as mean  $\pm$  SEM. \* $P < 0.05$  ( $n = 12$ ).

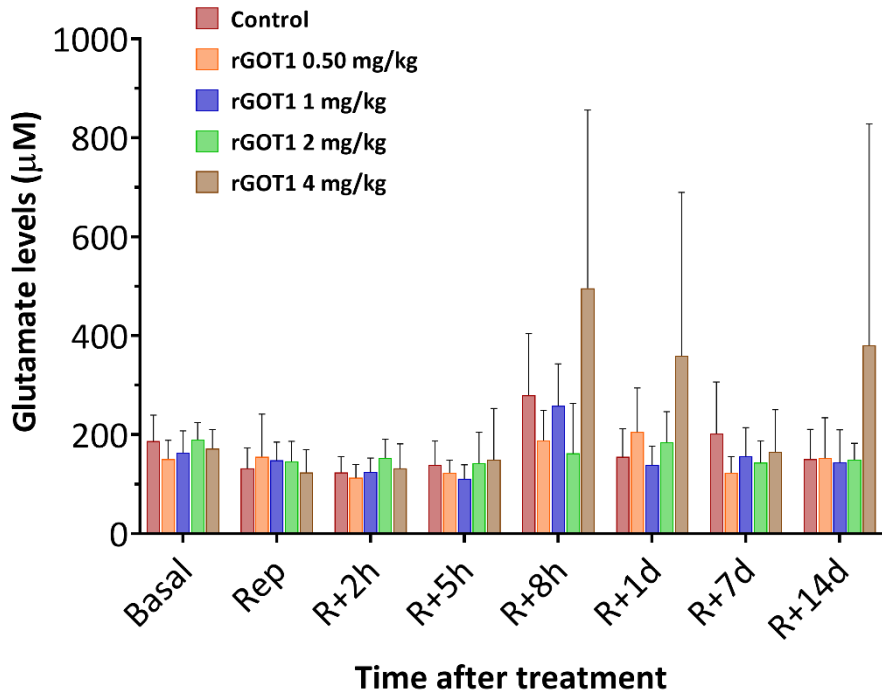


**Figure 42.** Temporal analysis of the effect of rGOT1 on blood glutamate levels in ischaemic animals. Control animals were treated (i.v.) with 1 mL of PBS (drug vehicle) and treated animals with 1 mL of rGOT1 (i.v.) at different concentrations. Basal samples were obtained before surgery. Data are shown as mean  $\pm$  SEM (n=6).

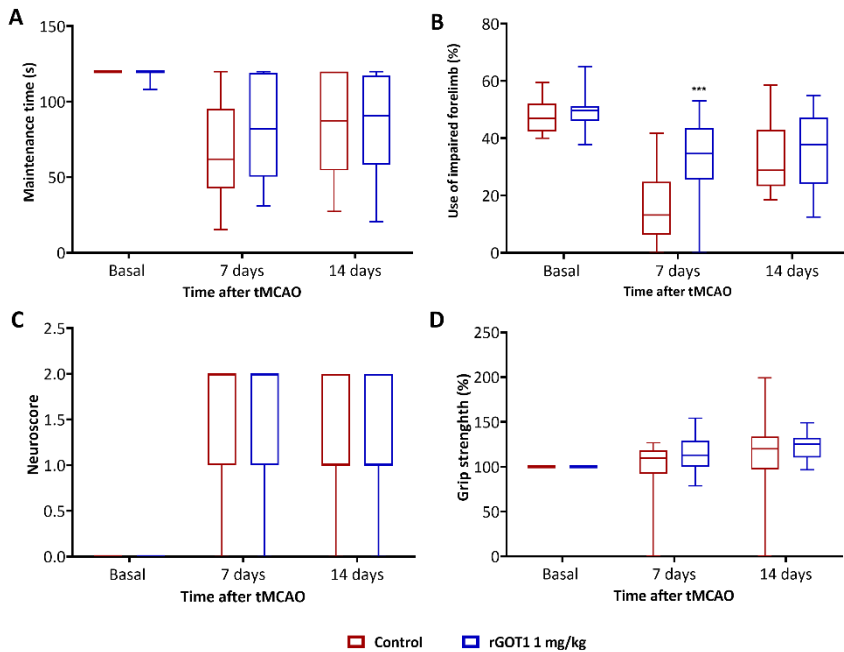


**Figure 43.** Box plots showing the assessment of sensorimotor function using rotarod test (A), cylinder test (B), neuroscore (C) and grip strength test (D). Functional tests were performed 1 day before ischaemic injury (baseline) and 7 and 14 days after injury in control (vehicle) and treated animals. Control animals were treated (I.V.) with 1 mL of PBS (drug vehicle), and rGOT1 treated animals with 1 mL (I.V.) at different concentrations. Treatments were injected right after reperfusion. tMCAO was induced during 75 minutes. Boxes represent interquartile ranges. The line across each box indicates the median, and the whiskers (T) are the highest and lowest values. Baseline reflects pre-treatment and preoperative functional evaluation. Data are shown as mean  $\pm$  SEM. \* $P < 0.05$ , \*\*\* $P < 0.001$  ( $n = 7$ ).

In a new independent study, we tested the delayed administration of the 1 mg/kg dose in order to analyse if we could expand the time window of rGOT1. We used the data from control and rGOT1 1 mg/kg groups from the previous study as reference values for the new set of animals. Once again, the analysis of blood GOT activity showed a significant increase with both administrations (Figure 44).

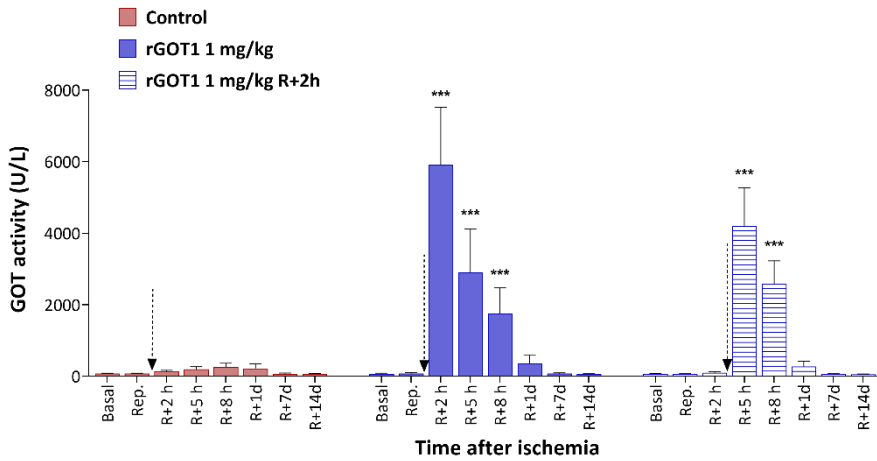


**Figure 44.** Temporal analysis of blood GOT activity in ischaemic animals. Control animals were injected (i.v.) with 1 mL of PBS (drug vehicle) and treated animals with 1 mL of rGOT1 (i.v.) 1 mg/kg. Treatments were injected 0 or 2 hours after reperfusion. tMCAO was induced during 75 minutes. Basal samples were obtained before treatment. Data are shown as mean  $\pm$  SEM. \*\*\* $P$ <0.001 compared to the control group ( $n=12$ ).

Nevertheless, both the reduction in infarct volume (**Figure 45**) and the improvement in the cylinder test (data not shown), observed with the group treated after reperfusion, disappeared once the administration of the drug was delayed. These results suggest that an early administration of the enzyme is critical for its neuroprotective effect on ischaemia.

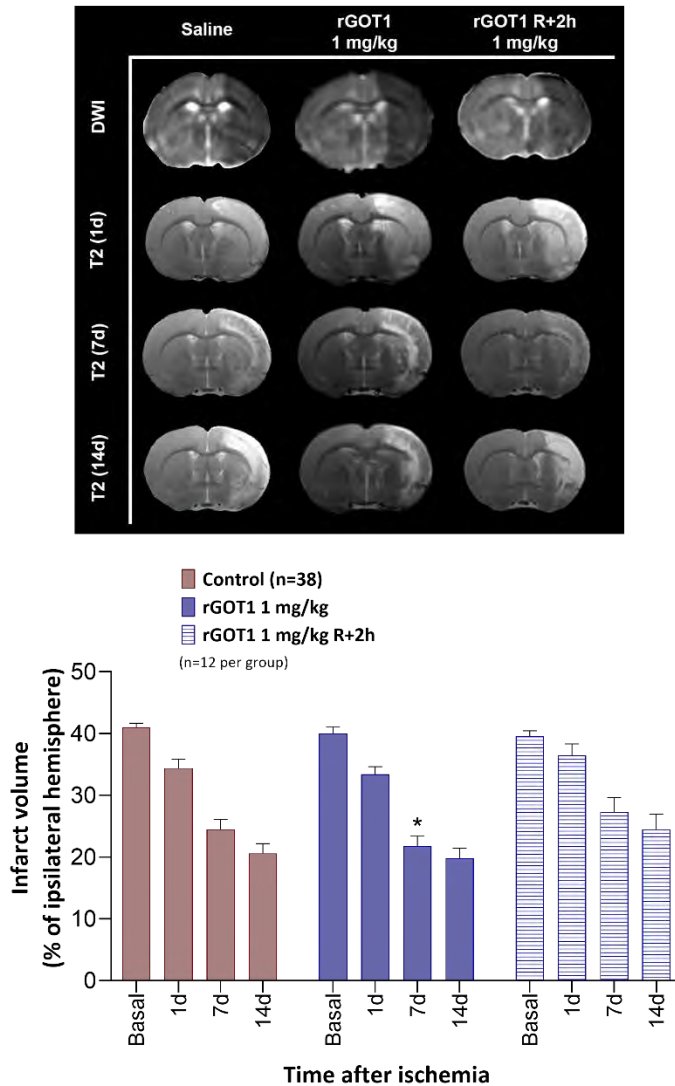


**Figure 45.** MRI assessments of ischaemic injury evolution. ADC maps were recorded during cerebral artery occlusion (defined as basal). Lesion volume evolution was assessed using T2-weighted images recorded 1, 7 and 14 days after ischaemia induction. Control animals were treated (I.V.) with 1 mL of PBS (drug vehicle), and rGOT1 animals were treated with 1 mL (I.V.) 1 mg/kg. Treatments were injected 0 or 2 hours after reperfusion. tMCAO was induced during 75 minutes. T2 lesions are represented as % adjusted to the ipsilateral hemisphere and corrected by oedema. Data are shown as mean  $\pm$  SEM. \* $P < 0.05$  ( $n = 12$ ).

#### 9.4.2.- MILD ISCHAEMIA

After analysing the therapeutic potential of the rGOT1 in cases of severe ischaemia, we also studied its effect on animals with a smaller infarct size. For this study we only used the 1 mg/kg dose, selected based on the results from the previous experiment. Following the same protocol, we first checked the GOT activity in blood before and after administration (**Figure 46**). Injection with 1 mg/kg of rGOT1 produced a significant increase of GOT activity levels in blood from 2 hours until at least 8 hours after reperfusion. Contrary to the group of severe ischaemia, rGOT1 did not have any impact on the infarct volume in the mild ischaemia model (**Figure 47**). In the same way, it did not show any effect on any of the sensorimotor tests performed either (data not shown). The reason behind the lack of results in this study compared with the severe ischaemia groups will be further debate in the discussion.

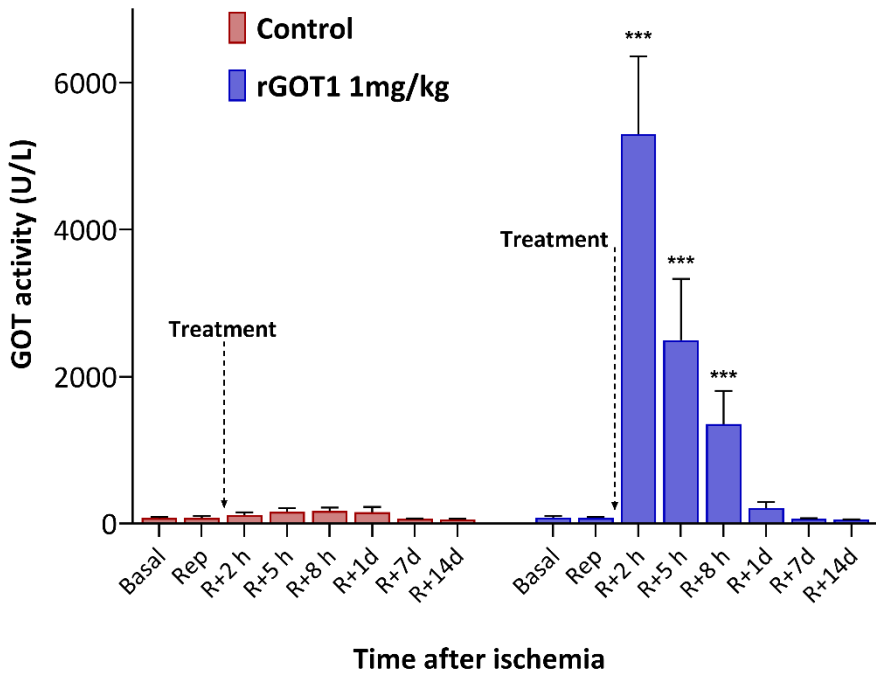


**Figure 46.** Temporal analysis of blood GOT activity in ischaemic animals. Control animals were injected (i.v.) with 1 mL of PBS (drug vehicle) and treated animals with 1 mL of rGOT1 (i.v.) 1 mg/kg. Treatments were injected right after reperfusion. tMCAO was induced during 45 minutes. Basal samples were obtained before surgery. Data are shown as mean  $\pm$  SEM. \*\*\* $P$ <0.001 compared to the control group (n=15).

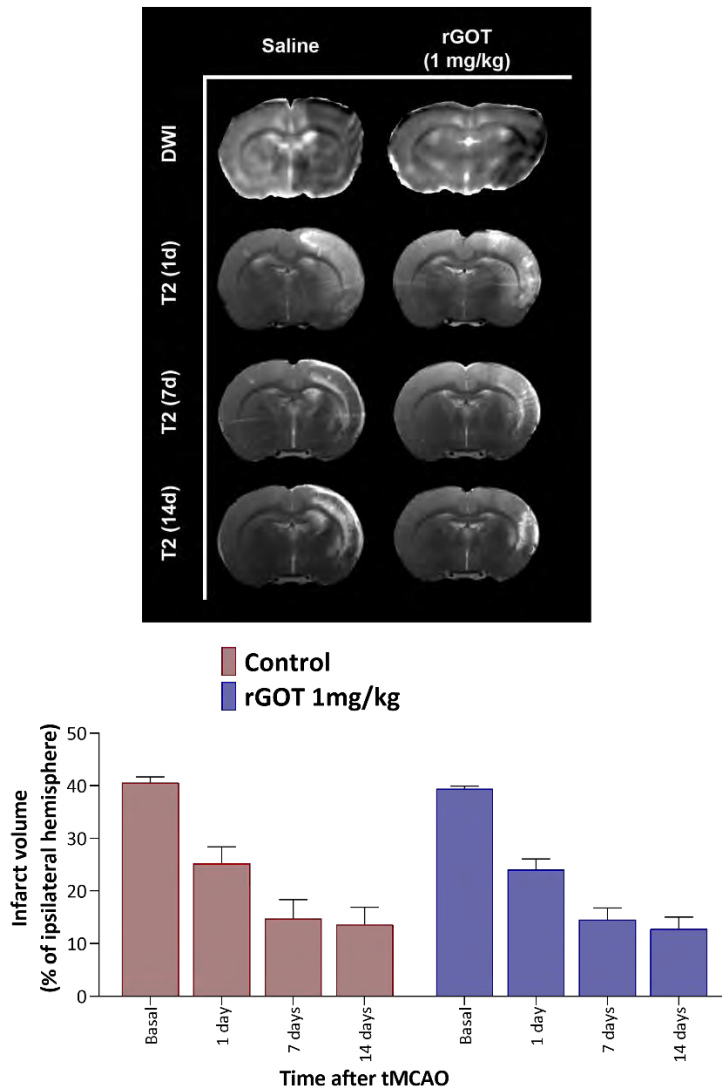


**Figure 47.** MRI assessments of ischaemic injury evolution. ADC maps were recorded during cerebral artery occlusion (defined as basal). Lesion volume evolution was assessed using T2-weighted images recorded 1, 7 and 14 days after ischaemia induction. Control animals were treated (I.V.) with 1 mL of PBS (drug vehicle), and rGOT1 animals were treated with 1 mL (I.V.) 1 mg/kg. Treatments were injected right after reperfusion. tMCAO was induced during 45 minutes. T2 lesions are represented as % adjusted to the ipsilateral hemisphere and corrected by oedema. Data are shown as mean  $\pm$  SEM (n=15).

## 9.5.- Injection Protocol

To increase the therapeutic efficacy of the rGOT1, we decided to test the effect on ischaemia of multiple injections of rGOT1. First, we tested different injection patterns to find the optimal protocol able to keep a stable rGOT1 activity in the first 8 hours after stroke (established as the therapeutic-time window for glutamate excitotoxicity)<sup>100,101</sup>. We tested three different protocols, varying in times of administration, volumes of injection and total amount of drug administered, and tested them in healthy rats (**Figure 48, A, B and C**). We selected the third protocol as the most suitable since it was the one maintaining a more stable GOT activity along time. The selected protocol was tested once again with a higher rGOT1 concentration to see if the temporal profile was time dose-dependent (**Figure 48, D**). Similar results as before were obtained, showing a relatively stable temporal profile with 4 injections of 1 mL of the treatment.

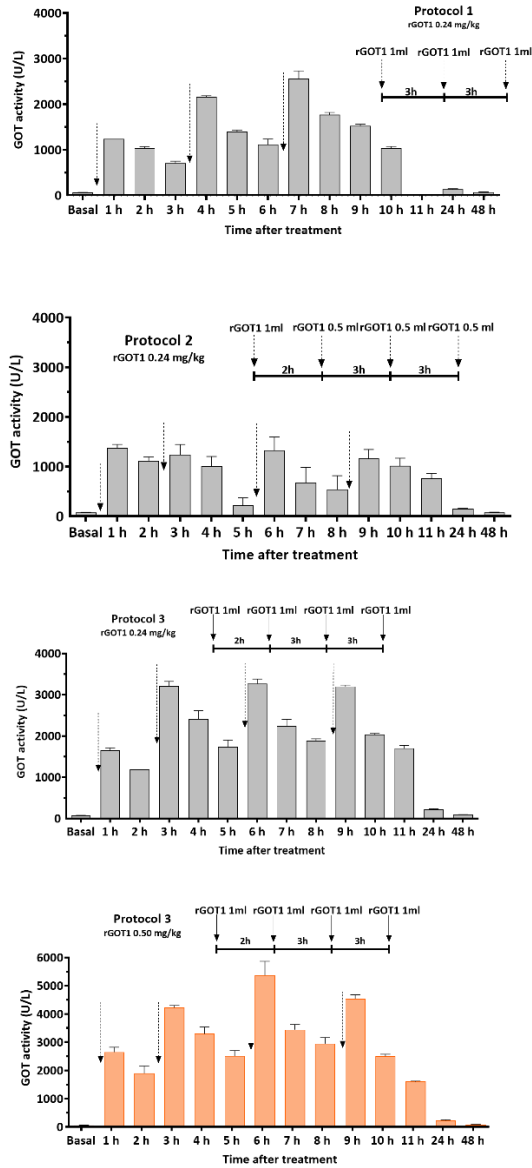


**Figure 48.** Temporal analysis of blood GOT activity in healthy animals. Three groups of animals were injected (I.V.) with several administrations of rGOT1 (I.V.) 0.24 mg/kg and one group with 0.50 mg/kg. Basal samples were obtained before treatment. Arrows indicate treatment administration. Data are shown as mean  $\pm$  SEM (n=3).

Finally, we tested the selected protocol in a new group of animals submitted to tMCAO in order to analyse if the ischaemic condition had some impact on the clearance and temporal profile of the enzyme (**Figure 49**). The results obtained from this study were similar to those observed in healthy rats and helped to choose Protocol 3 as the most suitable for the next experiments.

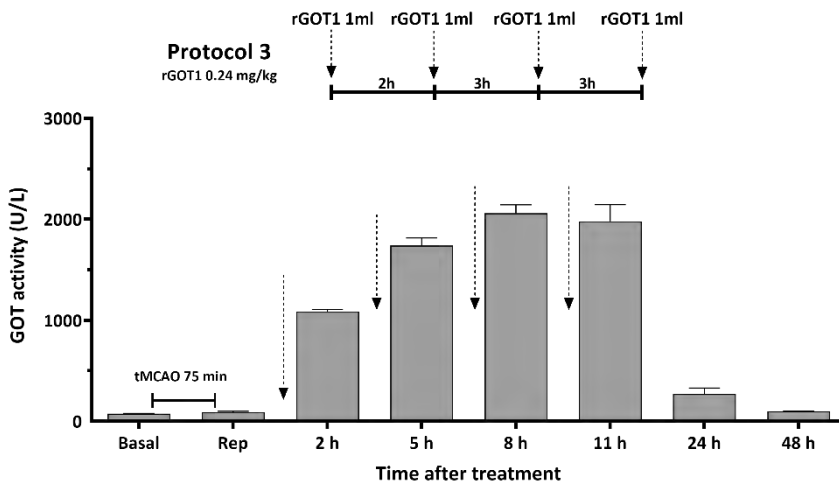


**Figure 49.** Temporal analysis of blood GOT activity in ischaemic animals. Animals were injected with 1 mL of rGOT1 (i.v.) 0.24 mg/kg. Treatments were injected at different times after reperfusion. tMCAO was induced during 75 minutes. Basal samples were obtained before surgery. Arrows indicate treatment administration. Data are shown as mean  $\pm$  SEM (n=3).

## 9.6.- Therapeutic Effect on Mild and Severe Ischaemia: 4 Injections Protocol

### 9.6.1.- SEVERE ISCHAEMIA

This four injections protocol was first tested in the model of severe ischaemia (tMCAO 75 min). rGOT1 administrations provoke a significant increase in blood GOT activity (**Figure 50**). This increase remained significantly high until 8 hours after

reperfusion (the time point of the last administration). In the group with the highest dose, 4 mg/kg, the rise of GOT activity was still detected 24 hours after reperfusion. Regarding the infarct volumes, both 0.50 and 1 mg/kg doses showed a significant reduction in the size of the lesion after 7 and 14 days, being especially remarkable for the 1 mg/kg dose (**Figure 51**). Similarly, the administration of 2 mg/kg also had a significant impact on the infarct volume after one week, although this effect disappeared at the end point of our study (14 days). Again, the 1 mg/kg dose showed the best therapeutic effect regarding the volume of the ischaemia. Despite corroborating and improving the results obtained in the previous study, where only one dose was used, once again we did not detect any significant changes in the blood glutamate levels (**Figure 52**) for any of the doses. In the sensorimotor tests, we saw an improving in the grip strength test at 14 days (**Figure 53, D**) with the 1 mg/kg dose, confirming it as the best therapeutic option.

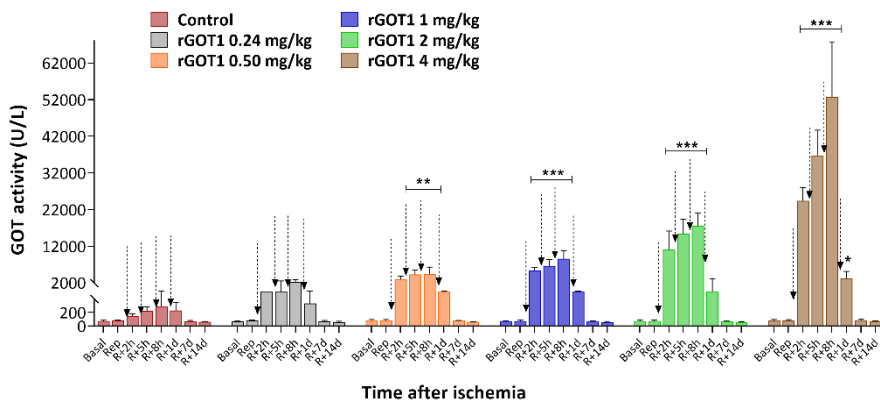


**Figure 50.** Temporal analysis of blood GOT activity in ischaemic animals. Control animals were injected (i.v.) with 1 mL of PBS (drug vehicle) and treated animals with 1 mL of rGOT1 (i.v.) at different concentrations. Treatments were injected right after reperfusion. tMCAO was induced during 75 minutes. Basal samples were obtained before surgery. Arrows indicate treatment administration. Data are shown as mean  $\pm$  SEM. \* $P$ <0.05, \*\* $P$ <0.01, \*\*\* $P$ <0.001 compared to the control group ( $n=12$ ).

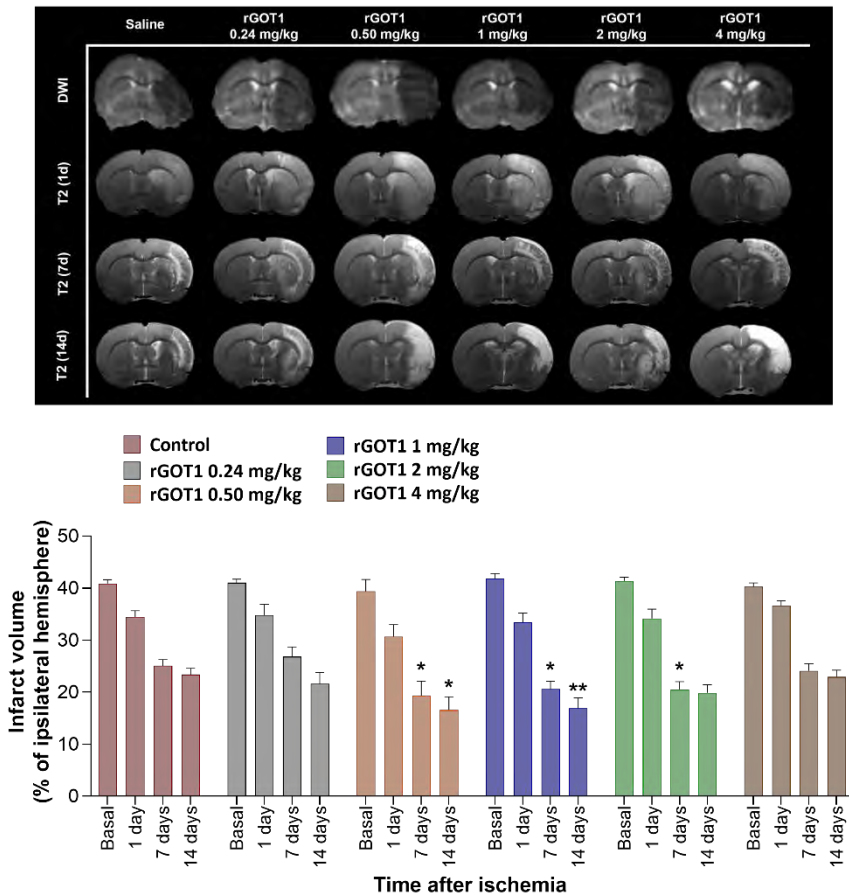


**Figure 51.** MRI assessments of ischaemic injury evolution. ADC maps were recorded during cerebral artery occlusion (defined as basal). Lesion volume evolution was assessed using T2-weighted images recorded 1, 7 and 14 days after ischaemia induction. Control animals were treated (I.V.) with 1 mL of PBS (drug vehicle), and rGOT1 animals were treated with 1 mL (I.V.) at different concentrations. Treatments were injected right after reperfusion. tMCAO was induced during 75 minutes. T2 lesions are represented as % adjusted to the ipsilateral hemisphere and corrected by oedema. Data are shown as mean  $\pm$  SEM (n=12).

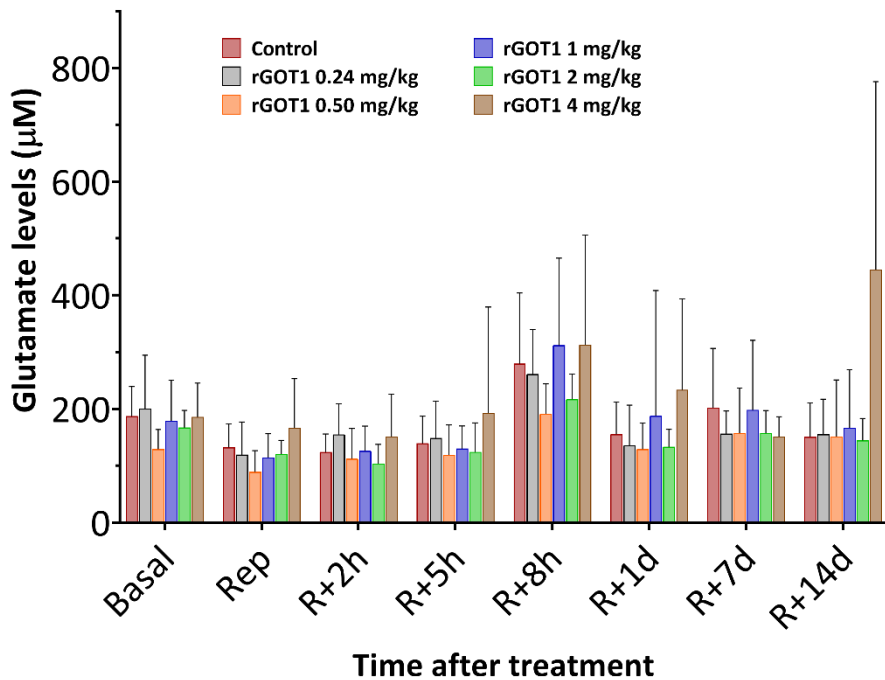


**Figure 52.** Temporal analysis of the effect of rGOT1 on blood glutamate levels in ischaemic animals. Control animals were treated (I.V.) with 1 mL of PBS (drug vehicle) and treated animals with 1 mL of rGOT1 (I.V.) at different concentrations. Basal samples were obtained before surgery. Data are shown as mean  $\pm$  SEM (n=6).

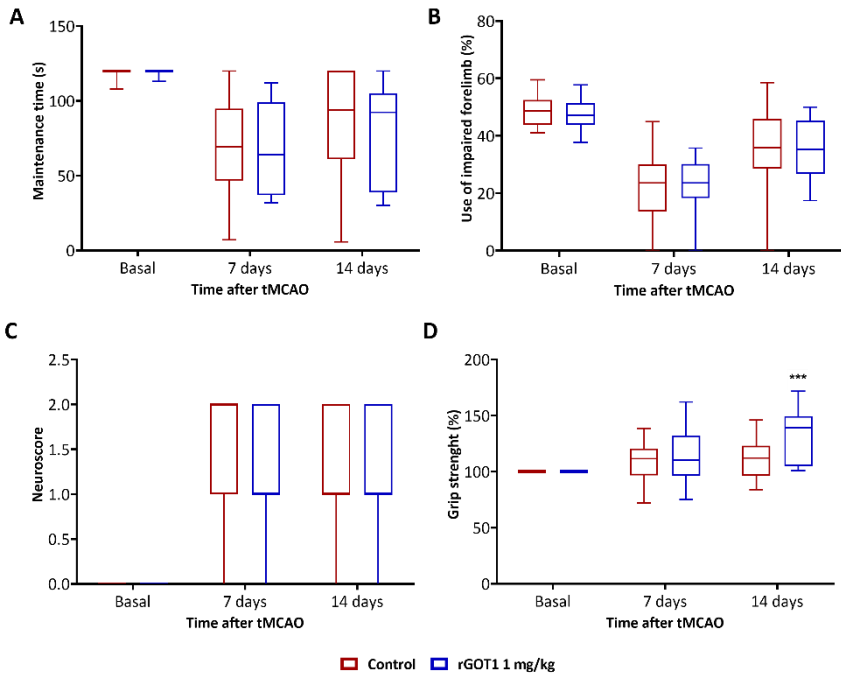


**Figure 53.** Box plots showing the assessment of sensorimotor function using rotarod test (A), cylinder test (B), neuroscore (C) and grip strength test (D). Functional tests were performed 1 day before ischaemic injury (baseline) and 7 and 14 days after injury in control (vehicle) and treated animals. Control animals were treated (i.v.) with 1 mL of PBS (drug vehicle), and rGOT1 treated animals with 1 mL (i.v.) at different concentrations. Treatments were injected right after reperfusion. tMCAO was induced during 75 minutes. Boxes represent interquartile ranges. The line across each box indicates the median, and the whiskers (T) are the highest and lowest values. Baseline reflects pre-treatment and preoperative functional evaluation. Data are shown as mean  $\pm$  SEM. \* $P < 0.05$ , \*\*\* $P < 0.001$  ( $n = 15$ ).

### 9.6.2.- MILD ISCHAEMIA

As we did before, we added a new study using a mild ischaemia model in order to observe the effect of the enzyme on smaller infarct volumes. In this case, we only used the doses of 0.50 and 1 mg/kg since they showed the best results in the previous experiments. Both treatments caused a significant increase of GOT activity in blood, as shown in **Figure 54**. In this occasion,

the 0.50 mg/kg dose did not show any effect on the infarct volume. However, the 1 mg/kg dose reduced, once again, the size of the lesion at 7 and 14 days to an even greater extent compared to the severe ischaemia animals (**Figure 55**). Furthermore, it also caused an improvement in the rotarod performance at 14 days, improvement also observed in the 0.50 mg/kg group, although to a lesser extent.

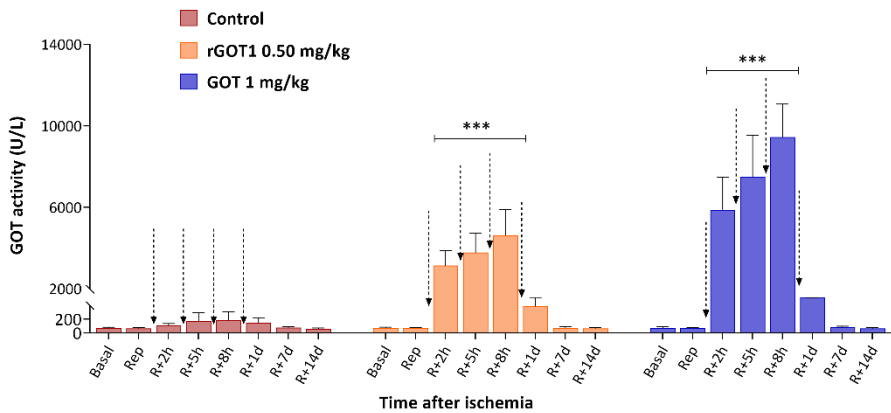


**Figure 54.** Temporal analysis of blood GOT activity in ischaemic animals. Control animals were injected (i.v.) with 1 mL of PBS (drug vehicle) and treated animals with 1 mL of rGOT1 (i.v.) 0.50 or 1 mg/kg. Treatments were injected right after reperfusion. tMCAO was induced during 45 minutes. Basal samples were obtained before surgery. Arrows indicate treatment administration. Data are shown as mean  $\pm$  SEM. \*\*\* $P < 0.001$  compared to the control group (n=12).

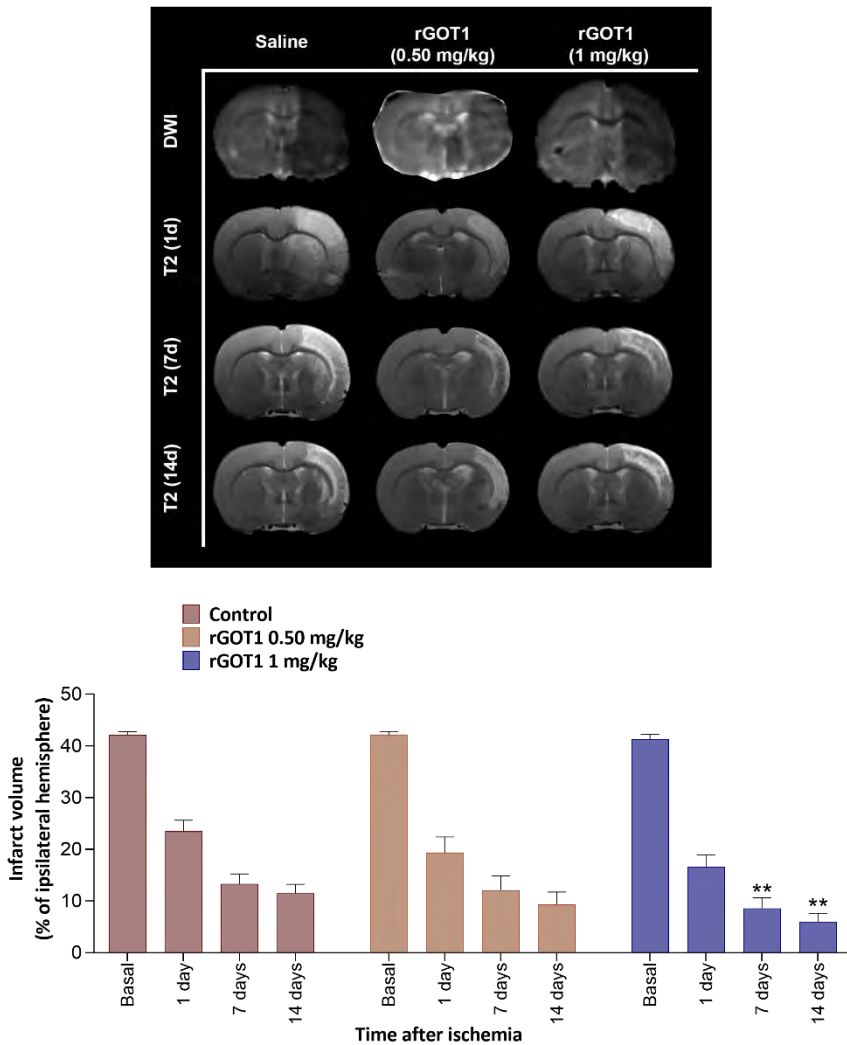


**Figure 55.** MRI assessments of ischaemic injury evolution. ADC maps were recorded during cerebral artery occlusion (defined as basal). Lesion volume evolution was assessed using T2-weighted images recorded 1, 7 and 14 days after ischaemia induction. Control animals were treated (i.v.) with 1 mL of PBS (drug vehicle), and rGOT1 animals were treated with 1 mL (i.v.) at 0.50 or 1 mg/kg. Treatments were injected right after reperfusion. tMCAO was induced during 45 minutes. T2 lesions are represented as % adjusted to the ipsilateral hemisphere and corrected by oedema. Data are shown as mean  $\pm$  SEM. \*\* $P < 0.01$  ( $n=12$ ).

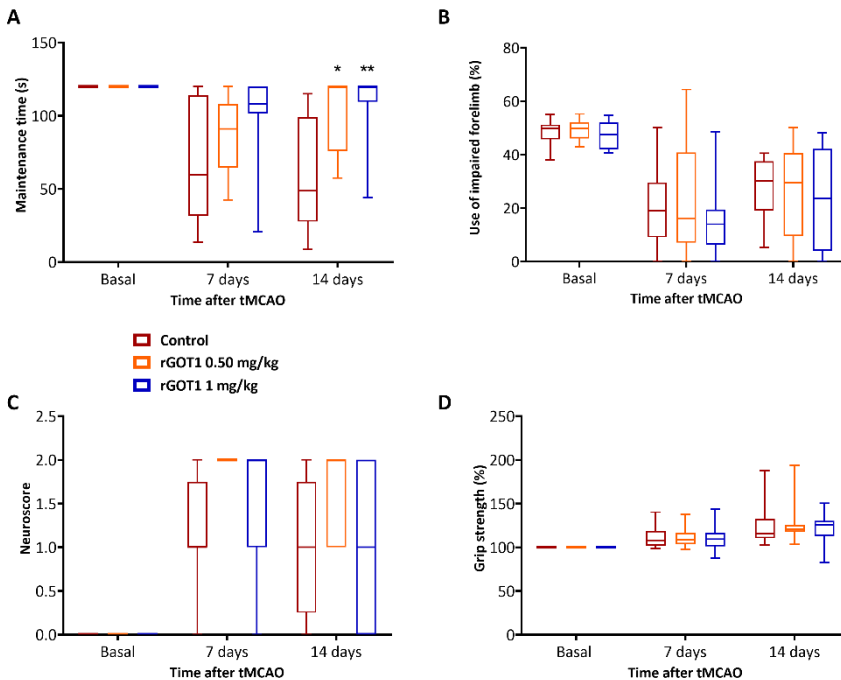


**Figure 56.** Box plots showing the assessment of sensorimotor function using rotarod test (A), cylinder test (B), neuroscore (C) and grip strength test (D). Functional tests were performed 1 day before ischaemic injury (baseline) and 7 and 14 days after injury in control (vehicle) and treated animals. Control animals were treated (I.V.) with 1 mL of PBS (drug vehicle), and rGOT1 treated animals with 1 mL (I.V.) at 0.50 or 1 mg/kg. Treatments were injected right after reperfusion. tMCAO was induced during 45 minutes. Boxes represent interquartile ranges. The line across each box indicates the median, and the whiskers (T) are the highest and lowest values. Baseline reflects pre-treatment and preoperative functional evaluation. Data are shown as mean  $\pm$  SEM. \* $P < 0.05$ , \*\* $P < 0.01$  ( $n = 12$ ).

Considering all these data, we decided to try once again a delayed administration of the drug (using for injections of the 1 mg/kg dose) to analyse the therapeutic window. rGOT1 administration caused an increase of the GOT activity in blood, (Figure 57). A delayed administration of the enzyme failed to show a significant reduction in the infarct volume of ischaemic animals. The only positive outcome observed were higher values in the grip strength test at 7 and 14 days after ischaemia (Figure 59). These results, combined with those obtained from the

single dose study, seem to confirm that a delayed injection of the drug is not effective, highlighting the importance of an early administration of the rGOT1, in accordance with the approved treatments for ischaemic stroke, where time is a crucial factor.

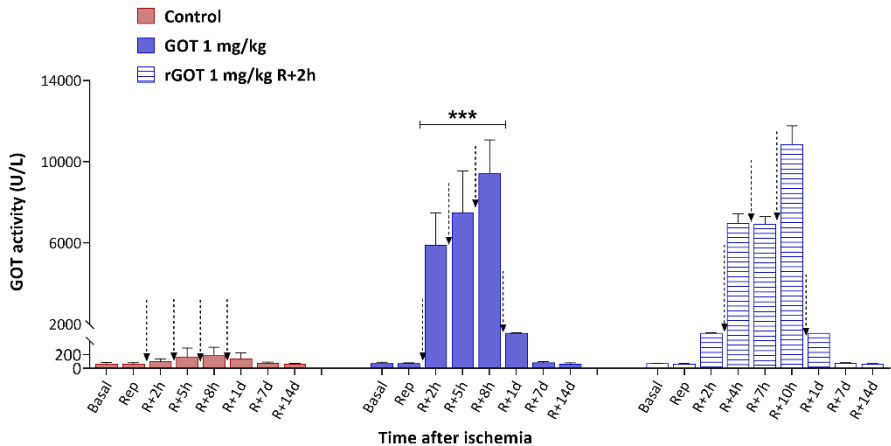


**Figure 57.** Temporal analysis of blood GOT activity in ischaemic animals. Control animals were injected (i.v.) with 1 mL of PBS (drug vehicle) and treated animals with 1 mL of rGOT1 (i.v.) 1 mg/kg. Treatments were injected at 0 or 2 hours after reperfusion. tMCAO was induced during 45 minutes. Basal samples were obtained before surgery. Arrows indicate treatment administration. Data are shown as mean  $\pm$  SEM. \*\*\* $P$ <0.001 compared to the control group ( $n=12$ ).

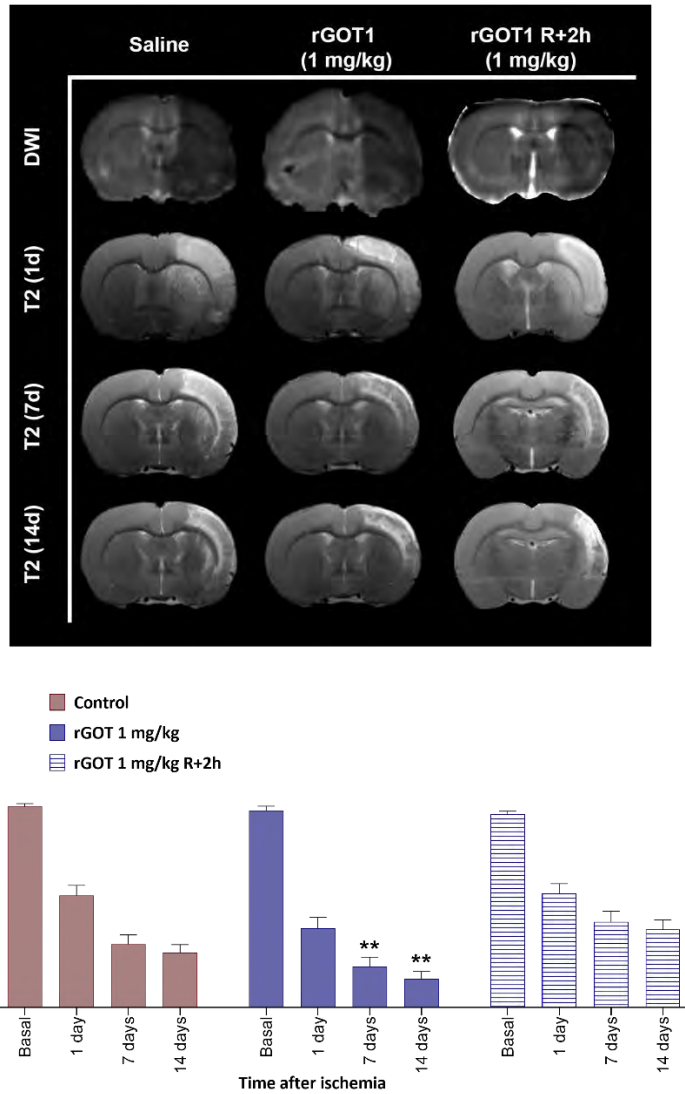


**Figure 58.** MRI assessments of ischaemic injury evolution. ADC maps were recorded during cerebral artery occlusion (defined as basal). Lesion volume evolution was assessed using T2-weighted images recorded 1, 7 and 14 days after ischaemia induction. Control animals were treated (I.V.) with 1 mL of PBS (drug vehicle), and rGOT1 animals were treated with 1 mL (I.V.) 1 mg/kg. Treatments were injected at 0 or 2 hours after reperfusion. tMCAO was induced during 45 minutes. T2 lesions are represented as % adjusted to the ipsilateral hemisphere and corrected by oedema. Data are shown as mean  $\pm$  SEM. \*\* $P < 0.01$  ( $n=12$ ).

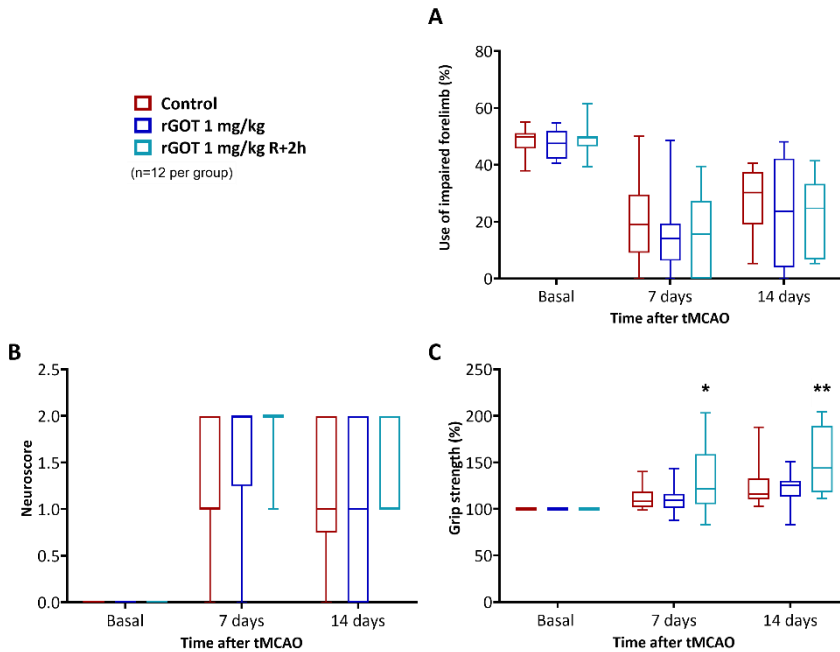


**Figure 59.** Box plots showing the assessment of sensorimotor function using cylinder test (A), neuroscore (B) and grip strength test (C). Functional tests were performed 1 day before ischaemic injury (baseline) and 7 and 14 days after injury in control (vehicle) and treated animals. Control animals were treated (i.v.) with 1 mL of PBS (drug vehicle), and rGOT1 treated animals with 1 mL (i.v.) 1 mg/kg. Treatments were injected at 0 or 2 hours after reperfusion. tMCAO was induced during 45 minutes. Boxes represent interquartile ranges. The line across each box indicates the median, and the whiskers (T) are the highest and lowest values. Baseline reflects pre-treatment and preoperative functional evaluation. Data are shown as mean  $\pm$  SEM. \* $P < 0.05$ , \*\* $P < 0.01$  ( $n = 12$ ).

## 9.7.- GOT1 Activity in CSF

Based on the lack of effect of rGOT1 on blood glutamate, we decided to study the GOT1 activity in CSF, both in healthy and ischaemic animals, in order to analyse if the enzyme was able to carry out its action directly in the cerebrospinal fluid. Animals were treated either with PBS, a single dose or four doses of 1

mg/kg of rGOT1 or with one dose of rGOT1 4 mg/kg. In all treated animals there was a significant increase in GOT activity in CSF, directly correlated with the amount of protein injected (**Figure 60**). This increase was higher 4 hours after treatment, both in healthy and ischaemic animals, for the 4 mg/kg dose and the 1 mg/kg dose when was administered four times.

Furthermore, in healthy animals, the increase of GOT activity 4 hours after treatment was higher in the group of 1 mg/kg (4 doses) than in the 4 mg/kg group, although this effect disappears in ischaemic animals, indicating that a sustained administration is more efficient than a single dose, even if the total amount of protein administered is the same. These results confirm that an exogenous rGOT1 administration has a significant effect on CSF GOT1 activity. However, if this is a secondary effect derived of the rGOT1 administration or if the protein is entering the CSF has yet to be elucidated.

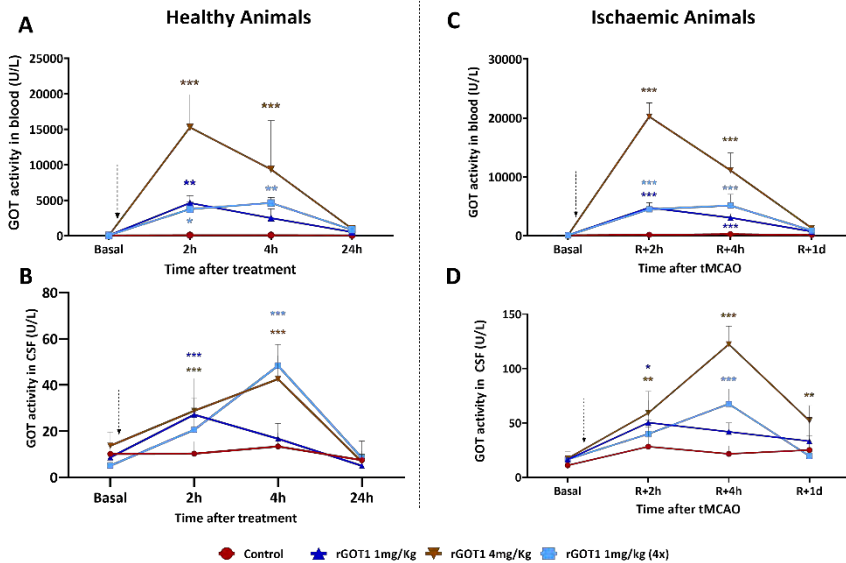


**Figure 60.** GOT1 activity was determined in blood and CSF from healthy (A, B) and ischaemic (C, D) animals. Control animals were treated (i.v.) with 1 mL of PBS (drug vehicle), and rGOT1 treated animals with 1 mL (i.v.) at 1 or 4 mg/kg (one dose) or 1 mg/kg (four doses). Treatments were injected right after reperfusion. tMCAO was induced during 75 minutes. Arrows indicate treatment administration. Data are shown as mean  $\pm$  SEM. \* $P < 0.05$ , \*\* $P < 0.01$ , \*\*\* $P < 0.001$  compared with the control group ( $n = 5$ ).

## 10.- SECTION III: rGOT1 BIOCONJUGATION

In order to extend the half-life of the rGOT1 and increase its therapeutic effect, a bioconjugate of the protein was designed. Furthermore, to try to target the rGOT1 towards the BBB and the brain, a second bioconjugate was synthesized. The characterization, pharmacokinetics and therapeutic effect of the bioconjugates are presented below.

## 10.1.- Synthesis of mPEG-rGOT1 and Angiopep-PEG-rGOT1

As shown in **Figure 61 (A)**, rGOT1 presents lysine residues (green) homogeneously distributed along the surface of the protein, which were selected as targets for random modifications with mPEG. Dimeric rGOT1 possesses 46 pendant amino groups (44 lysine residues and 2 N-terminal), although only 22 out of 46 are predicted to be solvent-accessible from the crystal structure of the protein. These were modified either with mPEG or Mal-PEG as determined by two complementary methods. Hence, bioconjugates bore approximately 22 polymer chains and possessed monomodal size-distribution profiles with dispersity (D) in the range of 1.4-1.9 (**Figure 61, B**).

In order to target rGOT1 to the BBB and promote transport to the brain, the terminal maleimide groups of Mal-PEG-rGOT1 were modified using a brain targeting peptide called Angiopep-2, which possesses a single thiol group. This targeting peptide is composed by 19 amino acids and it is derived from the common sequence of the low-density lipoprotein receptor-related protein 1 (LRP1) ligands. It is commonly used to target a wide range of nanocarriers, proteins or genetic material to the CNS.<sup>295</sup> LRP1 is highly expressed on the luminal side of the BBB and shows a high transcytosis efficacy and parenchymal accumulation.<sup>296</sup>

Grafting of Angiopep-2 to Mal-PEG-rGOT1 was measured by <sup>1</sup>H NMR spectroscopy (**Figure 61, D**). SEC analysis showed also an increase of hydrodynamic size (**Figure 61, B**). SDS-PAGE analysis of both rGOT1 bioconjugates under denaturing conditions can be seen in **Figure 61 (C)**, where two populations of bands were observed for the bioconjugates, corresponding to the monomeric or dimeric protein (some dimeric forms can be present due to incomplete denaturation) modified with polymer chains. No unmodified protein was observed and the size of the population increased slightly with the addition of Angiopep.

## 10.2.- Pharmacokinetics

Due to the association between PEGylation and catalytic activity loss,<sup>288</sup> the activity of the bioconjugates was measured using a GOT assay. Both conjugates preserved around 80% of the native rGOT1 activity, as shown in **Figure 61 (A)**. Additionally, the effect of the conjugation on blood exposure was analysed.

Equivalent amounts of native rGOT1 and both conjugates (based in protein concentration and similar activities) were I.V. injected in healthy and ischaemic animals. Blood samples were collected over a period of 30 days to analyse pharmacokinetics and pharmacodynamics of the conjugates. Initial activity (<1h) of rGOT1 and the bioconjugates was similar (**Figure 62, A**), but rGOT1 was rapidly clear from the blood. Furthermore, free PEG had no effect on GOT activity. On the other hand, both bioconjugates maintained high levels of GOT activity (between 3000 and 6000 U/L) until day 6. This suggests a tentative protection of rGOT1 from degradation (by serum proteases), as has been shown for other PEGylated proteins. Very little difference, if any, was observed between the mPEG-rGOT1 and Angiopep-PEG-rGOT1 groups. The pharmacokinetic profiles observed in healthy rats were also very similar to those observed for ischaemic rats (**Figure 62, B**), with negligible differences in half-lives of circulation/elimination or in area under the curves. This suggests that the routes of distribution and elimination of the bioconjugates were not affected by tMCAO and that the extended blood residence time correlated with a delayed elimination half-life.

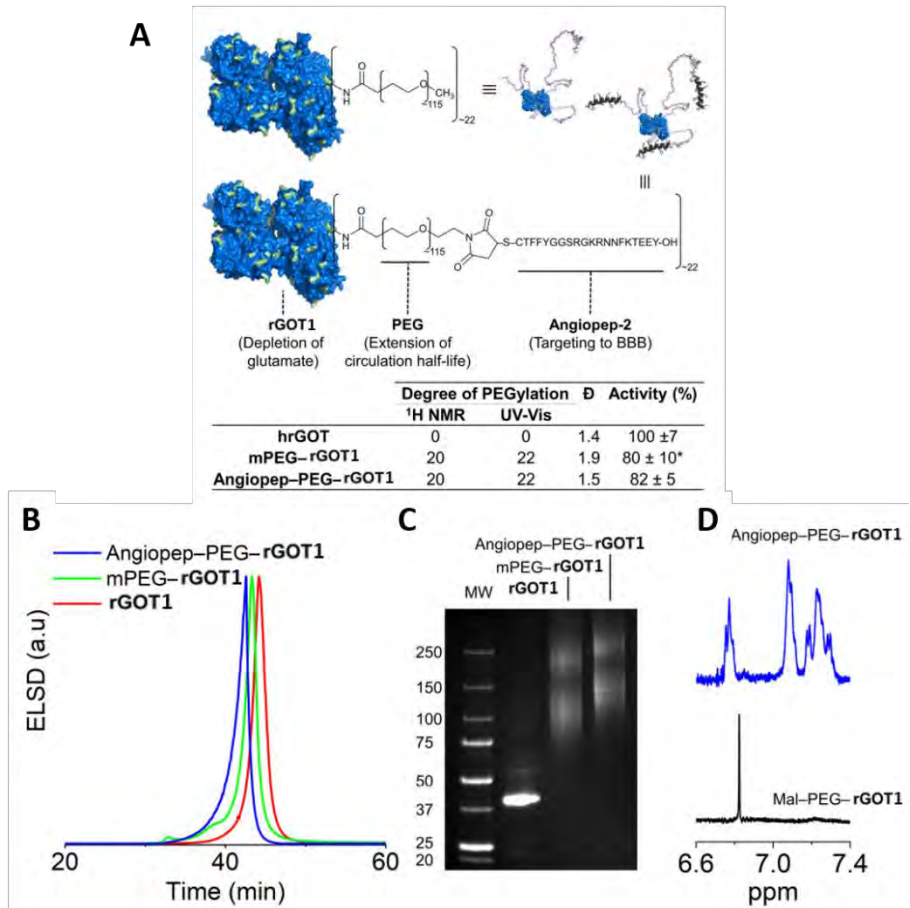


**Figure 61.** Design and characterization of protective bioconjugates. (A) rGOT1 was modified with mPEG or PEG bearing terminal Angiopep-2 ligands, with low loss of catalytic activity. The bioconjugates were designed for extended blood circulation and for BBB accumulation (via Angiopep-2). The degree of PEGylation was determined by UV-Vis and <sup>1</sup>H NMR spectroscopy. Dispersity was determined by size-exclusion chromatography. (B) Size exclusion chromatograms and SDS-PAGE (C) of the bioconjugates. (D) <sup>1</sup>H NMR spectra demonstrating quantitative modification of maleimide groups with Angiopep-2. ELSD: evaporative light scattering detector. Data are shown as mean ± SEM. \*P < 0.05, compared with native rGOT1 (n=3).

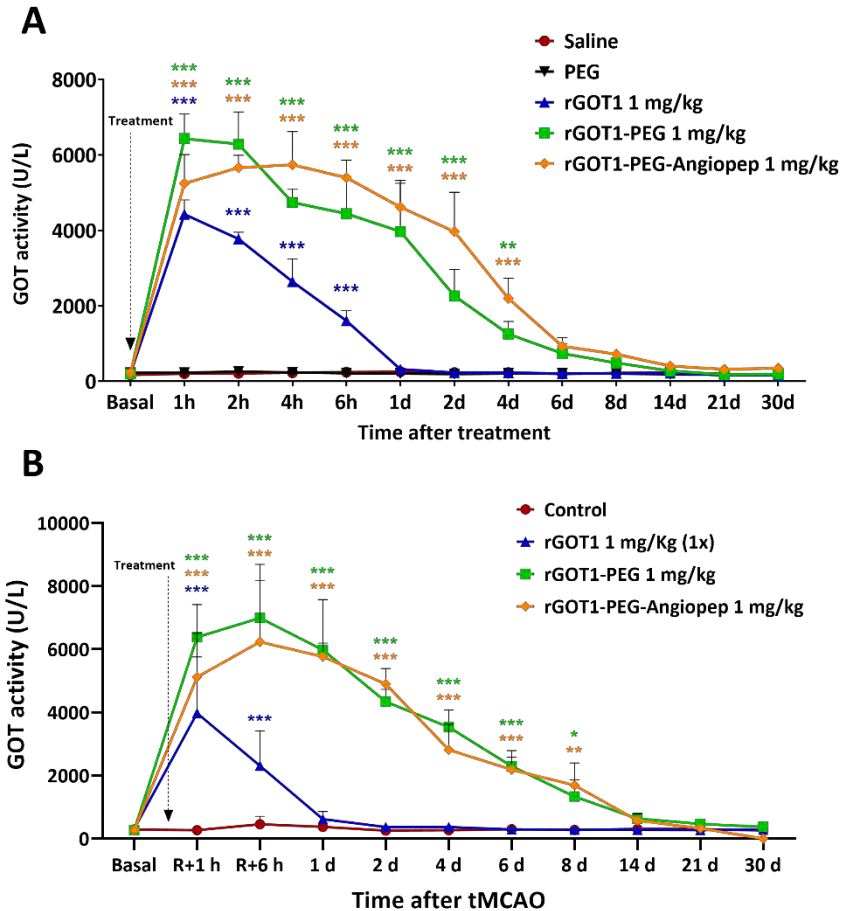


**Figure 62.** Temporal analysis of blood GOT activity in healthy (A) and ischaemic (B) animals. Control animals were injected (I.V.) with 1 mL of PBS (drug vehicle) and treated animals with 1 mL of rGOT1 or rGOT1 modifications (I.V.) 1 mg/kg. Treatments were injected right after reperfusion (ischaemic animals) or after basal measures (healthy animals). tMCAO was induced during 75 minutes. Basal samples were obtained before surgery. Data are shown as mean  $\pm$  SEM. \*\* $P < 0.01$ , \*\*\* $P < 0.001$  compared to the control group ( $n = 3-5$ ).

### 10.3.- Protective Study

In order to evaluate the effect of the enhanced rGOT1 blood exposure due to PEGylation, infarct volume was measured by MRI at different times after tMCAO. Representative images from central brain slices for each group are presented in **Figure 63 (A)** to illustrate the evolution of the infarct area. The slices show the occluded territory of the MCA, where the main ischaemic region is located. Infarct volume was measured in a 30-day period, as shown in **Figure 63 (B)**. ADC maps confirmed a similar baseline lesion volume, between 35-45% of the ipsilateral hemisphere (adjusted by oedema) in all groups. In this study, there was no significant difference between control group and animals treated with rGOT1. On the other hand, treatment with the bioconjugates showed a great reduction compared to control group (~40%). From day 7 onwards, reduction of infarct volume remained significant and evolved to a lesser extent. At day 30, the infarct volume for the bioconjugate groups was ~30% of their day 0 value, compared with ~60% for the saline and rGOT1 groups. The comparison of the infarct size measures with pharmacokinetics of the different treatments suggests that sustained GOT activity in blood, achieved with the bioconjugates, is beneficial for post-tMCAO recovery.

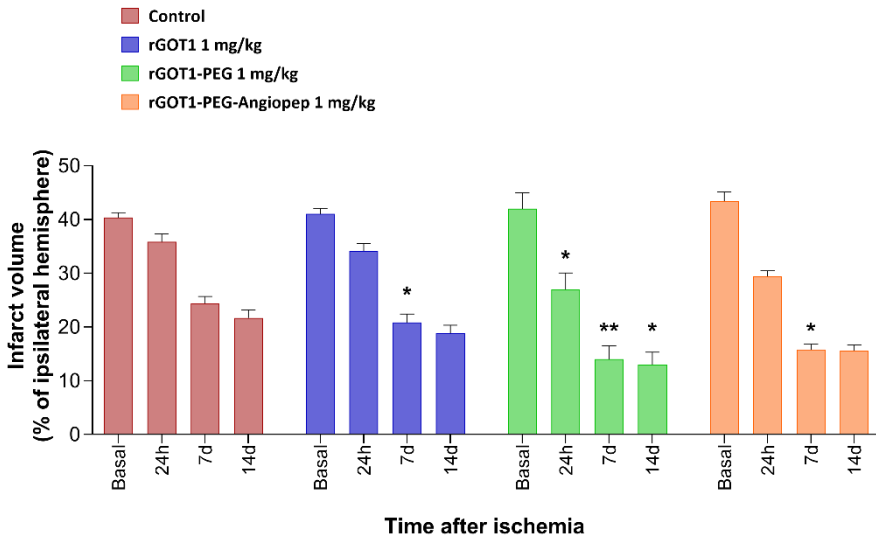


**Figure 63.** MRI assessments of ischaemic injury evolution. ADC maps were recorded during cerebral artery occlusion (defined as basal). Lesion volume evolution was assessed using T2-weighted images recorded 1, 7 and 14 days after ischaemia induction. Control animals were injected (i.v.) with 1 mL of PBS (drug vehicle), and treated animals with 1 mL of rGOT1 or rGOT1 modifications (i.v.) 1 mg/kg. Treatments were injected right after reperfusion. tMCAO was induced during 75 minutes. T2 lesions are represented as % adjusted to the ipsilateral hemisphere and corrected by oedema. Data are shown as mean  $\pm$  SEM. \* $P < 0.05$ , \*\* $P < 0.01$  ( $n = 5$ ).

To further study the protective effect of these new bioconjugates, motor functions of ischaemic rats were analysed using sensorimotor tests. Before surgery, all groups had similar results on rotarod test. At day 3, saline and rGOT1 groups showed a significant reduction in the rotarod performance compared with the bioconjugates groups (**Figure 64, A**). The retention time remained relatively stable for all groups until day 21 or 30, when it decreased in all groups. This reduction is likely to be due to the animals' loss of motivation to perform the physical exercise required to remain on the rotarod (lose their fear of falling), which is precisely one of the main limitations of this test. Intriguingly, performance appeared to degrade to a greater extent for the bioconjugate treated groups compared with the other groups at these late time points. This decline in

performance is believed to result from the caveat above rather than from real functional impairment, as it is not seen in the other functional test. In the cylinder test (**Figure 64, B**) animals treated with the bioconjugates displayed a significant increase in the use of the left (contralateral) forelimb ( $P<0.01$ ). They also showed an improved exploratory behaviour, evidenced by an increased amount of rearing. rGOT1 treated animals also presented an increase in left paw usage, compared to control group, at days 7, 14 and 21. On the other hand, grip strength test showed no significant differences between control and any of the treated groups. Overall, animals treated with rGOT1 had a better recovery than the control group, being said recovery higher in rats treated with the bioconjugates. Both infarct volume and sensorimotor tests results confirm that a sustained GOT activity in the blood contributes to protection after an ischaemic insult.

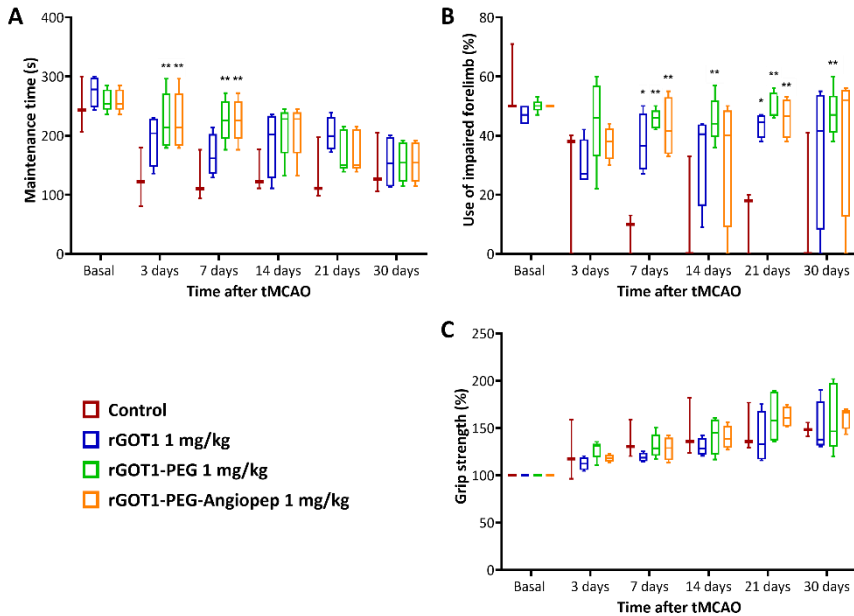


**Figure 64.** Box plots showing the assessment of sensorimotor function using rotarod test (A), cylinder test (B) and grip strength test (C). Functional tests were performed 1 day before ischaemic injury (baseline) and 3, 7, 14, 21 and 30 days after injury in control (vehicle) and treated animals. Control animals were injected (i.v.) with 1 mL of PBS (drug vehicle), and treated animals with 1 mL of rGOT1 or rGOT1 modifications (i.v.) 1 mg/kg. Treatments were injected right after reperfusion. tMCAO was induced during 75 minutes. Boxes represent interquartile ranges. The line across each box indicates the median, and the whiskers (T) are the highest and lowest values. Baseline reflects pre-treatment and preoperative functional evaluation. Data are shown as mean  $\pm$  SEM. \* $P < 0.05$ , \*\* $P < 0.01$  ( $n = 5$ ).

Blood glutamate concentration was not affected by any of the treatments thus leaving no correlation between enzymatic activity and blood glutamate levels (data not shown). These results can be related to a rapid homeostasis of glutamate in blood. Furthermore, no effect on CSF glutamate levels was detected (data not shown), suggesting a rapid glutamate homeostasis also in the brain.

Finally, we compared the results obtained with the administration of the pegylated version of the rGOT1 against the

data obtained in the 4 injections protocol with the native rGOT1 (**Figure 65**). The use of the rGOT1-PEG shows a less sharp profile of GOT activity in blood, as well as a prolonged enzyme activity, being significant at least until 8 days after administration, while the native rGOT1, even with 4 doses, lose its activity 1 day after treatment.

Regarding infarct volume (**Figure 66**), rGOT1-PEG shows an early effect in the infarct volume, being significant as soon as one day after ischaemia onset. Nevertheless, the use of a pegylated version of the enzyme did not show any significant changes respect to the native rGOT1 at the end point of our study (14 days). Although the size of the lesion seems to be smaller with the bioconjugate, the difference between both versions of the protein is not great enough to appreciate a substantial improvement.

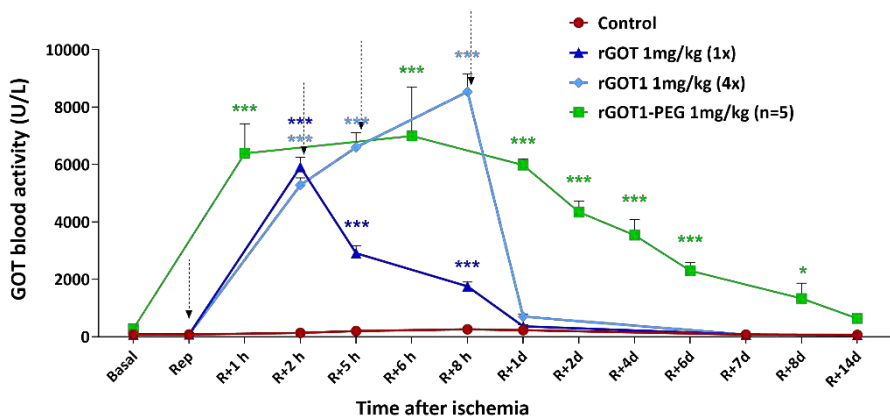


**Figure 65.** Temporal analysis of blood GOT activity in healthy (A) and ischaemic (B) animals. Control animals were injected (I.V.) with 1 mL of PBS (drug vehicle) and treated animals with 1 mL of rGOT1 or rGOT1 modifications (I.V.) 1 mg/kg. Treatments were injected right after reperfusion (ischaemic animals) or after basal measures (healthy animals). tMCAO was induced during 75 minutes. Basal samples were obtained before surgery. Arrows indicate treatment administration. Data are shown as mean  $\pm$  SEM. \*\* $P$ <0.01, \*\*\* $P$ <0.001 compared to the control group ( $n$ =3-5).

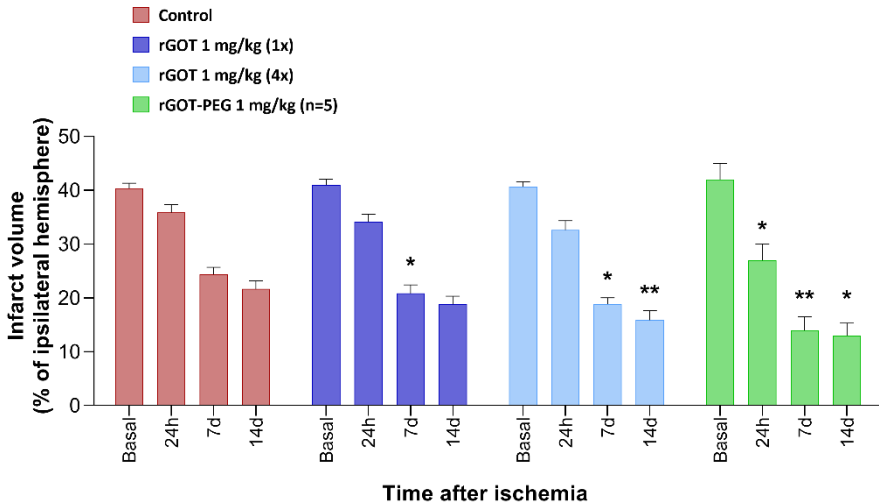


**Figure 66.** MRI assessments of ischaemic injury evolution. ADC maps were recorded during cerebral artery occlusion (defined as basal). Lesion volume evolution was assessed using T2-weighted images recorded 1, 7 and 14 days after ischaemia induction. Control animals were injected (i.v.) with 1 mL of PBS (drug vehicle). Treated animals were injected with 1 mL of rGOT1 (one or four doses) or rGOT1-PEG (i.v.) 1 mg/kg. Treatments were injected right after reperfusion. tMCAO was induced during 75 minutes. T2 lesions are represented as % adjusted to the ipsilateral hemisphere and corrected by oedema. Data are shown as mean  $\pm$  SEM. \* $P < 0.05$ , \*\* $P < 0.01$  ( $n = 5-12$ ).

#### 10.4.- GOT1 Activity in CSF

GOT activity was slightly increased in CSF 2 hours after rGOT1 administration, suggesting that a very small portion of the protein could be reaching the CSF (**Figure 67**). Nevertheless, this increase is very small, especially compared with the huge increase observed in blood. mPEG-rGOT1, on the other hand, showed no alteration of CSF GOT activity, indicating that the presence of the polymer could prevent passage through BBB or the blood-CSF barrier. The pharmacokinetics and pharmacodynamics observed for the targeted Angiopep-PEG-rGOT1 and the non-targeted mPEG-rGOT1 conjugates were not statistically different (data not shown), implying that brain or near-brain accumulation of the targeted bioconjugate

represents only a minor fraction of the total administered protein and does not contribute significantly to the results.

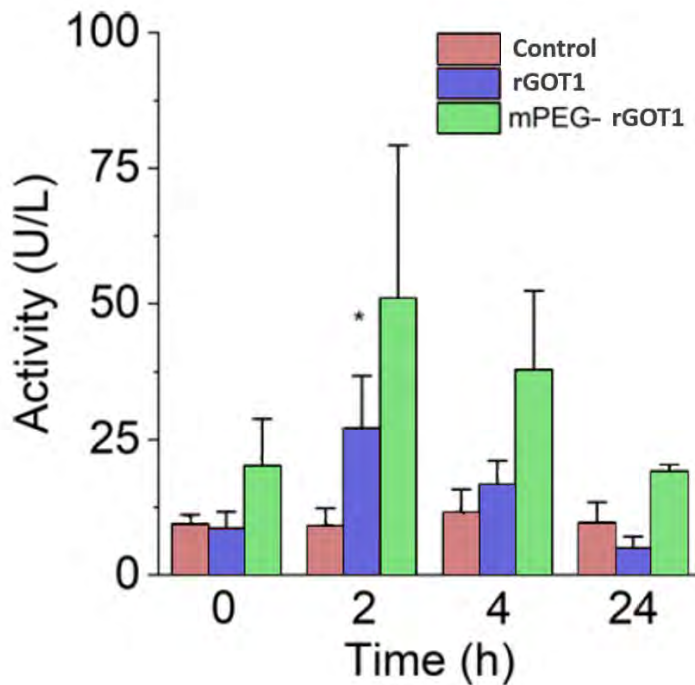


**Figure 67.** Pharmacokinetics in CSF. Saline, rGOT1, and mPEG-rGOT1 were administered to healthy rats. The catalytic activity was monitored in CSF samples taken at specific time points. Data are shown as mean  $\pm$  SEM. \* $P < 0.05$ , compared with the control group ( $n = 3$ ).

## 11.- SECTION IV: rGOT1 AND rtPA INTERACTION

As mentioned before, rtPA is the only pharmacological treatment currently approved for ischaemic stroke. Hence, for the development of a new therapeutic agent in stroke, it is of utmost importance to ensure a compatibility between the two drugs. In

order to do this, a series of analysis, including *in vitro* and *in vivo* studies, were performed.

### 11.1.- *In Vitro* Analysis

First, rtPA was incubated for 30 minutes with different concentrations of a rtPA inhibitor (leupeptin) and rGOT1 and its activity was measured using a fluorescence molecule as a reporter. A concentration of 100  $\mu\text{M}$  of the inhibitor was sufficient to induce a significant reduction in rtPA activity (**Figure 68, A**). Higher concentrations of the inhibitor had a greater impact in the rtPA activity reduction, with a maximum of ~90% reduction using a 10 mM concentration. On the other hand, none of the concentrations tested for rGOT1, up to 10 mM, had any effect on the rtPA activity (the estimated concentration for the 1 mg/kg treatment in the ischaemic animals is 0.15-0.20  $\mu\text{M}$ , assuming an animal weight of 250 grams and a blood volume of 13-18 mL).

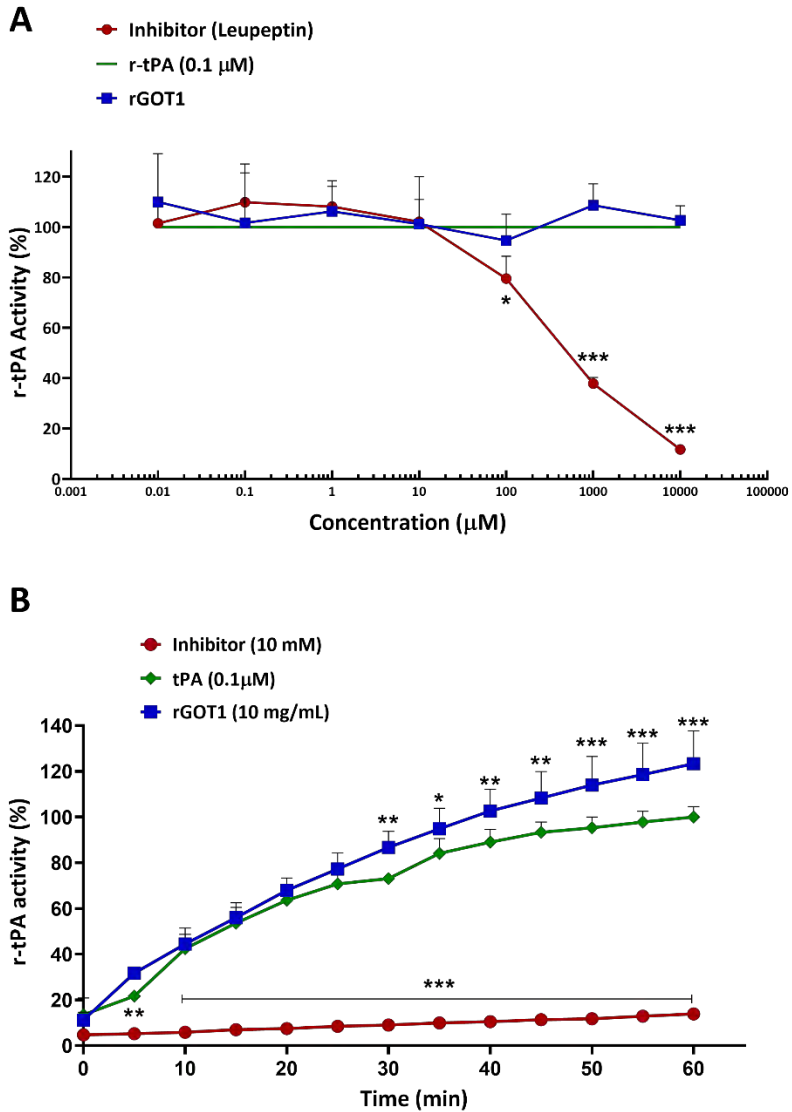


**Figure 68.** Analysis of rtPA activity *in vitro*. (A) rtPA activity at 30 minutes. rtPA was incubated with different concentrations of the inhibitor or rGOT1. Data are shown as a percentage relative to the activity of rtPA alone. (B) Kinetic profile of rtPA incubated with a fixed concentration of leupeptin (10 mM) or rGOT1 (10 mg/mL). Data are shown as a percentage relative to the activity of rtPA after 60 minutes. Data are shown as mean  $\pm$  SEM. \* $P$ <0.05, \*\* $P$ <0.01, \*\*\* $P$ <0.001 compared to the control group ( $n=4$ ).

Then, we carry out a kinetic profile of the rtPA activity using a fixed concentration of both the inhibitor and rGOT1 (**Figure 68, B**). The inhibitor showed a significant reduction of the rtPA activity as soon as 5 minutes after the start of the incubation. This reduction was significant for the entire duration of the assay. On the other hand, rGOT1 did not have any negative impact on the rtPA activity. Furthermore, from 30 minutes onwards the rtPA incubated with rGOT1 showed a higher activity compared with the rtPA alone, although this could be due to a background signal from the rGOT1, since a synergy between the two molecules is unlikely.

## 11.2.- Thrombin-Induced Stroke Model

For *in vivo* studies, we first utilized a thromboembolic model in mice. The usual parameters (GOT activity and infarct volume) were measured, as long as the reperfusion rate in control and treated animals. As expected, the rGOT1 administration had a significant impact on GOT activity in blood (**Figure 69**), measured 60 minutes after occlusion (30 minutes after administration). GOT activity levels were almost the same between animals treated with rGOT1 alone and animals with the double treatment (rtPA and rGOT1) suggesting that the use of rtPA has no impact on the rGOT1 performance. These data support the idea that there is no interaction between rtPA and rGOT1, in concordance with the data obtained in the *in vitro* analysis.

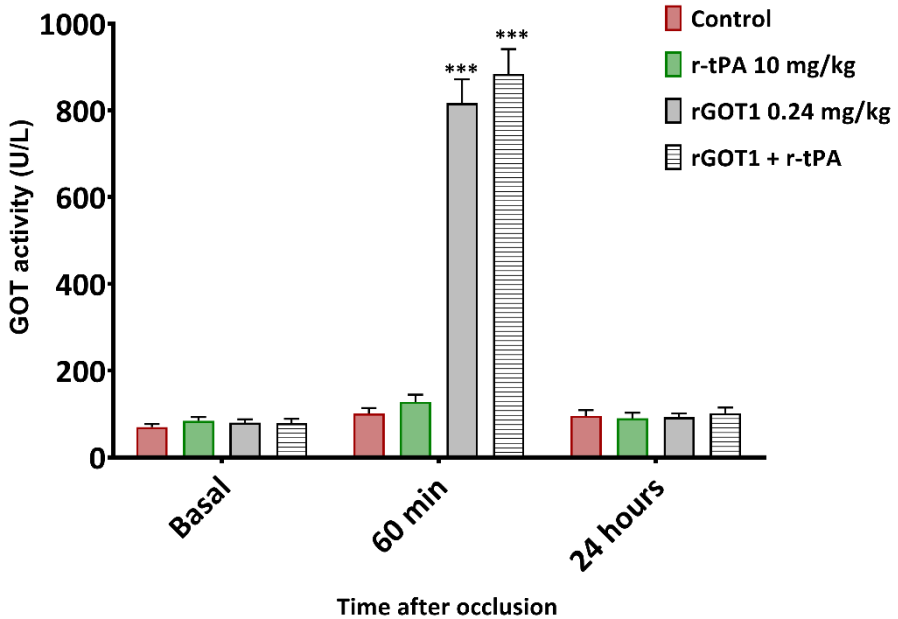


**Figure 69.** Temporal analysis of blood GOT activity in ischaemic animals. Treatments were injected 30 minutes after occlusion. Basal samples were obtained before treatment. Data are shown as mean  $\pm$  SEM. \*\*\* $P$ <0.001 compared to the control group (n=12).

Next, we analysed the recanalization rates of the animals. Recanalization rates showed a significant difference between rtPA (positive control) and control group (treated with PBS). This significance appeared also in the group treated with a combination of rtPA and rGOT1, proving no deleterious effect of the rGOT1 over rtPA activity *in vivo*. There was also a significant difference between rtPA and rGOT1 treated animals, as it was anticipated, since rGOT1 is not expected to have any thrombolytic activity.

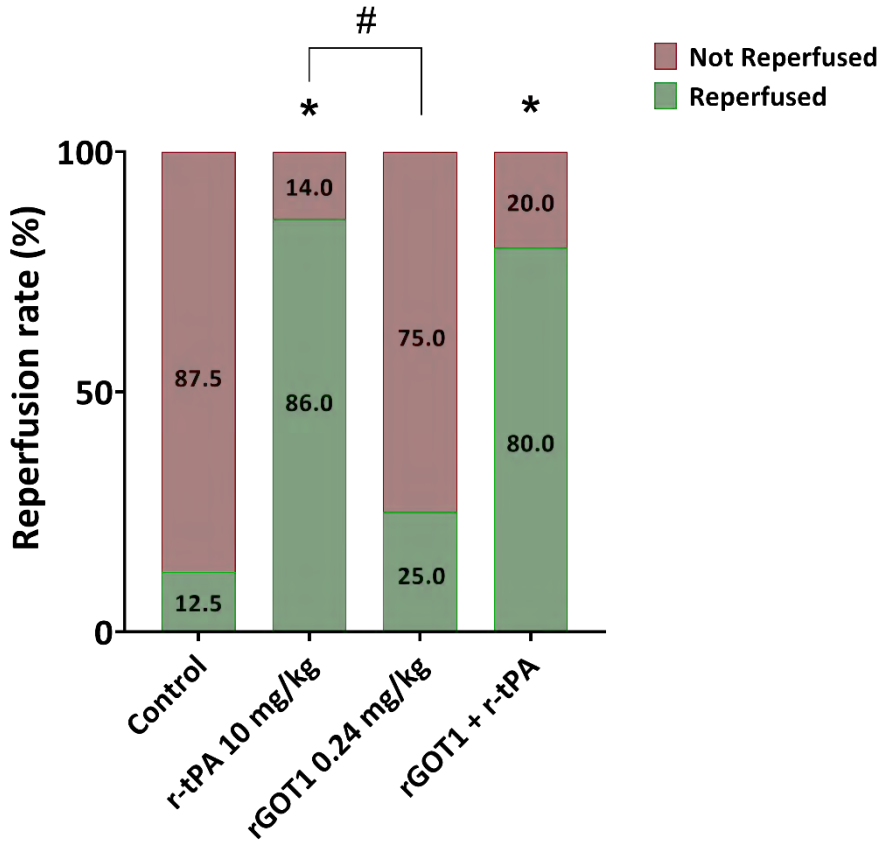


**Figure 70.** Reperfusion rate in ischaemic animals. Treatments were injected 30 minutes after occlusion. Reperfusion was considered successful when at least 50% of the basal CBF was restored within 30 minutes after treatment. Results are expressed as percentage of reperused and not reperused animals respect to the total number. Data are shown as mean  $\pm$  SEM. \* $P < 0.05$  compared to the control group. # $P < 0.05$  (n=8).

In relation to sensorimotor test (data not shown), only rotarod test showed a noteworthy difference, 1 day after ischaemia, between control and rGOT1 treated groups, although this disparity was not repeated in the other time points analysed.

### 11.3.- Embolic Stroke Model

After studying the rtPA and rGOT1 interaction in mice, we decided to analyse it once again using an embolic stroke model in rats. Besides the rtPA and rtPA combined with rGOT1 groups, equivalent to the ones studied before, we added a new group where rGOT1 was administered 30 minutes before rtPA in order to test if a pre-hospital administration of rGOT1 could be compatible with the reperfusion therapy with rtPA. Infarct volumes (**Figure 71**) showed a significant decrease in the lesion size (at 90 minutes after occlusion) when rGOT1 was administered 30 minutes before rtPA. However, the infarct volumes at this time point were assessed only 90 minutes after occlusion when the lesion was not fully well established, so these results should be taken with caution. In line with this appreciation, differences in the infarct volume disappeared at 24 hours.

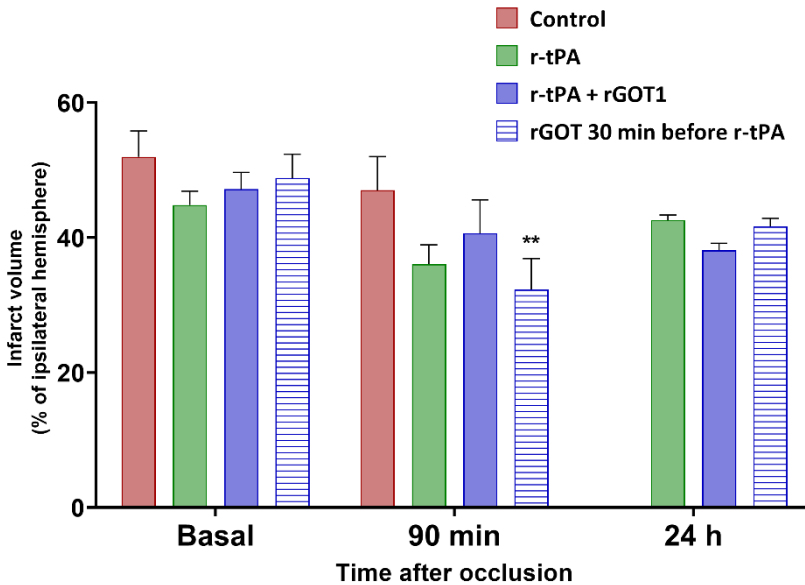


**Figure 71.** MRI assessments of ischaemic injury evolution. ADC maps were recorded during cerebral artery occlusion (defined as basal). Lesion volume evolution was assessed using ADC images (90 minutes after occlusion) and T2-weighted images (1 day after ischaemia induction). Treatments were injected 30 or 60 minutes after occlusion. Lesions are represented as % adjusted to the ipsilateral hemisphere and corrected by oedema. Data are shown as mean  $\pm$  SEM. \*\* $P < 0.01$  compared to the control group ( $n = 8$ ).

For the recanalization rates, results were similar to those obtained in mice, although the differences were not big enough to show any significance (**Figure 56**).

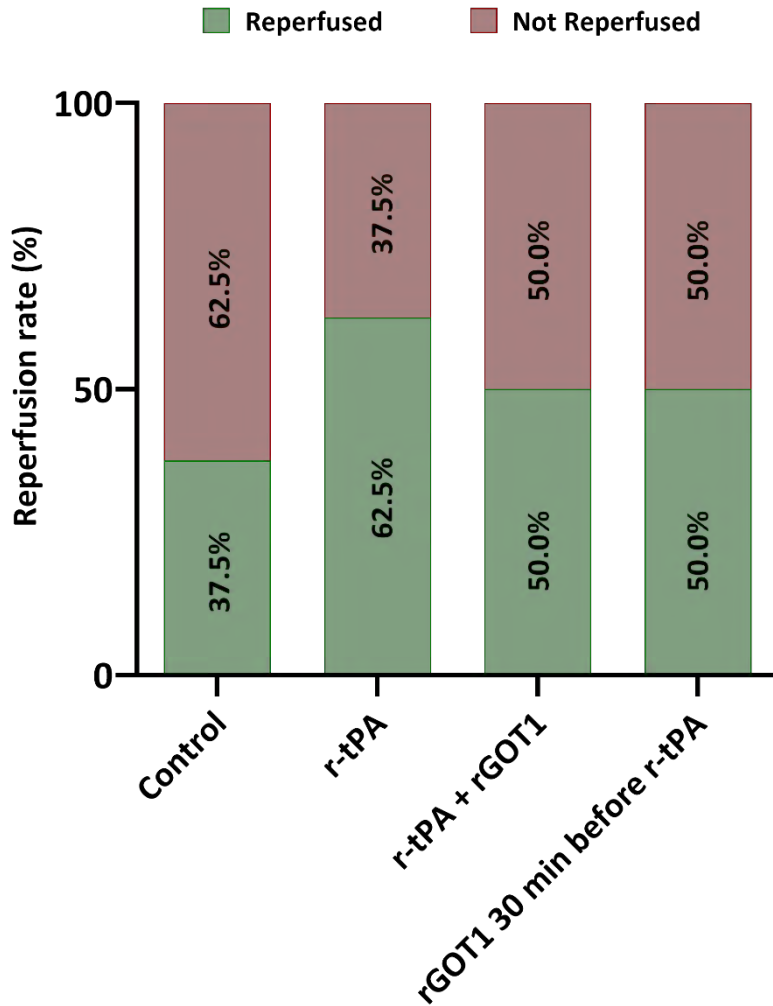


**Figure 72.** Reperfusion rate in ischaemic animals. Treatments were injected 30 or 60 minutes after occlusion. Reperfusion was determined by means of MRA. Results are expressed as percentage of reperfused and not reperfused animals respect to the total number. Data are shown as mean  $\pm$  SEM (n=8).

In this occasion, we also analysed the mortality at 24 hours (Figure 73). Control group (treated with PBS) had a 100% mortality rate at 24 hours, even in those animals with a spontaneous reperfusion. Groups treated with rtPA, either alone or combined with rGOT1, had a significant lower mortality compared to the control group.

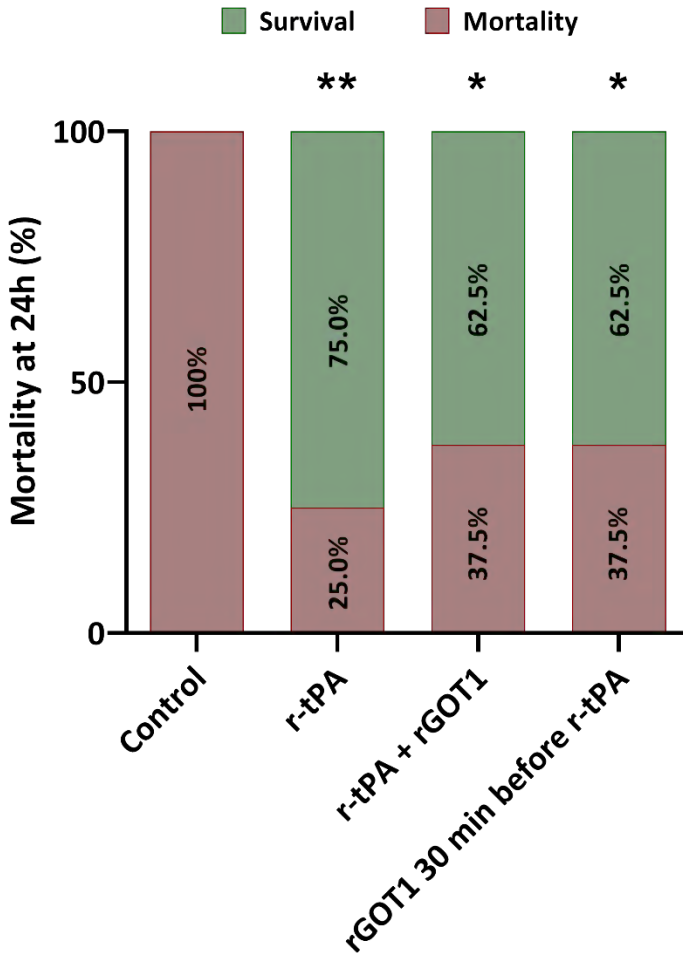


**Figure 73.** Mortality rate in ischaemic animals at 24 hours. Treatments were injected 30 or 60 minutes after occlusion. Results are expressed as percentage of deceased or living animals respect to the total number. Data are shown as mean  $\pm$  SEM. \* $P < 0.05$ , \*\* $P < 0.01$  (n=8).



## DISCUSSION

## 12.- SECTION I: ENDOGENOUS GOT1 INHIBITION STUDIES

Several studies have proposed GOT1 as a novel therapeutic drug based on its capacity to act as a blood glutamate scavenger; moreover, its use has been suggested for the acute phase of ischaemic stroke in order to reduce the neurological damage caused by glutamate excitotoxicity.<sup>125</sup> However, as mentioned before, GOT1 plays a major role, not only in glutamate metabolism and homeostasis, but also in other metabolic pathways. Due to this, this study was designed to produce, purify and test a polyclonal antibody against GOT1 to block its metabolic activity, allowing to evaluate its role and repercussions on an energetically compromised ischaemic brain. For this, the same animal model where rGOT1 beneficial effect was demonstrated, was used.<sup>125</sup>

One of the most crucial pathways GOT1 is involved in is the MAS, responsible for the transport of cytosolic reducing equivalents produced in different metabolic pathways, since the inner mitochondrial membrane is impermeable to NADH molecules. This shuttle has been observed to be crucial in the earliest stages of embryo development, as soon as the two-cell stage.<sup>297</sup> Due to this, the use of a knockout model for GOT1 had to be discarded as the animals were non-viable.

Therefore, another strategy had to be proposed in order to overcome this issue. One of the possibilities would be utilizing a conditional knockout, where the desired gene is normally flanked by two target sequences (LoxP) which are recognized by the recombinase Cre. The recombinase can then be activated at the desired time by administering tamoxifen. This technology allows to maintain a normal physiological function of the targeted cells until the recombinase is activated, overcoming some of the problems of the traditional knockouts. However,

and despite various efforts to address some of its limitations,<sup>298</sup> this method is still technically challenging, time consuming and expensive, in addition to requiring a greater number of animals.<sup>299</sup>

For all these reasons, we decided to use a polyclonal antibody instead, since its production is simpler, less expensive and it requires a reduced number of animals. The experiments conducted showed that the use of the AbGOT1 had a drastic impact on GOT1 normal function, reducing its activity for at least 8 days. Furthermore, we analysed the effect of the antibody in another serum transaminase very similar in structure and function to the GOT, the GPT, and results showed that the activity inhibition was specific to the GOT1. In view of this, we can conclude that the use of an antibody specifically designed against GOT1 is a viable approach to study the impact this protein has in a compromised ischaemic brain. Nevertheless, it should be noted that no study was conducted in order to analyse if the AbGOT1 had some impact in the other isoform of the protein, the mitochondrial GOT (GOT2). Further studies should be performed to discard any influence of a possible GOT2 inhibition in the results obtained and to confirm if the data presented in this manuscript is due solely to the inhibition of the GOT1.

Animals subjected to ischaemia and treated with the antibody showed that the inhibition of the blood GOT1 activity leads to an increased ischaemic damage and a poorer sensorimotor outcome, compared with non-treated ischaemic animals. These data are consistent with a similar observation reported in stroke patients, where patients with higher blood GOT levels (>18 U/L) had significantly less neurological damage 3 months after stroke compared to those whose blood GOT levels were lower.<sup>201,300</sup> These previous data, combined with the ones obtained from the present study, support the idea that cellular GOT1 has a crucial role during an ischaemic insult by maintaining cell viability and reducing neuronal damage.

Furthermore, MRS analysis of the brain parenchyma of animals treated with AbGOT1 demonstrated a significant increase in glutamate levels. In this regard, recent reports,<sup>203,204</sup> have proposed that, besides the blood glutamate grabbing property, GOT1 can, alternatively, metabolize glutamate in the cerebral ischaemic site as an alternative source of energy to maintain the cellular viability and to protect the brain against the excitotoxic damage. Thus, overexpression of GOT1 in the brain parenchyma caused a reduction of the ischaemic stroke lesion volume and improve the post-stroke sensorimotor functions. Based on these previous findings, we could observe that AbGOT1 induced a partial blocking of the GOT1 activity in the brain, and therefore this might contribute to the increase of glutamate in the extracellular space of the brain of ischaemic animals treated with AbGOT1, that could explain why they had a larger ischaemic lesion and poorer outcome.

Despite MRS results, where a clear increase in intracerebral glutamate can be observed, and contrary to the key role of GOT1 in glutamate metabolism, the expected raise in blood glutamate levels did not take place. HPLC analysis of serum samples of ischaemic rats treated with AbGOT1 showed no significant differences with the control group. A possible explanation for this could be the involvement of other enzymes in glutamate homeostasis. Although GOT represents a critical step in glutamate metabolism and homeostasis, both in blood and brain, as well as other organs, the presence of other serum enzymes capable of metabolising the glutamate could be reverting the effect of the AbGOT1 in glutamate levels. As we described before, we analysed the activity of other protein deeply related to glutamate metabolism, GPT, showing that the treatment with our antibody had no effect in the activity of this protein. GPT is another transaminase very similar, both in sequence, structure and function, to GOT1. This enzyme catalyses the reversible transamination between alanine and  $\alpha$ -ketoglutarate into pyruvate and glutamate, playing an important

role in glutamate homeostasis.<sup>301</sup> GPT activity, as in the case of GOT, was increased after ischaemic induction, but was not affected by the use of AbGOT1.

Furthermore, there are other enzymes involved in glutamate metabolism that were not tested in our studies, such as glutamate dehydrogenase, glutaminase synthetase or ornithine transaminase. Still, the reason why glutamate levels remain stable is yet to elucidate. Nevertheless, inhibition of GOT1 activity during the ischaemic period did cause an increase in infarct volume and a poorer neurological outcome. These results still support the use of rGOT1 as a promising drug for the acute phase of cerebral ischaemia.

Besides differences in the lesion size following ischaemia, animals treated with AbGOT1 also showed a bigger lesion size during arterial occlusion (defined as the basal time point and measured by ADC), contrary to our previous experience, where basal measures remained always stable among groups.<sup>275,302</sup> An analysis of the cerebral blood flow was performed in order to discard any possible changes in this physiological parameter due to the administration of AbGOT1. However, no detectable differences were observed in the blood flow of the middle cerebral artery during a 150 minutes monitoring. Nevertheless, previous studies conducted in tumoral cells have shown that an inhibition of GOT1 leads to an increase of lactate levels and generates a glucose-dependent metabolic stress.<sup>303,304</sup> This metabolic stress turns the cells more susceptible to damage, especially during a situation with a low glucose availability, such as ischaemic stroke. As presented in our study by MRS analysis, the inhibition of GOT1 by the action of the antibody increased the cerebral lactate levels, probably by the action of lactate dehydrogenase. Since AbGOT1 treatment is administered one hour before ischaemia onset, the brain parenchyma could already be in a susceptible state, explaining why the size of the lesion is bigger in treated animals even during artery occlusion.

Finally, results obtained from CSF and brain tissue analysis showed that the inhibition of GOT activity observed in blood is also present in cerebrospinal fluid and brain homogenates. Regarding the measures in CSF, two possibilities exist. Previous findings showed that proteins, antibodies and a large part of the molecules found in blood are capable of passively crossing the blood-CSF barrier.<sup>305</sup> Hence, the AbGOT1 could be entering the CSF through the choroid plexus epithelium, exerting its action directly in the GOT present in the CSF. Also, the already inhibited GOT, joined to the antibody, could be entering the CSF, replacing the normal functioning enzyme in the CSF. Although both scenarios are possible, passage of molecules from blood to CSF through the choroid plexus is inversely proportional to the size of the molecule,<sup>305</sup> so it is more likely that the antibody alone, and not the AbGOT1-GOT1 complex, is crossing the blood-CSF barrier and inhibiting the enzyme *in situ*.

On the other hand, it has been observed that antibodies are not capable of trespassing the BBB from blood to brain.<sup>306</sup> The BBB is composed by endothelial cells of the brain microvasculature, astrocytes and pericytes composing what is called the neurovascular unit. Additionally, neurons and microglia, despite not being part of the neurovascular unit, also play a significant role in BBB integrity, although the exact extent and nature of their involvement in this structure is not completely clear.<sup>307</sup> The BBB (**Figure 74**) is essential in regulating the influx and efflux of ions, oxygen and nutrients between the blood and brain compartments and protecting the delicate neural tissue by restricting the invasion of toxins and pathogens.

The transport of large molecules, such as antibodies, across the BBB exists, although it is highly regulated. Protein transport through BBB, carried out by transcytosis, is very limited. Endothelial cells in brain microvasculature present around 80-84% less endocytic vesicles compared to peripheral capillaries. Some of the known proteins transported by this method are insulin, leptin and transferrin. Nevertheless, some pathologies

are known to cause a BBB disruption, diminishing its integrity and increasing its non-specific permeability. Among these pathologies we can find different acute and chronic CNS diseases, including ischaemic stroke.<sup>308</sup> It has been observed that the number of endocytic vesicles in the endothelial cells of the BBB highly increase after ischaemic stroke, suggesting an increased transcytosis.<sup>309</sup> The detected inhibition of GOT1 activity in the brain in animals treated with AbGOT1 could be due to the crossing of the antibody into the brain parenchyma. However, it must be pointed that the present study does not provide enough data to completely clarify if this inhibition is due to a crossing of the AbGOT1 through transcytosis, a passive diffusion because of the compromised permeability of the BBB or another unknown cause. A further and deeper analysis must be performed in order to unravel the specific mechanism leading to the blockade of GOT1 activity in the brain parenchyma.

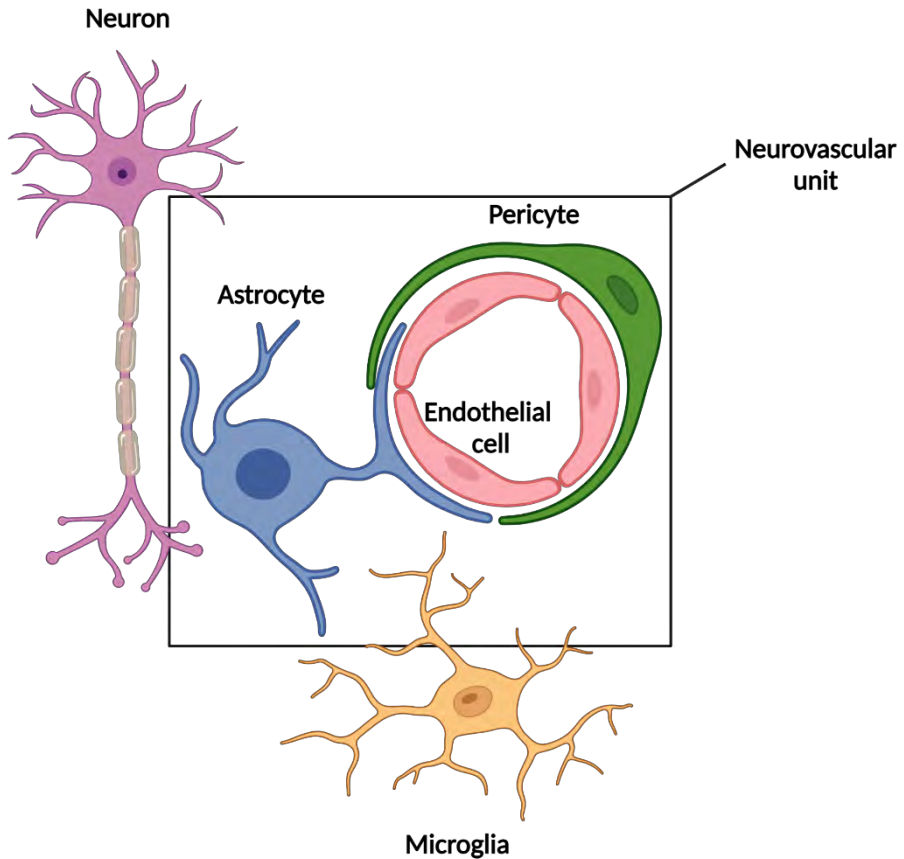


**Figure 74.** Schematic view of the blood-brain barrier with the neurovascular unit and auxiliary cell types. Self-created image using BioRender software.

## 13.- SECTION II: rGOT1 THERAPEUTIC EFFECT

In the past decade, the use of recombinant proteins, either for proteomic analysis, mechanistic studies or therapeutic approaches, has risen dramatically. This growing interest has led to an increasing number of methods in order to produce

these proteins, including yeast, bacteria, mammalian cells or even insects. One of the most common expression systems is *Escherichia coli*, which has been widely used for the expression of recombinant proteins. This bacterium has proven to be a very efficient tool as it is inexpensive, simple, easy to modify genetically and a user-friendly host for large-scale production. Nevertheless, there are some disadvantages in its use, such as low solubility, misfolding and degradation of the expressed protein and the lack of cellular machinery needed for post-translational modifications (e.g. glycosylation or phosphorylation).

In order to overcome these drawbacks, different fusion tags have been developed. One of the most promising is the addition of a SUMO sequence to the recombinant protein, which has demonstrated a significant improvement in expression and solubility.<sup>310</sup> SUMO acts as a chaperone, promoting the correct folding of the proteins and decreasing the proteolytic degradation. Furthermore, the peripheral hydrophilic and central hydrophobic core structure of SUMO peptide exhibits a detergent-like solubilizing effect leading to enhanced solubility of the aggregation-prone target proteins. Contrary to other common tags for specific proteases, SUMO does not leave any extraneous amino acids at the N-terminus after it is cleaved, maintaining the native N-terminal sequence of the target fusion proteins. Also, SUMO does not help in the purification step of the recombinant protein. However, this can be easily solved by adding to the SUMO sequence a His-tag, which is also removed after the proteolytic removal of the SUMO.<sup>311,312</sup> Taking all of these into account, SUMO technology has proven to be an excellent and a reliable method to synthesize recombinant proteins under the Current Good Manufacturing Practice (CGMP) regulations, meeting the FDA and other agencies standards.

The sequence analysis from rGOT1 and GOT1 extracted from RBC, showed a high coverage of the recombinant version of the protein once compared to the database sequence for human

GOT1. Additionally, size and secondary structure analysis demonstrated a really high similarity between the rGOT1 and the endogenous human GOT1. Finally, the activity test also showed an optimal enzymatic activity of the recombinant protein that matches de activity of the endogenous GOT1. In this study, SUMO technology has allowed to synthetize a recombinant form of the GOT1 identical to the human protein and is a promising procedure to scale-up the synthesis of this enzyme for a future clinical application.

The dose response studies in healthy rats showed an exponential increase in GOT activity with increasing doses of rGOT1, with a greater clearance of the protein in the highest concentrations. Nevertheless, all the doses tested failed to show any significant effect on blood glutamate levels, most likely due to the rapid homeostasis of glutamate. This rapid glutamate homeostasis was also observed when another set of healthy animals were pre-treated with a high dose of glutamate. Even with a starting concentration of glutamate in blood as high as 2000-2500  $\mu\text{M}$ , control animals managed to restore physiological levels of glutamate just around 2 hours later. Although animals treated with rGOT1 had a better glutamate clearance after these 2 hours, control animals showed the ability to rapidly restore normal levels of glutamate. These findings match those obtained from other studies, where glutamate kinetics after ingestion was analysed, showing that the concentration of this amino acid returned to normal levels between 60 and 120 minutes after its maximum value was established.<sup>313</sup> In addition, the other studies conducted in this Thesis in ischaemic rats also showed no significant reduction in blood glutamate levels, both in animals treated with a single dose or with four injections, in any of the doses tested. These results, along with those obtained in the AbGOT1 study, suggest a tight control in the homeostasis of this molecule. Different studies showed that most of the glutamate administered nasogastrically was sequestered by the splanchnic bed. When

glutamate was radioactively labelled (with  $^{15}\text{N}$ ) and administered orally, almost no  $^{15}\text{N}$ -glutamate was detected in arterial blood, while most of the  $^{15}\text{N}$  was recovered in the form of alanine and glutamine.<sup>314</sup> Finally, some other studies showed that there is a rapid efflux of glutamate from peripheral organs and tissues, allowing a quick replenishing of glutamate into the blood in case of need.<sup>315,316</sup> All these data indicate how strictly controlled are glutamate levels in blood, explaining why there are no observable changes in glutamate concentration in animals treated with rGOT1. Even if the enzyme is effectively lowering glutamate in blood or even increasing glutamate levels by causing a bigger gradient between brain and circulation promoting a greater efflux of glutamate from brain parenchyma, these changes can be quickly buffered by the normal homeostasis mechanisms of the animals, masking any detectable changes in glutamate concentration.

The analysis of the time window for rGOT1 did not show any improvement regarding either infarct volume or sensorimotor tests. First, a dosage of 0.24 mg/kg was selected according to previous studies conducted by our group,<sup>125</sup> but this dose proved to be insufficient to cause any beneficial effect even when administered right after reperfusion. The most likely explanation for this has to do with the synthesis process. In order to adapt the synthesis of the recombinant protein to the CGMP protocols (a set of guidelines aimed to ensure the safety and quality of food, cosmetics and drugs intended for their use in humans), a new synthesis process, different from the one used in our previous studies, had to be designed. One of the major changes in the new protocol was the elimination of the polyhistidine-tag in the N-terminal of the recombinant protein, in order to obtain an enzyme completely homologous to the human GOT1. Nevertheless, the effect of removing this His-Tag was not assessed. It cannot be discarded that this change affected the activity of the rGOT1 in terms of proteolysis, blood clearance or detection by the animal immune system, as it has been described that the addition of a His-Tag can alter protein

function.<sup>317-319</sup> This could explain the need of increasing the dose in order to obtain the same effect as in our previous analysis. Nevertheless, although the lack of results could initially be attributed to a problem with the dosage, subsequent analysis with increased doses that did have positive results in terms of lesion size and sensorimotor tests when administered right after reperfusion, failed to show any beneficial effects when the administration was delayed. This suggest that rGOT1 faces the same problem as the vast majority of treatments for ischaemic stroke, where time is crucial, a short therapeutic window.

Regarding infarct volume, rGOT1 showed a significant reduction in lesion size when administered immediately after reperfusion in most of the experiments performed, although the relative impact of the enzyme varied between the different analysis. In the case of a single administration, rGOT1 showed a significant reduction in the infarct size in animals submitted to a severe ischaemia (75 minutes occlusion) 7 days after ischaemia onset. However, this reduction disappeared in animals with a mild ischaemia (45 minutes occlusion) which had a smaller lesion volume. Interestingly, once the animals were treated with repeated doses of the rGOT1, the beneficial effect could be observed both in severe and mild ischaemia groups, being the effect even higher in the latter. Comparing the infarct volumes between control groups of animals submitted to mild and severe ischaemia, it can be noted that the lesion size is significantly smaller in the 45 minutes occlusion animals. As ischaemic damage is highly time-dependent, it is possible that a mild ischaemia would be insufficient to cause enough damage to see a positive result with the use of the rGOT1, allowing a sufficient recovery due to the intrinsic animal mechanisms and masking the potential therapeutic effect of the enzyme. However, by administering four doses of the protein, and therefore enhancing its effect, the difference in recovery between the control group and the treated group could be increased, finally observing this significant reduction in the lesion size, as in the present case. This enhanced therapeutic effect, achieved with

four administrations of the protein, allowed a better recovery of animals submitted to mild ischaemia compared to those subjected to a longer occlusion. Although no histology analyses were done, the brain tissue of animals suffering severe ischaemia is expected to be more damaged and, therefore, there is less tissue susceptible of being recovered.

In addition, it should be noted that the different doses of rGOT1 have a “valley effect”, where the doses in the middle present the best results, while smaller and greater doses had no effect on the lesion size. In the case of the smaller doses, it could be easily explained as an insufficient amount of protein to exert any visible effect, the case of greater doses presents a little more controversy. At first, it could be hypothesised that an excess of rGOT1 could be causing a deleterious effect, either by overdose derived toxicity or by disrupting a normal physiological process, such as glutamate homeostasis. Nevertheless, as mentioned before, no changes were observed in glutamate levels or blood glucose with any of the doses. Furthermore, greater doses of rGOT1 seem to simply fail to continue to exert a therapeutic benefit, rather than to show a toxic effect, since the infarct volumes are not greater than in control group and results for sensorimotor tests did not show a worst functional evolution. Further studies should be performed in order to determine if an excessive dosage of rGOT1 is indeed having a toxic effect or, at least, elucidate why this valley effect is present. One possible explanation could be that PLP would be acting as a limiting factor. As mentioned before, PLP is a cofactor involved in the enzymatic activity of different transaminases, and it has been described its critical role in the normal functioning of GOT.<sup>304</sup> Although the rGOT1 production process involves the synthesis of the protein with the cofactor included, it would be interesting to study the administration of rGOT1 along with PLP to observe if there is any possible synergic effect. In the same way, oxaloacetate, the cosubstrate of glutamate in the GOT reaction, could be acting as a limiting factor as well. Nevertheless, recent studies (data not published) from our group showed that the

double administration of rGOT1 and oxaloacetate had no further benefit compared with the administration of the rGOT1 alone.

Finally, as mentioned before, the use of serial doses of rGOT1 showed better results than using a single injection of the drug, even when the total amount of enzyme used was the same (e.g. 4 doses of 1 mg/kg of rGOT1, 4 mg/kg in total, versus a single injection of 4 mg/kg of the protein). These results are in concordance with those obtained from other researchers, where they observed that a sustained administration of GOT, rather than a single administration, had beneficial effects on different neuronal and cognitive parameters.<sup>267,268</sup>

In relation with sensorimotor tests, the dosage of 1 mg/kg, as in the case of infarct volume, showed the best results. The different studies showed diverse results in sensorimotor tests outcome, although it appears that the grip strength test was the most sensitive when it came to detect significant differences between control and treated animals. Although the better outcome measured by sensorimotor tests was not always associated with a significant reduction in the infarct volume, some studies have shown that these two parameters are not always correlated.<sup>320-323</sup>

Despite the lack of changes in blood glutamate levels, other mechanisms have been proposed that could explain the rGOT1 therapeutic effect without involving any significant reduction in peripheral glutamate. Khanna *et al.*<sup>203</sup> proved that oxygen-induced GOT could transform the neurotoxic glutamate released after ischaemia into metabolic fuel. Higher levels of GOT's mRNA expression and GOT enzymatic activity were correlated with a decreased of cortical glutamate levels in an ischaemic model performed in mice. Furthermore, they detected that this increased expression of GOT could reverse the loss of ATP production. Later, they identified the mechanism underlying this ATP recovery. GOT was able to use glutamate as metabolic fuel by an anaplerotic refilling of the TCA cycle intermediates.<sup>204</sup>

These results were accompanied by a reduction of the infarct volume and an improvement in sensorimotor function.

In a recently published article, Poyurovsky *et al.*<sup>324</sup> studied the effect of **KL-11743**, an inhibitor of the glucose metabolism in tumour xenografts in mice. They observed that the glucose metabolism inhibition by the blockade of the glucose transporters led to an increase of aspartate biosynthesis and an increased dependence on GOT1 mediated anaplerosis. Furthermore, GOT1 depletion led to an increased mortality in cells treated with **KL-11743**. These results are similar to our results obtained with the AbGOT1, where a blockade of GOT1 in a situation of low glucose availability (in our case, ischaemic conditions) led to a greater lesion volume. The results obtained by Poyurovsky *et al.* are also in concordance with those observed by Khanna *et al.* demonstrating the critical role of the GOT1 in the anaplerotic refilling of the TCA cycle in situations of metabolic stress.

Additionally, Lyssiotis *et al.*<sup>325</sup> observed the effect of the inhibition of GOT1 in pancreatic ductal adenocarcinoma. They observed that the inhibition of this enzyme led to a situation of metabolic stress and produced a cytostatic effect by arresting cells in the G1 phase. Moreover, GOT1 inhibition caused a disruption of normal mitochondrial metabolism and a greater sensitivity to ferroptosis, an of oxidative, non-apoptotic, and iron-dependent form of cell death. As in the previous cases, this deleterious effect of GOT1 inhibition is related to its function as part of the MAS. All these studies represent alternative mechanisms by which rGOT1 could be exerting its therapeutic effect.

Finally, as we did for AbGOT1, we analysed the GOT activity in the CSF of both healthy and ischaemic animals. All blood proteins are present in CSF due to a passive diffusion through the choroid plexus, with a final concentration in CSF of approximately 0.5% of blood levels.<sup>326</sup> Although enzymatic

activity is not a direct measure of protein concentration, we can observe, comparing blood and CSF measures, that GOT1 activity in CSF represents around 10-15% of blood GOT1 activity in basal conditions. However, once rGOT1 was administered, the ratio between blood and CSF GOT1 activity was reduced to an approximately 0.5% in the case of the 1 mg/kg dosage, matching the percentage described in bibliography. Although this result should be taken with caution, the existence of proteins that are actively transported across the CSF-blood barrier, such as prealbumin and transferrin,<sup>326</sup> opens the possibility to the existence of a mechanism to actively transport GOT1 at the choroid plexus. Other possibility for this abnormal high percentage, is the combined influx of GOT into CSF both from blood and brain parenchyma. As described before, interstitial solutes in brain can be cleared by draining into CSF,<sup>327,328</sup> through the glymphatic system. Furthermore, this could also explain why GOT activity in CSF is higher in ischaemic animals compared to healthy animals. The cell death caused after the ischaemic insult releases cellular content into the brain parenchyma, increasing the interstitial concentration of all kinds of cellular components, including proteins. This increased interstitial concentration of proteins could lead to a bigger efflux of GOT into the CSF, explaining these differences. Nevertheless, new studies (labelling the rGOT1 with a radioisotope for example) should be performed in order to reliably determine the origin of the GOT detected in the CSF.

#### 14.- SECTION III: rGOT1 BIOCONJUGATION

The modification of the rGOT1 by adding PEG to its structure increased the circulation half-life from hours to days, promoting a better blood exposure and an improved therapeutic effect. Same as before, a more stable and prolonged exposure time, obtained before with the administration of 4 doses of the enzyme, showed a better therapeutic effect than that obtained in animals treated with a single dose of the enzyme. The rapid

clearance of the native rGOT1 can be related to its peripheral uptake. In fact, previous studies have shown, through a  $^{125}\text{I}$ -labeled GOT, that the enzyme can be taken up and metabolized by several tissues (spleen, kidney, liver and intestines). The radioactivity associated with liver and spleen reached its maximum 2 hours after the injection and the time course coincided with that for the plasma clearance in the fast phase.<sup>329</sup> The subsequent decrease in radioactivity in these tissues was followed by an increase in radioactivity in the urine. Therefore, the prolonged blood residence time is most likely due to the hindrance of rGOT1 uptake by peripheral organs. Additionally, the addition of PEG chains to the enzyme surface was able to reduce the immunogenicity (if existent) and protect the enzyme for proteolytic degradation. However, these mechanisms are believed to have a lesser impact than those involving liver, spleen and kidney uptake.

Besides the protective effect on the lesion size, the use of the bioconjugates also showed a significant improvement in functional impairment, the most important parameter for patients' outcome. tMCAO caused an important deficit in neurological function and motor performance, with animals mostly showing weakened limbs. Several studies have shown that the infarct volume does not necessarily correlate with functional deficit, proving that this measure alone can be insufficient to correctly evaluate the protective effect of the rGOT1.<sup>320-323</sup> Improvement in the motor functions, assessed by the accelerated rotarod test, was significantly greater in groups treated with rGOT1 and bioconjugates. These results are also correlated with those obtained in the cylinder test, although the outcome of both tests was slightly different. However, the targeting of the rGOT1 to the BBB, by using an Angiopep-2 ligand, did not show any additional therapeutic effect compared to stabilizing and increasing the circulation lifetime of rGOT1 using mPEG. These results, along with those obtained in the previous studies, suggest that glutamate transport across the BBB is not the rate-limiting step to protection. Further studies to

achieve brain accumulation or overexpression of endogenous GOT1 directly in the brain could help to elucidate if the therapeutic effect of the enzyme is related to a local process in brain parenchyma or a systemic effect due to its action in blood.

Once again, and contrary to what has been reported in other studies,<sup>125</sup> rGOT1 and rGOT1 bioconjugates did not show any significant effect on serum glutamate levels. However, most of the published works do not mention the specific activity of their rGOT1 protein, making it impossible to reliably compare doses between studies. Although new dose escalation studies with the bioconjugate could be performed, data obtained from the previous studies exposed in this manuscript indicate that the lack of changes in blood glutamate levels responds more to a rapid and a tightly controlled glutamate homeostasis rather than a low dose of the enzyme or its bioconjugates. Nevertheless, present results are consistent with observations obtained from other groups of a clockwise hysteresis on the pharmacokinetics/pharmacodynamics curves, suggesting that it takes a certain time to deplete peripheral glutamate sufficiently for there to be a noticeable difference in the blood.<sup>301</sup> As exposed before, in general, glutamate homeostasis is a rapid and maintained process through a variety of peripheral transporters and receptors,<sup>315,316</sup> yielding rapid efflux of glutamate towards the blood from organs (e.g., brain) and peripheral tissues. A previous work has shown that radioactivity of intravenously injected (radioactive) glutamate decayed with a half-life of ~3min, owing to metabolic reactions occurring in the liver or in the plasma, which provides some insight into the timescale of glutamate homeostasis.<sup>330</sup> This is the most probable explanation for the lack of noticeable depletion of glutamate in the blood concurrent with neuroprotection in the brain.

In order to analyse if a more local effect of rGOT1 and its bioconjugates could be observed, GOT activity and glutamate levels were measured in CSF of healthy rats treated either with the native rGOT1 or with the rGOT1-PEG. Although a significant

increase of GOT activity was detected in CSF in the treated groups, no significant effect on CSF glutamate concentration was observed. These results are in accordance with a recently published study that showed that a daily administration of a recombinant version of GOT (every 12 hours on days 1-4) reversed the disruption of synaptic plasticity in a rat model of TBI by decreasing the glutamate levels in hippocampus interstitial fluid, but not in ventricular CSF.<sup>222</sup> Overall, these observations provide strong support for the effect of sustained blood glutamate depletion by the bioconjugates on ischaemic damage, which merits further investigation. Indeed, these findings raise new questions related to the safety and tolerability of such treatments. New protective or healing mechanisms (yet to be identified) may be involved in addition to those expected for rGOT1. Overall, glutamate scavenging strategies are highly suited to overcome many of the drawbacks of the receptor-based therapies (e.g., cognitive impairments, hallucinations, and even coma)<sup>331</sup> and this concept is an attractive protective strategy to remove excess glutamate in the brain interstitial fluid. The most significant observation of this study is that maintaining high and relatively stable rGOT1 blood activity over a period of several days had a very beneficial effect on infarct volume as well as sensorimotor function.<sup>125,332-334</sup> This was achieved with a single administration of rGOT1 bioconjugate. Remarkably, equivalent doses of native rGOT1 alone yielded results equivalent to saline controls for certain tests, and did not alter blood or CSF glutamate levels. Overall, the efficacy of this strategy holds great potential as a therapy for stroke,<sup>125</sup> as well as other pathologies associated with acute excitotoxicity such as spinal cord injury<sup>335</sup> or traumatic brain injury.<sup>222</sup>

## 15.- SECTION IV: rGOT1 AND rtPA INTERACTION

Since rtPA is the most common fibrinolytic agent in clinical use, any new therapy applied in the same therapeutic time-window must not interfere with it. A good example of the importance of this is the case of **nerinetide**. PSD-95 is a scaffold protein which directly interacts with NMDAR and has a major role in shaping a framework of multiple proteins at excitatory synapses, organizes signal transduction and is central to glutamatergic synaptic signalling.<sup>336</sup> **Nerinetide**, a PSD-95 inhibitor, is an eicosapeptide which acts by uncoupling NMDAR from nNOS neurotoxic signalling, suppressing NO production and reducing neuronal death.<sup>336</sup> After promising preclinical results, a multicentre clinical trial showed that a larger percentage of patients who underwent endovascular thrombectomy had a good clinical outcome when treated with **nerinetide**. However, patients who received pharmacological treatment with alteplase (the commercial name of rtPA) in addition to thrombectomy did not show any further beneficial effect once compared to placebo.<sup>337</sup> Additional studies showed that **nerinetide** is subjected to proteolytic cleavage when administered after rtPA.<sup>338</sup> The experience learned from **nerinetide** case illustrates why it is important to assess a possible interaction between rtPA and rGOT1.

First, an *in vitro* analysis of rGOT1 and rtPA interaction was performed, either in a dose response manner or with a kinetics of rtPA activity. In both cases, no changes were observed in rtPA activity with none of the rGOT1 doses tested, even when the highest dose (10 mM), which is, roughly, 100.000 times the expected concentration of rGOT1 in blood when injected I.V. Using a known inhibitor of the rtPA (leupeptin) as a positive control, it was clear that the tested concentrations of rGOT1 *in vitro* were not causing any deleterious effect on rtPA activity.

Furthermore, in the kinetics study, from the 30 minutes timepoint and onwards, the combination of rGOT1 and rtPA showed an even higher activity compared with the rtPA alone. Since activity measures were done in a plate reader by measuring fluorescence, it is possible that the addition of rGOT1 caused some background, hence increasing the activity measures. The other possibility, a synergic action of rGOT1 and rtPA resulting in a higher activity of the latter, is highly unlikely and it has not been described anywhere in the bibliography.

When reperfusion rates were examined in a thrombin-induced stroke model, where a small volume of thrombin is directly injected in the MCA bifurcation in order to cause a thrombus, no changes were detected between animals treated only with rtPA or with a combination of rtPA and rGOT1, while control group and animals treated only with rGOT1, as expected, had a significantly lower reperfusion rate. When GOT activity in blood was measure, no differences were observed between animals treated only with rGOT1 or animals treated with a combination of the enzyme and the fibrinolytic agent. These results, along with the ones obtained in the *in vitro* analysis, and the reperfusion rates of both groups suggest that there is no interaction between rGOT1 and rtPA, in either direction. The *in vitro* study showed that rGOT1 is not interfering with the normal activity of the rtPA, and the reperfusion rates proved that an administration of the recombinant GOT has no impact in the therapeutic effect of the rtPA in the ischaemic insult. On the other hand, the analysis of blood GOT activity demonstrated that rtPA is not causing a loss of rGOT1 activity.

Finally, after sensorimotor tests analysis, only a small improvement in the rotarod test was detected at 24 hours after ischaemia onset in animals treated only with rGOT1. Nevertheless, this isolated significance is not enough to affirm a therapeutic effect of rGOT1 in these animals.

In the case of the embolic stroke model, no differences in recanalization rates were detected between any of the groups tested. The lack of significant differences could be due to the limitations of the model, since the percentage of animals reperfused between control and rtPA groups are also more similar than in the thrombin-induced stroke model. Nevertheless, there is a trend toward a higher reperfusion rate in rtPA treated groups, with or without rGOT1, suggesting, as before, that rGOT1 treatment does not interfere with the normal activity of the rtPA. In this model, mortality at 24 hours was also analysed. Contrary to reperfusion rates, there was a clear improvement in mortality between treated animals and the control group, where all the animals included died within the first 24 hours, even those which had a spontaneous reperfusion. No differences were detected between animals treated only with rtPA or with rtPA combined with rGOT1, suggesting once again no interaction between our enzyme and the fibrinolytic agent.

Although infarct volume was not the primary endpoint in this study, the animals that were treated with rGOT1 30 minutes before administering rtPA showed a smaller infarct volume 90 minutes after ischaemia onset, after the end of rtPA administration, when recanalization was assessed by MRA. This opens a really interesting possibility in terms of therapeutic potential. As mentioned before, one of the major issues of neuroprotective drugs for ischaemic stroke, including rGOT1, is the short therapeutic window of the vast majority of them, mostly due to stroke being a highly time-dependant pathology. However, as it was demonstrated here, rGOT1 does not interfere with the normal functioning of rtPA. Furthermore, as previously described by our group,<sup>339</sup> although rGOT1 has no beneficial effects in intracerebral haemorrhage, it has no negative effect on the volume of the haematoma either. The beneficial effect of rGOT1 once administered before rtPA, the lack of interference with rtPA and the safety study in ICH suggest the possibility of using rGOT1 in pre-hospital stages in case of suspected stroke, without the need of neuroimaging techniques to establish the

type of stroke. Although more safety studies in terms of toxicity or possible deleterious effects in other pathologies (one possible complication could be an undesirable side effect after administration of rGOT1 in the case of a stroke mimic) should be performed, the possibility of an early administration could further improve the therapeutic effect of rGOT1 demonstrated in this manuscript, overcoming one of the major problems in stroke therapy.

In conclusion, the studies presented in this manuscript showed the importance of the rGOT1 in the ischaemic stroke pathology. AbGOT1 studies demonstrated the central role of GOT1 in the extent of the damage after ischaemia as well as its implication in cerebral glutamate homeostasis, as showed by the MRS study. More importantly, the use of rGOT1 as a therapeutic agent proved to have beneficial effects both in infarct volume and sensorimotor deficits. This therapeutic effect can be improved by increasing the residence time of the protein in the blood, either by administering multiple doses or by increasing the half-life of the rGOT1 with the development of bioconjugates of the enzyme. Although more experiments should be performed in order to clarify the mechanism of action of the rGOT1, the presence of the enzyme in CSF could indicate that the enzyme is exerting its effect in a local, rather than a systemic, way, hence the lack of changes in peripheral glutamate. Currently, different mechanistic studies are being conducted, from histological and proteomic analysis to permeability assays by using BBB models to analyse a possible crossing of the rGOT1. Finally, the lack of any noticeable interaction between rtPA and rGOT1 and the safety studies performed by our group open the possibility of using the rGOT1 in pre-hospital stages in case of a suspected stroke, bringing forward the start of the treatment, which is of great importance in a pathology where time is a crucial factor. All these results convert rGOT1 into a promising therapeutic option and open the possibility of more ambitious studies to be developed in the future.

## CONCLUSIONS



Based on the objectives established at the beginning of this Thesis, and once the results have been properly analysed and discussed, several conclusions can be drawn.

### SECTION I: ENDOGENOUS GOT1 INHIBITION STUDIES

1. The use of a polyclonal antibody against GOT1 is capable of inhibiting GOT1 activity in blood, leading to a higher infarct volume and a worse sensorimotor deficit, highlighting the main role of this enzyme in the ischaemic injury.
2. The inhibitory effect of the AbGOT1 also affects GOT1 activity in CSF and brain tissue, increasing the intracerebral levels of glutamate and lactate.

### SECTION II: rGOT1 THERAPEUTIC EFFECT

1. rGOT1 treatment successfully increases GOT1 activity in blood, reduces the infarct volume and improves the neurological outcome in animal models of stroke.
2. The administration of several doses of rGOT1 enhances its therapeutic effect compared with a single administration, even when the total amount of rGOT1 used is the same, showing that a sustained rGOT1 activity in blood is crucial.
3. An early administration of rGOT1 is critical to obtain the beneficial effect of the enzyme and should therefore be administered as soon as possible.

### SECTION III: rGOT1 BIOCONJUGATION

1. The bioconjugation of the rGOT1 increases the half-life of the protein without affecting its normal enzymatic activity.
2. The bioconjugation of rGOT1 with PEG improves the therapeutic effect of the rGOT1, showing that the enzyme works more in a time-dependent rather than a dose-dependent manner.

### SECTION IV: rGOT1 AND rtPA INTERACTION

1. There is no interaction between rGOT1 and rtPA neither *in vitro* nor *in vivo* and the use of the rGOT1 does not affect the reperfusion efficiency of rtPA.
2. rGOT1 can be administered together with or before rtPA, allowing the use of the rGOT1 in pre-hospital stages in case of suspected stroke.

## CONCLUSIONES



Basándose en los objetivos que fueron establecidos previamente, y una vez que los resultados han sido debidamente analizados y discutidos, diversas conclusiones pueden ser extraídas.

### SECCIÓN I: ESTUDIOS SOBRE LA INHIBICIÓN DE LA GOT1 ENDÓGENA

1. El uso de un anticuerpo policlonal contra la GOT1 es capaz de inhibir la actividad de la GOT1 en sangre, lo que provoca un mayor volumen de infarto y un peor déficit sensoriomotor, demostrando el papel crítico de esta encima en el daño isquémico.
2. El efecto inhibitorio del anticuerpo contra la GOT1 también afecta a su actividad en el líquido cefalorraquídeo y el tejido cerebral, lo que conlleva un incremento de los niveles intracerebrales de glutamato y lactato.

### SECCIÓN II: EFECTO TERAPÉUTICO DE LA rGOT1

1. El tratamiento con rGOT1 aumenta la actividad de la GOT1 en sangre, reduce el volumen de infarto y mejora el déficit neurológico en modelos animales de isquemia.
2. La administración de múltiples dosis de rGOT1 incrementa su efecto terapéutico comparado con una única administración, aun cuando la cantidad total de proteína inyectada fuese la misma, demostrando que una actividad sostenida en sangre de la GOT1 es crucial.

3. Una administración temprana de la rGOT1 es crítica a la hora de obtener un efecto beneficioso de la enzima y debe ser, por lo tanto, administrada lo antes posible.

### SECCIÓN III: BIOCONJUGACIÓN DE LA rGOT1

1. La bioconjugación de la rGOT1 incrementa la vida media de la proteína sin afectar a su actividad enzimática normal.
2. La bioconjugación de la rGOT1 con PEG mejora su efecto terapéutico, demostrando que la enzima funciona más de una manera tiempo dependiente que dosis dependiente.

### SECCIÓN IV: INTERACCIÓN ENTRE LA rGOT1 Y EL rtPA

1. No existe interacción entre la rGOT1 y el rtPA, ni *in vitro* ni *in vivo*, y el uso de la rGOT1 no afecta a la eficacia reperfusora del rtPA.
2. La rGOT1 puede ser administrada tanto de forma previa como conjuntamente con el rtPA, lo que permite el uso de la rGOT1 de forma prehospitalaria en casa de sospecha de ictus.

## BIBLIOGRAPHY



1. Sacco RL, Kasner SE, Broderick JP, Caplan LR, Connors JJ (Buddy), Culebras A, et al. An Updated Definition of Stroke for the 21st Century. *Stroke*. 2013;44(7):2064-2089. doi:10.1161/STR.0B013E318296AECA
2. Castillo J, Luna A, Rodríguez-Yáñez M, Ugarriza I, Zarranz JJ. Neurología. In: *Neurología*. 6th ed. Elsevier; 2018:301-358.
3. Global, regional, and national life expectancy, all-cause mortality, and cause-specific mortality for 249 causes of death, 1980–2015: a systematic analysis for the Global Burden of Disease Study 2015. *Lancet*. 2016;388(10053):1459. doi:10.1016/S0140-6736(16)31012-1
4. INE. Defunciones según la causa de muerte. Published online 2019.
5. Singh RJ, Chen S, Ganesh A, Hill MD. Long-term neurological, vascular, and mortality outcomes after stroke. *Int J Stroke*. 2018;13(8):787-796. doi:10.1177/1747493018798526
6. Wolfe CDA. The impact of stroke. *Br Med Bull*. 2000;56(2):275-286. doi:10.1258/0007142001903120
7. Clua-Espuny JL, Piñol-Moreso JL, Panisello-Tafalla A, Lucas-Noll J, Gil-Guillen VF, Orozco-Beltran D, Queralt-Tomas ML. Estudio Ebrictus. Resultados funcionales, supervivencia y años potenciales de vida perdidos después del primer episodio de ictus. *Aten Primaria*. 2012;44(4):223. doi:10.1016/J.APRIM.2011.04.004
8. Adamson J, Beswick A, Ebrahim S. Is stroke the most common cause of disability? *J Stroke Cerebrovasc Dis*. 2004;13(4):171-177. doi:10.1016/j.jstrokecerebrovasdis.2004.06.003
9. Alvarez-Sabín J, Quintana M, Masjuan J, Oliva-Moreno J, Mar J, Gonzalez-Rojas N, Becerra V, Torres C, Yebenes M. Economic impact of patients admitted to stroke units in Spain. *Eur J Health Econ*. 2017;18(4):449-458. doi:10.1007/S10198-016-0799-9
10. Sociedad Española de Neurología. El Atlas del Ictus en España 2019. Accessed December 8, 2021. [https://www.sen.es/images/2020/atlas/Atlas\\_del\\_Ictus\\_de\\_Espana\\_version\\_web.pdf](https://www.sen.es/images/2020/atlas/Atlas_del_Ictus_de_Espana_version_web.pdf)
11. Carod Artal FJ. Coste directo de la enfermedad cerebrovascular en el primer año de seguimiento. *Rev Neurol*. 1999;29(12):1354. doi:10.33588/rn.2912.99571
12. Beguiristain JM, Mar J, Arrazola A. The cost of cerebrovascular accident. *Rev Neurol*. 2005;40(7):406-411. doi:10.33588/rn.4007.2004436
13. Oliva J, Osuna R, Jorgensen N. Estimación de los costes de los cuidados informales asociados a enfermedades neurológicas de alta prevalencia en España. *Pharmacoeconomics - Spanish Res Artic*. 2007;4(3):83-96.

doi:10.1007/BF03320929

14. Calandre L, Arnal C, Fernandez Ortega J, Bermejo F, Felgeroso B, Del Ser T, Vallejo A. Risk Factors for Spontaneous Cerebral Hematomas. Case-Control Study. *Stroke*. 1986;17(6). Accessed October 14, 2021. <http://ahajournals.org>
15. Arboix A. Cardiovascular risk factors for acute stroke: Risk profiles in the different subtypes of ischemic stroke. *World J Clin Cases WJCC*. 2015;3(5):418. doi:10.12998/WJCC.V3.I5.418
16. H P Adams J, Bendixen BH, Kappelle LJ, Biller J, Love BB, Gordon DL, E Marsh 3rd. Classification of subtype of acute ischemic stroke. Definitions for use in a multicenter clinical trial. TOAST. Trial of Org 10172 in Acute Stroke Treatment. *Stroke*. 1993;24(1):35-41. doi:10.1161/01.STR.24.1.35
17. Collaborators GLRoS. GLOBAL, REGIONAL, AND COUNTRY-SPECIFIC LIFETIME RISK OF STROKE,1990-2016. *N Engl J Med*. 2018;379(25):2429. doi:10.1056/NEJMOA1804492
18. Bushnell CD, Chaturvedi S, Gage KR, Herson PS, Hurn PD, Jiménez MC, Kittner SJ, Madsen TE, McCullough LD, McDermott M, Reeves MJ, Rundek T. Sex differences in stroke: Challenges and opportunities. *J Cereb Blood Flow Metab*. 2018;38(12):2179. doi:10.1177/0271678X18793324
19. O'Donnell MJ, Chin SL, Rangarajan S, Xavier D, Liu L, Zhang H, et al. Global and regional effects of potentially modifiable risk factors associated with acute stroke in 32 countries (INTERSTROKE): a case-control study. *Lancet*. 2016;388(10046):761-775. doi:10.1016/S0140-6736(16)30506-2
20. Arboix A, Garcia-Eroles L, Oliveres M, Massons JB, Targa C. Clinical predictors of early embolic recurrence in presumed cardioembolic stroke. *Cerebrovasc Dis*. 1998;8(6):345-353. doi:10.1159/000015878
21. Castillo J. Fisiopatología de la isquemia cerebral. *Rev Neurol*. 2000;30(05):459. doi:10.33588/rn.3005.99500
22. Back T. Pathophysiology of the ischemic penumbra - Revision of a concept. *Cell Mol Neurobiol*. 1998;18(6):621-638. doi:10.1023/A:1020265701407
23. Astrup J, Symon L, Branston NM, Lassen NA. Cortical evoked potential and extracellular K<sup>+</sup> and H<sup>+</sup> at critical levels of brain ischemia. *Stroke*. 1977;8(1):51-57. doi:10.1161/01.STR.8.1.51
24. Hansen AJ. Effect of Anoxia on Ion Distribution in the Brain. *Physiol Rev*. 1985;65(1).

25. Blank W, Kirshner H. The kinetics of extracellular potassium changes during hypoxia and anoxia in the cat cerebral cortex. *Brain Res.* 1977;123:113-124.
26. Choi D. Ionic dependence of glutamate neurotoxicity. *J Neurosci.* 1987;7(2):369. doi:10.1523/JNEUROSCI.07-02-00369.1987
27. Choi DW, Rothman SM. The role of glutamate neurotoxicity in hypoxic-ischemic neuronal death. *Annu Rev Neurosci.* 1990;13:171-182.
28. White BC, Sullivan JM, DeGracia DJ, O'Neil BJ, Neumar RW, Grossman LI, Rafols JA, Krause GS. *Brain Ischemia and Reperfusion: Molecular Mechanisms of Neuronal Injury.* Vol 179.; 2000. doi:10.1016/S0022-510X(00)00386-5
29. Choi DW. Excitotoxic cell death. *J Neurobiol.* 1992;23(9):1261-1276. doi:10.1002/neu.480230915
30. Schiene K, Bruehl C, Zilles K, Qu M, Hagemann G, Kraemer M, Witte OW. Neuronal Hyperexcitability and Reduction of GABAA-Receptor Expression in the Surround of Cerebral Photothrombosis: <http://dx.doi.org/101097/00004647-199609000-00014>. 2016;16(5):906-914. doi:10.1097/00004647-199609000-00014
31. Banasiak KJ, Xia Y, Haddad GG. Mechanisms underlying hypoxia-induced neuronal apoptosis. *Prog Neurobiol.* 2000;62(3):215-249. doi:10.1016/S0301-0082(00)00011-3
32. Nogawa S, Zhang F, Ross ME, Iadecola C. Cyclo-Oxygenase-2 Gene Expression in Neurons Contributes to Ischemic Brain Damage. *J Neurosci.* 1997;17(8):2746. doi:10.1523/JNEUROSCI.17-08-02746.1997
33. Grandati M, Verrecchia C, Revaud ML, Allix M, Boulu RG, Plotkine M. Calcium-independent NO-synthase activity and nitrites/nitrates production in transient focal cerebral ischaemia in mice. *Br J Pharmacol.* 1997;122(4):625. doi:10.1038/SJ.BJP.0701427
34. McDonald ES, Windebank AJ. Mechanisms of neurotoxic injury and cell death. *Neurol Clin.* 2000;18(3):525-540. doi:10.1016/S0733-8619(05)70209-7
35. Jander S, Kraemer M, Schroeter M, Witte OW, Stoll G. Lymphocytic Infiltration and Expression of Intercellular Adhesion Molecule-1 in Photochemically Induced Ischemia of the Rat Cortex: <http://dx.doi.org/101038/jcbfm19955>. 2016;15(1):42-51. doi:10.1038/JCBFM.1995.5
36. Rami A, Agarwal R, Botez G, Winckler J.  $\mu$ -Calpain activation, DNA fragmentation, and synergistic effects of caspase and calpain inhibitors

- in protecting hippocampal neurons from ischemic damage. *Brain Res.* 2000;866(1-2):299-312. doi:10.1016/S0006-8993(00)02301-5
37. Thiebaut AM, Gauberti M, Ali C, Martinez De Lizarrondo S, Vivien D, Yepes M, Roussel BD. The role of plasminogen activators in stroke treatment: fibrinolysis and beyond. *Lancet Neurol.* 2018;17(12):1121-1132. doi:10.1016/S1474-4422(18)30323-5
38. Correa-Paz C, da Silva-Candal A, Polo E, Parcq J, Vivien D, Maysinger D, Pelaz B, Campos F. New Approaches in Nanomedicine for Ischemic Stroke. *Pharmaceutics.* 2021;13(5):757. doi:10.3390/PHARMACEUTICS13050757
39. Fang MC, Cutler DM, Rosen AB. Trends in Thrombolytic Use for Ischemic Stroke in the United States. *J Hosp Med.* 2010;5(7):409. doi:10.1002/JHM.689
40. Rha JH, Saver JL. The Impact of Recanalization on Ischemic Stroke Outcome. *Stroke.* 2007;38(3):967-973. doi:10.1161/01.STR.0000258112.14918.24
41. Flottmann F, Leischner H, Broocks G, Nawabi J, Bernhardt M, Faizy TD, Deb-Chatterji M, Thomalla G, Fiehler J, Brekenfeld C. Recanalization Rate per Retrieval Attempt in Mechanical Thrombectomy for Acute Ischemic Stroke. *Stroke.* 2018;49(10):2523-2525. doi:10.1161/STROKEAHA.118.022737
42. McMeekin P, White P, James MA, Price CI, Flynn D, Ford GA. Estimating the number of UK stroke patients eligible for endovascularthrombectomy. *Eur Stroke J.* 2017;2(4):326. doi:10.1177/2396987317733343
43. Rodríguez-Yáñez M, Sobrino T, Arias S, Vázquez-Herrero F, Brea D, Blanco M, Leira R, Castellanos M, Serena J, Vivancos J, Dávalos A, Castillo J. Early Biomarkers of Clinical-Diffusion Mismatch in Acute Ischemic Stroke. *Stroke.* 2011;42(10):2813-2818. doi:10.1161/STROKEAHA.111.614503
44. Kaur H, Prakash A, Medhi B. Drug Therapy in Stroke: From Preclinical to Clinical Studies. *Pharmacology.* 2013;92(5-6):324-334. doi:10.1159/000356320
45. Paul S, Candelario-Jalil E. *Emerging Neuroprotective Strategies for the Treatment of Ischemic Stroke: An Overview of Clinical and Preclinical Studies.* Vol 335. Elsevier Inc; 2021. doi:10.1016/j.expneurol.2020.113518
46. Ginsberg MD. Current Status of Neuroprotection for Cerebral Ischemia Synoptic Overview. *Stroke.* 2009;40(3 Suppl):S111. doi:10.1161/STROKEAHA.108.528877

47. Jia M, Njapo SAN, Rastogi V, Hedna VS. Taming glutamate excitotoxicity: Strategic pathway modulation for neuroprotection. *CNS Drugs*. 2015;29(2):153-162. doi:10.1007/s40263-015-0225-3
48. Shuaib A, Lees KR, Lyden P, Grotta J, Davalos A, Davis SM, Diener HC, Ashwood T, Wasiewski WW, Emeribe U. NXY-059 for the Treatment of Acute Ischemic Stroke. <http://dx.doi.org/101056/NEJMoa070240>. 2009;357(6):562-571. doi:10.1056/NEJMoa070240
49. Chamorro Á, Amaro S, Castellanos M, Segura T, Arenillas J, Martí-Fàbregas J, Gállego J, Krupinski J, Gomis M, Cánovas D, Carné X, Deulofeu R, Román LS, Oleaga L, Torres F, Planas AM. Safety and efficacy of uric acid in patients with acute stroke (URICO-ICTUS): A randomised, double-blind phase 2b/3 trial. *Lancet Neurol*. 2014;13(5):453-460. doi:10.1016/S1474-4422(14)70054-7
50. JJ S, JL L. Citicoline: pharmacological and clinical review. *Methods Find Exp Clin Pharmacol*. 2006;28 Supplem(June):1-56.
51. Hurtado O, Moro MA, Cárdenas A, Sánchez V, Fernández-Tomé P, Leza JC, Lorenzo P, Secades JJ, Lozano R, Dávalos A, Castillo J, Lizasoain I. Neuroprotection afforded by prior citicoline administration in experimental brain ischemia: Effects on glutamate transport. *Neurobiol Dis*. 2005;18(2):336-345. doi:10.1016/j.nbd.2004.10.006
52. Hurtado O, Cárdenas A, Pradillo JM, Morales JR, Ortego F, Sobrino T, Castillo J, Moro MA, Lizasoain I. A chronic treatment with CDP-choline improves functional recovery and increases neuronal plasticity after experimental stroke. *Neurobiol Dis*. 2007;26(1):105-111. doi:10.1016/j.nbd.2006.12.005
53. Dávalos A, Castillo J, Álvarez-Sabín J, Secades JJ, Mercadal J, López S, Cobo E, Warach S, Sherman D, Clark WM, Lozano R. Oral Citicoline in Acute Ischemic Stroke. *Stroke*. 2002;33(12):2850-2857. doi:10.1161/01.STR.0000038691.03334.71
54. Dávalos A, Alvarez-Sabín J, Castillo J, Díez-Tejedor E, Ferro J, Martínez-Vila E, Serena J, Segura T, Cruz VT, Masjuan J, Cobo E, Secades JJ. Citicoline in the treatment of acute ischaemic stroke: An international, randomised, multicentre, placebo-controlled study (ICTUS trial). *Lancet*. 2012;380(9839):349-357. doi:10.1016/S0140-6736(12)60813-7
55. Castillo J, Blanco M, Rodríguez-Yáñez M, Sobrino T, Leira R, Montaner J. Estrategias neuroprotectoras. In: ICG Marge S, ed. *Tratamiento Del Ictus Isquémico*. 1st ed. ; 2009:109-124.
56. Liu J, Zhang J, Wang LN. Gamma aminobutyric acid (GABA) receptor agonists for acute stroke. *Cochrane database Syst Rev*. 2018;10(10). doi:10.1002/14651858.CD009622.PUB5

57. Zhang ZG, Chopp M. Neurorestorative therapies for stroke: underlying mechanisms and translation to the clinic. *Lancet Neurol.* 2009;8(5):500. doi:10.1016/S1474-4422(09)70061-4
58. Alvarez-Buylla A, García-Verdugo JM. Neurogenesis in Adult Subventricular Zone. *J Neurosci.* 2002;22(3):634. doi:10.1523/JNEUROSCI.22-03-00629.2002
59. Martí-Fàbregas J, Romaguera-Ros M, Gómez-Pinedo U, Martínez-Ramírez S, Jiménez-Xarrié E, Marín R, Martí-Vilalta JL, García-Verdugo JM. Proliferation in the human ipsilateral subventricular zone after ischemic stroke. *Neurology.* 2010;74(5):357-365. doi:10.1212/WNL.0b013e3181cbccec
60. Belle JE Le, Orozco NM, Paucar AA, Saxe JP, Mottahedeh J, Pyle AD, Wu H, Kornblum HI. Proliferative Neural Stem Cells Have High Endogenous ROS Levels that Regulate Self-Renewal and Neurogenesis in a PI3K/Akt-Dependant Manner. *Cell Stem Cell.* 2011;8(1):71. doi:10.1016/J.STEM.2010.11.028
61. Arenillas JF, Sobrino T, Castillo J, Dávalos A. The role of angiogenesis in damage and recovery from ischemic stroke. *Curr Treat Options Cardiovasc Med.* 2007;9(3):205-212. doi:10.1007/s11936-007-0014-5
62. Brea López D, Sobrino Moreiras T, Ramos Cabrer P, Castillo Sánchez J. Reorganización de la vascularización cerebral tras la isquemia. *Rev Neurol.* 2009;49(12):645. doi:10.33588/rn.4912.2009564
63. Seevinck PR, Deddens LH, Dijkhuizen RM. Magnetic resonance imaging of brain angiogenesis after stroke. *Angiogenesis.* 2010;13(2):111. doi:10.1007/S10456-010-9174-0
64. Sobrino T, Hurtado O, Moro MA, Rodríguez-Yañez M, Castellanos M, Brea D, Moldes O, Blanco M, Arenillas JF, Leira R, Dávalos A, Lizasoain I, Castillo J. The Increase of Circulating Endothelial Progenitor Cells After Acute Ischemic Stroke Is Associated With Good Outcome. *Stroke.* 2007;38(10):2759-2764. doi:10.1161/STROKEAHA.107.484386
65. Zacharek A, Chen J, Cui X, Li A, Li Y, Roberts C, Feng Y, Gao Q, Chopp M. Angiopoietin1/Tie2 and VEGF/Flk1 induced by MSC treatment amplifies angiogenesis and vascular stabilization after stroke. *J Cereb Blood Flow Metab.* 2007;27(10):1691. doi:10.1038/SJ.JCBFM.9600475
66. Font MA, Arboix A, Krupinski J. Angiogenesis, Neurogenesis and Neuroplasticity in Ischemic Stroke. *Curr Cardiol Rev.* 2010;6(3):238. doi:10.2174/157340310791658802
67. Liu XS, Chopp M, Zhang RL, Hozeska-Solgot A, Gregg SC, Buller B, Lu M, Zhang ZG. Angiopoietin 2 Mediates the Differentiation and Migration of Neural Progenitor Cells in the Subventricular Zone after Stroke. *J Biol*

- Chem.* 2009;284(34):22680. doi:10.1074/JBC.M109.006551
68. Teng H, Zhang ZG, Wang L, Zhang RL, Zhang L, Morris D, Gregg SR, Wu Z, Jiang A, Lu M, Zlokovic B V, Chopp M. Coupling of angiogenesis and neurogenesis in cultured endothelial cells and neural progenitor cells after stroke. *J Cereb Blood Flow Metab.* 2008;28(4):764. doi:10.1038/SJJCBFM.9600573
  69. Chopp M, Zhang ZG, Jiang Q. Neurogenesis, Angiogenesis, and MRI Indices of Functional Recovery From Stroke. *Stroke.* 2007;38(2 PART 2):827-831. doi:10.1161/01.STR.0000250235.80253.E9
  70. Jiang Q, Zheng GZ, Guang LD, Zhang L, Ewing JR, Wang L, Zhang RL, Li L, Lu M, Meng H, Arbab AS, Hu J, Qing JL, Nejad D SP, Athiraman H, Chopp M. Investigation of neural progenitor cell induced angiogenesis after embolic stroke in rat using MRI. *Neuroimage.* 2005;28(3):698-707. doi:10.1016/j.neuroimage.2005.06.063
  71. Parr AM, Tator CH, Keating A. Bone marrow-derived mesenchymal stromal cells for the repair of central nervous system injury. *Bone Marrow Transplant.* 2007;40(7):609-619. doi:10.1038/sj.bmt.1705757
  72. Mifsud G, Zammit C, Muscat R, Giovanni G Di, Valentino M. Oligodendrocyte Pathophysiology and Treatment Strategies in Cerebral Ischemia. *CNS Neurosci Ther.* 2014;20(7):612. doi:10.1111/CNS.12263
  73. Moriyama Y, Hayashi M, Yamada H, Yatsushiro S, Ishio S, Yamamoto A. Synaptic-like microvesicles, synaptic vesicle counterparts in endocrine cells, are involved in a novel regulatory mechanism for the synthesis and secretion of hormones. *J Exp Biol.* 2000;203(Pt 1):117-125. Accessed October 18, 2021. <https://pubmed.ncbi.nlm.nih.gov/10600680/>
  74. Schousboe A. Transport and metabolism of glutamate and GABA in neurons and glial cells. *Int Rev Neurobiol.* 1981;22(C):1-45. doi:10.1016/S0074-7742(08)60289-5
  75. Boyko M, Gruenbaum SE, Gruenbaum BF, Shapira Y, Zlotnik A. Brain to blood glutamate scavenging as a novel therapeutic modality: a review. *J Neural Transm.* 2014;121(8):979. doi:10.1007/S00702-014-1181-7
  76. Rodriguez-Rodriguez P, Almeida A, Bolaños JP. Brain energy metabolism in glutamate-receptor activation and excitotoxicity: Role for APC/C-Cdh1 in the balance glycolysis/pentose phosphate pathway. *Neurochem Int.* 2013;62(5):750-756. doi:10.1016/J.NEUINT.2013.02.005
  77. Mangia S, Giove F, DiNuzzo M. Metabolic pathways and activity-

- dependent modulation of glutamate concentration in the human brain. *Neurochem Res.* 2012;37(11):2561. doi:10.1007/S11064-012-0848-4
78. Hawkins RA. The blood-brain barrier and glutamate. *Am J Clin Nutr.* 2009;90(3):867-874. doi:10.3945/AJCN.2009.27462BB
79. Cooper- AJL, McDonald JM, Gelbard AS, Gledhill RF, Duffyg TE. The Metabolic Fate of <sup>13</sup>N-labeled Ammonia in Rat Brain. *J Biol Chem.* 1979;254(12):4982-4992. doi:10.1016/S0021-9258(18)50550-0
80. Cooper AJ, Plum F. Biochemistry and physiology of brain ammonia. *Physiol Rev.* 1987;67(2):440-519. doi:10.1152/PHYSREV.1987.67.2.440
81. Martinez-Hernandez A, Bell KP, Norenberg MD. Glutamine Synthetase: Glial Localization in Brain. *Science (80- ).* 1977;195(4284):1356-1358. doi:10.1126/SCIENCE.14400
82. Shigeri Y, Seal RP, Shimamoto K. Molecular pharmacology of glutamate transporters, EAATs and VGLUTs. *Brain Res Rev.* 2004;45(3):250-265. doi:10.1016/J.BRAINRESREV.2004.04.004
83. Krzyżanowska W, Pomierny B, Filip M, Pera J. Glutamate transporters in brain ischemia: to modulate or not? *Acta Pharmacol Sin.* 2014;35(4):462. doi:10.1038/APS.2014.1
84. Zhou Y, Danbolt NC. Glutamate as a neurotransmitter in the healthy brain. *J Neural Transm.* 2014;121(8):817. doi:10.1007/S00702-014-1180-8
85. Hans Christian Cederberg H, Carsten Uhd N, Brodin B. Glutamate Efflux at the Blood-Brain Barrier: Cellular Mechanisms and Potential Clinical Relevance. *Arch Med Res.* 2014;45(8):639-645. doi:10.1016/J.ARCMED.2014.11.004
86. Maragakis NJ, Dietrich J, Wong V, Xue H, Mayer-Proschel M, Rao MS, Rothstein JD. Glutamate transporter expression and function in human glial progenitors. *Glia.* 2004;45(2):133-143. doi:10.1002/GLIA.10310
87. Liguz-Leczna M, Skangiel-Kramska J. Vesicular glutamate transporters (VGLUTs): The three musketeers of glutamatergic system. *Acta Neurobiol Exp (Wars).* 2007;67(3):207-218.
88. Zou J, Wang YX, Dou FF, Lü HZ, Ma ZW, Lu PH, Xu XM. Glutamine synthetase downregulation reduces astrocyte protection against glutamate excitotoxicity to neurons. *Neurochem Int.* 2010;56(4):584. doi:10.1016/J.NEUINT.2009.12.021
89. Hertz L, Rothman DL. Glucose, Lactate,  $\beta$ -Hydroxybutyrate, Acetate, GABA, and Succinate as Substrates for Synthesis of Glutamate and

- GABA in the Glutamine-Glutamate/GABA Cycle. *Adv Neurobiol.* 2016;13:9-42. doi:10.1007/978-3-319-45096-4
90. Westbrook GL. Glutamate receptors and excitotoxicity. *Res Publ Assoc Res Nerv Ment Dis.* 1993;71:35-50. Accessed October 18, 2021. <https://pubmed.ncbi.nlm.nih.gov/8380238/>
  91. Fremeau RT, Voglmaier S, Seal RP, Edwards RH. VGLUTs define subsets of excitatory neurons and suggest novel roles for glutamate. *Trends Neurosci.* 2004;27(2):98-103. doi:10.1016/J.TINS.2003.11.005
  92. McBean GJ. Cerebral cystine uptake: a tale of two transporters. *Trends Pharmacol Sci.* 2002;23(7):299-302. doi:10.1016/S0165-6147(02)02060-6
  93. Bridges RJ, Natale NR, Patel SA. System xc- cystine/glutamate antiporter: an update on molecular pharmacology and roles within the CNS. *Br J Pharmacol.* 2012;165(1):34. doi:10.1111/J.1476-5381.2011.01480.X
  94. Zerangue N, Kavanaugh MP. Flux coupling in a neuronal glutamate transporter. *Nature.* 1996;383:634-637. doi:10.1038/383634a0
  95. Oldendorf W, Szabo J. Amino acid assignment to one of three blood-brain barrier amino acid carriers. *Am J Physiol.* 1976;230(1):94-98. doi:10.1152/AJPLEGACY.1976.230.1.94
  96. Mann GE, Yudilevich DL, Sobrevia L. Regulation of Amino Acid and Glucose Transporters in Endothelial and Smooth Muscle Cells. *Physiol Rev.* 2003;83(1):183-252. doi:10.1152/PHYSREV.00022.2002
  97. Zauner A, Bullock R, Kuta AJ, Woodward J, Young HF. Glutamate release and cerebral blood flow after severe human head injury. *Acta Neurochir Suppl.* 1996;67(67):40-44. doi:10.1007/978-3-7091-6894-3\_9
  98. Leibowitz A, Boyko M, Shapira Y, Zlotnik A. Blood Glutamate Scavenging: Insight into Neuroprotection. *Int J Mol Sci.* 2012;13(8):10041-10066. doi:10.3390/IJMS130810041
  99. Castillo MR, Babson JR. Ca(2+)-dependent mechanisms of cell injury in cultured cortical neurons. *Neuroscience.* 1998;86(4):1133-1144. doi:10.1016/S0306-4522(98)00070-0
  100. Castillo J, Dávalos A, Naveiro J, Noya M. Neuroexcitatory Amino Acids and Their Relation to Infarct Size and Neurological Deficit in Ischemic Stroke. *Stroke.* 1996;27(6):1060-1065. doi:10.1161/01.STR.27.6.1060
  101. Castillo J, Dávalos A, Noya M. Progression of ischaemic stroke and excitotoxic aminoacids. *Lancet.* 1997;349(9045):79-82. doi:10.1016/S0140-6736(96)04453-4

102. Castillo J, Dávalos A, Noya M. Aggravation of Acute Ischemic Stroke by Hyperthermia Is Related to an Excitotoxic Mechanism. *Cerebrovasc Dis.* 1999;9(1):22-27. doi:10.1159/000015891
103. Zlotnik A, Sinelnikov I, Gruenbaum BF, Gruenbaum SE, Dubilet M, Dubilet E, Leibowitz A, Ohayon S, Regev A, Boyko M, Shapira Y, Teichberg VI. Effect of Glutamate and Blood Glutamate Scavengers Oxaloacetate and Pyruvate on Neurological Outcome and Pathohistology of the Hippocampus after Traumatic Brain Injury in Rats. *Anesthesiology.* 2012;116(1):73-83. doi:10.1097/ALN.0B013E31823D7731
104. Andreadou E, Kapaki E, Kokotis P, Paraskevas GP, Katsaros N, Libitaki G, Zis V, Sfagos C, Vassilopoulos D. Plasma glutamate and glycine levels in patients with amyotrophic lateral sclerosis: The effect of riluzole treatment. *Clin Neurol Neurosurg.* 2008;110(3):222-226. doi:10.1016/J.CLINEURO.2007.10.018
105. Stojanovic IR, Kostic M, Ljubisavljevic S. The role of glutamate and its receptors in multiple sclerosis. *J Neural Transm.* 2014;121(8):945-955. doi:10.1007/S00702-014-1188-0
106. Campos F, Sobrino T, Blanco M, López-Arias E, Baluja A, Álvarez J, Castillo J. Glutamate neurotoxicity is involved in the neurological damage in patients undergoing extracorporeal circulation. *Int J Cardiol.* 2014;172(2):481-483. doi:10.1016/J.IJCARD.2014.01.004
107. O’Kane RL, Martínez-López I, DeJoseph MR, Viña JR, Hawkins RA. Na<sup>+</sup>-dependent Glutamate Transporters (EAAT1, EAAT2, and EAAT3) of the Blood-Brain Barrier: A MECHANISM FOR GLUTAMATE REMOVAL \*. *J Biol Chem.* 1999;274(45):31891-31895. doi:10.1074/JBC.274.45.31891
108. Caldeira M V., Salazar IL, Curcio M, Canzoniero LMT, Duarte CB. Role of the ubiquitin-proteasome system in brain ischemia: Friend or foe? *Prog Neurobiol.* 2014;112:50-69. doi:10.1016/j.pneurobio.2013.10.003
109. Sattler R, Tymianski M. Molecular mechanisms of calcium-dependent excitotoxicity. *J Mol Med (Berl).* 2000;78(1):3-13. doi:10.1007/S001090000077
110. Lau A, Tymianski M. Glutamate receptors, neurotoxicity and neurodegeneration. *Pflügers Arch - Eur J Physiol* 2010 4602. 2010;460(2):525-542. doi:10.1007/S00424-010-0809-1
111. Campos F, Sobrino T, Pérez-Mato M, Rodríguez-Orsorio X, Leira R, Blanco M, Mirelman D, Castillo J. Glutamate oxaloacetate transaminase: A new key in the dysregulation of glutamate in migraine patients: <https://doi.org/10.1177/0333102413487444>. 2013;33(14):1148-1154. doi:10.1177/0333102413487444

112. Zlotnik A, Gurevich B, Cherniavsky E, Tkachov S, Matuzani-Ruban A, Leon A, Shapira Y, Teichberg VI. The Contribution of the Blood Glutamate Scavenging Activity of Pyruvate to its Neuroprotective Properties in a Rat Model of Closed Head Injury. *Neurochem Res* 2007 336. 2007;33(6):1044-1050. doi:10.1007/S11064-007-9548-X
113. Aarts M, Liu Y, Liu L, Besshoh S, Arundine M, Gurd JW, Wang YT, Salter MW, Tymianski M. Treatment of Ischemic Brain Damage by Perturbing NMDA Receptor- PSD-95 Protein Interactions. *Science* (80- ). 2002;298(5594):846-850. doi:10.1126/SCIENCE.1072873
114. Jones N. Disruption of the nNOS-PSD-95 complex is neuroprotective in models of cerebral ischemia. *Nat Rev Neurol* 2011 72. 2011;7(2):61-61. doi:10.1038/nrneurol.2010.203
115. Zhou L, Li F, Xu HB, Luo CX, Wu HY, Zhu MM, Lu W, Ji X, Zhou QG, Zhu DY. Treatment of cerebral ischemia by disrupting ischemia-induced interaction of nNOS with PSD-95. *Nat Med*. 2010;16(12):1439-1443. doi:10.1038/nm.2245
116. Lee JM, Zipfel GJ, Choi DW. The changing landscape of ischaemic brain injury mechanisms. *Nature*. 1999;399:A7-A14. doi:10.1038/399a007
117. Dykens JA. Isolated Cerebral and Cerebellar Mitochondria Produce Free Radicals when Exposed to Elevated Ca<sup>2+</sup> and Na<sup>+</sup>: Implications for Neurodegeneration. *J Neurochem*. 1994;63(2):584-591. doi:10.1046/J.1471-4159.1994.63020584.X
118. Ogden KK, Traynelis SF. New advances in NMDA receptor pharmacology. *Trends Pharmacol Sci*. 2011;32(12):733. doi:10.1016/J.TIPS.2011.08.003
119. Kalia L V., Kalia SK, Salter MW. NMDA Receptors in Clinical Neurology: Excitatory Times Ahead. *Lancet Neurol*. 2008;7(8):755. doi:10.1016/S1474-4422(08)70165-0
120. Muir KW. Glutamate-based therapeutic approaches: clinical trials with NMDA antagonists. *Curr Opin Pharmacol*. 2006;6(1):53-60. doi:10.1016/J.COPH.2005.12.002
121. Ikonomidou C, Turski L. Why did NMDA receptor antagonists fail clinical trials for stroke and traumatic brain injury? *Lancet Neurol*. 2002;1(6):383-386. doi:10.1016/S1474-4422(02)00164-3
122. Danbolt NC. Glutamate uptake. *Prog Neurobiol*. 2001;65(1):1-105. doi:10.1016/S0301-0082(00)00067-8
123. Castillo J, Loza MI, Mirelman D, Brea J, Blanco M, Sobrino T, Campos F. A novel mechanism of neuroprotection: Blood glutamate grabber. *J Cereb Blood Flow Metab*. 2016;36(2):292-301.

doi:10.1177/0271678X15606721

124. Gottlieb M, Wang Y, Teichberg VI. Blood-mediated scavenging of cerebrospinal fluid glutamate. *J Neurochem.* 2003;87(1):119-126. doi:10.1046/J.1471-4159.2003.01972.X
125. Pérez-Mato M, Ramos-Cabrer P, Sobrino T, Blanco M, Ruban A, Mirelman D, Menendez P, Castillo J, Campos F. Human recombinant glutamate oxaloacetate transaminase 1 (GOT1) supplemented with oxaloacetate induces a protective effect after cerebral ischemia. *Cell Death Dis.* 2014;5(1):e992. doi:10.1038/cddis.2013.507
126. Karmen A, Wróblewski F, LaDue JS. Transaminase Activity in Human Blood. *J Clin Invest.* 1955;34(1):133. doi:10.1172/JCI103055
127. Otto-Ślusarczyk D, Graboń W, Mielczarek-Putka M. [Aspartate aminotransferase--key enzyme in the human systemic metabolism]. *Postepy Hig Med Dosw.* 2016;70:219-230. doi:10.5604/17322693.1197373
128. Ford GC, Eichele G, Jansonius JN. Three-dimensional structure of a pyridoxal-phosphate-dependent enzyme, mitochondrial aspartate aminotransferase. *Proc Natl Acad Sci U S A.* 1980;77(5):2563. doi:10.1073/PNAS.77.5.2559
129. Borisov V V., Borisova SN, Kachalova GS, Sosfenov NI, Vainshtein BK, Torchinsky YM, Braunstein AE. Three-dimensional structure at 5 Å resolution of cytosolic aspartate transaminase from chicken heart. *J Mol Biol.* 1978;125(3):275-292. doi:10.1016/0022-2836(78)90403-5
130. Harutyunyan EG, Malashkevich VN, Tersyan SS, Kochkina VM, Torchinsky YM, Braunstein AE. Three-dimensional structure at 3.2 Å resolution of the complex of cytosolic aspartate aminotransferase from chicken heart with 2-oxoglutarate. *FEBS Lett.* 1982;138(1):113-116. doi:10.1016/0014-5793(82)80407-9
131. Jeong SY, Jin H, Chang JH. Crystal structure of L-aspartate aminotransferase from *Schizosaccharomyces pombe*. *PLoS One.* 2019;14(8). doi:10.1371/JOURNAL.PONE.0221975
132. Ulusu NN. Evolution of Enzyme Kinetic Mechanisms. *J Mol Evol.* 2015;80(5-6):257. doi:10.1007/S00239-015-9681-0
133. Kirsch JF, Eichele G, Ford GC, Vincent MG, Jansonius JN, Gehring H, Christen P. Mechanism of action of aspartate aminotransferase proposed on the basis of its spatial structure. *J Mol Biol.* 1984;174(3):497-525. doi:10.1016/0022-2836(84)90333-4
134. Toney MD. Aspartate Aminotransferase: an old dog teaches new tricks. *Arch Biochem Biophys.* 2014;0:127. doi:10.1016/J.ABB.2013.10.002

135. Rej R. Aspartate aminotransferase activity and isoenzyme proportions in human liver tissues. *Clin Chem.* 1978;24(11):1971-1979.
136. Teranishi H, Kagamiyama H, Teranishi K, Wada H, Yamano T. Cytosolic and mitochondrial isoenzymes of glutamic-oxalacetic transaminase from human heart. *J Biol Chem.* 1978;253(24):8842-8847. doi:10.1016/S0021-9258(17)34254-0
137. Rej R. Aminotransferase in disease. *Clin Lab Med.* 1989;9(4):667-687. doi:10.1016/s0272-2712(18)30598-5
138. Leung FY, Henderson AR. Isolation and purification of aspartate aminotransferase isoenzymes from human liver by chromatography and isoelectric focusing. *Clin Chem.* 1981;27(2):232-238.
139. Van Der Laarse A, Dijkshoorn NJ, Hollaar L, Caspers T. The (ISO)enzyme activities of lactate dehydrogenase,  $\alpha$ -hydroxybutyrate dehydrogenase, creatine kinase and aspartate aminotransferase in human myocardial biopsies and autopsies. *Clin Chim Acta.* 1980;104(3):381-391. doi:10.1016/0009-8981(80)90397-6
140. Uhlén M, Fagerberg L, Hallström BM, Lindskog C, Oksvold P, Mardinoglu A, et al. Tissue-based map of the human proteome. *Science (80- ).* 2015;347(6220). doi:10.1126/SCIENCE.1260419
141. The Human Protein Atlas. Published November 2021. Accessed December 8, 2021. <https://www.proteinatlas.org>
142. Rej R. Immunochemical quantitation of isoenzymes of aspartate aminotransferase and lactate dehydrogenase. *Clin Biochem.* 1983;16(1):17-19. doi:10.1016/S0009-9120(83)94262-5
143. Hirano K, Matsuda K, Adachi T, Ito Y, Hayashi K, Okuno F, Muto Y. Determination of mitochondrial aspartate aminotransferase in serum. *Clin Chim Acta.* 1986;155(3):251-262. doi:10.1016/0009-8981(86)90245-7
144. Niblock AE, Jablonsky G, Leung FY, Henderson AR. Changes in mass and catalytic activity concentrations of aspartate aminotransferase isoenzymes in serum after a myocardial infarction. *Clin Chem.* 1986;32(3):496-500.
145. Dawson AG. Oxidation of cytosolic NADH formed during aerobic metabolism in mammalian cells. *Trends Biochem Sci.* 1979;4(8):171-176. doi:10.1016/0968-0004(79)90417-1
146. Broeks MH, Karnebeek CDM van, Wanders RJA, Jans JJM, Verhoeven-Duif NM. Inborn disorders of the malate aspartate shuttle. *J Inherit Metab Dis.* 2021;44(4):808. doi:10.1002/JIMD.12402
147. McKenna MC, Waagepetersen HS, Schousboe A, Sonnewald U. Neuronal

- and astrocytic shuttle mechanisms for cytosolic-mitochondrial transfer of reducing equivalents: Current evidence and pharmacological tools. *Biochem Pharmacol.* 2006;71(4):399-407. doi:10.1016/J.BCP.2005.10.011
148. Pardo B, Contreras L, Satrústegui J. De novo Synthesis of Glial Glutamate and Glutamine in Young Mice Requires Aspartate Provided by the Neuronal Mitochondrial Aspartate-Glutamate Carrier Aralar/AGC1. *Front Endocrinol (Lausanne).* 2013;4:149. doi:10.3389/FENDO.2013.00149
149. Safer B. The Metabolic Significance of the Malate-Aspartate Cycle in Heart. *Circ Res.* 1975;37(5):527-533. doi:10.1161/01.RES.37.5.527
150. Sluse FE, Ranson M, Liébecq C. Mechanism of the Exchanges Catalysed by the Oxoglutarate Translocator of Rat-Heart Mitochondria. *Eur J Biochem.* 1972;25(2):207-217. doi:10.1111/J.1432-1033.1972.TB01686.X
151. Ferré P, Williamson DH. Evidence for the participation of aspartate aminotransferase in hepatic glucose synthesis in the suckling newborn rat. *Biochem J.* 1978;176(1):338. doi:10.1042/BJ1760335
152. Rognstad R, Clark DG. Effects of aminoxyacetate on the metabolism of isolated liver cells. *Arch Biochem Biophys.* 1974;161(2):638-646. doi:10.1016/0003-9861(74)90348-8
153. Smith SB, Briggs S, Triebwasser KC, Freedland RA. Re-evaluation of amino-oxyacetate as an inhibitor. *Biochem J.* 1977;162(2):455. doi:10.1042/BJ1620453
154. Horio Y, Fukui H, Taketoshi M, Tanaka T, Wada H. Induction of Cytosolic Aspartate Aminotransferase by Glucagon in Primary Cultured Rat Hepatocytes. *Biochem Biophys Res Commun.* 1988;153(1):410-416.
155. Smith BC, Clotfelter LA, Cheung JY, LaNoue KF. Differences in 2-oxoglutarate dehydrogenase regulation in liver and kidney. *Biochem J.* 1992;284(Pt 3):826. doi:10.1042/BJ2840819
156. Fahien LA, MacDonald MJ. The Succinate Mechanism of Insulin Release. *Diabetes.* 2002;51(9):2669-2676. doi:10.2337/DIABETES.51.9.2669
157. Carmena R, Betteridge DJ. Diabetogenic Action of Statins: Mechanisms. *Curr Atheroscler Rep.* 2019;21(6):1-9. doi:10.1007/s11883-019-0780-z
158. Yokoi N, Ghani G, Takahashi H, Seino S.  $\beta$ -Cell glutamate signaling: Its role in incretin-induced insulin secretion. *J Diabetes Investig.* 2016;7:38-43. doi:10.1111/JDI.12468
159. Campbell JE, Newgard CB. Mechanisms controlling pancreatic islet cell

- function in insulin secretion. *Nat Rev Mol Cell Biol.* 2021;22(2):158. doi:10.1038/S41580-020-00317-7
160. Maechler P, Wollheim CB. Mitochondrial glutamate acts as a messenger in glucose-induced insulin exocytosis. *Nat* 1999 4026762. 1999;402(6762):685-689. doi:10.1038/45280
161. Murao N, Yokoi N, Honda K, Han G, Hayami T, Gheni G, Takahashi H, Minami K, Seino S. Essential roles of aspartate aminotransferase 1 and vesicular glutamate transporters in  $\beta$ -cell glutamate signaling for incretin-induced insulin secretion. *PLoS One.* 2017;12(11). doi:10.1371/JOURNAL.PONE.0187213
162. Tordjman J, Leroyer S, Chauvet G, Quette J, Chauvet C, Tomkiewicz C, Chapron C, Barouki R, Forest C, Aggerbeck M, Antoine B. Cytosolic Aspartate Aminotransferase, a New Partner in Adipocyte Glyceroneogenesis and an Atypical Target of Thiazolidinedione. *J Biol Chem.* 2007;282(32):23591-23602. doi:10.1074/JBC.M611111200
163. Reshef L, Olswang Y, Cassuto H, Blum B, Croniger CM, Kalhan SC, Tilghman SM, Hanson RW. Glyceroneogenesis and the triglyceride/fatty acid cycle. *J Biol Chem.* 2003;278(33):30413-30416. doi:10.1074/jbc.R300017200
164. Hanson RW, Reshef L. Glyceroneogenesis revisited. *Biochimie.* 2003;85(12):1199-1205. doi:10.1016/j.biochi.2003.10.022
165. Gorin E, Tal-Or Z, Shafir E. Glyceroneogenesis in Adipose Tissue of Fasted, Diabetic and Triamcinolone Treated Rats. *Eur J Biochem.* 1969;8(3):370-375. doi:10.1111/J.1432-1033.1969.TB00537.X
166. Plee-Gautier E, Grimal H, Aggerbeck M, Barouki R, Forest C. Cytosolic aspartate aminotransferase gene is a member of the glucose-regulated protein gene family in adipocytes. *Biochem J.* 1998;329(Pt 1):40. doi:10.1042/BJ3290037
167. Plee-Gautier E, Aggerbeck M, Beurton F, Antoine B, Grimal H, Barouki R, Forest C. Identification of an Adipocyte-Specific Negative Glucose Response Region in the Cytosolic Aspartate Aminotransferase Gene. *Endocrinology.* 1998;139(12):4936-4944. doi:10.1210/ENDO.139.12.6342
168. Ubuka T, Umemura S, Yuasa S, Kinuta M, Watanabe K. Purification and characterization of mitochondrial cysteine aminotransferase from rat liver. *Physiol Chem Phys.* 1978;10(6):483-500. doi:10.18926/AMO/30697
169. Akagi R. Purification and characterization of cysteine aminotransferase from rat liver cytosol. *Acta Med Okayama.* 1982;36(3):187-197. doi:10.18926/AMO/30697

170. Kimura H. Physiological role of hydrogen sulfide and polysulfide in the central nervous system. *Neurochem Int.* 2013;63(5):492-497. doi:10.1016/j.neuint.2013.09.003
171. Wu D, Wang J, Li H, Xue M, Ji A, Li Y. Role of Hydrogen Sulfide in Ischemia-Reperfusion Injury. *Oxid Med Cell Longev.* 2015;2015. doi:10.1155/2015/186908
172. Jiang Z, Li C, Manuel ML, Yuan S, Kevil CG, McCarter KD, Lu W, Sun H. Role of Hydrogen Sulfide in Early Blood-Brain Barrier Disruption following Transient Focal Cerebral Ischemia. *PLoS One.* 2015;10(2). doi:10.1371/JOURNAL.PONE.0117982
173. Shibuya N, Koike S, Tanaka M, Ishigami-Yuasa M, Kimura Y, Ogasawara Y, Fukui K, Nagahara N, Kimura H. A novel pathway for the production of hydrogen sulfide from D-cysteine in mammalian cells. *Nat Commun* 2013 41. 2013;4(1):1-7. doi:10.1038/ncomms2371
174. Miyamoto R, Otsuguro K ichi, Yamaguchi S, Ito S. Contribution of cysteine aminotransferase and mercaptopyruvate sulfurtransferase to hydrogen sulfide production in peripheral neurons. *J Neurochem.* 2014;130(1):29-40. doi:10.1111/JNC.12698
175. Shibuya N, Mikami Y, Kimura Y, Nagahara N, Kimura H. Vascular Endothelium Expresses 3-Mercaptopyruvate Sulfurtransferase and Produces Hydrogen Sulfide. *J Biochem.* 2009;146(5):623-626. doi:10.1093/JB/MVP111
176. Guidetti P, Amori L, Sapko MT, Okuno E, Schwarcz R. Mitochondrial aspartate aminotransferase: a third kynurenate-producing enzyme in the mammalian brain. *J Neurochem.* 2007;102(1):103-111. doi:10.1111/J.1471-4159.2007.04556.X
177. Han Q, Robinson H, Cai T, Tagle DA, Li J. Biochemical and structural characterization of mouse mitochondrial aspartate aminotransferase, a newly identified kynurenine aminotransferase-IV. *Biosci Rep.* 2011;31(5):332. doi:10.1042/BSR20100117
178. Jiang X, Wang J, Chang H, Zhou Y. Recombinant expression, purification and crystallographic studies of the mature form of human mitochondrial aspartate aminotransferase. *Biosci Trends.* 2016;10(1):79-84. doi:10.5582/BST.2015.01150
179. Rossi F, Miggiano R, Ferraris DM, Rizzi M. The Synthesis of Kynurenic Acid in Mammals: An Updated Kynurenine Aminotransferase Structural KATalogue. *Front Mol Biosci.* 2019;6(FEB):9. doi:10.3389/FMOLB.2019.00007
180. Kubicova L, Hadacek F, Bachmann G, Weckwerth W, Chobot V. Coordination Complex Formation and Redox Properties of Kynurenic

- and Xanthurenic Acid Can Affect Brain Tissue Homeodynamics. *Antioxidants*. 2019;8(10):476. doi:10.3390/ANTIOX8100476
181. Németh H, Toldi J, Vécsei L. Kynurenines, Parkinson's disease and other neurodegenerative disorders: preclinical and clinical studies. *J Neural Transm Suppl*. 2006;(70):285-304. doi:10.1007/978-3-211-45295-0\_45
  182. Chess AC, Simoni MK, Alling TE, Bucci DJ. Elevations of Endogenous Kynurenic Acid Produce Spatial Working Memory Deficits. *Schizophr Bull*. 2007;33(3):804. doi:10.1093/SCHBUL/SBL033
  183. Gao J, Xu K, Liu H, Liu G, Bai M, Peng C, Li T, Yin Y. Impact of the Gut Microbiota on Intestinal Immunity Mediated by Tryptophan Metabolism. *Front Cell Infect Microbiol*. 2018;8(FEB):13. doi:10.3389/FCIMB.2018.00013
  184. Fazio F, Lionetto L, Curto M, Iacovelli L, Copeland CS, Neale SA, Bruno V, Battaglia G, Salt TE, Nicoletti F. Cinnabarinic acid and xanthurenic acid: Two kynurenine metabolites that interact with metabotropic glutamate receptors. *Neuropharmacology*. 2017;112:365-372. doi:10.1016/j.neuropharm.2016.06.020
  185. Akbal E, Koçak E, Akyürek Ö, Köklü S, Batgi H, Şenes M. Liver fatty acid-binding protein as a diagnostic marker for non-alcoholic fatty liver disease. *Cent Eur J Med*. 2014;128(1-2):48-52. doi:10.1007/s00508-014-0680-8
  186. Xu H, Diolintzi A, Storch J. Fatty acid-binding proteins: Functional understanding and diagnostic implications. *Curr Opin Clin Nutr Metab Care*. 2019;22(6):407-412. doi:10.1097/MCO.0000000000000600
  187. Berk PD, Wada H, Horio Y, Potter BJ, Sorrentino D, Zhou SL, Isola LM, Stump D, Kiang CL, Thung S. Plasma membrane fatty acid-binding protein and mitochondrial glutamic-oxaloacetic transaminase of rat liver are related. *Proc Natl Acad Sci U S A*. 1990;87(9):3488. doi:10.1073/PNAS.87.9.3484
  188. Stump DD, Zhou SL, Berk PD. Comparison of plasma membrane FABP and mitochondrial isoform of aspartate aminotransferase from rat liver. *Am J Physiol*. 1993;265(5 Pt 1). doi:10.1152/AJPGI.1993.265.5.G894
  189. Zhou SL, Stump D, Kiang CL, Isola LM, Berk PD. Mitochondrial Aspartate Aminotransferase Expressed on the Surface of 3T3-L1 Adipocytes Mediates Saturable Fatty Acid Uptake. *Proc Soc Exp Biol Med*. 1995;208(3):263-270.
  190. Isola LM, Zhou SL, Kiang CL, Stump DD, Bradbury MW, Berk PD. 3T3 fibroblasts transfected with a cDNA for mitochondrial aspartate aminotransferase express plasma membrane fatty acid-binding protein

- and saturable fatty acid uptake. *Proc Natl Acad Sci U S A*. 1995;92(21):9870. doi:10.1073/PNAS.92.21.9866
191. Roepstorff C, Wulff Helge J, Vistisen B, Kiens B. Studies of plasma membrane fatty acid-binding protein and other lipid-binding proteins in human skeletal muscle. *Proc Nutr Soc*. 2004;63(2):239-244. doi:10.1079/pns2004332
192. Bradbury MW, Stump D, Guarnieri F, Berk PD. Molecular Modeling and Functional Confirmation of a Predicted Fatty Acid Binding Site of Mitochondrial Aspartate Aminotransferase. *J Mol Biol*. 2011;412(3):422. doi:10.1016/J.JMB.2011.07.034
193. Thumser AE, Moore JB, Plant NJ. Fatty acid binding proteins: Tissue-specific functions in health and disease. *Curr Opin Clin Nutr Metab Care*. 2014;17(2):124-129. doi:10.1097/MCO.0000000000000031
194. Lipton P. Ischemic Cell Death in Brain Neurons. *Physiol Rev*. 1999;79(4):1431-1568. doi:10.1152/PHYSREV.1999.79.4.1431
195. Castillo J, Martínez F, Corredera E, Aldrey JM, Noya M. Amino Acid Transmitters in Patients With Headache During the Acute Phase of Cerebrovascular Ischemic Disease. *Stroke*. 1995;26(11):2035-2039. doi:10.1161/01.STR.26.11.2035
196. Nagy D, Marosi M, Kis Z, Farkas T, Rakos G, Vecsei L, Teichberg VI, Toldi J. Oxaloacetate Decreases the Infarct Size and Attenuates the Reduction in Evoked Responses after Photothrombotic Focal Ischemia in the Rat Cortex. *Cell Mol Neurobiol*. 2009;29(6):827-835. doi:10.1007/S10571-009-9364-8
197. Campos F, Sobrino T, Ramos-Cabrer P, Castillo J. Oxaloacetate: A novel neuroprotective for acute ischemic stroke. *Int J Biochem Cell Biol*. 2012;44(2):262-265. doi:10.1016/J.BIOCEL.2011.11.003
198. Marosi M, Fuzik J, Nagy D, Rákos G, Kis Z, Vécsei L, Toldi J, Ruban-Matuzani A, Teichberg VI, Farkas T. Oxaloacetate restores the long-term potentiation impaired in rat hippocampus CA1 region by 2-vessel occlusion. *Eur J Pharmacol*. 2009;604(1-3):51-57. doi:10.1016/J.EJPHAR.2008.12.022
199. Campos F, Sobrino T, Ramos-Cabrer P, Argibay B, Agulla J, Pérez-Mato M, Rodríguez-González R, Brea D, Castillo J. Neuroprotection by glutamate oxaloacetate transaminase in ischemic stroke: an experimental study. *J Cereb Blood Flow Metab*. 2011;31(6):1378-1386. doi:10.1038/JCBFM.2011.3
200. Boyko M, Zlotnik A, Gruenbaum BF, Gruenbaum SE, Ohayon S, Kuts R, Melamed I, Regev A, Shapira Y, Teichberg VI. Pyruvate's blood glutamate scavenging activity contributes to the spectrum of its

- neuroprotective mechanisms in a rat model of stroke. *Eur J Neurosci.* 2011;34(9):1432-1441. doi:10.1111/J.1460-9568.2011.07864.X
201. Campos F, Rodríguez-Yáñez M, Castellanos M, Arias S, Pérez-Mato M, Sobrino T, Blanco M, Serena J, Castillo J. Blood levels of glutamate oxaloacetate transaminase are more strongly associated with good outcome in acute ischaemic stroke than glutamate pyruvate transaminase levels. *Clin Sci.* 2011;121(1):11-17. doi:10.1042/CS20100427
  202. Campos F, Pérez-Mato M, Agulla J, Blanco M, Barral D, Almeida Á, Brea D, Waeber C, Castillo J, Ramos-Cabrer P. Glutamate Excitotoxicity Is the Key Molecular Mechanism Which Is Influenced by Body Temperature during the Acute Phase of Brain Stroke. *PLoS One.* 2012;7(8):44191. doi:10.1371/JOURNAL.PONE.0044191
  203. Rink C, Gnyawali S, Peterson L, Khanna S. Oxygen-inducible glutamate oxaloacetate transaminase as protective switch transforming neurotoxic glutamate to metabolic fuel during acute ischemic stroke. *Antioxidants Redox Signal.* 2011;14(10):1777-1785. doi:10.1089/ars.2011.3930
  204. Rink C, Gnyawali S, Stewart R, Teplitsky S, Harris H, Roy S, Sen CK, Khanna S. Glutamate oxaloacetate transaminase enables anaplerotic refilling of TCA cycle intermediates in stroke-affected brain. *FASEB J.* 2017;31(4):1709-1718. doi:10.1096/fj.201601033R
  205. Campos F, Sobrino T, Ramos-Cabrer P, Argibay B, Agulla J, Pérez-Mato M, Rodríguez-González R, Brea D, Castillo J. Neuroprotection by glutamate oxaloacetate transaminase in ischemic stroke: an experimental study. *J Cereb Blood Flow Metab.* 2011;31(6):1386. doi:10.1038/JCBFM.2011.3
  206. Khanna S, Stewart R, Gnyawali S, Harris H, Balch M, Spieldenner J, Sen CK, Rink C. Phytoestrogen isoflavone intervention to engage the neuroprotective effect of glutamate oxaloacetate transaminase against stroke. *FASEB J.* 2017;31(10):4544. doi:10.1096/FJ.201700353
  207. Ghajar J. Traumatic brain injury. *Lancet.* 2000;356(9233):923-929. doi:10.1016/S0140-6736(00)02689-1
  208. Cole TB. Global Road Safety Crisis Remedy Sought. *J Am Med Assoc.* 2004;291(21):2531-2532. doi:10.1001/JAMA.291.21.2531
  209. Warden DL, French L. Traumatic Brain Injury in the War Zone. *N Engl J Med.* 2005;352(20):2043-2047. doi:10.1056/NEJMP058102
  210. Xydakis LCMS, Fravell LCMD, Nasser LCKE, Casler CJD. Analysis of Battlefield Head and Neck Injuries in Iraq and Afghanistan. *Otolaryngol Neck Surg.* 2016;133(4):497-504.

doi:10.1016/J.OTOHNS.2005.07.003

211. Hoge CW, McGurk D, Thomas JL, Cox AL, Engel CC, Castro CA. Mild Traumatic Brain Injury in U.S. Soldiers Returning from Iraq. *N Engl J Med.* 2008;358(5):453-463. doi:10.1056/NEJMOA072972
212. Mock C, Quansah R, Krishnan R, Arreola-Risa C, Rivara F. Strengthening the prevention and care of injuries worldwide. *Lancet.* 2004;363(9427):2172-2179. doi:10.1016/S0140-6736(04)16510-0
213. Maas AI, Stocchetti N, Bullock R. Moderate and severe traumatic brain injury in adults. *Lancet Neurol.* 2008;7(8):728-741. doi:10.1016/S1474-4422(08)70164-9
214. Hutchinson PJ, O'Connell MT, Rothwell NJ, Hopkins SJ, Nortje J, Carpenter KLH, Timofeev I, Al-Rawi PG, Menon DK, Pickard JD. Inflammation in Human Brain Injury: Intracerebral Concentrations of IL-1 $\alpha$ , IL-1 $\beta$ , and Their Endogenous Inhibitor IL-1ra. *J Neurotrauma.* 2007;24(10):1545-1557. doi:10.1089/NEU.2007.0295
215. Kroemer G, Galluzzi L, Brenner C. Mitochondrial Membrane Permeabilization in Cell Death. *Physiol Rev.* 2007;87(1):99-163. doi:10.1152/PHYSREV.00013.2006
216. Rose ME, Huerbin MB, Melick J, Marion DW, Palmer AM, Schiding JK, Kochanek PM, Graham SH. Regulation of interstitial excitatory amino acid concentrations after cortical contusion injury. *Brain Res.* 2002;943(1):15-22. doi:10.1016/S0006-8993(02)02471-X
217. Bullock R, Zauner A, Woodward JJ, Myseros J, Choi SC, Ward JD, Marmarou A, Young HF. Factors affecting excitatory amino acid release following severe human head injury. *J Neurosurg.* 1998;89(4):507-518. doi:10.3171/JNS.1998.89.4.0507
218. Richards DA, Toliaas CM, Sgouros S, Bowery NG. Extracellular glutamine to glutamate ratio may predict outcome in the injured brain: a clinical microdialysis study in children. *Pharmacol Res.* 2003;48(1):101-109. doi:10.1016/S1043-6618(03)00081-1
219. Orrenius S, Zhivotovsky B, Nicotera P. Regulation of cell death: the calcium-apoptosis link. *Nat Rev Mol Cell Biol.* 2003;4(7):552-565. doi:10.1038/nrm1150
220. Zlotnik A, Gurevich B, Tkachov S, Maoz I, Shapira Y, Teichberg VI. Brain neuroprotection by scavenging blood glutamate. *Exp Neurol.* 2007;203(1):213-220. doi:10.1016/J.EXPNEUROL.2006.08.021
221. Zlotnik A, Gruenbaum SE, Artru AA, Rozet I, Dubilet M, Tkachov S, Brotfain E, Klin Y, Shapira Y, Teichberg VI. The neuroprotective effects of oxaloacetate in closed head injury in rats is mediated by its blood

- glutamate scavenging activity: Evidence from the use of maleate. *J Neurosurg Anesthesiol.* 2009;21(3):235-241. doi:10.1097/ANA.0B013E3181A2BF0B
222. Zhang D, Xiao M, Wang L, Jia W. Blood-Based Glutamate Scavengers Reverse Traumatic Brain Injury-Induced Synaptic Plasticity Disruption by Decreasing Glutamate Level in Hippocampus Interstitial Fluid, but Not Cerebral Spinal Fluid, In Vivo. *Neurotox Res* 2018 352. 2018;35(2):360-372. doi:10.1007/S12640-018-9961-8
223. Cross DT, Tirschwell DL, Clark MA, Tuden D, Derdeyn CP, Moran CJ, Dacey RG. Mortality rates after subarachnoid hemorrhage: variations according to hospital case volume in 18 states. *J Neurosurg.* 2003;99(5):810-817. doi:10.3171/JNS.2003.99.5.0810
224. Gijn J van, Kerr RS, Rinkel CJ. Subarachnoid haemorrhage. *Lancet.* 2007;369(9558):306-318. doi:10.1016/S0140-6736(07)60153-6
225. Harmsen P, Tsipogianni A, Wilhelmsen L. Stroke incidence rates were unchanged, while fatality rates declined, during 1971-1987 in Göteborg, Sweden. *Stroke.* 1992;23(10):1410-1415. doi:10.1161/01.STR.23.10.1410
226. Stegmayr B, Eriksson M, Asplund K. Declining Mortality From Subarachnoid Hemorrhage. *Stroke.* 2004;35(9):2059-2063. doi:10.1161/01.STR.0000138451.07853.B6
227. Sehba FA, Bederson JB. Mechanisms of acute brain injury after subarachnoid hemorrhage. *Neurol Res.* 2013;28(4):381-398. doi:10.1179/016164106X114991
228. Johnston M V, Trescher WH, Ishida A, Nakajima W, Zipursky A. Neurobiology of Hypoxic-Ischemic Injury in the Developing Brain. *Pediatr Res.* 2001;49(6):735-741. doi:10.1203/00006450-200106000-00003
229. Hillered L, Vespa PM, Hovda DA. Translational Neurochemical Research in Acute Human Brain Injury: The Current Status and Potential Future for Cerebral Microdialysis. *J Neurotrauma.* 2005;22(1):3-41. doi:10.1089/NEU.2005.22.3
230. Huang CY, Wang LC, Wang HK, Pan CH, Cheng YY, Shan YS, Chio CC, Tsai KJ. Memantine Alleviates Brain Injury and Neurobehavioral Deficits after Experimental Subarachnoid Hemorrhage. *Mol Neurobiol.* 2014;51(3):1038-1052. doi:10.1007/S12035-014-8767-9
231. Schulz MK, Wang LP, Tange M, Bjerre P. Cerebral microdialysis monitoring: determination of normal and ischemic cerebral metabolisms in patients with aneurysmal subarachnoid hemorrhage. *J Neurosurg.* 2000;93(5):808-814. doi:10.3171/JNS.2000.93.5.0808

232. Park S, Yamaguchi M, Zhou C, Calvert JW, Tang J, Zhang JH. Neurovascular Protection Reduces Early Brain Injury After Subarachnoid Hemorrhage. *Stroke*. 2004;35(10):2412-2417. doi:10.1161/01.STR.0000141162.29864.E9
233. Sehba FA, Chereshevnev I, Maayani S, Friedrich V, Bederson JB. Nitric Oxide Synthase in Acute Alteration of Nitric Oxide Levels after Subarachnoid Hemorrhage. *Neurosurgery*. 2004;55(3):671-678. doi:10.1227/01.NEU.0000134557.82423.B2
234. Dawson V, Kizushi V, Huang P, Snyder S, Dawson T. Resistance to neurotoxicity in cortical cultures from neuronal nitric oxide synthase-deficient mice. *J Neurosci*. 1996;16(8):2487. doi:10.1523/JNEUROSCI.16-08-02479.1996
235. Bloudek LM, Stokes M, Buse DC, Wilcox TK, Lipton RB, Goadsby PJ, Varon SF, Blumenfeld AM, Katsarava Z, Pascual J, Lanteri-Minet M, Cortelli P, Martelletti P. Cost of healthcare for patients with migraine in five European countries: results from the International Burden of Migraine Study (IBMS). *J Headache Pain*. 2012;13(5):378. doi:10.1007/S10194-012-0460-7
236. Ferrari A, Spaccapelo L, Pinetti D, Tacchi R, Bertolini A. Effective prophylactic treatments of migraine lower plasma glutamate levels. *Cephalalgia*. 2009;29(4):423-429. doi:10.1111/J.1468-2982.2008.01749.X
237. Martínez F, Castillo J, Rodríguez JR, Leira R, Noya M. Neuroexcitatory Amino Acid Levels in Plasma and Cerebrospinal Fluid During Migraine Attacks: *Cephalalgia*. 2016;13(2):89-93. doi:10.1046/J.1468-2982.1993.1302089.X
238. Edvinsson L, Villalón CM, Maassenvandenbrink A. Basic mechanisms of migraine and its acute treatment. *Pharmacol Ther*. 2012;136(3):319-333. doi:10.1016/J.PHARMTHERA.2012.08.011
239. Hoffmann J, Charles A. Glutamate and Its Receptors as Therapeutic Targets for Migraine. *Neurotherapeutics*. 2018;15(2):370. doi:10.1007/S13311-018-0616-5
240. Goadsby PJ, Classey JD. Glutamatergic transmission in the trigeminal nucleus assessed with local blood flow. *Brain Res*. 2000;875(1-2):119-124. doi:10.1016/S0006-8993(00)02630-5
241. Ramadan NM. The link between glutamate and migraine. *CNS Spectr*. 2003;8(6):446-449. doi:10.1017/S1092852900018757
242. Kertész S, Kapus G, Gacsályi I, Lévy G. Deramciclane improves object recognition in rats: Potential role of NMDA receptors. *Pharmacol Biochem Behav*. 2010;94(4):570-574. doi:10.1016/J.PBB.2009.11.012

243. Wang M, Chazot PL, Ali S, Duckett SF, Obrenovitch TP. Effects of NMDA receptor antagonists with different subtype selectivities on retinal spreading depression. *Br J Pharmacol*. 2012;165(1):244. doi:10.1111/J.1476-5381.2011.01553.X
244. Pandit V, Seshadri S, Rao SN, Samarasinghe C, Kumar A, Valsalan R. A case of organophosphate poisoning presenting with seizure and unavailable history of parenteral suicide attempt. *J Emergencies, Trauma Shock*. 2011;4(1):134. doi:10.4103/0974-2700.76825
245. Santos MD, Pereira EFR, Aracava Y, Castro NG, Fawcett WP, Randall WR, Albuquerque EX. Low Concentrations of Pyridostigmine Prevent Soman-Induced Inhibition of GABAergic Transmission in the Central Nervous System: Involvement of Muscarinic Receptors. *J Pharmacol Exp Ther*. 2003;304(1):254-265. doi:10.1124/JPET.102.043109
246. Lallement G, Delamanche IS, Pernot-Marino I, Baubichon D, Denoyer M, Carpentier P, Blanchet G. Neuroprotective activity of glutamate receptor antagonists against soman-induced hippocampal damage: quantification with an  $\omega 3$  site ligand. *Brain Res*. 1993;618(2):227-237. doi:10.1016/0006-8993(93)91270-3
247. McDonough JH, McLeod CG, Nipwoda MT. Direct microinjection of soman or VX into the amygdala produces repetitive limbic convulsions and neuropathology. *Brain Res*. 1987;435(1-2):123-137. doi:10.1016/0006-8993(87)91593-9
248. Raveh L, Brandeis R, Gilat E, Cohen G, Alkalay D, Rabinovitz I, Sonogo H, Weissman BA. Anticholinergic and Antiglutamatergic Agents Protect against Soman-Induced Brain Damage and Cognitive Dysfunction. *Toxicol Sci*. 2003;75(1):108-116. doi:10.1093/TOXSCI/KFG166
249. Tattersall J. Seizure activity post organophosphate exposure. *Front Biosci (Landmark Ed)*. 2009;14(14):3711. doi:10.2741/3481
250. Lallement G, Denoyer M, Collet A, Pernot-Marino I, Baubichon D, Monmaur P, Blanchet G. Changes in hippocampal acetylcholine and glutamate extracellular levels during soman-induced seizures: Influence of septal cholinceptive cells. *Neurosci Lett*. 1992;139(1):104-107. doi:10.1016/0304-3940(92)90868-8
251. Capacio BR, Shih TM. Anticonvulsant Actions of Anticholinergic Drugs in Soman Poisoning. *Epilepsia*. 1991;32(5):604-615. doi:10.1111/J.1528-1157.1991.TB04699.X
252. Gilat E, Kadar T, Levy A, Rabinovitz I, Cohen G, Kapon Y, Sahar R, Brandeis R. Anticonvulsant treatment of sarin-induced seizures with nasal midazolam: An electrographic, behavioral, and histological study in freely moving rats. *Toxicol Appl Pharmacol*. 2005;209(1):74-85. doi:10.1016/J.TAAP.2005.03.007

253. Ruban A, Mohar B, Jona G, Teichberg VI. Blood glutamate scavenging as a novel neuroprotective treatment for paraoxon intoxication. *J Cereb Blood Flow Metab.* 2014;34(2):227. doi:10.1038/JCBFM.2013.186
254. Griesmaier E, Keller M. Glutamate receptors - prenatal insults, long-term consequences. *Pharmacol Biochem Behav.* 2012;100(4):835-840. doi:10.1016/J.PBB.2011.04.011
255. Zlotnik A, Tsesis S, Gruenbaum BF, Ohayon S, Gruenbaum SE, Boyko M, Sheiner E, Brotfain E, Shapira Y, Teichberg VI. Relationship between glutamate, GOT and GPT levels in maternal and fetal blood: A potential mechanism for fetal neuroprotection. *Early Hum Dev.* 2012;88(9):773-778. doi:10.1016/J.EARLHUMDEV.2012.05.001
256. Holopainen IE, Laurén HB. Glutamate signaling in the pathophysiology and therapy of prenatal insults. *Pharmacol Biochem Behav.* 2012;100(4):825-834. doi:10.1016/J.PBB.2011.03.016
257. Ruban A, Malina KCK, Cooper I, Graubardt N, Babakin L, Jona G, Teichberg VI. Combined Treatment of an Amyotrophic Lateral Sclerosis Rat Model with Recombinant GOT1 and Oxaloacetic Acid: A Novel Neuroprotective Treatment. *Neurodegener Dis.* 2015;15(4):233-242. doi:10.1159/000382034
258. Groot J de, Sontheimer H. Glutamate and the Biology of Gliomas. *Glia.* 2011;59(8):1189. doi:10.1002/GLIA.21113
259. Sontheimer H. Malignant gliomas: perverting glutamate and ion homeostasis for selective advantage. *Trends Neurosci.* 2003;26(10):543-549. doi:10.1016/J.TINS.2003.08.007
260. Sontheimer H. Ion Channels and Amino Acid Transporters Support the Growth and Invasion of Primary Brain Tumors. *Mol Neurobiol.* 2004;29(1):71. doi:10.1385/MN:29:1:61
261. Ye ZC, Sontheimer H. Glioma cells release excitotoxic concentrations of glutamate. *Cancer Res.* 1999;59(17):4383-4391.
262. Ye ZC, Rothstein JD, Sontheimer H. Compromised Glutamate Transport in Human Glioma Cells: Reduction-Mislocalization of Sodium-Dependent Glutamate Transporters and Enhanced Activity of Cystine-Glutamate Exchange. *J Neurosci.* 1999;19(24):10777. doi:10.1523/JNEUROSCI.19-24-10767.1999
263. Behrens PF, Langemann H, Strohschein R, Draeger J, Hennig J. Extracellular glutamate and other metabolites in and around RG2 rat glioma: an intracerebral microdialysis study. *J Neurooncol.* 2000;47(1):11-22. doi:10.1023/A:1006426917654
264. Rijpkema M, Schuurung J, Meulen Y van der, Graaf M van der, Bernsen

- H, Boerman R, Kogel A van der, Heerschap A. Characterization of oligodendrogliomas using short echo time 1H MR spectroscopic imaging. *NMR Biomed.* 2003;16(1):12-18. doi:10.1002/NBM.807
265. Roslin M, Henriksson R, Bergström P, Ungerstedt U, Bergenheim AT. Baseline levels of glucose metabolites, glutamate and glycerol in malignant glioma assessed by stereotactic microdialysis. *J Neurooncol.* 2003;61(2):151-160. doi:10.1023/A:1022106910017
266. Ruban A, Berkutzki T, Cooper I, Mohar B, Teichberg VI. Blood glutamate scavengers prolong the survival of rats and mice with brain-implanted gliomas. *Invest New Drugs.* 2012;30(6):2235. doi:10.1007/S10637-012-9794-X
267. Kobayashi R, Tohda C. Extracellular Cytosolic Aspartate Aminotransferase Promotes Axonal Growth and Object Recognition Memory. *Neurochem Res.* 2017;42(12):3465-3473. doi:10.1007/s11064-017-2394-6
268. Zhang D, Qi Y, Klyubin I, Ondrejcek T, Sarell CJ, Cuellar AC, Collinge J, Rowan MJ. Targeting glutamatergic and cellular prion protein mechanisms of amyloid  $\beta$ -mediated persistent synaptic plasticity disruption: Longitudinal studies. *Neuropharmacology.* 2017;121:231-246. doi:10.1016/j.neuropharm.2017.03.036
269. Zhang D, Mably AJ, Walsh DM, Rowan MJ. Peripheral Interventions Enhancing Brain Glutamate Homeostasis Relieve Amyloid  $\beta$ - and TNF $\alpha$ -Mediated Synaptic Plasticity Disruption in the Rat Hippocampus. *Cereb Cortex.* 2017;27(7):3724-3735. doi:10.1093/CERCOR/BHW193
270. Cheng SY, Zhao YD, Li J, Chen XY, Wang RD, Zeng JW. Plasma levels of glutamate during stroke is associated with development of post-stroke depression. *Psychoneuroendocrinology.* 2014;47(183):126-135. doi:10.1016/j.psycheneu.2014.05.006
271. Gruenbaum BF, Kutz R, Zlotnik A, Boyko M. Blood glutamate scavenging as a novel glutamate-based therapeutic approach for post-stroke depression. *Ther Adv Psychopharmacol.* 2020;10. doi:10.1177/2045125320903951
272. Levite M. Glutamate, T cells and multiple sclerosis. *J Neural Transm.* 2017;124(7):775-798. doi:10.1007/s00702-016-1661-z
273. Dopico-López A, Pérez-Mato M, da Silva-Candal A, Iglesias-Rey R, Rabinov A, Bugallo-Casal A, Sobrino T, Mirelman D, Castillo J, Campos F. Inhibition of endogenous blood glutamate oxaloacetate transaminase enhances the ischemic damage. *Transl Res.* 2021;230:68-81. doi:10.1016/j.trsl.2020.10.004
274. Zlotnik A, Gurevich B, Tkachov S, Maoz I, Shapira Y, Teichberg VI. Brain

- neuroprotection by scavenging blood glutamate. *Exp Neurol.* 2007;203(1):213-220. doi:10.1016/j.expneurol.2006.08.021
275. Fernández-Susavila H, Iglesias-Rey R, Dopico-López A, Pérez-Mato M, Sobrino T, Castillo J, Campos F. Inclusion criteria update for the rat intraluminal ischaemic model for preclinical studies. *Dis Model Mech.* 2017;10(12):1433-1438. doi:10.1242/dmm.029868
276. Stroke Therapy Academic Industry Roundtable (STAIR). Recommendations for standards regarding preclinical neuroprotective and restorative drug development. *Stroke.* 1999;30(12):2752-2758. doi:10.1161/01.STR.30.12.2752
277. Philip M, Benatar M, Fisher M, Savitz SI. Methodological Quality of Animal Studies of Neuroprotective Agents Currently in Phase II/III Acute Ischemic Stroke Trials. *Stroke.* 2009;40(2):577-581. doi:10.1161/STROKEAHA.108.524330
278. Reith W, Hasegawa Y, Latour LL, Dardzinski BJ, Sotak CH, Fisher M. Multislice diffusion mapping for 3-D evolution of cerebral ischemia in a rat stroke model. *Neurology.* 1995;45(1):172-177. doi:10.1212/WNL.45.1.172
279. Higuchi T, Graham SH, Fernandez EJ, Rooney WD, Gaspary HL, Weiner MW, Maudsley AA. Effects of Severe Global Ischemia on N-Acetylaspartate and other Metabolites in the Rat Brain. *Magn Reson Med.* 1997;37(6):851. Accessed July 7, 2021. /pmc/articles/PMC2744638/
280. Tkáč I, Starčuk Z, Choi IY, Gruetter R. In Vivo 1 H NMR Spectroscopy of Rat Brain at 1 ms Echo Time. *Magn Reson Med.* 1999;41:649-656. doi:10.1002/(SICI)1522-2594(199904)41:4
281. Jokinen V, Lilius TO, Laitila J, Niemi M, Rauhala PV, Kalso EA. Pregabalin enhances the antinociceptive effect of oxycodone and morphine in thermal models of nociception in the rat without any pharmacokinetic interactions. *Eur J Pain.* 2016;20(2):297-306. doi:10.1002/EJP.728
282. Reglodi D, Tamás A, Lengvári I. Examination of sensorimotor performance following middle cerebral artery occlusion in rats. *Brain Res Bull.* 2003;59(6):459-466. doi:10.1016/S0361-9230(02)00962-0
283. Schallert T, Fleming SM, Leasure JL, Tillerson JL, Bland ST. CNS plasticity and assessment of forelimb sensorimotor outcome in unilateral rat models of stroke, cortical ablation, parkinsonism and spinal cord injury. *Neuropharmacology.* 2000;39(5):777-787. doi:10.1016/S0028-3908(00)00005-8
284. White JA, Hart RJ, Fry JC. An evaluation of the Waters Pico-Tag system for the amino-acid analysis of food materials. *J Automat Chem.*

- 1986;8(4):170. doi:10.1155/S1463924686000330
285. Pegg CC, He C, Stroink AR, Kattner KA, Wang CX. Technique for collection of cerebrospinal fluid from the cisterna magna in rat. *J Neurosci Methods*. 2010;187(1):8-12. doi:10.1016/J.JNEUMETH.2009.12.002
286. Fernández-Susavila H, Rodríguez-Yáñez M, Dopico-López A, Arias S, Santamaría M, Ávila-Gómez P, Doval-García JM, Sobrino T, Iglesias-Rey R, Castillo J, Campos F. Heads and tails of natriuretic peptides: Neuroprotective role of brain natriuretic peptide. *J Am Heart Assoc*. 2017;6(12). doi:10.1161/JAHA.117.007329
287. Zaghmi A, Dopico-López A, Pérez-Mato M, Iglesias-Rey R, Hervella P, Greschner AA, Bugallo-Casal A, da Silva A, Gutiérrez-Fernández M, Castillo J, Pérez FC, Gauthier MA. Sustained blood glutamate scavenging enhances protection in ischemic stroke. *Commun Biol*. 2020;3(1). doi:10.1038/s42003-020-01406-1
288. Zaghmi A, Greschner AA, Mendez-Villuendas E, Liu JY, Haan HW de, Gauthier MA. Determination of the degree of PEGylation of protein bioconjugates using data from proton nuclear magnetic resonance spectroscopy. *Data Br*. 2019;25. doi:10.1016/J.DIB.2019.104037
289. Orset C, Macrez R, Young AR, Panthou D, Angles-Cano E, Maubert E, Agin V, Vivien D. Mouse Model of In Situ Thromboembolic Stroke and Reperfusion. *Stroke*. 2007;38(10):2771-2778. doi:10.1161/STROKEAHA.107.487520
290. Overgaard K, Sereghy T, Boysen G, Pedersen H, Høyer S, Diemer NH. A Rat Model of Reproducible Cerebral Infarction Using Thrombotic Blood Clot Emboli: <http://dx.doi.org/101038/jcbfm199266>. 1992;12:484-490. doi:10.1038/JCBFM.1992.66
291. Niessen F, Hilger T, Hoehn M, Hossmann KA. Differences in Clot Preparation Determine Outcome of Recombinant Tissue Plasminogen Activator Treatment in Experimental Thromboembolic Stroke. *Stroke*. 2003;34(8):2019-2024. doi:10.1161/01.STR.0000080941.73934.30
292. Boyko M, Stepensky D, Gruenbaum BF, Gruenbaum SE, Melamed I, Ohayon S, Glazer M, Shapira Y, Zlotnik A. Pharmacokinetics of glutamate-oxaloacetate transaminase and glutamate-pyruvate transaminase and their blood glutamate-lowering activity in naïve rats. *Neurochem Res*. 2012;37(10):2198-2205. doi:10.1007/s11064-012-0843-9
293. Woo CW, Lee BS, Kim ST, Kim KS. Correlation between lactate and neuronal cell damage in the rat brain after focal ischemia: An in vivo 1H magnetic resonance spectroscopic (1H-MRS) study: *Acta radiol*. 2010;51(3):344-350. doi:10.3109/02841850903515395

294. Brouns R, Sheorajpanday R, Wauters A, De Surgeloose D, Mariën P, De Deyn PP. Evaluation of lactate as a marker of metabolic stress and cause of secondary damage in acute ischemic stroke or TIA. *Clin Chim Acta*. 2008;397(1-2):27-31. doi:10.1016/J.CCA.2008.07.016
295. Oller-Salvia B, Sánchez-Navarro M, Giralt E, Teixidó M. Blood-brain barrier shuttle peptides: an emerging paradigm for brain delivery. *Chem Soc Rev*. 2016;45(17):4690-4707. doi:10.1039/C6CS00076B
296. Bertrand Y, Currie JC, Demeule M, Régina A, Ché C, Abulrob A, Fatehi D, Sartelet H, Gabathuler R, Castaigne JP, Stanimirovic D, Béliveau R. Transport characteristics of a novel peptide platform for CNS therapeutics. *J Cell Mol Med*. 2010;14(12):2839. doi:10.1111/J.1582-4934.2009.00930.X
297. Lane M, Gardner DK. Mitochondrial malate-aspartate shuttle regulates mouse embryo nutrient consumption. *J Biol Chem*. 2005;280(18):18361-18367. doi:10.1074/JBC.M500174200
298. Nishizono H, Hayano Y, Nakahata Y, Ishigaki Y, Yasuda R. Rapid generation of conditional knockout mice using the CRISPR-Cas9 system and electroporation for neuroscience research. *Mol Brain*. 2021;14(1):148. doi:10.1186/S13041-021-00859-7
299. Williams RW, Flaherty L, Threadgill DW. The math of making mutant mice. *Genes, Brain Behav*. 2003;2(4):191-200. doi:10.1034/J.1601-183X.2003.00017.X/FORMAT/PDF
300. Campos F, Sobrino T, Ramos-Cabrer P, Castellanos M, Blanco M, Rodríguez-Yáez M, Serena J, Leira R, Castillo J. High blood glutamate oxaloacetate transaminase levels are associated with good functional outcome in acute ischemic stroke. *J Cereb Blood Flow Metab*. 2011;31(6):1393. doi:10.1038/JCBFM.2011.4
301. Boyko M, Stepensky D, Gruenbaum BF, Gruenbaum SE, Melamed I, Ohayon S, Glazer M, Shapira Y, Zlotnik A. Pharmacokinetics of Glutamate-Oxaloacetate Transaminase and Glutamate-Pyruvate Transaminase and Their Blood Glutamate-Lowering Activity in Naïve Rats. *Neurochem Res*. 2012;37(10):2198-2205. doi:10.1007/S11064-012-0843-9
302. Pérez-Mato M, Iglesias-Rey R, Vieites-Prado A, Dopico-López A, Argibay B, Fernández-Susavila H, da Silva-Candal A, Pérez-Díaz A, Correa-Paz C, Günther A, Ávila-Gómez P, Isabel Loza M, Baumann A, Castillo J, Sobrino T, Campos F. Blood glutamate EAAT2-cell grabbing therapy in cerebral ischemia. *EBioMedicine*. 2019;39:118-131. doi:10.1016/j.ebiom.2018.11.024
303. Zhou X, Curbo S, Li F, Krishnan S, Karlsson A. Inhibition of glutamate oxaloacetate transaminase 1 in cancer cell lines results in altered

- metabolism with increased dependency of glucose. *BMC Cancer*. 2018;18(1). doi:10.1186/s12885-018-4443-1
304. Yoshida T, Yamasaki S, Kaneko O, Taoka N, Tomimoto Y, Namatame I, Yahata T, Kuromitsu S, Cantley LC, Lyssiotis CA. A covalent small molecule inhibitor of glutamate-oxaloacetate transaminase 1 impairs pancreatic cancer growth. *Biochem Biophys Res Commun*. 2020;522(3):638. doi:10.1016/j.bbrc.2019.11.130
305. Reiber H. Proteins in cerebrospinal fluid and blood: barriers, CSF flow rate and source-related dynamics. *Restor Neurol Neurosci*. 2003;21(3-4):79-96. doi:10.1016/0022-510X(94)90298-4
306. Pardridge WM. CSF, blood-brain barrier, and brain drug delivery. *Expert Opin Drug Deliv*. 2016;13(7):963-975. doi:10.1517/17425247.2016.1171315
307. Keaney J, Campbell M. The dynamic blood-brain barrier. *FEBS J*. 2015;282(21):4067-4079. doi:10.1111/febs.13412
308. Jiang X, Andjelkovic A V., Zhu L, Yang T, Bennett MVL, Chen J, Keep RF, Shi Y. Blood-brain barrier dysfunction and recovery after ischemic stroke. *Prog Neurobiol*. 2018;163-164:171. doi:10.1016/j.pneurobio.2017.10.001
309. Knowland D, Arac A, Sekiguchi KJ, Hsu M, Lutz SE, Perrino J, Steinberg GK, Barres BA, Nimmerjahn A, Agalliu D. Stepwise Recruitment of Transcellular and Paracellular Pathways Underlies Blood-Brain Barrier Breakdown in Stroke. *Neuron*. 2014;82(3):617. doi:10.1016/j.neuron.2014.03.003
310. Jentsch S, Pyrowolakis G. Ubiquitin and its kin: how close are the family ties? *Trends Cell Biol*. 2000;10(8):335-342. doi:10.1016/S0962-8924(00)01785-2
311. Yadav DK, Yadav N, Yadav S, Haque S, Tuteja N. *An Insight into Fusion Technology Aiding Efficient Recombinant Protein Production for Functional Proteomics*. Vol 612. Elsevier Ltd; 2016. doi:10.1016/j.abb.2016.10.012
312. Peroutka RJ, Orcutt SJ, Strickler JE, Butt TR. SUMO fusion technology for enhanced protein expression and purification in prokaryotes and eukaryotes. *Methods Mol Biol*. 2011;705:15-30. doi:10.1007/978-1-61737-967-3\_2
313. Cynober L. Metabolism of Dietary Glutamate in Adults. *Ann Nutr Metab*. 2018;73 Suppl 5(Suppl 5):5-14. doi:10.1159/000494776
314. Johnson AW, Berrington JM, Walker I, Manning A, Losowsky MS. Measurement of the transfer of the nitrogen moiety of intestinal lumen

- glutamic acid in man after oral ingestion of l-[15N]glutamic acid. *Clin Sci*. 1988;75(5):499-502. doi:10.1042/CS0750499
315. Hinoi E, Takarada T, Ueshima T, Tsuchihashi Y, Yoneda Y. Glutamate signaling in peripheral tissues. *Eur J Biochem*. 2004;271(1):1-13. doi:10.1046/J.1432-1033.2003.03907.X
316. Nemkov T, Sun K, Reisz JA, Yoshida T, Dunham A, Wen EY, Wen AQ, Roach RC, Hansen KC, Xia Y, D'Alessandro A. Metabolism of Citrate and Other Carboxylic Acids in Erythrocytes As a Function of Oxygen Saturation and Refrigerated Storage. *Front Med*. 2017;4:175. doi:10.3389/FMED.2017.00175
317. Ferenc-Mrozek A, Bojarska E, Stepinski J, Darzynkiewicz E, Lukaszewicz M. Effect of the His-Tag Location on Decapping Scavenger Enzymes and Their Hydrolytic Activity toward Cap Analogs. *ACS Omega*. 2020;5(19):10759-10766. doi:10.1021/ACSOMEGA.0C00304
318. Mason AB, He QY, Halbrooks PJ, Everse SJ, Gumerov DR, Kaltashov IA, Smith VC, Hewitt J, MacGillivray RTA. Differential effect of a his tag at the N- and C-termini: functional studies with recombinant human serum transferrin. *Biochemistry*. 2002;41(30):9448-9454. doi:10.1021/B1025927L
319. Parshin PD, Pometun AA, Martysuk UA, Kleymentov SY, Atroshenko DL, Pometun E V., Savin SS, Tishkov VI. Effect of His 6-tag Position on the Expression and Properties of Phenylacetone Monooxygenase from *Thermobifida fusca*. *Biochemistry (Mosc)*. 2020;85(5):575-582. doi:10.1134/S0006297920050065
320. Hunter AJ, Hatcher J, Virley D, Nelson P, Irving E, Hadingham SJ, Parsons AA. Functional assessments in mice and rats after focal stroke. *Neuropharmacology*. 2000;39(5):806-816. doi:10.1016/S0028-3908(99)00262-2
321. Bouët V, Freret T, Toutain J, Divoux D, Boulouard M, Schumann-Bard P. Sensorimotor and cognitive deficits after transient middle cerebral artery occlusion in the mouse. *Exp Neurol*. 2007;203(2):555-567. doi:10.1016/J.EXPNEUROL.2006.09.006
322. Zhang L, Chen J, Li Y, Zhang ZG, Chopp M. Quantitative measurement of motor and somatosensory impairments after mild (30 min) and severe (2 h) transient middle cerebral artery occlusion in rats. *J Neurol Sci*. 2000;174(2):141-146. doi:10.1016/S0022-510X(00)00268-9
323. Hattori K, Lee H, Hurn PD, Crain BJ, Traystman RJ, DeVries AC. Cognitive Deficits After Focal Cerebral Ischemia in Mice. *Stroke*. 2000;31(8):1939-1944. doi:10.1161/01.STR.31.8.1939
324. Olszewski K, Barsotti A, Feng XJ, Momcilovic M, Liu KG, Kim JI, Morris

- K, Lamarque C, Gaffney J, Yu X, Patel JP, Rabinowitz JD, Shackelford DB, Poyurovsky M V. Inhibition of glucose transport synergizes with chemical or genetic disruption of mitochondrial metabolism and suppresses TCA cycle-deficient tumors. *Cell Chem Biol.* 2021;0(0). doi:10.1016/J.CHEMBIOL.2021.10.007
325. Kremer DM, Nelson BS, Lin L, Yarosz EL, Halbrook CJ, Kerk SA, et al. GOT1 inhibition promotes pancreatic cancer cell death by ferroptosis. *Nat Commun.* 2021;12(1). doi:10.1038/S41467-021-24859-2
326. Rapoport SI. *Passage of Proteins from Blood to Cerebrospinal Fluid.* Springer, Boston, MA; 1983. doi:10.1007/978-1-4615-9269-3\_16
327. Iliff JJ, Wang M, Liao Y, Plogg BA, Peng W, Gundersen GA, Benveniste H, Vates GE, Deane R, Goldman SA, Nagelhus EA, Nedergaard M. A paravascular pathway facilitates CSF flow through the brain parenchyma and the clearance of interstitial solutes, including amyloid  $\beta$ . *Sci Transl Med.* 2012;4(147). doi:10.1126/SCITRANSLMED.3003748
328. Mestre H, Hablitz LM, Xavier ALR, Feng W, Zou W, Pu T, et al. Aquaporin-4-dependent glymphatic solute transport in the rodent brain. *Elife.* 2018;7. doi:10.7554/ELIFE.40070
329. Kamimoto Y, Horiuchi S, Tanase S, Morino Y. Plasma clearance of intravenously injected aspartate aminotransferase isozymes: evidence for preferential uptake by sinusoidal liver cells. *Hepatology.* 1985;5(3):367-375. doi:10.1002/HEP.1840050305
330. Klin Y, Zlotnik A, Boyko M, Ohayon S, Shapira Y, Teichberg VI. Distribution of radiolabeled L-glutamate and D-aspartate from blood into peripheral tissues in naive rats: Significance for brain neuroprotection. *Biochem Biophys Res Commun.* 2010;399(4):694-698. doi:10.1016/J.BBRC.2010.07.144
331. Lipton SA. Pathologically activated therapeutics for neuroprotection. *Nat Rev Neurosci.* 2007;8(10):803-808. doi:10.1038/NRN2229
332. Nakajima M, Nito C, Sowa K, Suda S, Nishiyama Y, Nakamura-Takahashi A, Nitahara-Kasahara Y, Imagawa K, Hirato T, Ueda M, Kimura K, Okada T. Mesenchymal Stem Cells Overexpressing Interleukin-10 Promote Neuroprotection in Experimental Acute Ischemic Stroke. *Mol Ther Methods Clin Dev.* 2017;6:111. doi:10.1016/J.OMTM.2017.06.005
333. Milani D, Cross JL, Anderton RS, Blacker DJ, Knuckey NW, Meloni BP. Neuroprotective efficacy of poly-arginine R18 and NA-1 (TAT-NR2B9c) peptides following transient middle cerebral artery occlusion in the rat. *Neurosci Res.* 2017;114:9-15. doi:10.1016/J.NEURES.2016.09.002
334. Milani D, Knuckey NW, Anderton RS, Cross JL, Meloni BP. The R18 Polyarginine Peptide Is More Effective Than the TAT-NR2B9c (NA-1)

- Peptide When Administered 60 Minutes after Permanent Middle Cerebral Artery Occlusion in the Rat. *Stroke Res Treat.* 2016;2016. doi:10.1155/2016/2372710
335. Goldshmit Y, Jona G, Schmukler E, Solomon S, Pinkas-Kramarski R, Ruban A. Blood Glutamate Scavenger as a Novel Neuroprotective Treatment in Spinal Cord Injury. *J Neurotrauma.* 2018;35(21):2581-2590. doi:10.1089/NEU.2017.5524
336. Ugalde-Triviño L, Díaz-Guerra M. PSD-95: An Effective Target for Stroke Therapy Using Neuroprotective Peptides. *Int J Mol Sci.* 2021;22(22):12585. doi:10.3390/IJMS222212585
337. Hill MD, Goyal M, Menon BK, Nogueira RG, McTaggart RA, Demchuk AM, et al. Efficacy and safety of nerinetide for the treatment of acute ischaemic stroke (ESCAPE-NA1): a multicentre, double-blind, randomised controlled trial. *Lancet.* 2020;395(10227):878-887. doi:10.1016/S0140-6736(20)30258-0
338. Nunez DM, Ji Z, Sun X, Teves L, Garman JD, Tymianski M. Plasmin-resistant PSD-95 inhibitors resolve effect-modifying drug-drug interactions between alteplase and nerinetide in acute stroke. *Sci Transl Med.* 2021;13(588). doi:10.1126/SCITRANSLMED.ABB1498
339. da Silva-Candal A, Vieites-Prado A, Gutiérrez-Fernández M, Rey RI, Argibay B, Mirelman D, Sobrino T, Rodríguez-Frutos B, Castillo J, Campos F. Blood glutamate grabbing does not reduce the hematoma in an intracerebral hemorrhage model but it is a safe excitotoxic treatment modality. *J Cereb Blood Flow Metab.* 2015;35(7):1212. doi:10.1038/JCBFM.2015.28

# ANNEXES





## RESOLUCIÓN DE AUTORIZACIÓN DE PROXECTOS DE EXPERIMENTACIÓN ANIMAL

**Expediente núm.:** 15010/2019/004      **Data de inicio:** 05.02.2019  
**Persoa interesada:** Francisco Campos Pérez      **Procedemento:** resolución de autorización  
**Forma de inicio:** solicitude da persoa interesada

### ANTECEDENTES

A persoa interesada, como representante do centro CIMUS (Universidade de Santiago de Compostela), presentou con data 05.02.2019 unha solicitude para a realización do proxecto de experimentación animal (entrada no Rexistro Electrónico da Xunta de Galicia 2019/246024), cuxos datos se detallan a continuación:

**Denominación do proxecto:** *Nanopartículas biomiméticas para a administración dirixida de nanomedicinas*

**Nome do centro usuario:** Animalario do CIMUS

**Persoa responsable do proxecto:** Francisco Campos Pérez

**Establecemento onde se realizarán os procedementos do proxecto (ou lugar xeográfico no caso de traballos de campo):** Animalario do CIMUS

**Clasificación do proxecto :** Tipo I     Tipo II     Tipo III

### CONSIDERACIÓNS LEGAIS E TÉCNICAS

1 O Real decreto 53/2013, de 1 de febreiro (BOE 34, do 8 de febreiro), polo que se establecen as normas básicas aplicables para a protección dos animais utilizados en experimentación e outros fins científicos, incluíndo a docencia, establece no seu artigo 33 as condicións de autorizacións dos proxectos con animais de experimentación.

2 O artigo 88 da Lei 39/2015, de 1 de outubro, do procedemento administrativo común das administracións públicas (BOE 236, do 2 de outubro de 2015) establece que a resolución que poña fin o procedemento decidirá todas as cuestións expostas polos interesados e aquelas outras derivadas deste.

3 O Servizo de Gandaría da Coruña revisou a documentación achegada na solicitude e o resultado favorable da avaliación do proxecto, realizada polo órgano habilitado da Sección de Experimentación Animal do Comité de Bioética da Universidade de Santiago de Compostela.

Esta xefatura territorial é competente para ditar unha resolución, de conformidade co Decreto 149/2018, do 5 de decembro, polo que se establece a estrutura orgánica da



Consellería do Medio Rural e se modifica parcialmente o Decreto 177/2016, do 15 de decembro, polo que se fixa a estrutura orgánica da Vicepresidencia e das consellerías da Xunta de Galicia (DOG 235, do 11 de novembro).

De acordo con todo o indicado, RESOLVO:

- 1 Autorizar o proxecto solicitado.
- 2 O mencionado proxecto precisa someterse a unha avaliación retrospectiva tras finalizar a súa autorización.
- 3 A autorización deste proxecto terá unha duración de dous anos e unha vez transcorrido este tempo deberá ser autorizado de novo.

A citada autorización é unicamente válida nas condicións que figuran no expediente. Ante calquera cambio significativo no proxecto que poida ter efectos negativos sobre o benestar dos animais, deberá solicitar a confirmación da autorización ao Servizo Provincial de Gandería.

Esta autorización poderá ser suspendida, no caso de que o proxecto non se leve a cabo de acordo coas condicións de autorización e retirada, previo expediente tramitado ao que se lle dará audiencia.

Contra a presente resolución, que non lle pon fin á vía administrativa, poderá interpoñer un recurso de alzada ante o conselleiro de Medio Rural. O prazo comezará a contar dende o día seguinte ao da recepción desta resolución. Todo isto, segundo o disposto nos artigos 121 e 122 da citada Lei 39/2015.

Mediante este escrito notifícasele ao CIMUS da USC esta resolución segundo o esixido no artigo 40.1 da antedita Lei 39/2015.

JOSÉ MANUEL CIFUENTES MARTÍNEZ, PRESIDENTE DEL COMITÉ DE BIOÉTICA DE LA UNIVERSIDAD DE SANTIAGO DE COMPOSTELA, cuya Sección de Experimentación animal ha sido designada como Órgano Habilitado para la evaluación de proyectos de experimentación animal por resolución de la Xunta de Galicia, con fecha 11 de noviembre de 2013, de acuerdo con lo exigido por el RD 53/2013 de 1 de febrero, por el que se establecen las normas básicas aplicables para la protección de los animales utilizados en experimentación y otros fines científicos, incluyendo la docencia,

#### INFORMA:

Que el proyecto de investigación titulado: “Nanopartículas biomiméticas para la administración dirigida de nanomedicinas” del que es investigador responsable D. Francisco Campos Pérez, ha sido examinado por el Comité de Bioética de esta Universidad, Sección de Experimentación Animal, llegando a las siguientes conclusiones:

Con respecto a su finalidad, se trata de un proyecto de investigación traslacional o aplicada cuyo objetivo fundamental es el desarrollo de nanosistemas biomiméticos basados en cubiertas celulares (extraídas de células madre mesenquimales y/o plaquetas) para dirigir nanomedicinas a su lugar de acción (diana).

- Con respecto a los requisitos de las 3Rs,
  - No cabe la posibilidad de reemplazo ya que no se han encontrado otros métodos o estrategias de ensayo que permitan llevar a cabo los experimentos propuestos en este trabajo.
  - La experimentación se realizará en un centro registrado como usuario de animales de experimentación por lo que la manipulación, manejo y supervisión de los animales durante todo el proyecto será llevada a cabo por personas capacitadas. El grupo investigador lo componen personas con capacitaciones A, B y C, lo que asegura su preparación para garantizar el bienestar animales durante todos los procedimientos (requisito de refinamiento).
  - Finalmente, con respecto al requisito de reducción, se considera que el número de animales a utilizar es el mínimo imprescindible para la obtención de los resultados.
- La clasificación de los procedimientos en función de su grado de severidad es de “leve para los procedimientos 1, 3 y “severo” para los procedimientos 2 y 4.
- Con respecto al balance de los daños y los beneficios, los procedimientos se efectúan bajo analgesia y anestesia previa a la administración de sustancias e intervenciones quirúrgicas por lo que se minimiza el dolor, angustia y sufrimiento. Los métodos de sacrificio descritos (sobredosis de anestesia) se encuentran entre los indicados por el propio RD 53/2013.
- Se han examinado las situaciones y excepciones previstas en el punto e) del artículo 34. 2 encontrando que ninguna de ellas es aplicable en este proyecto.
- El proyecto se clasifica como tipo III y por tanto debe ser sometido a evaluación retrospectiva. Este Comité considera que dicha evaluación debería efectuarse a los dos años de la concesión de la autorización.

Por todas estas razones, este Comité acordó emitir un INFORME FAVORABLE.

En la evaluación de este proyecto NO HA EXISTIDO CONFLICTO DE INTERESES.

Lugo, 17 de abril de 2018



MÓDULOS FUNDAMENTAIS OU TRONCAIS E ESPECÍFICOS CORRESPONDENTES Á CATEGORÍA "A"  
COIDADADO DOS ANIMAIS – ORDE ECC/566/2015, DE 20 DE MARZO

MÓDULOS FUNDAMENTAIS OU TRONCAIS

- 1.- Lexislación nacional (1 hora).
- 2.- Ética, benestar animal e as "tres erres", nivel 1 (2 horas).
- 3.- Bioloxía básica e adecuada, nivel 1 (3 horas).
- 4.- Coidado, saúde e manexo dos animais, nivel 1 (5 horas).
- 5.- Recoñecemento do dolor, o sufrimento e a angustia ( 3 horas).
- 6.- Métodos incruentos de sacrificio, nivel 1 (2 horas)

MÓDULOS ESPECÍFICOS DA CATEGORÍA "A"

- 1.-Bioloxía básica e adecuada, nivel 2 (3 horas)
- 

MÓDULOS FUNDAMENTALES O TRONCALES

- 1.- Legislación nacional (1 hora).
- 2.- Ética, bienestar animal y las "tres erres", nivel 1 (2 horas).
- 3.- Biología básica y adecuada, nivel 1 (3 horas).
- 4.- Cuidado, salud y manejo de los animales, nivel 1 (5 horas).
- 5.- Reconocimiento del dolor, el sufrimiento y la angustia ( 3 horas).
- 6.- Métodos incruentos de sacrificio, nivel 1 (2 horas)

MÓDULOS ESPECÍFICOS DE LA CATEGORÍA "A"

- 1.-Biología básica y adecuada, nivel 2 (3 horas)

**Certificado de capacitación en materia de protección de animais utilizados, criados ou suministrados con fins de experimentación e outros fins científicos, incluíndo a docencia conforme coa Orde ECC/566/2015 de 20 de marzo.**

*Certificado de capacitación en materia de protección de animales utilizados, criados o suministrados con fines de experimentación y otros fines científicos, incluyendo la docencia conforme con la Orden ECC/566/2015 de 20 de marzo.*

<b>1. IDENTIFICACIÓN</b>		
1.1. Apelidos / <i>Apellidos / Surnames</i> : <b>DOPICO LÓPEZ</b>		
1.2. Nome / <i>Nombre / First names</i> : <b>ANTONIO</b>		DNI / <i>IDNI / Identity card number</i> : <b>79336909L</b>
1.3. Categoría / <i>Categoría / Category</i> : <b>"a"</b>	1.4. Especies / <i>Especies / Species</i> : <b>ROEDORES</b>	1.5. Válido ata / <i>válido hasta/expire</i> : <b>1/07/2029</b>
<b>2. Nº DO CERTIFICADO / Nº DEL CERTIFICADO / CERTIFICATE NUMBER</b>		
<b>A310</b>		
<b>3. ORGANISMO QUE EXPIDE O CERTIFICADO / ORGANISMO QUE EXPIDE EL CERTIFICADO / BODY ISSUING THE CERTIFICATE:</b>		
3.1. Nome e enderezo do organismo que expide o certificado / <i>Nombre y dirección del organismo que expide el certificado / Name and address of the body issuing the certificate</i> :  <b>AXENCIA GALEGA DA CALIDADE ALIMENTARIA CONSELLERÍA DO MEDIO RURAL – XUNTA DE GALICIA Rúa do Camiño Francés, 10 baixo 15781 Santiago de Compostela A Coruña (España)</b>		
3.2. Teléfono / <i>Teléfono / telephone</i> : <b>981 546 657</b>	3.3. Fax / <i>Fax / Fax</i> : <b>981 546 651</b>	3.4. Correo electrónico / <i>Correo electrónico / Email</i> : <b>formacion.cmr@xunta.es</b>
3.5. Data / <i>Fecha / Date</i> :	3.6. Lugar / <i>Lugar / Place</i> : <b>Santiago de Compostela</b>	
3.7. Nome e sinatura / <i>Nombre y firma / Name and signature</i>  <b>Asdo.: Xiana María Perales Arroyo Xefa do Departamento de Formación (asinado dixitalmente)</b>		

## **MÓDULOS FUNDAMENTAIS OU TRONCAIS E ESPECÍFICOS CORRESPONDENTES Á CATEGORÍA "B" EUTANASIA DOS ANIMAIS – ORDE ECC/566/2015, DE 20 DE MARZO**

### **MÓDULOS FUNDAMENTAIS OU TRONCAIS**

- 1.- *Legislación nacional (1 hora).*
- 2.- *Ética, benestar animal e as "tres erres", nivel 1 (2 horas).*
- 3.- *Bioloxía básica e adecuada, nivel 1 (3 horas).*
- 4.- *Coidado, saúde e manexo dos animais, nivel 1 (5 horas).*
- 5.- *Recoñecemento do dolor, o sufrimento e a angustia (3 horas).*
- 6.- *Métodos incruentos de sacrificio, nivel 1 (2 horas)*

### **MÓDULOS ESPECÍFICOS DA CATEGORÍA "B"**

- 1.- *Bioloxía básica e adecuada, nivel 2 (3 horas)*
- 2.- *Métodos incruentos de sacrificio, nivel 2 (3 horas)*

---

### **MÓDULOS FUNDAMENTALES O TRONCALES**

- 1.- *Legislación nacional (1 hora).*
- 2.- *Ética, bienestar animal y las "tres erres", nivel 1 (2 horas).*
- 3.- *Biología básica y adecuada, nivel 1 (3 horas).*
- 4.- *Cuidado, salud y manejo de los animales, nivel 1 (5 horas).*
- 5.- *Reconocimiento del dolor, el sufrimiento y la angustia (3 horas).*
- 6.- *Métodos incruentos de sacrificio, nivel 1 (2 horas)*

### **MÓDULOS ESPECÍFICOS DE LA CATEGORÍA "B"**

- 1.- *Biología básica y adecuada, nivel 2 (3 horas)*
- 2.- *Métodos incruentos de sacrificio, nivel 2 (3 horas)*

**Certificado de capacitación en materia de protección de animais utilizados, criados ou subministrados con fins de experimentación e outros fins científicos, incluíndo a docencia conforme coa Orde ECC/566/2015 de 20 de marzo.**

*Certificado de capacitación en materia de protección de animales utilizados, criados o suministrados con fines de experimentación y otros fines científicos, incluyendo la docencia conforme con la Orden ECC/566/2015 de 20 de marzo.*

<b>1. IDENTIFICACIÓN</b>		
1.1. Apellidos / Apellidos / Surname <b>DOPICO LÓPEZ</b>		
1.2. Nome / Nome / First names <b>ANTONIO</b>		DNI (DNI) / Identity card number <b>79336909L</b>
1.3. Categoría / Categoría / Category <b>"b"</b>	1.4. Especies / Especies / Species <b>ROEDORES</b>	1.5. Válido ata / Valid to / Validity <b>01/07/2029</b>
<b>2. Nº DO CERTIFICADO / Nº DEL CERTIFICADO / CERTIFICATE NUMBER</b> <b>B593</b>		
<b>3. ORGANISMO QUE EXPIDE O CERTIFICADO / ORGANISMO QUE EMITE EL CERTIFICADO / BODY ISSUING THE CERTIFICATE:</b>		
3.1. Nome e endereço do organismo que expide o certificado / Nombre y dirección del organismo que expide el certificado / Name and address of the body issuing the certificate: <b>CONSELLERÍA DO MEDIO RURAL – XUNTA DE GALICIA AXENCIA GALEGA DA CALIDADE ALIMENTARIA Avda. Do Camiño Francés, 10 baixo 15781 Santiago de Compostela A Coruña (España)</b>		
3.3. Teléfono / Teléfono / Telephone <b>981 546 857</b>	3.5. Fax / Fax / Fax <b>981 546 851</b>	3.4. Correo electrónico / Correo electrónico / Email <b>formacion.emmm@xunta.es</b>
3.5. Data / Data / Date	3.6. Lugar / Lugar / Place <b>Santiago de Compostela</b>	
3.7. Nome e sinatura / Nombre y firma / Name and signature  <b>Asdo.: Xiana María Perales Arroyo Xefa do Departamento de Formación (asinado dixitalmente)</b>		

## **MÓDULOS FUNDAMENTAIS OU TRONCAIS E ESPECÍFICOS CORRESPONDENTES Á CATEGORÍA "C" REALIZACIÓN DOS PROCEDIMENTOS – ORDE ECC/566/2015, DE 20 DE MARZO**

### **MÓDULOS FUNDAMENTAIS OU TRONCAIS**

- 1.- *Legislación nacional (1 hora).*
- 2.- *Ética, benestar animal e as "tres erres", nivel 1 (2 horas).*
- 3.- *Bioloxía básica e adecuada, nivel 1 (3 horas).*
- 4.- *Cuidado, saúde e manexo dos animais, nivel 1 (5 horas).*
- 5.- *Recoñecemento do dolor, o sufrimento e a angustia (3 horas).*
- 6.- *Métodos incruentos de sacrificio, nivel 1 (2 horas)*

### **MÓDULOS ESPECÍFICOS DA CATEGORÍA "C"**

- 1.- *Biología básica e adecuada, nivel 2 (3 horas)*
- 2.- *Procedementos minimamente invasores sen anestesia, nivel 1 (5 horas)*
- 3.- *Procedementos minimamente invasores sen anestesia, nivel 2 (10 horas)*
- 4.- *Anestesia para procedementos menores (5 horas)*
- 5.- *Anestesia avanzada para intervencións cirúrxicas ou procedementos prolongados (8 horas)*
- 6.- *Principios de cirurxía (5 horas)*

---

### **MÓDULOS FUNDAMENTALES O TRONCALES**

- 1.- *Legislación nacional (1 hora).*
- 2.- *Ética, bienestar animal y las "tres erres", nivel 1 (2 horas).*
- 3.- *Biología básica y adecuada, nivel 1 (3 horas).*
- 4.- *Cuidado, salud y manejo de los animales, nivel 1 (5 horas).*
- 5.- *Reconocimiento del dolor, el sufrimiento y la angustia (3 horas).*
- 6.- *Métodos incruentos de sacrificio, nivel 1 (2 horas)*

### **MÓDULOS ESPECÍFICOS DE LA CATEGORÍA "C"**

- 1.- *Biología básica y adecuada, nivel 2 (3 horas)*
- 2.- *Procedimientos mínimamente invasivos sin anestesia, nivel 1 (5 horas)*
- 3.- *Procedimientos mínimamente invasivos sin anestesia, nivel 2 (10 horas)*
- 4.- *Anestesia para procedimientos menores (5 horas)*
- 5.- *Anestesia avanzada para intervenciones quirúrgicas o procedimientos prolongados (8 horas)*
- 6.- *Principios de cirugía (5 horas)*

**Certificado de capacitación en materia de protección de animais utilizados, criados ou subministrados con fins de experimentación e outros fins científicos, incluíndo a docencia conforme coa Orde ECC/566/2015 de 20 de marzo.**

*Certificado de capacitación en materia de protección de animales utilizados, criados o suministrados con fines de experimentación y otros fines científicos, incluyendo la docencia conforme con la Orden ECC/566/2015 de 20 de marzo.*

<b>1. IDENTIFICACIÓN</b>		
1.1 Apellidos / Apellidos / Surname <b>DOPICO LÓPEZ</b>		
1.2 Name / Nombre / First name: <b>ANTONIO</b>		DNI / DNI / Identity card number: <b>79336909L</b>
1.3 Categorical / Categorical / Category: <b>"C"</b>	1.4. Especies / Especies / Species: <b>ROEDORES</b>	1.6. Válido ata / Valid until / Expiry: <b>1/07/2029</b>
<b>2. Nº DO CERTIFICADO / Nº DEL CERTIFICADO / CERTIFICATE NUMBER</b>		
<b>C621</b>		
<b>3. ORGANISMO QUE EXPIDE O CERTIFICADO / ORGANISMO QUE EXPIDE EL CERTIFICADO / BODY ISSUING THE CERTIFICATE:</b>		
3.1 Nome e endereço do organismo que expide o certificado / Nombre y dirección del organismo que expide el certificado / Name and address of the body issuing the certificate:  <b>CONSELLERÍA DO MEDIO RURAL – XUNTA DE GALICIA AXENCIA GALEGA DA CALIDADE ALIMENTARIA Avda. Do Camiño Francés, 10 baixo 15781 Santiago de Compostela A Coruña (España)</b>		
1.1. Teléfono / Teléfono / Telephone: <b>981 546 657</b>	1.3. FAX / Fax / Fax: <b>981 546 651</b>	1.4. Correo electrónico / Correo electrónico / Email: <b>formacion.ccmrj@xunta.es</b>
1.5. Data / Fecha / Date:	1.6. Lugar / Lugar / Place: <b>Santiago de Compostela</b>	
1.7. Nome e sinatura / Nombre y firma / Name and signature:  <b>Asdo.: Xiana Maria Perales Arroyo Xefa do Departamento de Formación (asinado dixitalmente)</b>		

## Publications

This Thesis presents results, totally or partially, of the following publications, of which the PhD is co-author:

### **Publication 1: Sustained blood glutamate scavenging enhances protection in ischemic stroke**

-Year:

2020

-Authors:

Ahlem Zaghmi<sup>1</sup>, Antonio Dopico López<sup>2</sup>, María Pérez Mato<sup>2,3</sup>, Ramón Iglesias Rey<sup>2</sup>, Pablo Hervella<sup>2</sup>, Andrea A. Greschner<sup>1</sup>, Ana Bugallo Casal<sup>2</sup>, Andrés da Silva<sup>2</sup>, María Gutiérrez Fernández<sup>3</sup>, José Castillo<sup>2</sup>, Francisco Campos Pérez<sup>2</sup>, Marc A. Gauthier<sup>1</sup>.

-Affiliation:

1) Institut National de la Recherche Scientifique (INRS), EMT Research Center, Varennes, Québec, Canada.

2) Clinical Neuroscience Research Laboratory, Health Research Institute of Santiago de Compostela (IDIS), Santiago de Compostela, Spain.

3) Neuroscience and Cerebrovascular Research Laboratory, Department of Neurology and Stroke Center, La Paz University Hospital, Neuroscience Area of IdiPAZ Health Research Institute, Universidad Autónoma de Madrid, Madrid, Spain.

-Publisher and ISSN:

Springer Nature, 2399-3642.

-Quality indexes:

Impact factor: 5.49

h-Index: 26

Quartile: Q1 (Biochemistry, Genetics and Molecular Biology)

-PhD contribution:

The PhD contributed to the conduct of the experiments.

-Content present in this Thesis:

Chapters 6 and 10.

-Reference:

Zaghmi A, Dopico-López A, Pérez-Mato M, Iglesias-Rey R, Hervella P, Greschner AA, Bugallo-Casal A, da Silva A, Gutiérrez-Fernández M, Castillo J, Pérez FC, Gauthier MA. Sustained blood glutamate scavenging enhances protection in ischemic stroke. *Commun Biol.* 2020;3(1). doi:10.1038/s42003-020-01406-1.

## **Publication 2: Inhibition of endogenous blood glutamate oxaloacetate transaminase enhances the ischemic damage**

-Year:

2021

-Authors:

Antonio Dopico López<sup>1</sup>, María Pérez Mato<sup>2</sup>, Andrés da Silva Candal<sup>1</sup>, Ramón Iglesias Rey<sup>1</sup>, Aharon Rabinkov<sup>3</sup>, Ana Bugallo Casal<sup>1</sup>, Tomás Sobrino<sup>1</sup>, David Mirelman<sup>3</sup>, José Castillo<sup>1</sup>, Francisco Campos<sup>1</sup>.

-Affiliation:

1) Clinical Neuroscience Research Laboratory, Health Research Institute of Santiago de Compostela (IDIS), Santiago de Compostela, Spain.

2) Neuroscience and Cerebrovascular Research Laboratory, Department of Neurology and Stroke Center, La Paz University Hospital, Neuroscience Area of IdiPAZ Health Research Institute, Universidad Autónoma de Madrid, Madrid, Spain.

3) Department of Biomolecular Sciences, Weizmann Institute of Science, Rehovot, Israel.

-Publisher and ISSN:

Mosby Inc., 1931-5244.

-Quality indexes:

Impact factor: 6.54

h-Index: 98

Quartile: Q1 (Physiology)

-PhD contribution:

The PhD contributed to the conduct of the experiments, the writing of the manuscript and the discussion of the results and their implications.

-Content present in this Thesis:

Chapters 4 and 8.

-Reference:

Dopico-López A, Pérez-Mato M, da Silva-Candal A, Iglesias-Rey R, Rabinkov A, Bugallo-Casal A, Sobrino T, Mirelman D, Castillo J, Campos F. Inhibition of endogenous blood glutamate oxaloacetate transaminase enhances the ischemic damage. *Transl Res.* 2021;230:68-81. doi:10.1016/j.trsl.2020.10.004



A pesar de los avances en las últimas décadas, el ictus sigue siendo una de las principales causas de muerte y discapacidad en nuestro país. Es por ello que el desarrollo de nuevas terapias para esta enfermedad continúa vigente. En la presente Tesis se analiza el efecto terapéutico de una nueva versión recombinante de la enzima humana GOT1 (rGOT1), una transaminasa implicada profundamente en el metabolismo del glutamato y otros procesos celulares. Mediante la utilización de modelos animales de isquemia cerebral, se ha podido demostrar que el uso de esta enzima recombinante ejerce un efecto beneficioso sobre la lesión isquémica, así como sobre el déficit neurológico de los animales. El desarrollo de esta Tesis profundiza en el conocimiento de esta enzima y apoya el uso de la rGOT1 como terapia frente al ictus.